RNAi and Chemical-Based High Content Screening for the Normalization of XPC Phenotyope

Farah Kobaisi

THÈSE

Pour obtenir le grade de

DOCTEUR DE L'UNIVERSITE GRENOBLE ALPES

Spécialité: **Modelés, Méthodes et Algorithmes en Biologie.**

Arrêté ministériel : 25 mai 2016

Présentée par

Farah Kobaisi

Thèse dirigée par **le Professeur Walid Rachidi, UGA** et codirigée par le **Professeur Hussein Fayyad-Kazan, Université Libanaise** avec **le Dr Xavier Gidrol, CEA**

préparée au sein du **Laboratoire Biomics/IRIG/CEA**
dans **l'École Doctorale Ingénierie Pour la Santé, la Cognition et l'Environnement.**

Criblage à Haut Contenu à Base d'ARNi et de Produits Chimiques pour la Normalisation du Phénotype XPC

Thèse soutenue publiquement le **15/07/2021**,
devant le jury composé de :

Mr. Patrice Marche
Directeur De Recherche INSERM, Grenoble, Président

Mrs. Laure Favot
Maitre de conférences, Université de Poitiers, Rapporteur

Mr. Jerome Lamartine
Professeur des Universités, Université de Lyon, Rapporteur

Mr. Thierry Magnaldo
Directeur De Recherche CNRS, Nice, Membre

Mrs. Eva Hamade
Professeur des Universités, Université Libanaise, Membre

Mr. Eric Sulpice
Chercheur, CEA Grenoble, Invité

Mr. Bassam Badran
Professeur des Universités, Université Libanaise, Liban, Invité

RÉSUMÉ

La Xeroderma Pigmentosium C (XP-C) est une génodermatose autosomique récessive rare. Les patients de cette pathologie sont porteurs d'une mutation dans la protéine XPC de reconnaissance des dommages de l'AND. Cette mutation génère un phénotype pathologique caractérisé par une photosensibilité extrême et l'accumulation de dommages à l'ADN induits par les UV. Par conséquent, l'objectif de ce projet est de cribler des molécules chimiques et biologiques afin d'identifier les hits qui peuvent inverser ce phénotype malade. Des cellules XP-C et normales dérivées de patients seront utilisées pour cribler une bibliothèque chimique de 1280 médicaments approuvés par la FDA ou une bibliothèque de siRNA visant à diminuer l'expression de toutes les kinases humaines, étant donné l'implication des kinases dans les différentes voies de réparation de l'ADN. Les cellules seront ensuite irradiées par des UVB pour induire des lésions de l'ADN, puis l'inversion phénotypique sera surveillée au niveau de la photosensibilité ou au niveau de la réparation des lésions de l'ADN pour visualiser quel traitement permet une diminution du niveau de lésions et donc une réparation. Une caractérisation plus poussée des effets des hits sera ensuite effectuée au niveau de l'apoptose et de la prolifération, par cytométrie de flux, et de la signalisation en aval via le western blot. Pour le criblage chimique, 1280 médicaments différents ont été utilisés pour traiter les cellules. Après l'induction de dommages à l'ADN, les cellules ont également été post-traitées avec les mêmes médicaments, puis incubées pendant vingt-quatre heures pour permettre leur récupération. La viabilité des cellules traitées a été. Seize médicaments ont permis une augmentation de plus de 25% de la viabilité des cellules. Ensuite, après le marquage des dommages à l'ADN et leur quantification, deux médicaments, l'isoconazole et le chlorhydrate de clemizole, ont permis de diminuer de 20% la quantité de dommages à l'ADN. L'un des deux médicaments, l'isoconazole, a permis de réduire la mort apoptotique des cellules XPC mais n'a eu aucun effet sur leur taux de prolifération. Le mode d'action connu des deux médicaments sélectionnés est un antifongique pour l'isoconazole et un antagoniste des récepteurs de l'histamine pour le chlorhydrate de clémizole. Cela n'explique pas leurs effets dans la protection des cellules XPC contre la mort induite par l'irradiation. Par conséquent, une étude plus approfondie du mécanisme d'action possible est nécessaire en comparant le profil d'expression des protéines des cellules traitées et non traitées afin d'identifier un nouveau mécanisme d'action possible pour ces deux médicaments. Quant à criblage biologique, une bibliothèque de siRNAs ciblant l'ensemble des kinases humaines a été utilisée pour traiter les XPC et les cellules normales, puis pour détecter si une inversion phénotypique se produit. 1292 siRNA différents ont été utilisés pour traiter les cellules XPC afin de les irradier et leur permettre de récupérer pendant 24 heures avant de mesurer leur viabilité. Vingt-huit siRNA différents ont été sélectionnés sur la base de leur capacité à induire une augmentation de 25 % de la viabilité cellulaire. Parmi eux, le ciblage de deux kinases a permis une réparation de 20% des dommages induits à l'ADN. Une kinase en particulier a eu un effet exclusif dans la photo-protection des cellules XPC et aucun effet sur les cellules normales. Le knock down de l'expression de la kinase induit par ce siRNA a été validé au niveau de l'ARNm par PCR et au niveau de la protéine par western blot. L'effet photo-protecteur de ce knock down de la kinase dans les cellules XPC a également été validé dans un test de réponse aux UVB. Le

XPC est un excellent modèle pour comprendre l'initiation du cancer de la peau, car il est accéléré dans ces cellules. En améliorant ce phénotype, nous pouvons donc trouver des moyens de retarder ou de prévenir l'initiation du cancer.

Mots clés: XPC, criblage chmique, criblage ARNi, dommage ADN, reparation d'ADN

ABSTRACT

Xeroderma Pigmentosium C (XP-C) is a rare autosomal recessive genodermatosis. Patients with this disorder carry a mutation in the DNA damage recognition protein XPC belonging to the nucleotide excision repair (NER) pathway. This mutation generates a pathological phenotype characterized by extreme photosensitivity and accumulation of UV-induced DNA damage without repair. XP-C and normal patient-derived cells will be used to screen a chemical library of 1280 FDA-approved drugs or a library of siRNAs aimed at decreasing the expression of all human kinases, given the involvement of kinases in different DNA repair pathways. Cells will then be irradiated with UVB to induce DNA damage, and then the phenotypic reversal will be monitored for photosensitivity or for DNA damage repair to visualize which treatment results in a decrease in the level of damage and thus repair. Further characterization of the effects of the hits will then be performed at the level of apoptosis and proliferation, by flow cytometry, and of downstream signaling via western blot. The screening procedure was performed on XPC and normal cell lines. For chemical screening, 1280 different drugs were used to treat cells in duplicate in the wells of a 96-well plate. After induction of DNA damage, the cells were also post-treated with the same drugs and then incubated for twenty-four hours to allow recovery. The viability of treated cells was measured and compared to the positive control of untreated unirradiated cells and the negative control of untreated irradiated cells. Of the drugs tested in the library, sixteen drugs resulted in an increase of more than 25% in cell viability. Then, after DNA damage labeling and quantification, two drugs, isoconazole and clemizole hydrochloride, decreased the amount of DNA damage by 20%. Further characterization of these two drugs by separating the treatment into pre-irradiation or post-irradiation treatment revealed that post-irradiation was more effective in inducing photoresistance in XPC cells. One of the two drugs, isoconazole, reduced apoptotic death of XPC cells but had no effect on their proliferation rate. The known mode of action of the two selected drugs is an antifungal for isoconazole and a histamine receptor antagonist for clemizole hydrochloride. This does not explain their effects in protecting XPC cells from irradiation-induced death. Therefore, further investigation of the possible mechanism of action is needed by comparing the protein expression profile of treated and untreated cells to identify a possible new mechanism of action for these two drugs. As for biological screening. A library of siRNAs targeting all human kinases was used to treat XPCs and normal cells, and then to detect whether a phenotypic reversal occurs. 1292 different siRNAs were used to treat XPC cells to irradiate them and allow them to recover for 24 hours before measuring their viability. Twenty-eight different siRNAs were selected based on their ability to induce a 25% increase in cell viability compared to controls transfected with non-targeted siRNA. Among them, targeting two kinases resulted in a 20% repair of induced

DNA damage. One kinase, in particular, had an exclusive effect in the photoprotection of XPC cells and no effect on normal cells. The knockdown of the kinase expression induced by this siRNA was validated at the mRNA level by PCR and at the protein level by western blot. The photoprotective effect of this kinase knockdown in XPC cells was also validated in a UVB response assay where it was able to induce higher viability in transfected XPC cells compared to non-transfected cells as a function of increasing UVB doses. The regulation of downstream signaling induced by the knockdown of this kinase is also studied by western blot. XPC is an excellent model to understand skin cancer initiation, as it is accelerated in these cells. By improving this phenotype, we can therefore find ways to delay or prevent cancer initiation.

Keywords: XPC, chemical screen, RNAi screen, DNA damage, DNA repair

TABLE OF CONTENTS

LIST OF TABLES

LIST OF FIGURES

TABLE OF ABBREVIATIONS

Abbreviation	Description	Alternative Symbol
3'UTR	3' untranslated region	
4E-BP1	Eukaryotic Translation Initiation Factor 4E Binding Protein 1	
5'UTR	5' untranslated region	
6-4PP	6-4 pyrimidine-pyrimidone photoproduct	
ABL	ABL Proto-Oncogene 1, Non-Receptor Tyrosine Kinase	
ACQ	alanine cysteine glutamine	
ADP	adenosine di-phosphate	
AHR	aryl hydrocarbon receptor	
AK2	Adenylate Kinase 2	
AKT	AKT Serine/Threonine Kinase 1	
AP	apyrimidinic site	
AP-1	Jun Proto-Oncogene, AP-1 Transcription Factor Subunit	JUN
APAF1	Apoptotic Peptidase Activating Factor 1	
APE1	Apurinic/Apyrimidinic Endodeoxyribonuclease 1	
ARE	antioxidant response element	
ARF	ADP Ribosylation Factor	
Arg	aregenine	
ASA	ascorbic acid	
ASNR	non-irradiated allstar transfected cells	
ASR	irradiated allstar transfected cells	
ATAC	histone acetyl transferase	
ATM	Ataxia Telangiectasia mutated protein	
Atp1	ATP synthase subunit	
ATR	Ataxia Telangiectasia and Rad3-related protein	
BACH1	BTB Domain And CNC Homolog 1	
Bad	BCL2 Associated Agonist Of Cell Death	
Bak	BCL2 Antagonist/Killer 1	
Bax	BCL2 Associated X, Apoptosis Regulator	
BCC	Basal Cell Carcinoma	
Bcl-xl	BCL2 Apoptosis Regulator	BCL2
BCR	B cell receptor	
BER	base excision repair	
BLM	BLM RecQ Like Helicase	
BRAF	B-Raf Proto-Oncogene, Serine/Threonine Kinase	
BRCA1	BRCA1 DNA Repair Associated	
BRL1	brassinosteroid receptor	

bZip	leucine xipper motif	
C.elegans	Caenorhabditis elegans	
CALM2	Calmodulin 2	
CAMK2G	Calcium/Calmodulin Dependent Protein Kinase II Gamma	
CBP	CREB Binding Protein	CREBBP
cdc25	Cell Division Cycle 25C	
CDK	Cyclin Dependent Kinase	
CDK2	Cyclin Dependent Kinase 2	
CDK4	Cyclin Dependent Kinase 4	
CDKN1A	Cyclin Dependent Kinase Inhibitor 1A	P16INK4A
CDKN1B	Cyclin Dependent Kinase Inhibitor 1B	
cDNA	complementary DNA	
CDNR	non-irradiated cell death transfected cells	RSK1
CDR	irradiated cell death transfected cells	
CEBPG	CCAAT Enhancer Binding Protein Gamma	
CETN2	Centrin 2	
c-FOS	Fos Proto-Oncogene, AP-1 Transcription Factor Subunit	
CH	chaperon	
ChK1/2	Checkpoint kinases 1/2	
CLK1	CDC Like Kinase 1	
Clock-BMAL	Cryptochrome Circadian Regulator 1	CRY1
COFS	Cerebro-oculo-facio-skeletal syndrome	
COX2	Cytochrome C Oxidase	
CPD	Cyclobutane Pyrimidine Dimer	
CRISPR-Cas9	clustered regularly interspaced short palindromic repeats-CRISPR associated protein 9	
CS	Cockayne Syndrome	
CSA	ERCC Excision Repair 8, CSA Ubiquitin Ligase Complex Subunit	ERCC8
CSB	ERCC Excision Repair 6, Chromatin Remodeling Factor	ERCC6
CSNK2A1	Casein Kinase 2 Alpha 1	CK2
CUL4	Culin 4/DDB1- And CUL4-Associated Factor 2	
Cyn	Cuynaropicrin	
CYP1A1	Cytochrome P450 Family 1 Subfamily A Member 1	
Cys	Cysteine	
DCLK1	Doublecortin Like Kinase 1	
DDB1	Damage Specific DNA Binding Protein 1	
DDR	DNA Damage Response	
DDR2	Discoidin Domain Receptor Tyrosine Kinase 2	
DEVD	aspartate glutamine valline aspartate amino acid peptide	

DGKZ	Diacylglycerol Kinase Zeta	
DGUOK	Deoxyguanosine Kinase	
DMSO	Dimethyl sulfoxide	
DNA	Deoxyribo Nucleic Acid	
DNA-PK	DNA protein kinase	
DNMT1	DNA Methyltransferase 1	
dNTP	deoxyribo nucleotide tri-phosphate	
dpy-31	collagen processing protease	
DSB	Double Strand Breaks	
DTT	Dithiothreitol	
DUOX	Dual Oxidase	
E. Coli	Escherichia Coli	
E2F4-p130	E2F Transcription Factor 4	
EDU	5-Ethynyl-2´-deoxyuridine	
EGFR	Epidermal Growth Factor Receptor	
eIF-4E	Eukaryotic Translation Initiation Factor 4E	
EP300	E1A Binding Protein P300	
EPIGEN	Epithelial Mitogen	EPGN
ERCC1	ERCC Excision Repair 1, Endonuclease Non-Catalytic Subunit	
ERK	Mitogen-Activated Protein Kinase 1	MAPK1
FA	Fanconi anemia	
FANCC	FA Complementation Group C	
FANCM	FA Complementation Group M	
FASTK	Fas Activated Serine/Threonine Kinase	
FBS	fetal bovine serum	
FDA	food and drug administration	
FOXO	Forkhead Box O	
GADD45α	Growth Arrest And DNA Damage Inducible Alpha	
GAK	Cyclin G Associated Kinase	
GFP	green fluorescence protein	
GG-NER	Global Genome Nucleotide Excision Repair	GGR
Gli	Glioma zinc finger transcriptions factors	
GPX2	Glutathione Peroxidase 2	
GRK6	G Protein-Coupled Receptor Kinase 6	
GSH	glutathione	
GSK3	Glycogen Synthase Kinase 3 Beta	
GSK3A	Glycogen Synthase Kinase 3 Alpha	
GST	glutathione S transferase	
GTP	guanosine triphosphate	

GWAS	genome-wide association studies	
H2DCFA	2',7'-dichlorodihydrofluorescein diacetate	
H2O2	hydrogen peroxide	
HAP1	Huntingtin Associated Protein 1	
HAT	histone acetyl transferase	
HBV	hepatitis B virus	
HBx	Late Endosomal/Lysosomal Adaptor, MAPK And MTOR Activator 5	LAMTOR5
HDR	homologous recombination	
HERC2	HECT And RLD Domain Containing E3 Ubiquitin Protein Ligase 2	
HIF1A	Hypoxia Inducible Factor 1 Subunit Alpha	
His	Histidine	
HMGA1	High Mobility Group AT-Hook 1	
HMGN1	High Mobility Group Nucleosome Binding Domain 1	
HPLC	high performance liquid chromatography	
HRP	horseradish peroxidase	
Hsp90	Heat Shock Protein 90 Alpha Family Class A Member 1	HSP90AA1
IKB	NFKB Inhibitor Alpha	NFKBIA
IKKB	Inhibitor Of Nuclear Factor Kappa B Kinase Subunit Beta	IKBKB
IL1β	interleukin 1	
IL6	interleukin 6	
IL10	interleukin 10	
IPMK	Inositol Polyphosphate Multikinase	
IR	Ioninzing Radiation	
Ira1	inhibitory regulator protein	
IRAK1	Interleukin 1 Receptor Associated Kinase 1	
ITK	IL2 Inducible T Cell Kinase	
JNK	Mitogen-Activated Protein Kinase 8	MAPK8
KEAP1	Kelch Like ECH Associated Protein 1	
KGF	Keratinocytes growth factor	
KIF11	Kinesin Family Member 11	EG5
KRAS	KRAS Proto-Oncogene, GTPase	
LacY	Lactose permease	
LATS1	Large Tumor Suppressor Kinase 1	
LATS2	Large Tumor Suppressor Kinase 2	
LD50	lethal dose 50	
Leu	leucine	
MAF	MAF BZIP Transcription Factor	
MAL	Mal, T Cell Differentiation Protein	
MAP3K6	Mitogen-Activated Protein Kinase Kinase Kinase 6	

MAPK	Mitogen-Activated Protein Kinase 1	
MAPKAPK2	MAPK Activated Protein Kinase 2	
MC1R	Melanocortin 1 Receptor	
MDM2	MDM2 Proto-Oncogene	
Mek	Mitogen-Activated Protein Kinase Kinase 1	MAP2K1
miRNA	microRNA	
MMC	mitomycin C	
MMP1	Matrix Metallopeptidase 1	
Mrpl3	mitochondrial ribosomal protein	
MS	mass spectrometry	
MSK1	Ribosomal Protein S6 Kinase A5	RPS6KA5
mTORC	Mechanistic Target Of Rapamycin Kinase	MTOR
MTT	3-(4,5-Dimethylthiazol-2-yl)-2,5-diphenyltetrazolium bromide	
MUTYH	MutY DNA Glycosylase	
MYC	MYC Proto-Oncogene, BHLH Transcription Factor	
NAC	N-acetyl cysteine	
NAD	nicotinamide	
NEK3	NIMA Related Kinase 3	
NEK4	NIMA Related Kinase 4	
NER	Nucleotide Excision Repair	
NFkB	Nuclear Factor Kappa B Subunit 1	
NHEJ	non-homologous end joining	
NMD	nonsense mediated mRNA decay	
NOX	NADPH Oxidase	
NOXA	Phorbol-12-Myristate-13-Acetate-Induced Protein 1	PMAIP1
NQO1	NAD(P)H Quinone Dehydrogenase 1	D3T
NRAS	NRAS Proto-Oncogene, GTPase	
NRF2	Nuclear Factor, Erythroid 2 Like 2	NFE2L2
Nth1	Nth Like DNA Glycosylase 1	
NUP116	Nucleoporin 98 And 96 Precursor	NUP98
ODD	oxidative DNA damage	
OGG1	8-Oxoguanine DNA Glycosylase	
P21	Cyclin Dependat Kinase Inhibitor 1A	CDKN1
P38	Mitogen-Activated Protein Kinase 14	MAPK14
P53	Tumor Protein 53	
p70s6k	Ribosomal Protein S6 Kinase B1	RPS6KB1
p90rsk	Ribosomal Protein S6 Kinase A1	RPS6KA1
PANK2	Pantothenate Kinase 2	
PARP1	Poly(ADP-Ribose) Polymerase 1	

PARP4	Poly(ADP-Ribose) Polymerase Family Member 4	
PBS	phosphate buffer saline	
PCNA	Proliferating Cell Nuclear Antigen	
PDK1	Pyruvate Dehydrogenase Kinase 1	
PFA	paraform aldahyde	
PGC	Progastricsin	
PGH2	Prostaglandin-Endoperoxide Synthase 2	
PI3K	Phosphatidylinositol-4,5-Bisphosphate 3-Kinase Catalytic Subunit Alpha	PIK3CA
PIK3C3	Phosphatidylinositol 3-Kinase Catalytic Subunit Type 3	
PIK3R3	Phosphoinositide-3-Kinase Regulatory Subunit 3	
PKC	Protein Kinase C Alpha	PRKCA
Pol	polymerase	
PRC2	Polycomb repressive complex 2	
PREX2	Phosphatidylinositol-3,4,5-triphosphate dependent RAC exchange factor	
PRKACG	Protein Kinase CAMP-Activated Catalytic Subunit Gamma	
Pro	Proline	
PTC	premature termination codon	
PTCH1	Patched 1	
PTEN	Phosphatase And Tensin Homolog	
PTP-κ	Pyruvoyltetrahydropterin	
PUMA	BCL2 Binding Component 3	BBC3
qPCR	quantitaitve PCR	
Rac	Rac Family Small GTPase	
RAD23B	RAD23 Homolog B, Nucleotide Excision Repair Protein	
RAD52	RAD52 Homolog, DNA Repair Protei	
RAF	Raf Proto-Oncogene, Serine/Threonine Kinase	
RAS	RAS Proto-Oncogene, GTPase	
RBX1	Ring-Box 1	
RFC	Replication factor C	
RNAi	interfering RNA	
ROI	region of interest	
ROS	Reactive Oxygen Species	
RPA1	Replication Protein A1	
RPS6KB1	Ribosomal Protein S6 Kinase B1	
RSV	resveratrol	
Rzscore	robust Z score	
S6K	Ribosomal Protein S6 Kinase B1	RPS6KB1
san1	ubiquitin protein kinase	

SCC	Squamous Cell Carcinoma	
SDS	Sodium dodecyl sulfate	
Ser	Serine	
SFN	sulforaphane	
sgRNA	single guide RNA	
SHH	sonic hedgehog	
shRNA	Short hairpin RNA	
siAS	siRNA all star	
siCD	siRNA cell death	
siRNA	short interferring RNA	
SIRT1	Sirtuin 1	
SLC30A8	solute carrier family 30 member 8	
SLP1	Synaptotagmin Like 1	SYTL1
sMASE	Neutral Sphingomyelinase Activation Associated Factor	NSMAF
SMO	smoothened	
SNAIL	zinc finger protein SNAl1	
SNF5	SWI/SNF Related, Matrix Associated, Actin Dependent Regulator Of Chromatin, Subfamily B, Member 1	SMARCB1
SP1	Sp1 Transcription Factor	
SPRR2D	Small Proline Rich Protein 2D	
SRP	simgle recognition paticle	
SRP	abasic deoxyribose phosphate	
SSB	Single Strand Breaks	
STK17B	Serine/Threonine Kinase 17b	
SWI/SNF	**SWItch**/Sucrose Non-Fermentable chromatin remodeling complex	
TCEA1	Transcription Elongation Factor A1	
TC-NER	Transcription coupled Nucleotide Excision Repair	TCR
TEK	TEK Receptor Tyrosine Kinase	
TF	transcirption factor	
TFIIH	Transcription factor II H	
Thr	Threonine	
TIE1	Tyrosine Kinase With Immunoglobulin Like And EGF Like Domains 1	
TNFα	Tumor Necrosis Factor	
TP63	Tumor Protein P63	
tRNA	transfer ribonucleotide acid	
Trp	tryptophan	
TSC2	TSC Complex Subunit 2	
TSSK6	Testis Specific Serine Kinase 6	
TTD	Trichothiodystrophy	

Tyr	Tyrosine	
UCA	urocanic acid	
unc-52	SMU1 DNA Replication Regulator And Spliceosomal Factor	SMU1
USP1	Ubiquitin Specific Peptidase 1	
USP24	Ubiquitin Specific Peptidase 24	
USP45	Ubiquitin Specific Peptidase 25	
USP48	Ubiquitin Specific Peptidase 48	
USP7	Ubiquitin Specific Peptidase 7	
UV	Ultraviolet	
UVA	Ultraviolet radiation A	
UVB	Ultra violet radiation B	
UVC	Ultra violet radiation C	
UVR	Ultraviolet radiation	
UVRAG	Ultra violet radiation resistance associated gene	
UVSSA	UV Stimulated Scaffold Protein A	
VDR	vitamin D receptor	
WIP1	Protein Phosphatase, Mg2+/Mn2+ Dependent 1D	PPM1D
Wnt	Wingless-related integration site	
WT	wild type	
XAB2	XPA Binding Protein 2	
XP	Xeroderma Pigmentosum	
XPA	Xeroderma Pigmentosum protein A	
XPB	ERCC Excision Repair 3, TFIIH Core Complex Helicase Subunit	ERCC3
XPC	Xeroderma Pigmentosum protein C	
XPD	ERCC Excision Repair 2, TFIIH Core Complex Helicase Subunit	ERCC2
XPE	Damage Specific DNA Binding Protein 2	DDB2
XPF	ERCC Excision Repair 4, Endonuclease Catalytic Subunit	ERCC4
XPG	ERCC Excision Repair 5, Endonuclease	ERCC5
XPV	DNA Polymerase Eta	POLH
XRCC1	X-Ray Repair Cross Complementing 1	
YY1	YY1 Transcription Factor	
αMSH	melanotropin	
γH2AX	phosphorylated H2A histone family member X	

BIBLIOGRAPHIC REVIEW

CHAPTER 1. SKIN, DNA DAMAGE, AND UV RADIATION

Our study is concerned with the normalization of the photosensitive profile of the rare genetic autosomal recessive disease XP-C. XP-C mainly manifests in increased skin cancer incidence upon UV irradiation. For that, we will first explore the different aspects of the skin cells and the effect of UV irradiation on the downstream signaling and the associated carcinogenesis.

1. THE SKIN AND ITS LAYERS

The skin provides the first line of defense against pathogens and protects the body from mechanical stress and water loss [3]. However, being in direct contact with the environment renders it highly susceptible to different stimulants like xenobiotics, UV radiation, and thermal stress disrupting skin cells' metabolism [4]. The skin consists of epidermis, dermis and subcutaneous fat layer [5]. The epidermal cells, keratinocytes and melanocytes, and the dermal fibroblasts are of great concern being the major skin cells affected in XP patients.

1.1 EPIDERMIS

It is the outermost layer of the skin that includes mainly keratinocytes but also other cells like melanocytes, Langerhans cells and Merkel cells. Keratinocytes render the epidermis continually renewable due to the proliferation of keratinocyte stem cells [6] These cells produce keratin which protects them against UV radiation [7]. Malignant transformation of keratinocytes leads to non-melanoma skin cancer like squamous cell carcinoma (SCC) and basal cell carcinoma (BCC). Other cells of interest are the melanocytes. They are located near the basal membrane of the epidermis and have cytoplasmic appendixes that penetrate the keratinocytes' layers. Melanin is produced by these cells and it is responsible for pigmentation hence protecting skin from radiation [8]. Melanin is considered to have UV absorptive properties. Any abnormalities in these cells can give rise to melanomas.

1.2 DERMIS

Fibroblasts are the main constituents of the dermis and they are located between the nerves, blood vessels and connective tissue. They secrete collagen, elastin and glucosaminoglycans thus strengthening the skin and mediating its elasticity [4]. Moreover, in case of cancer, these cells play a role in progression and metastasis due to the various molecules they express [9].

2. OVERVIEW OF THE DNA DAMAGE RESPONSE

DNA damage is the outcome of a wide variety of physiological-chemical aberrations [10]. The sources of DNA damage can be either endogenous, originating from within the cell, or exogenous. The first includes reactive oxygen species (ROS) and oxygen radicals generated during cellular metabolism. These ROS can result in the formation of base modifications including abasic sites

from depurination or deamination, 8-oxoguanine lesions and single-strand breaks. It is noteworthy that ROS generation can also be triggered by exogenous factors. For example, the skin contains endogenous chromophores like tryptophan, riboflavin and mitochondrial cytochrome c oxidase that favor the generation of ROS from sunlight [11, 12]. Replication errors are other endogenous sources of DNA damage that lead to base mismatches, insertions or deletions in the nucleotide sequence. On the other hand, external causes of DNA lesions comprise ionizing radiations, X rays and antitumor drugs that generate double-strand breaks (DSB), single-strand breaks, and interstrand cross-links (figure 1) [13]. In addition, nucleotide modifications such as pyrimidine dimers and the addition of bulky adducts are triggered upon exposure to UV light or certain pollutants or chemicals (figure 1) [12]. Therefore, a DNA damage response (DDR) is required for the correction of these DNA insults to ensure the accurate transmission of genetic information. DNA damage detection is the first step in the repair pathway and it involves molecules termed sensors. The latter transmits signals to transducers, that are mostly protein kinases [14], which in turn act on effectors, including cell cycle regulators, nucleases and helicases, to halt the cell cycle in order to ensure DNA repair or to induce apoptosis or senescence in case of irreparable damage [15] Any failure in this pathway can lead to the accumulation of DNA damage and ultimately premature aging or tumorigenesis [13].

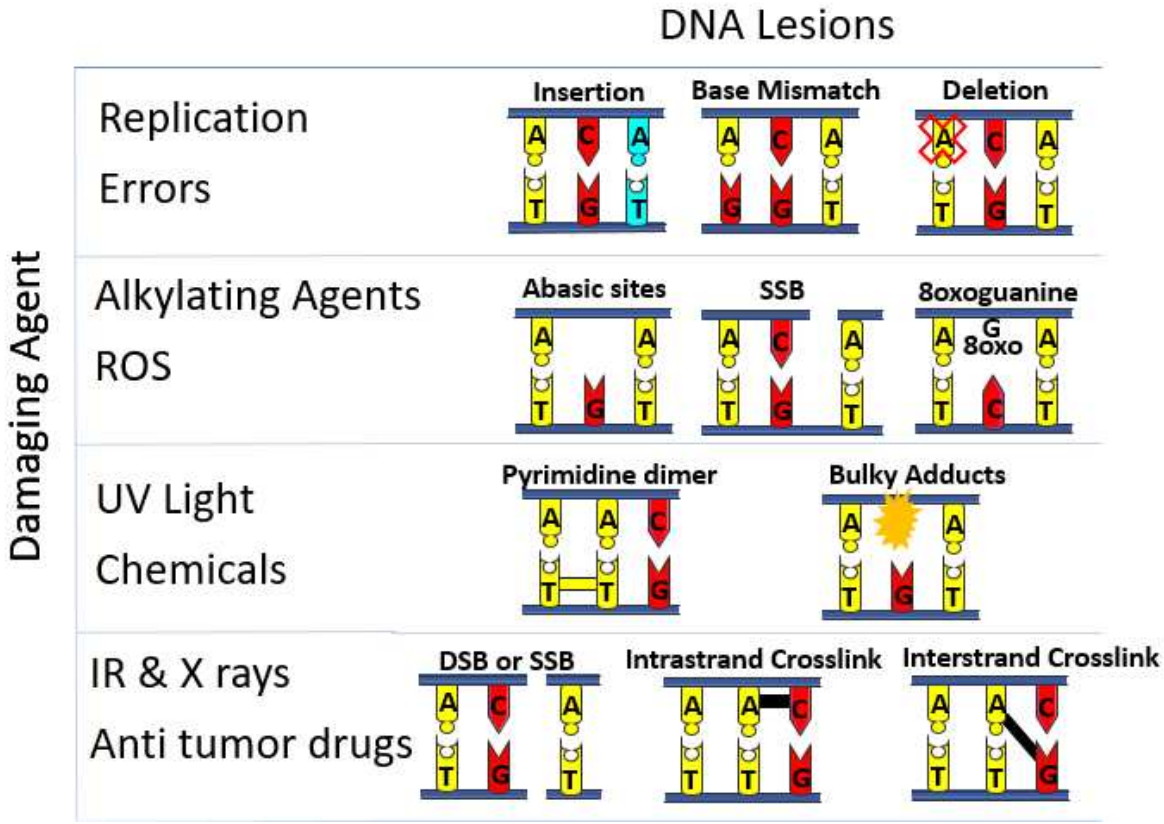

Figure 1 DNA lesions induced by damaging agents

Several DNA lesions are formed upon the exposure of the DNA to harmful insults. Replication Errors can give rise to insertion, deletion, or base mismatch mutations. Alkylating agents and reactive oxygen species (ROS) can lead to the formation of abasic sites, single strand breaks (SSB) and 8-oxoguanines. On the other hand, UV radiation and chemical agents mediate the formation of pyrimidine dimers and the addition of bulky adducts. Finally, ionizing

radiation including X rays and antitumor drugs can lead to single strand breaks, double-strand breaks, together with inter and intra strand crosslinks. Abbreviations: ROS: reactive oxygen species, SSB: single-strand breaks, DSB: double-strand breaks, IR: ionizing radiation.

3. UV RADIATION AND SKIN PENETRATION

Solar UV radiation is sub-classified into UVA (320-400nm), UVB (280-320nm) and UVC (200-280nm). UVC is absorbed by the ozone layer rendering the UV spectrum reaching earth restricted to 95% UVA and 5% UVB. These two solar rays allow the induction of DNA lesions, thus playing a critical role in skin carcinogenesis. The more energetic UVB can be absorbed by the epidermis and superficial dermis; whereas the less energetic more penetrating UVA can reach deep into the dermis. On one hand, UVB irradiation generates direct damages to the DNA in the form of dimeric pyrimidine photoproducts including Cyclobutane pyrimidine dimers (CPDs), 6-4 pyrimidine-pyrimidone photoproducts (6-4PPs) and Dewar isomers [16]. The latter are formed between two adjacent pyrimidine sites TT, CT, TC or CC. The 6-4 PPs are readily repaired in faster kinetics compared to CPDs where the TC and CC-CPD are the most mutagenic ones [17]. UVB also contributes to the generation of double-strand breaks via collapsing the replication forks at dimer sites and formation of reactive oxygen species (ROS) [18]. The generation of 8-hydroxy-2-deoxyguanosines (8-OHdG) was reported post UVB irradiation that leads to G→T transversion. The majority of UVB-induced mutations are C→T or CC→TT transitions designated as the UVB signature mutation [19]. On the other hand, UVA damage to the DNA is indirect via reactive oxygen species that are generated at bigger amounts than UVB-induced ROS. The most common UVA-induced lesion is 8-oxo guanine. CPDs' indirect formation post UVA are mediated by chemically generated excited electronic states [20]. In addition to DNA damage, ROS can also contribute to lipid peroxidation and protein oxidation (figure 2).

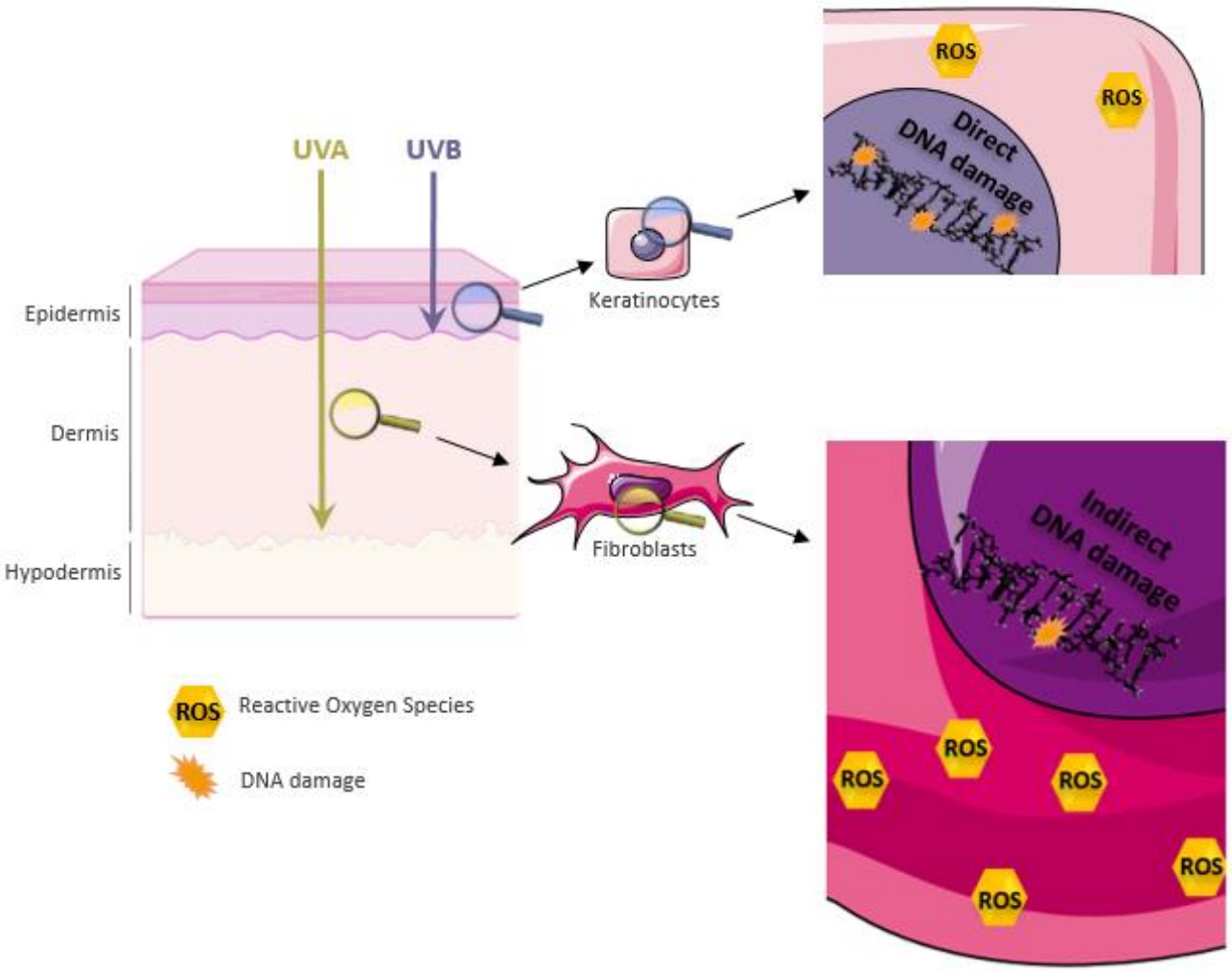

Figure 2 UV skin penetration and molecular outcomes

Out of solar rays, UVA and UVB can penetrate the skin to reach deep into the dermis or be restricted to the epidermis respectively. UVB rays induce direct damages to the DNA and the formation of reactive oxygen species (ROS). UVA's damage to the DNA is indirect via photosensitization reactions by ROS produced at a high rate.

3.1. UV INDUCED APOPTOSIS

Apoptosis is triggered in irradiated cells by three different mechanisms. UV-induced DNA damage favors the activation of ataxia telangiectasia and rad3 related (ATR), ataxia telangiectasia mutated (ATM) and DNA-PK kinases that ultimately activates p53 via checkpoint kinase ChK1/2 as part of the DNA damage response. p53 regulates the transcription of cell cycle protein p21 and several pro-apoptotic factors including APAF1, NOXA, PUMA, Bax and Bak. This contributes to the arrest of the cell cycle. If damage repair fails, P53 via downstream effectors modulate mitochondrial permeability to allow the release of cytochrome c. APAF1, procaspase 9 and cytochrome c favor the formation of the apoptosome leading to the activation of caspase 9 then

caspase 3 [2]. Moreover, the production of reactive oxygen species post UV induces, in addition to DNA damage, lipid peroxidation, protein oxidation and the release of cytochrome c to mediate another intrinsically triggered apoptotic pathway. One final mechanism of apoptosis is mediated via the extrinsic effect of UV in clustering death receptors, including the tumor necrosis factor (TNF) receptor superfamily members the CD95 (Fas/APO-1) or TRAIL, leading to the activation of a cascade of caspases from caspase 8 till caspase 3 [21] (figure 3).

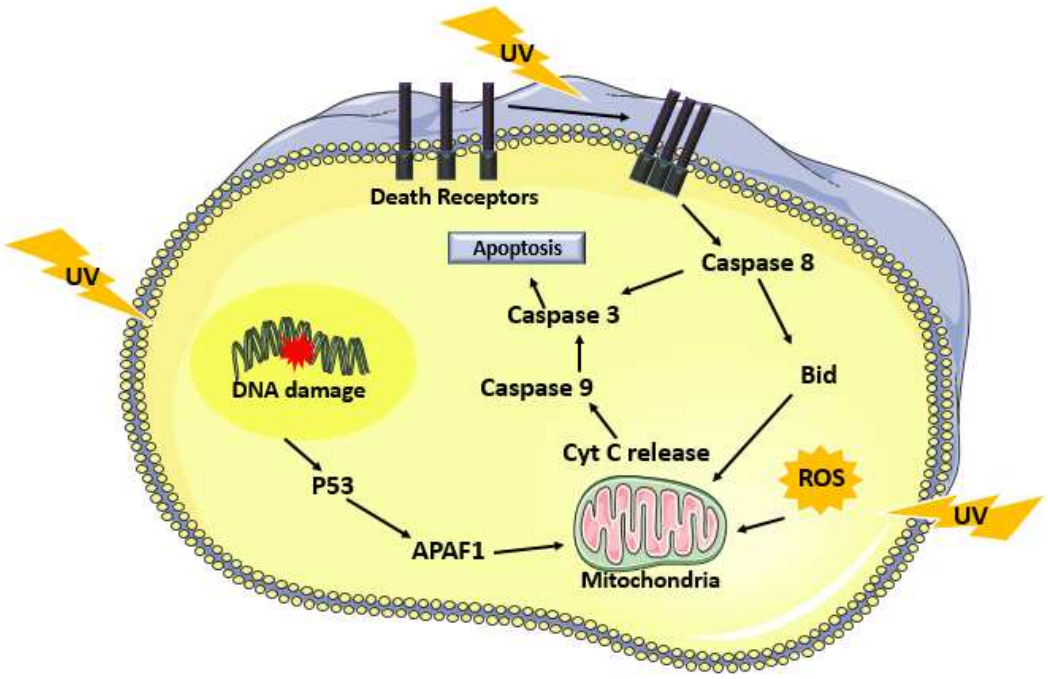

Figure 3 Mechanisms of UV induced apoptosis

UV irradiation triggers cell apoptosis by three different mechanisms. The first is mediated by P53 activation due to DNA damage that ultimately leads to the activation of caspase 9 followed by caspase 3. Reactive oxygen species generated by UV also induce apoptosis by enabling the release of cytochrome c from the mitochondria. One final mechanism is via UV mediated clustering of death receptors leading to the activation of caspase 8.

3.2. UV INDUCED SIGNAL TRANSDUCTION

3.2.1 AKT PATHWAY

The full kinase activity of Akt is achieved on one hand by its phosphorylation at two distinct sites, Thr308 phosphorylation via receptor tyrosine kinase activated PI3K and Ser473 by mTOR complex 2 (mTOR/Rictor; mTORC2) [22]. Its inhibition, on the other hand, is achieved by the tumor suppressor PTEN [23]. UV triggers tyrosine kinase receptors as well as the inhibition of PTEN to enable Akt activation post-irradiation [24]. This further permits the activation of anti-apoptotic transcription factor NFκB [23] and p53 negative regulator MDM2 [25]. The latter together with Akt mediated inhibition of FOXO [26], pro-apoptotic forkhead transcription factor, and apoptotic proteins Bad and caspase 9 [27] infers an anti-apoptotic Akt mediated signal. Cell

cycle progression is also achieved via the inhibition of nuclear translocation of cell cycle inhibitors p21 and p27 [28]. Akt also increases metabolic activity via the phosphorylation and thus inhibition of glycogen synthase kinase (GSK3) [29]. The outcome involves the modulation of protein synthesis and autophagy. The Akt-mediated inhibition of TSC2, tuberous sclerosis protein 2, leads to activation of mTOR/Raptor (mTORC1) that promotes translation via phosphorylation of

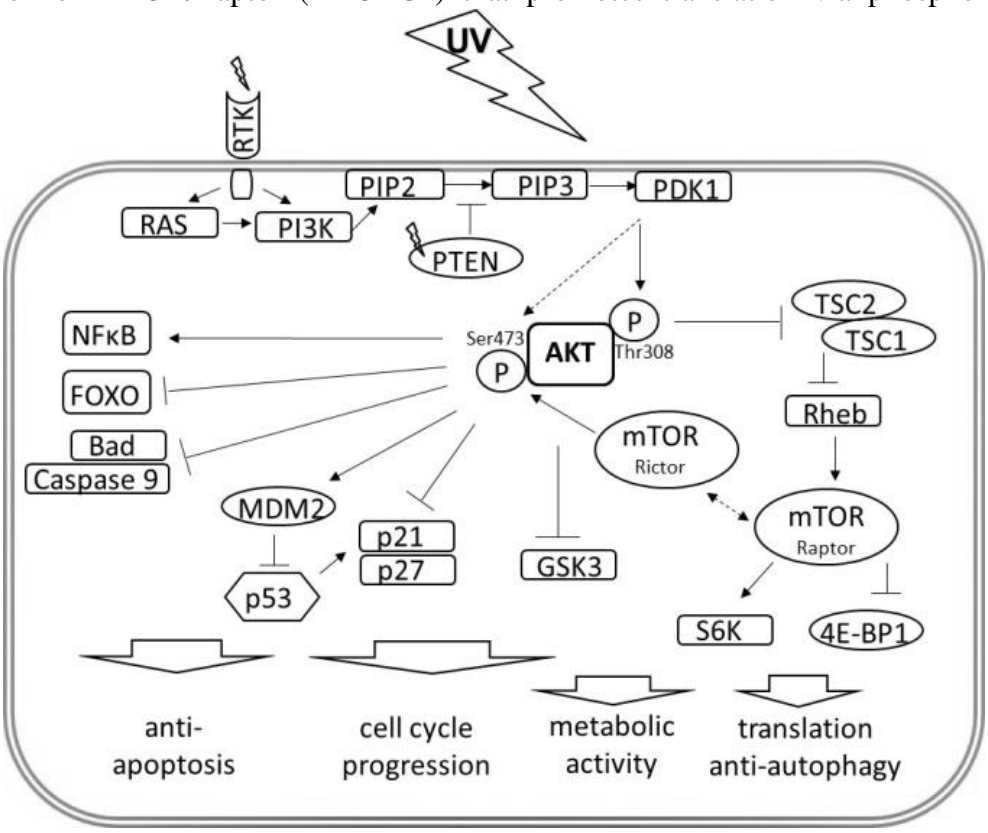

Figure 4 Physiological functions triggered by UV induced Akt signaling

UV induced Akt activation can induce the activation of several downstream cellular functions including inhibition of apoptosis, cell cycle progression, metabolic activity inductions and translation. Detailed description available in the text [2].

eukaryotic initiation factor 4E (eIF-4E) binding protein-1 (4E-BP1) and p70/p85 S6 kinase (S6K) [30] (figure 4).

3.2.2 MAPK PATHWAY

Another UV activated pathway is the mitogen activated protein kinase (MAPK) pathway with final effectors including the c-JUN NH2 terminal kinases (JNKs), the extracellular signal regulated kinases (ERKs) and p38 kinases that regulate the activity of transcription factors NFκB and AP-1. The different forms of UV irradiation (UVA, UVB, UVC) explicit different modes of MAPK activation that are dose dependent.

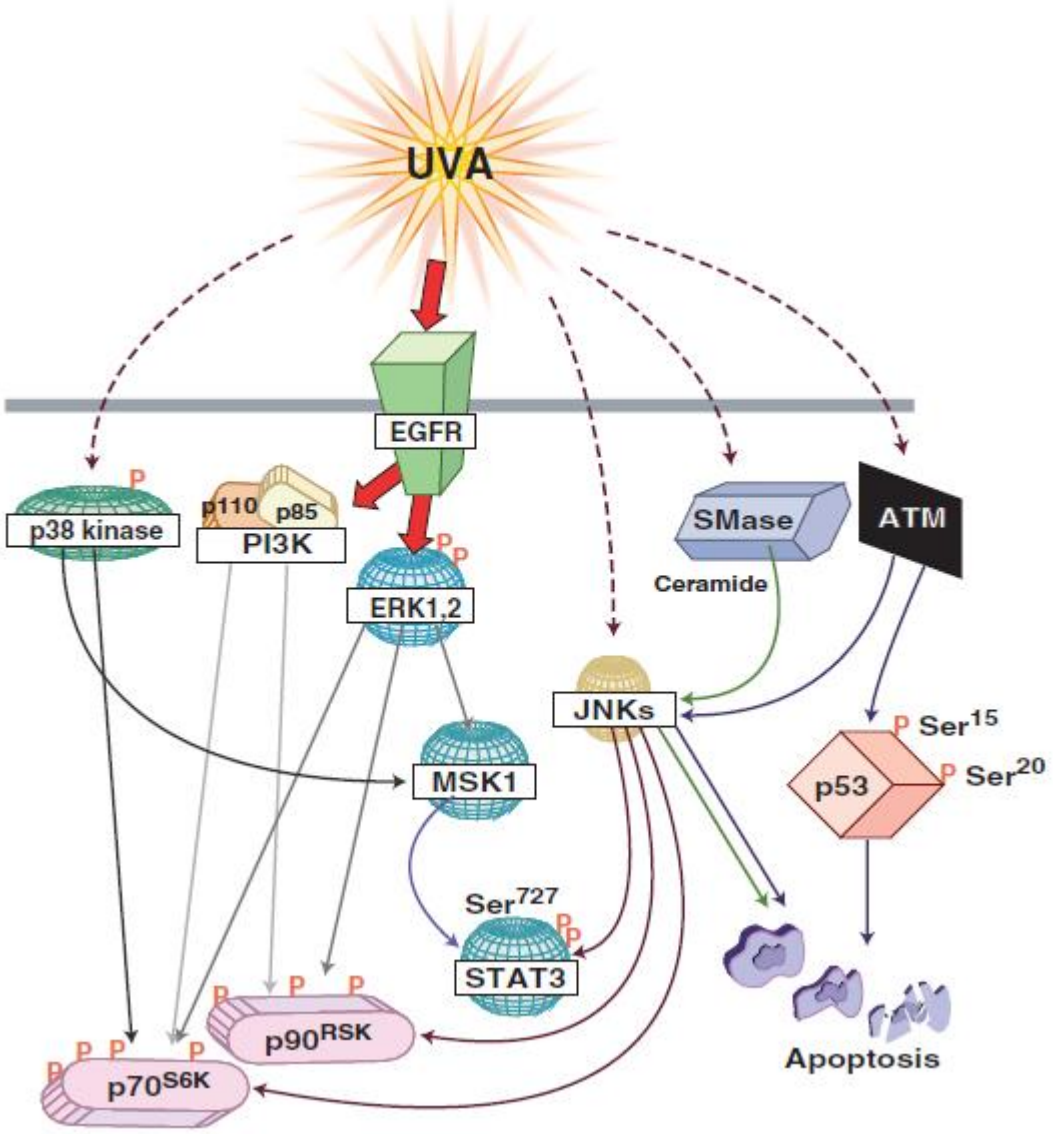

Figure 5 UVA induced MAPK signaling

UVA activates EGFR that leads to the phosphorylation/activation of several downstream effectors including $p70^{S6K}$ and $p90^{RSK}$. UVA mediated apoptosis is mediated by the activation of JNK, ATM, or SMase [1].

I. UVA INDUCED MAPK SIGNALING

UVA induces the activation of epidermal growth factor receptor (EGFR) that then leads to the phosphorylation of the 40*S* ribosomal protein S6 by $p70^{S6K}$ (70-kD ribosomal S6 kinase) and $p90^{RSK}$ (90-Kd ribosomal S6 kinase, also known as MAPKAP-K1) [31, 32]. The activation of $p70^{S6K}$, on one hand, is achieved by different MAPK pathways phosphorylating four distinct sites. PI3K activation induces the phosphorylation at Ser411, Thr421 and Ser424 while mTOR phosphorylates the Thr389 site. These four sites are phosphorylated by ERK1/2. P38 phosphorylates Thr389 and JNK added phosphate groups on both Ser411 and Thr389 [33]. On

the other hand, ERK and JNK but not p38 enable the phosphorylation/activation of $p90^{RSK}$ at Ser381 [34]. It should be noted that the inhibition of EGFR abrogated the UV induced phosphorylation of ERK but not p38 and JNK implying that EGFR mediated signaling to $p90^{RSK}$ and $p70^{S6K}$ is ERK [35] and PI3K dependent. These ribosomal kinases regulate various cellular functions like proliferation and differentiation. Moreover, UVA irradiation can direct cellular decision towards apoptosis triggered by P53 and JNK [36]. The latter being activated by sphingomyelinase (SMase) and thus ceramide hydrolysis [37] (figure 5).

II. UVB INDUCED MAPK SIGNALING

A) MAPK MEDIATED UVB INDUCED ACTIVATION OF AP-1 VIA PKC

UVB induced activation of AP-1 implicates PKC that favors activation of JNK and ERK [38]. ERK further on mediates activation of AP-1 [39]. P38, however, was shown to be activated in EGFR dependent mechanism post UVB and that it further on led to apoptosis [40] (figure 6A).

B) MAPK MEDIATED UVB INDUCED APOPTOSIS

UVB induced P53 dependent apoptosis is mediated via the phosphorylation of the latter at Ser20 by JNK [41]. Nonetheless, p38 and ERK phosphorylate P53 at Ser15 [42] (figure 6B). Apoptosis is also mediated by the activation of the pro-apoptotic protein BAD. The phosphorylation of BAD is carried out by several kinases including JNK1, ERK downstream kinases RSK1 and MSK1 and by p38 kinase allowing BAD's dissociation from the anti-apoptotic Bcl-XL [43] (figure 6C).

C) MAPK MEDIATED UVB INDUCED CHROMATIN REMODELING

The phosphorylation of nucleosome structural protein histone H3 regulates its role in enabling gene expression and chromatin remodeling. Two phosphorylation sites are present on histone H3 which are the Ser10 and Ser28. Ser10 phosphorylation is mediated via ERK and p38 [42] whereas Ser28's phosphorylation is mediated by JNK, ERK and p38 kinases together with ERK and p38 downstream kinase MSK1[44, 45] (figure 6D).

D) MAPK MEDIATED UVB INDUCED GROWTH CONTROL

Growth control regulation can be mediated at either the transcriptional level via ribosomal kinases or at the translational level by translation initiation factors. UVB activates PI3K pathway triggering the phosphorylation of several downstream effectors like Akt and $p70^{S6K}$ [46]. Akt UVB-induced activation is mediated via MSK1 [47] (figure 6E). Moreover, the p38 kinase through its downstream effector MSK1 phosphorylates eukaryotic initiation factor 4E (eIF-4E)-binding protein (4E-BP1) allowing its dissociation from eIF-4F, relieving the translational block and allowing cap-dependent translation initiation [48] (figure 6F).

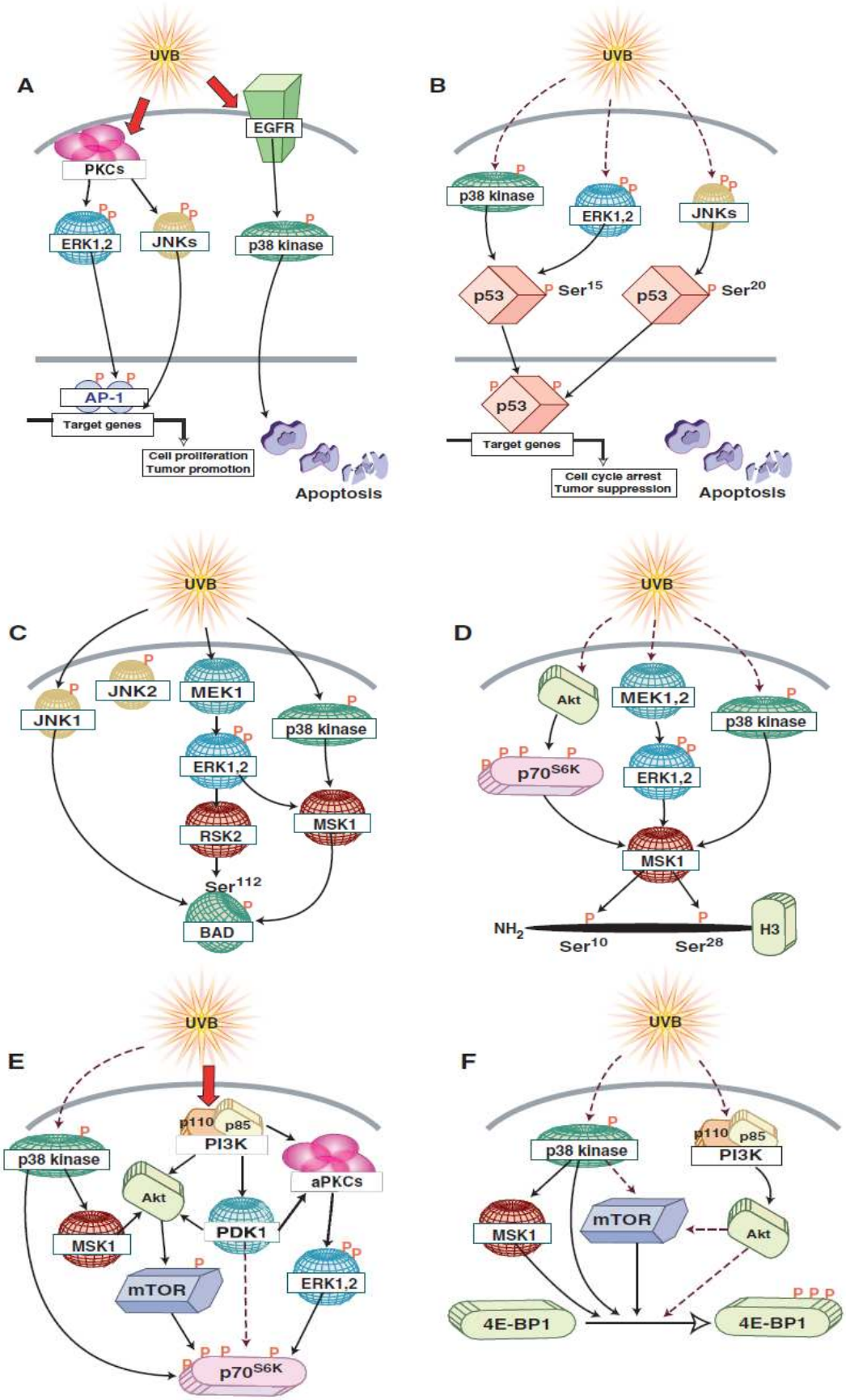
A
UVB
EGFR
PKCs
ERK1,2
JNKs
p38 kinase
AP-1
Target genes
Cell proliferation
Tumor promotion
Apoptosis
B
UVB
p38 kinase
ERK1,2
JNKs
p53
Ser15
p53
Ser20
p53
Target genes
Cell cycle arrest
Tumor suppression
Apoptosis
C
UVB
JNK1
JNK2
MEK1
p38 kinase
ERK1,2
RSK2
MSK1
Ser112
BAD
D
UVB
Akt
MEK1,2
p38 kinase
p70S6K
ERK1,2
MSK1
NH2
Ser10
Ser28
H3
E
UVB
p110
p85
PI3K
p38 kinase
aPKCs
Akt
MSK1
PDK1
mTOR
ERK1,2
p70S6K
F
UVB
p38 kinase
p110
p85
PI3K
MSK1
mTOR
Akt
4E-BP1
4E-BP1

Figure 6 UVB induced MAPK signaling

UVB can trigger different cellular functions via the activation of the diverse MAPK effectors. (A) UVB can, on one hand, activate PKC leading to the activation of AP-1 and, on the other hand, mediate the activation of p38 via EGFR that leads to apoptosis. (B) P53 phosphorylation is achieved by both ERK and p38 at Ser15 and by JNK on Ser15. (C) BAD phosphorylation at Ser112 is facilitated by JNK1, RSK2 and MSK1. (D) Histone H3 is phosphorylated at two sites: Ser10 by ERK and p38 kinase and at Ser28 by ERK, p38 and JNK. MSK1, a downstream effector of ERK and p38, also favors the phosphorylation at Ser28. (E) UVB mediated activation of Akt is PI3K dependent and MSK1 can also be involved in such activation. (F) 4EBP1 phosphorylation by the p38 kinase to MSK1 pathway favors its activation and dissociation from eIF-4E [1].

4. UV-INDUCED MUTATIONS AND CARCINOGENESIS

4.1 P53

p53 plays a critical role in the cell cycle arrest post-stress induction. It activates cell cycle checkpoints halting cycle progression allowing enough time for DNA damage repair. If the repair was unsuccessful, p53 aids in the commitment of the cell to apoptosis by the expression of several pro-apoptotic proteins. UV-induced activation of p53 is mainly mediated via (ATR) that phosphorylates checkpoint kinases (chk1/2) ultimately leading to p53 phosphorylation at Ser15 and Ser20 [49]. Mutations in *p53* can be mainly detected in squamous cell carcinoma and less in basal cell carcinoma. Such mutations carry the UV fingerprint C → T transition [50]. Such mutations hinder the pro-apoptotic activity of p53 resulting in amplification of DNA damage accumulating cells. That combined with UVR-induced upregulation of heat shock proteins poses a combined effect on carcinogenesis evident via their co-localization with mutant p53 in squamous cell carcinoma [51].

4.2 PTEN

Phosphate tensin homolog is a known inhibitor of the PI3K/Akt leading to the deregulation of cell proliferation and induction of apoptosis. Besides, PTEN also has a role in the regulation of DNA damage repair of NER and DSB. In the course of NER, Ming et al. showed that downregulation of PTEN expression in the epidermis of mice predisposes them to skin tumorigenesis upon UV irradiation [52]. One hypothesis involves the reduction of xeroderma pigmentosum C (XPC) expression upon PTEN downregulation via the Akt/p38 pathway. XPC is a DNA damage recognition protein in the nucleotide excision repair pathway required for the identification of the UV induced DNA damages. The decrease of XPC thus allows the accumulation of CPDs and 6-4PPs. In DSB, PTEN downregulation leads to decreased Rad51 expression [53].

4.3 PTCH

PTCH gene encodes for a membrane receptor in the sonic hedgehog (Shh) pathway. The latter plays an important role in regeneration and re-differentiation of adult tissue. The canonical signaling in the Shh pathway starts with the biding of the Shh ligand to the transmembrane receptor

Patched (PTCH) inactivating it. This will relieve the PTCH-mediated inhibition of smoothened (SMO). SMO will further activate the downstream signaling to result in the translocation of the Glioma zinc finger transcriptions factors (Gli) to the nucleus to initiate transcription [54]. Some of the downstream expressed genes are involved in tumorigenesis and they include BCL2 for apoptosis resistance, SNAIL for epithelial-mesenchymal transition, Wnt2 for cell stemness, and TGFβ for immune suppression among others [55]. PTCH mutations bear the UV signature C→T or CC→TT transitions. The latter allows the inactivation of PTCH and its role in the inhibition of smoothened (SMO) expression. Therefore, SMO can then mediate the activation of Gli1 transcriptional factor resulting in tumor formation [56] (figure 7). Such deficiency was recorded in 85% of BCC [57]. Gorlin syndrome is characterized by an increased predisposition to basal cell carcinomas due to a mutation in PTCH1 tumor suppressor gene. Charazac et al. reported that fibroblasts from Gorlin patients exhibit high radio-sensitivity. These cells appeared to manifest low expression and activity of base excision repair pathway proteins thus linking Gorlin clinical manifestations to possible defects in DNA damage response or repair capacity [58].

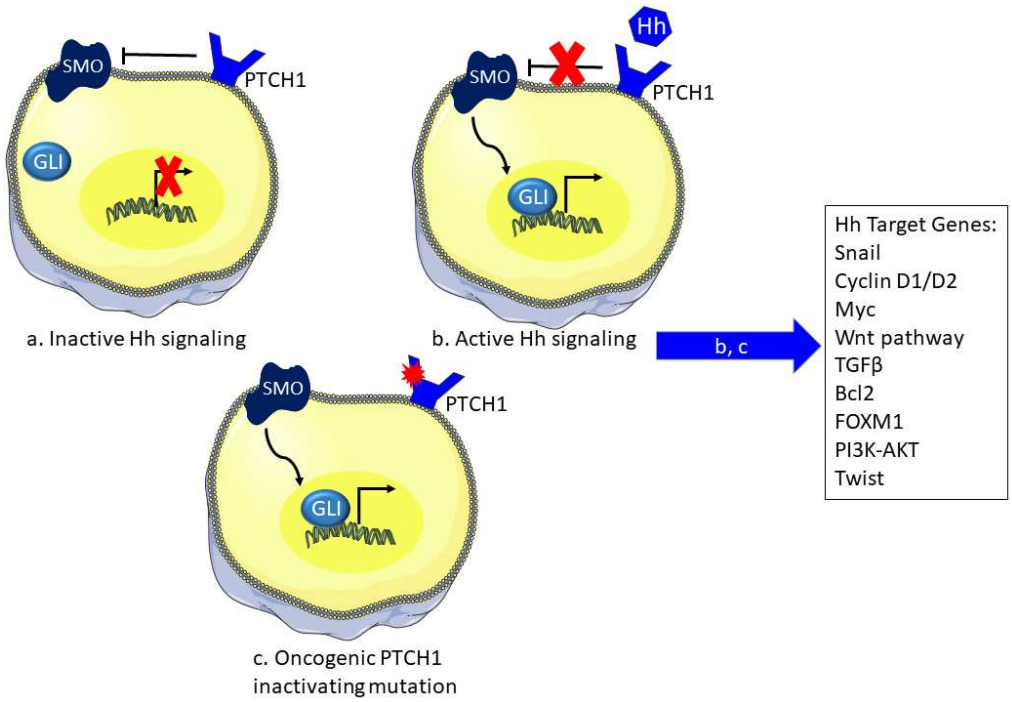

Figure 7 The sonic hedgehog pathway and the effect of UV irradiation.

The SHH pathway controls the expression of several downstream effectors. a) In the inactive state, PTCH receptor inhibits SMO and thus preventing the translocation of Gli to the nucleus blocking transcription of underlying genes. b) However, in the presence of the Hh ligand the PTCH receptor becomes inactive losing its inhibitory effect on SMO favoring the activity of Gli in transcription. c) Inactivating mutation of PTCH induced by UV irradiation annuls SMO inhibition and activates the pathway to express downstream genes via Gli. SHH: sonic hedgehog, PTCH: patched receptor, SMO: smoothened, Gli: glioma transcription factor

4.4 NRAS AND BRAF

NRAS and BRAF play a major role in the mitogen-activated protein kinase (MAPK) pathway. The binding of growth factors to their respective tyrosine kinase receptor activates this pathway. RAS GTPase then conveys the intracellular signaling. Active Ras bound to GTP allows the recruitment of effectors including the RAF family of serine/threonine kinases that regulate cell proliferation. RAF further on activates MAP kinase kinase (MEK1/2) and then MAP kinase (ERK1/2). The latter promotes cell proliferation [59]. Activating mutations in these genes are mainly found in melanoma. Only a single mutation in either gene can exist at a time [60]. Mutations in either are of the activating type enhancing the MAPK signaling. BRAF most frequent mutation is a T→A transversion.[61]. NRAS most frequent mutation is either a C→A transversion or A→G transitions in sun-exposed areas [62]. These mutations are not exactly a C→T UV signature mutation, however, their comparison with the mutagenic profile in bacteria reveals that they may be derived from UVA mediated oxidative DNA damage [63].

4.5 RAC1 AND PREX2

PREX2 is a GTP/GDP exchange factor that can promote tumorigenesis via the inhibition of PTEN, a known regulator of the PI3K signaling pathway [64]. PREX2 also mediates the activation of the GTPase RAC involved in cell migration [65]. Large scale cancer genomic profiling revealed the involvement of mutations in these two genes with melanoma oncogenesis [66, 67]. These genes interact to promote the PI3K/Akt [65, 68]. Mutations in the RAC1 gene possess the typical UV signature C→T transition mutation in sun-exposed areas that allows the activation of RAC1 and the underlying signaling pathways [69]. PREX2 mutations are also mainly found in sun-exposed areas [67] where it inhibits PTEN annulling its effect in the inhibition of the PI3K pathway.

Although other genes have been recorded to be involved in skin carcinogenesis, they do not possess a UV signature mutation profile signifying a different origin other than UV as their carcinogenesis initiator. The latter includes mutations in the cell cycle genes found in both basal and squamous cell carcinoma [70]. In addition, loss of $p16^{INK4A}$ was also identified in melanoma leading to the enhancement of CDK4 activity promoting proliferation [71].

5. UV-IRRADIATION INDUCED IMMUNOSUPPRESSION

Genetic mutations alone do not represent the only initiators of skin tumorigenesis. An intricate signaling network interplays with such mutations leading ultimately to tumor generation one of which is UV irradiation-induced immune suppression. The first form of suppression is mediated via the defective antigen presentation activity of Langerhans cells. UVR leads to the elevation of IL6, IL10 and TNFα levels thus inhibiting the skin immune response by downregulating Langerhans cells activity [72]. Moreover, UV irradiation was found to have a negative effect on the number of natural killer cells in a UV dose-dependent manner. The latter cells are implicated in anti-tumor and anti-viral infection [73]. UVB exposure also increases the expression of

cyclooxygenase (COX-2) enzyme that catalyzes the first step for the conversion of arachidonic acid to active prostaglandin involved in the inflammatory response. COX-2 is implicated in the development of several types of tumors [74]. Finally, one last activator of immune suppression is urocanic acid (UCA), a histamine deamination product highly available in the skin [75]. The inhibition of UCA with an antibody against it enabled the delay of tumor formation in irradiated skin [76].

Despite the filtration of the harmful UVC radiation by the ozone layer, the two remaining solar ultraviolet rays reaching the earth's surface are proving to be hazardous. UVB radiation can directly damage the DNA of exposed cells while UVA can indirectly create such damage via the generation of reactive oxygen species. After such induced stress, the cells that fail to repair the damage can either be committed to apoptosis or persist where their damaged DNA progresses to the UV signature C→T transition. These mutations have been identified in several genes correlated with skin carcinogenesis signifying a link between UV exposure and tumorigenesis. Moreover, UV irradiation activates several downstream signaling pathways including the Akt and MAPK pathways implicated in the regulation of cell proliferation, apoptosis and tumor promotion among many others. Finally, an additional instigator of tumor formation can be the UV-induced immune suppression where the inhibition of the action of some immune cells allows the cells' harboring damage and tumors to escape from the surveillance of the body. For that, possessing an active repair system is essential to eliminate such dangerous UV-induced lesions where any defect will give rise to diseases like Xeroderma Pigmenstosum and others with increased risks of skin cancers and neurodegeneration.

CHAPTER 2. NUCLEOTIDE EXCISION REPAIR

DNA damaging agents result in the formation of a wide variety of DNA lesions. Over the past years, several repair mechanisms specific to each lesion have been discovered. One of these mechanisms is the nucleotide excision repair (NER) required for the removal of bulky adducts and dimers. Cyclobutane pyrimidine dimers (CPD), and pyrimidine-pyrimidone photoproducts (6-4PP), are the main UV photoproducts formed following exposure to UV radiation [77]. NER starts with the recognition of the lesion and then the incision 5' and 3' to the damage to allow its removal creating a gap. This gap will be filled by synthesizing damage free DNA by polymerases to finally be ligated sealing the nick [78]. NER constitutes two sub-pathways: global genome NER (GG-NER) that occurs all over the genome and transcription-coupled NER (TC-NER) that mends lesions in actively transcribed genes where such damages can block the progression of RNA polymerases [79]. These pathways differ mainly in the recognition step. Deficiencies in TC-NER sub-pathway underlies CS and UVsS, while patients with XP, TTD, XP-CS, XP-TTD and COFS are lacking proficiency in either GG-NER or both of the sub-pathways. NER pathway can be modulated by various signaling pathways, biological or chemical compounds. The modulation of this pathway can pave away to the possible regulation of the NER pathway in XP-C patients.

1. REPAIR SUB-PATHWAYS

1.1. GLOBAL GENOME NUCLEOTIDE EXCISION REPAIR (GG-NER)

In GG-NER, helix-distorting lesions are initially recognized by a complex that includes XPC, Rad 23 homolog B (RAD23B) and centrin 2 (CETN2) proteins (figure 8). RAD23B stabilizes XPC while CETN2 enhances XPC damage recognition [80]. Recent studies indicated that DNA lesions (such as CPDs) that induce very mild disruptions in the DNA double helix are poor XPC substrates. In this case, UV-damaged DNA-binding protein (UV-DDB) complex, also known as the DDB1–DDB2 heterodimer, initially recognizes the lesions and then creates a kink that will be recognized by XPC [81]. It is noteworthy to state that XPC binds to the strand opposite of the adduct [78]. DDB2-DDB1-CUL4-RBX1 E3 ligase forms a $CRL4^{DDB2}$ ubiquitin ligase complex that ubiquitylates XPC, DDB2, and histones [82]. XPC poly-ubiquitination increases its affinity to DNA rather than its degradation [80]. The next step starts with the recruitment of the pre-incision TFIIH complex that encompasses ATPase/helicase XPD and XPB. These proteins unwind the DNA around the lesion, XPD at the 5' and XPB at 3' of the lesion, creating a 20-30 nucleotide bubble. This complex allows the recruitment of XPA, XPG and replication protein A (RPA1) that bind to single-stranded DNA of the bubble [81]. XPA binds at 5' of the bubble and interacts with the pre-incision complex. This interaction allows the release of TFIIH component CDK activating kinase (CDK7) to facilitate both the recruitment of XPF-ERCC1 that binds to XPA and the release of the XPC-RAD23B complex. XPF-ERCC1endonuclease mediates the cleavage at 5' of the lesion. Pol ε/δ/κ-PCNA-RFC-RPA1, the DNA replicative machinery, can then synthesize the damage free strand while displacing the damaged one and TFIIH. Afterwards, the incision at the 3' end will be catalyzed by XPG. Finally, the generated nick will be sealed by DNA ligase. It should be emphasized that replicating cells utilize polymerase epsilon (Pol ε) and Ligase I while non-replicating cells use polymerase delta/kappa (Pol δ/κ) and Ligase III α and X ray repair cross-complementing protein 1 (XRCC1) [83] (figure 8).

1.2. TRANSCRIPTION COUPLED NUCLEOTIDE EXCISION REPAIR (TC-NER)

TC-NER pathway is triggered once RNA polymerase progression in actively transcribed genes is blocked due to the presence of bulky adducts (figure 8). This allows the recruitment of Cockayne syndrome group B protein (CSB), also called excision repair cross-complementing protein 6 (ERCC6), which binds the polymerase and changes the DNA conformation [84]. CSB recruits CSA, EP300, and NER factors excluding XPC and UV-DDB [81]. The CSA-DDB1-CUL4-RBX1 E3 ligase form $CRL4^{CSA}$ ubiquitin ligase complex that ubiquitylates CSB mediating its degradation. However, UV-stimulated scaffold protein A (UVSSA) interacts with RNAPII and delivers the deubiquitinating enzyme ubiquitin specific processing protease 7 (USP7) that inhibits the CSA-dependent CSB degradation [82]. In addition, CSA allows the recruitment of the nucleosome remodeling factors HMGN1, XAB2 and TCEA1 [85]. The remaining steps are similar to those of GG-NER involving the recruitment of TFIIH, incision, and synthesis (figure 8).

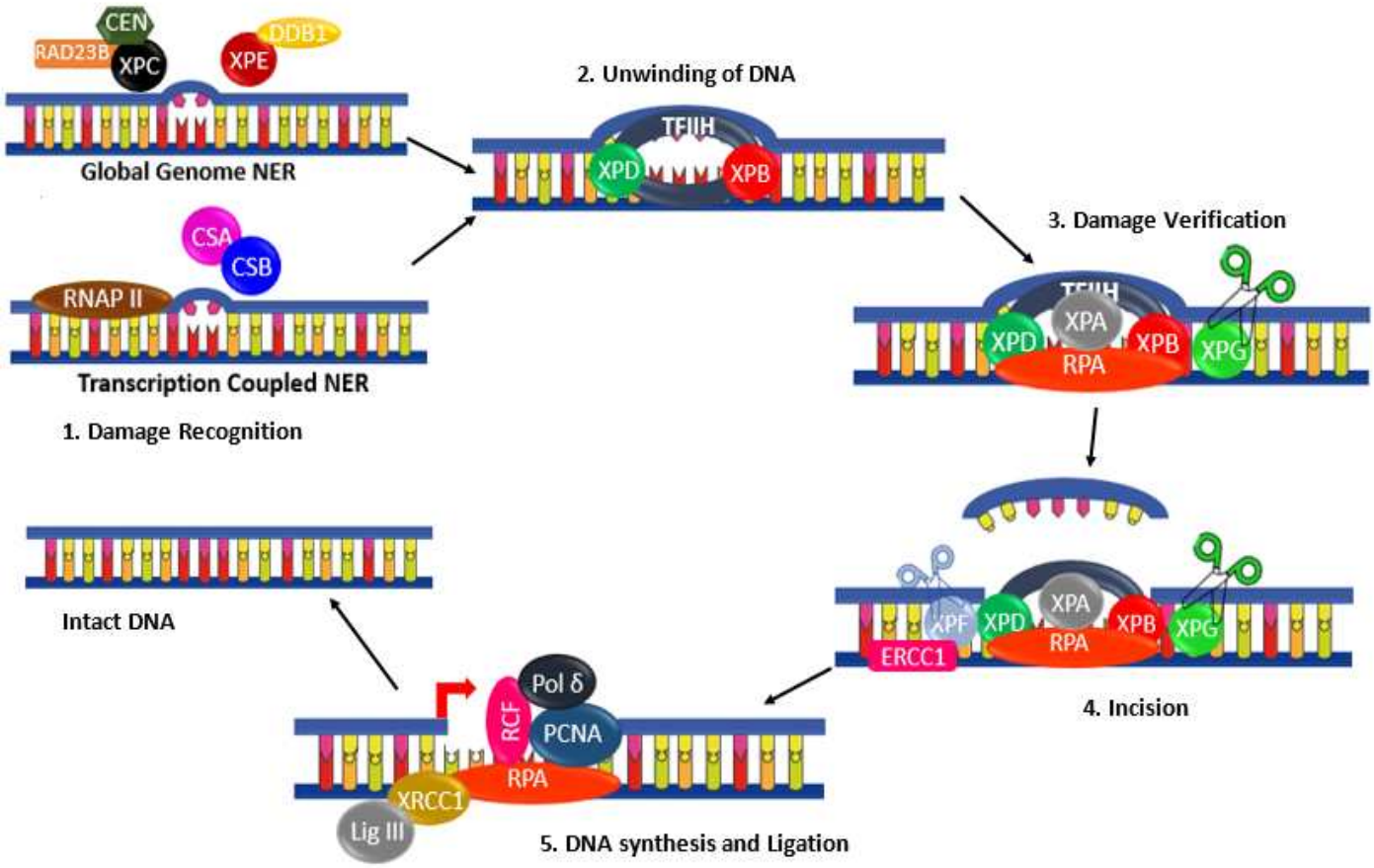

Figure 8 Schematic representation of Nucleotide excision repair

Recognition of DNA damage differs between Transcription Coupled NER (TC-NER) and Global Genome NER (GG-NER). (1) Damage Recognition. In TC-NER the stalled RNA polymerase in transcriptionally active genes favors the recruitment of cockayne syndrome proteins A and B (CSA & CSB). In GG-NER the damage is recognized by XPC and its partners RAD23B (Rad 23 homologue B) and CEN (centrin 2) if it is a helix distorting lesion. A mild distorting lesion in this sub-pathway is recognized by XPE and DDB1 (DNA damage binding protein 1). The following steps are the same for both GG-NER and TC-NER. (2) DNA unwinding. TFIIH is recruited and it contains XPB and XPD helicases that catalyze the opening of the DNA. (3) Damage Verification. XPA, XPG and RPA1 are recruited. XPA verifies the DNA damage while RPA1 binds to the single stranded DNA. (4) Incision. XPF that is in a complex with ERCC1 is recruited. Both XPF and XPG are nucleases that catalyze the incision of 5' and 3' of the damage respectively. (5) DNA synthesis and Ligation. The missing DNA sequence is synthesized by polymerase delta with the assistance of PCNA, RCF and RPA1. DNA ligase 3 interacting with XRCC1 ligates the produced fragment leading to the formation of intact DNA. It should be noted that XPF-ERCC1 mediates the incision at the 5' end then the polymerase with PCNA, RCF and PCNA will aid in displacing the damaged strand to be finally followed by the incision at the 3' end by XPG. Abbreviation: XPA-XPG: Xeroderma Pigmentosum protein A-G; NER: Nucleotide Excision Repair; TC-NER: Transcription Coupled Nucleotide Excision Repair; GG-NER: Global Genome Nucleotide Excision Repair, CSA and CSB: Cockayne Syndrome Protein A and B; DDB1: DNA Damage Binding protein 1; RAD23B: RAD 23 homologue B; Cen: Centrin 2; TFIIH: Transcription Factor II H; RPA1: Replication Protein A; ERCC1: Excision Repair Cross Complementation group 1; PCNA: Proliferating Cell Nuclear Antigen; RCF: Replication Factor C; Polδ: Polymerase delta; LIG3: DNA ligase III; XRCC1: X ray Repair Cross Complementing protein 1.

2. TRANSCRIPTIONAL AND POSTTRANSLATIONAL REGULATION OF NER

2.1. TRANSCRIPTIONAL REGULATION

The transcription of the different NER factors is under tight balance due to the effects of both transcription factors and their repressors. The rate-limiting factor of NER is XPA that verifies the damage and leads to the recruitment of the incision proteins. The expression of XPA is controlled by the circadian clock which is higher in the daytime than at night with Clock Circadian Regulator-aryl hydrocarbon receptor nuclear translocator like protein (Clock-Bmal1) transcriptional activator and a cryptochrome circadian regulator-period circadian regulator (CRY-PER) transcriptional repressor to enable repair in UV exposed cells [86]. Its expression is also regulated by other transcription factors including hypoxia-inducible factor 1 (HIF1A) that upregulates XPA expression and high mobility group protein A1 (HMGA1) that down-regulates XPA expression [87, 88].

The ATP-dependent helicases XPB and XPD favor the opening of the double strand around the site of damage. Specificity protein 1 (SP1) binds to XPB promoter and activates its expression while hepatitis B virus x (HBx) inhibits it [89, 90]. On the other hand, XPD expression is promoted by HIF1α and insulin while being repressed by HBx as well [91, 92]. However, long-term exposure to glucose at high concentrations can mitigate the insulin-dependent increase in XPD mRNA [93].

The expression of the GG-NER sensors, XPC and XPE, is regulated in a TP53 dependent manner [94]. Overexpression is also mediated by transactivation isoform of p63 gamma (TP63) and breast cancer 1 (BRCA1) [95, 96]. Moreover, XPC expression is up-regulated by SP1, Sirtuin 1 (SIRT1), ARF, MC1R, and E-cadherin but down-regulated by HIF1α and E2F4-p130. SP1's binding sequence overlaps that of HRE at the XPC promoter. This implies that competition exists between HIF1α and SP1 in the binding to XPC promoter. HIF1α binds to the promoter in normal condition. Upon the exposure to UV radiation, HIF1α is downregulated mediating the SP1 induced increase in XPC expression [91, 92] In line with negative regulation of NER pathway by HIF1A, it has been shown that decreased HIF1A expression in the mouse epidermis is associated with an increase in the removal rate of UVB irradiation-induced DNA damage via direct up-regulation of several components of the DNA repair machinery, such as XPC and XPB. This upregulation of NER efficiency led to decreased UVB-induced carcinogenesis in HIF1A ablated mice [97]On the other hand, SIRT1 stimulates the expression of XPC by preventing the nuclear localization of the E2F4-p130 transcriptional repressor. The accumulation of the latter is mediated by AKT1 activation resulting from SITR1 inhibition. SIRT1 can interact with p130 and deacetylate it [98, 99]. The role of SIRT1 in enhancing XPC expression was also reported by Ming et al. where the knockdown of SIRT1 by siRNA not only decreased XPC expression but also inhibited CPD repair [100].

Finally, the expression of the incision enzymes, XPF and XPG, is up-regulated by c-Fos/AP-1 [101]. In addition, CCAAT/enhancer-binding protein gamma (CEBPG) whose expression is modulated by E2F1 and YY1 favors the overexpression of XPG [102].

2.2. POSTTRANSLATIONAL REGULATION

2.2.1. UBIQUITINATION AND SUMOYLATION

$CRL4^{DDB2}$ can ubiquitinate histones, XPC and DDB2. Ubiquitination of DDB2 leads to its degradation that can be counteracted by the deubiquitinating enzyme ubiquitin-specific processing protease 24 (USP24) [103]. DDB2 ubiquitination and degradation require the activity of the mitogen-activated protein kinase MAPK14 that mediates the phosphorylation at serine moieties [104]. On the other hand, XPC ubiquitination enhances its DNA binding ability rather than triggering its degradation [105]. XPC SUMOylation can either promote or hinder its activity depending on the targeted residues while SUMOylation of lysine 655 favors the UV-induced XPC degradation, SUMOylation of Lysine residues 81, 89, and 183 of XPC stimulates NER [106].

CSA-dependent ubiquitination leads to the degradation of CSB which could be prevented by the action of the UV-sensitive syndrome A protein (UVSSA) and its recruitment of USP7 that mediates CSB deubiquitination and phosphoinositide-dependent [107]. SUMOylation of CSB enhances the recruitment of CSA [108]. Moreover, XPA ubiquitination by HERC2 (E3 ubiquitin protein ligase) leads to its degradation [109]. Finally, XPF-ERCC1 is deubiquitinated by USP45 that favors its recruitment to the site of damage [110].

In conclusion, the enhancement of NER can be mediated by the ubiquitination of XPC, and SUMOylation of CSB and XPC but at particular residues. On the other hand, the ubiquitination of DDB2, CSB or even XPA leads to their degradation and the impairment of NER rendering the ubiquitination enzymes targets for therapy (figure 9).

2.2.2. PHOSPHORYLATION, ACETYLATION, PARYLATION

Phosphorylation of XPA by Ataxia Telangiectasia and Rad3-related protein (ATR), involved in the damage recognition of single-strand breaks, stimulates NER by blocking the HERC2-mediated ubiquitination. However, the dephosphorylation of XPA by wild-type TP53 induced phosphatase 1 (PPM1D (WIP1)) reduces NER activity [111, 112], therefore, repressing NER by inactivating XPA and XPC. The phosphorylation of XPB does not interfere with the helicase activity of TFIIH but inhibits the XPF-ERCC1 5' end incision. XPC phosphorylation at serine 94 is mediated by casein kinase 2 (CSNK2A1) that promotes NER by allowing the recruitment of ubiquitinated XPC and other NER factors to the chromatin [113].

XPA activity is also regulated by acetylation favoring a decrease in NER activity while deacetylation enhances it by enabling the interaction with replication protein RPA132. On the other hand, the acetylation of XPG by EP300 acetyltransferase allows its accumulation at sites of damage [91].

Finally, PARylation, mediated by PARP1, regulates some of the NER proteins. First, DDB2 PARylation inhibits its ubiquitination and favors PARP1 and XPC interaction and the latter's

recruitment to DNA lesions [114]. CSB is another NER protein PARylated by PARP1 leading to inhibition of its ATP hydrolysis activity [115].

Therefore, NER enhancement in this case can be mediated by phosphorylating XPA and XPC, deacetylating XPG, and PARylating XPC. NER inhibition, however, necessitates the phosphorylation of XPB, acetylation of XPA, and PARylation of CSB (figure 9).

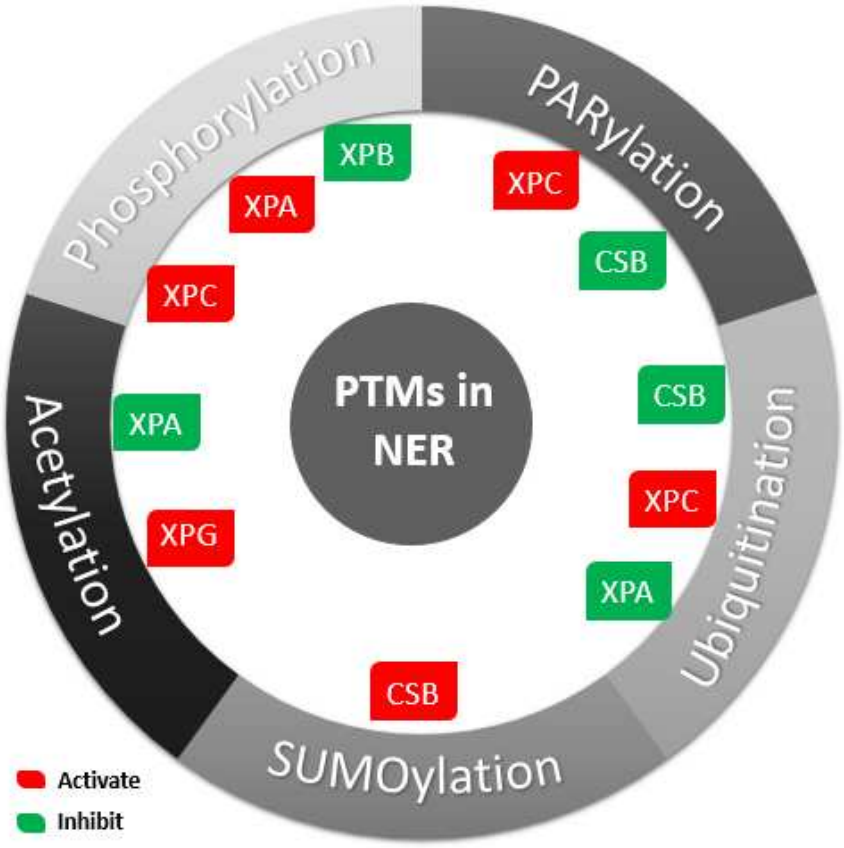

Figure 9 Post translational modifications of NER factors.

Several NER factors including XPC.XPB.XPG.XPA and CSB are subjected to different forms of posttranslational modifications that can either activate them favoring NER enhancement or the direct opposite via their inhibition.

3. MODULATION OF NER PATHWAY

NER function can be regulated by distinct signaling pathways. Moreover, this repair pathway could be modulated by the cellular redox status as it has been shown that it is inhibited by oxidative stress [116]. Moreover, molecular components such as miRNAs, being able to regulate the expression of several elements in the NER pathway [117], can affect the overall activity of this repair mechanism (figure 13). These data suggest that NER activity can be manipulated to

potentiate the repair response, thus, preventing the accumulation of DNA damage and photocarcinogenesis.

3.1. SIGNALING PATHWAYS REGULATING NER FUNCTION

3.1.1. NFE2L2 (NRF2) SIGNALING PATHWAY

Oxidative stress products, including peroxidized lipids, inhibit NER [118]. Trans-4-hydroxy-2-nonenal (4-HNE), one of the lipid peroxidation products, inhibits NER capacity in host cell reactivation framework [119]. On the other hand, the inflammation derived monochloramine (NH2CL) inhibits NER via the inhibition of TP53 phosphorylation [120]. Langie et al. showed that the exposure of epithelial cells to hydrogen peroxide decreases the NER capacity to less than 50% [116]. Therefore, since NER is inhibited by oxidative stress, antioxidants can help prevent such inhibition. One of such mechanisms can be achieved by Nrf2, a transcription factor enabling the expression of antioxidant genes. NFE2L2 has a basic leucine zipper motif (bZip), allowing it to interact with other bZip containing proteins, and another basic region that binds DNA by hydrogen bonds to favor transcription [121]. NFE2L2 activity is inhibited once bound to Kelch-like ECH-associated protein 1 (KEAP1) that triggers its ubiquitination by the ubiquitin ligase Cul 3. Binding of 4 ubiquitin residues leads to the degradation of NFE2L2 [122]. In oxidative stress conditions, the cysteine residues of KEAP1 are oxidized leading to a change in KEAP1 conformation and the ultimate release of NFE2L2 from the KEAP1-Cul 3 complex. The free NFE2L2 will be translocated to the nucleus where it forms a complex with MAF transcription factors and binds to DNA at an antioxidant responsive element (ARE) [123]. This binding allows the transcription of antioxidant enzymes including catalase, Glutathione S-transferase (GST), glutathione reductase (GR), superoxide dismutase, etc... [124-126]. PARP1 (poly (ADP) ribose polymerase) enhances NFE2L2 transcriptional activity. It forms a complex with antioxidant response element (ARE) in NFE2L2 target genes enhancing the latter's activity without physically binding or even populating it. However, PARP1 is said to interact with MAF proteins and ARE to enhance NFE2L2 interaction with ARE. For that, PARP1 acts as transcriptional co-activator [127]. Other co-activators include CBP/EP300 that binds and acetylates NFE2L2 at multiple lysines promoting NFE2L2 specific binding [128]. It is noteworthy that Nrf2 can be inhibited by BACH1 that competes with it for the binding to ARE. The phosphorylation of BACH1 by MAPK1 abolishes this role [4].

Notably, the NFE2L2 pathway is involved in the protection of keratinocytes, melanocytes and fibroblasts against the harmful effects of UV radiation.

I. KERATINOCYTES

Keratinocytes Growth Factor (KGF) binds to its receptors to increase the proliferation of keratinocytes and elevate their NFE2L2 activity. This activity is essential against ROS generated during aerobic respiration or during the protection of the skin against pathogens [129, 130]. In addition, coal tar activates the aryl hydrocarbon receptor (AHR) that binds to NFE2L2 gene and increases its expression [131]. Extracellular activators of NFE2L2 in keratinocytes are numerous. For instance arsenic, a potent carcinogen, that increases ROS levels enabling an increase in NFE2L2 activity [132]. In addition, Xenobiotics like formaldehyde, eugenol or dinitrochlorobenzene bind covalently to cysteine of KEAP1 enabling NFE2L2 release and activation [133]. This release is also mediated by either plant sterols that activate IKB while IKKβ

will bind to KEAP1 preventing its interaction with NFE2L2 [134] or by carbonitriles that nitrosylate KEAP1 cysteine [135]. Other activators include flavonoids that protect cells from UV radiation [136]. Sulforaphane (SFN) found in broccoli and Brussels sprouts reduce GSH levels altering KEAP1 conformation releasing NFE2L2 and enhancing the expression of antioxidant enzymes [137]. Furthermore, D3T increases the mRNA levels and elevates phosphorylation of NFE2L2 by MAPK1 kinase [138]. Finally, ketoconazole activates AHR to increase NFE2L2 transcriptional activity [139] (figure 10).

However, it should be noted that NFE2L2 overactivation leads to abnormal proliferation of keratinocytes inducing hyperkeratosis due to the expression of various downstream target genes. Among those genes is *EPIGEN*, encoding a growth factor, which causes the enlargement of the sebaceous gland and cyst formation all via EGFR signaling [140]. Small proline-rich protein 2d (*SPRR2D*), another NFE2L2 target gene, weakens the epidermal barrier leading to inflammation and enhances keratinocyte proliferation. Finally, Secretory leukocyte peptidase inhibitor (SLPI) mediates hyperkeratosis [3].

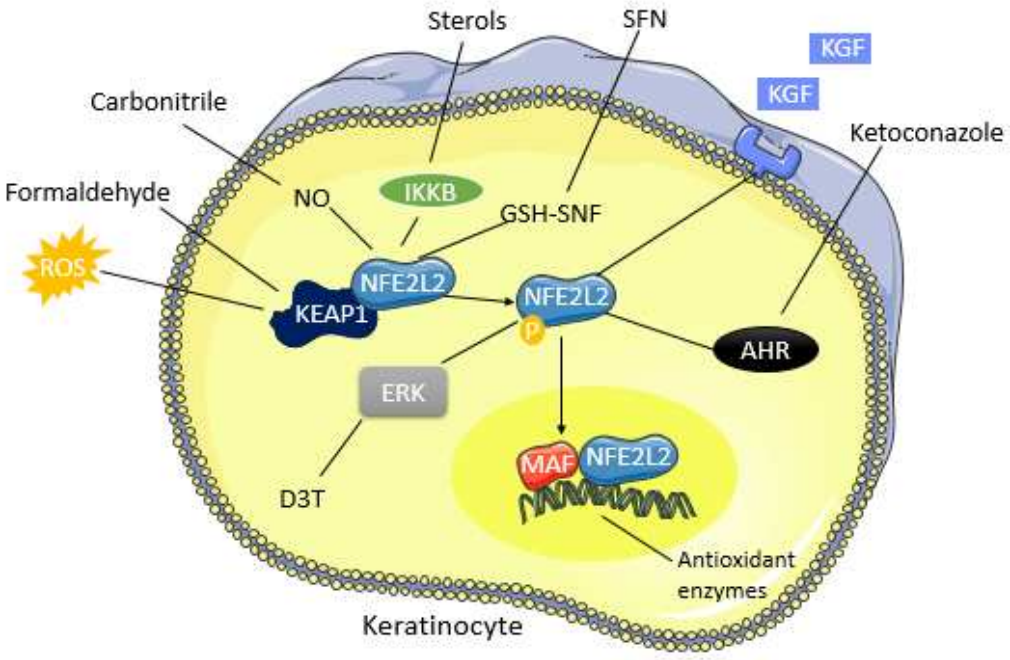

Figure 10 Modulation of the NFE2L2 pathway in Keratinocytes

Several compounds can potentiate the NFE2L2 response in Keratinocytes leading to enhanced expression of antioxidant enzymes. The binding of Keratinocytes Growth Factor (KGF) to their receptors, activation of MAPK1 by D3T and the activation of AHR by Ketoconazole all enhance NFE2L2 transcriptional activity. On the other hand, ROS, formaldehyde, carbonitriles, sterols and sulforaphane (SFN) lead to the release of NFE2L2 from KEAP1 mediating its activity each in its unique mechanism. Activated NFE2L2 will be translocated to the nucleus to interact with MAF and favour the expression of antioxidant enzymes.

II. MELANOCYTES

Melanocytes produce melanin in a process termed melanogenesis which requires tyrosinases possessing both a diphenylene activity leading to H_2O_2 generation and a catalase activity for H_2O_2 decomposition. NFE2L2 is required to protect these cells against the generated ROS during melanin synthesis [141]. NFE2L2 activation can be mediated by the binding of melanotropin (αMSH) to MC1R to form a complex that initiates the transcription of ARE-containing genes [142]. Stress that leads to unbalanced redox status sends a signal to IRES (internal ribosome entry sites) in NFE2L2 mRNA increasing its synthesis [143]. In addition, ERK1/2 activation by RAS/RAF/Mek/MAPK1 pathway favours the phosphorylation of NFE2L2 [144]. Extracellular activators of NFE2L2 include afamelanotide and curcumin even though the latter increases apoptosis of keratinocytes [124, 145] (figure 11).

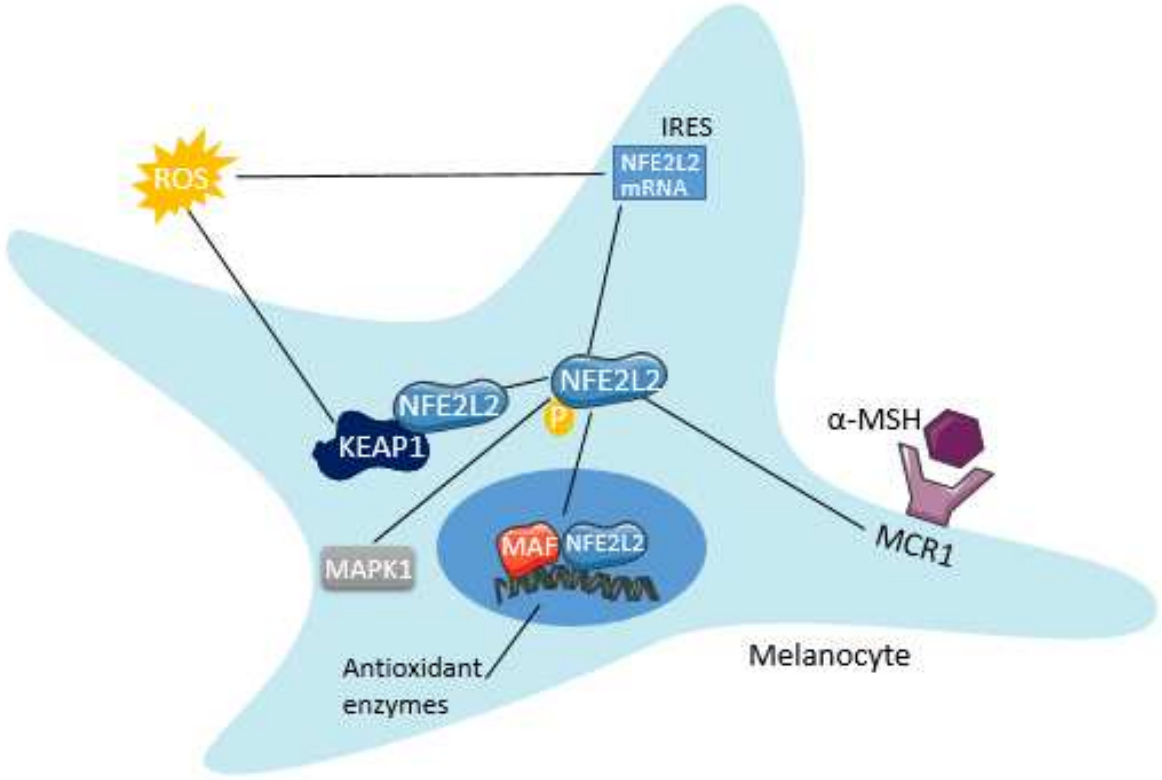

Figure 11 Modulation of the NFE2L2 pathway in Melanocytes

The expression of antioxidant enzymes in melanocytes is mediated by the NFE2L2 pathway whose activity can be enhanced due to the effects of ROS that mediated the release of NFE2L2 from its inhibitor KEAP1 or through the enhancement of its mRNA expression. Moreover, activated MAPK1 or even α-MSH binding to its receptor MCR1 increases NFE2L2 activity where it is translocated to the nucleus to interact with MAF and express the enzymes. It should be noted that the activation of NFE2L2 necessitates its phosphorylation mainly by MAPK1.

Hydrogen peroxide inducesNFE2L2 activation as well as the expression of antioxidants and anti-apoptotic proteins [146]. Eotaxin chemokine also mediates an increase in NFE2L2 expression or activation. Together with flavone that activates MAPK1 mediating NFE2L2's phosphorylation [147, 148]. Moreover, curcumin disrupts TGFβ signaling by the phosphorylation of SMAD2 and increases the TGF induced factor, a TGFβ inhibitor, leading to NFE2L2 activation and the ultimate decrease of ROS [149]. On the other hand, thioredoxin inhibits NFE2L2 due to its free thiol that prevents KEAP1 oxidation [150]. The caveolae formed by dent fibroblast membrane can favor NFE2L2 degradation. Finally, diethyl malate increases the expression of Mrp1 that removes glutathione conjugates with harmful substances including drugs only in NFE2L2 positive cells [151] (figure 12).

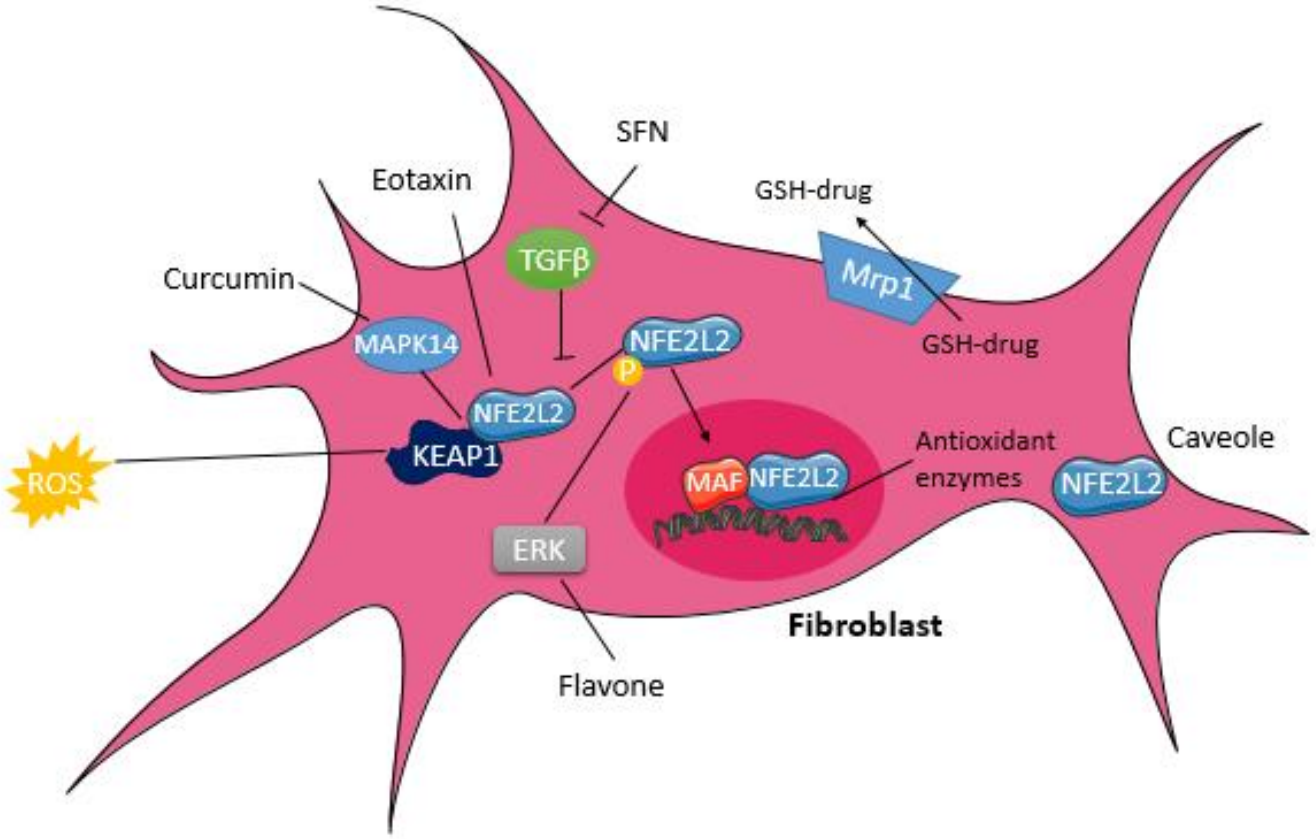

Figure 12 Modulation of the NFE2L2 pathway in Fibroblasts

The NFE2L2 pathway in fibroblasts can be either activated or inhibited depending on the administered compound. ROS, Eotaxin and curcumin mediate the release of NFE2L2 from the inhibitor KEAP1. Flavone via the activation of MAPK1 facilitates the phosphorylation of NFE2L2. In addition, Mrp1 removes glutathione conjugates to drugs in an NFE2L2 dependent manner. However, TGFB signalling inhibits NFE2L2 activity which can be counteracted by the administration of SFN. Finally, the fibroblast caveolae can also inhibit NFE2L2 function preventing the expression of antioxidant enzymes that require the translocation of an NFE2L2 transcription factor to the nucleus and its interaction with MAF.

NRF1was also linked to the enhancement of NER. Keratinocytes with Nrf1 loss are sensitive to killing by UVB exposure. Analysis of DNA damage repair in the cell population surviving UVB exposure showed a decrease in CPD repair by slot blot assay. Han et al. linked the latter to a decrease in XPC expression as it was reversed by the overexpression of XPC in Nrf1 inhibited cells enabling the repair. It is not through the inhibition of XPC repressors that Nrf1 mediated such function but rather due to the maintenance of GSH levels [152]. Therefore, the stimulation of NRF pathway by these various compounds should be further explored as a method for NER enhancement.

3.1.2. AHR PATHWAY

The Aryl Hydrocarbon receptor (AHR) is found in the cytosol and it senses various chemicals including flavonoids and dioxin. The binding of ligands to the AHR induces a conformational change favoring its translocation to the nucleus. There it will bind to the xenobiotic response element (XRE) of genes to increase their transcription. One of these target genes is cytochrome P450 family enzyme CYP1A1. The latter allows the detoxification of pollutants and generates ROS and mutagenic metabolites [153]. This receptor was shown to decrease the clearance of CPD in the course of global genome repair. AHR compromised cells manifested elevated CPD repair in a CDKN1B dependent manner as the latter was increased in AHR silenced cells and enhanced NER [154].

However, other studies have shown that some ligands of AHR including ketoconazole and quercetin do not lead to ROS generation but induce an antioxidant response due to the activation of NFE2L2-NQO1 [155].

Cynaropicrin (Cyn), a sesquiterpene lactone found in artichoke, is an antioxidant that activates the AHR-NFE2L2-NQO1 pathway. Cyn favors the activation and translocation of AHR to the nucleus which in turn mediates the nuclear translocation of NFE2L2 and the increase in NFE2L2 and NQO1 (NAD (P) H- Quinone oxidoreductase 1) mRNA levels. In addition, it decreased the levels of ROS and pro-inflammatory cytokines IL6 and tumour necrosis factor α (TNFα) [156]. Other phytochemicals that operate on the AHR-NFE2L2-NQO1 pathway include the labasia pumila that decreases the UVB-induced TNFα production [157] which is also reduced by curcumin that reduces IL6 production as well [158]. Finally, phenols from lonicera caverula and Vaccinium myrtillus fruit protect keratinocytes against UVB-induced ROS generation and IL 6 production [159].

3.1.3. PI3K/AKT1 PATHWAY

PI3K/AKT1 pathway is induced following tyrosine kinase receptor mediated activation of PI3K. The latter converts PIP2 (phosphatidylinositol biphosphate) into PIP3 allowing the recruitment of both PDK1 (phosphoinositide dependent kinase) and AKT1 allowing the phosphorylation of its threonine 308. In addition, the Target of Rapamycin Complex 2, MTORC2, phosphorylates serine 473 of AKT1. All that leads to AKT1 activation that can be counteracted by PTEN phosphatase [2]. The involvement of this pathway in the modulation of NER function is still controversial. AKT activates MDM2 that favors the degradation of TP53 [160]. Therefore, AKT1 inhibits NER due to the decrease in XPC and DDB2-TP53 dependent transcription [161]. Another mode of inhibition

is mediated by the AKT1-dependent localization of XPC transcriptional repressors (P130). This is reversed by the action of deacetylase and longevity factor (SIRT1) that deacetylates PTEN to inhibit AKT1. In addition, the abundance of lysine acetylation sites in GG-NER proteins DDB1, DDB2, CUL4A, and RAD23A suggest that they can be possibly regulated by deacytelases including SIRT1 [99]. Moreover, AKT1 is known for its contribution in cell cycle progression as it prevents the translocation of CDKN1A and CDKN1B cell cycle inhibitors, stabilizes cyclin and increase metabolic activity by the phosphorylation and inhibition of GSK [28, 29, 162] Further, it activates nuclear factor kappa B (NFKβ), IAPS, CASP8 and FADD like apoptosis regulator (FLIP) but inactivates the pro-apoptotic protein Bad and caspase 9. Nonetheless, AMP activated protein kinase (AMPK) can counteract the AKT1 mediated MTOR activation during UV radiation [2]. Finally, AKT1 can enhance TC-NER via the phosphorylation of EP300 that relaxes the chromatin to allow the recruitment of repair factors [163].

3.1.4. MAPK PATHWAY

MAPK pathway starts with RAS-GTP that allows the stimulation of MAPK-KK (RAF) activating MAPK-K (MEK) via phosphorylation that further actuates MAPK (ERK1/2, JNK, or MAPK14) by dual phosphorylation of tyrosine and threonine residues. MAPK1 controls differentiation and proliferation while MAPK14 and JNK regulate apoptosis, cell cycle arrest, invasion and others [164]. It has been reported that ERK1/2 activation enhances NER, hence, decreases mutagenicity [165]. In addition, this MAPK post translationally modifies RAD23A, RAD23B, and RPA12 [166]. Similarly, to AKT1, MAPK can also mediate phosphorylation of EP300, whereupon UV radiation, EP300 is recruited to damage site in heterochromatin and is phosphorylated by both MAPK14 MAPK and AKT1 increasing histone acetyltransferase (HAT) activity to acetylate H3 and H4 leading to chromatin relaxation. After that, EP300 phosphorylation conditions it for proteasomal degradation enabling the recruitment of DDB2, XPC, and other NER factors [167]. However, MAPK pathway can also mediate metastasis. High ROS levels or UVA radiation activates MAPKs JNK, MAPK1, and MAPK14 leading to activation of AP-1 c-Jun and c-FOS mediating the expression of matrix metalloproteinase 1 (MMP1) [168]. MMPs break down extracellular matrixes and are highly expressed by XPC fibroblasts with enhanced MMP1 promoter activity and ROS activation leading to the predisposition to invasive skin carcinomas [9]. Moreover, Zhao et al demonstrated a role of MAPK14 in mediating repair of CPD by utilizing SB203580, MAPK14 inhibitor, and measuring the repair kinetics using slot blot assay. They also reported a MAPK14 dependent ubiquitination of DDB2 favoring its degradation and clearance from damaged chromatin [104].

3.1.5 CSNK2A1 (CK21) PATHWAY

Casein Kinase 2 (CSNK2A1) is a serine/threonine kinase involved in various signaling pathways including PI3K/AKT1, epidermal growth factor receptor (EGFR), Heat shock protein 90 (Hsp90) and nuclear factor kappa B (NFkB) [169-174]. It was recently linked to the regulation of single and double strand break repair [175, 176]. One of CSNK2A1 substrates is X ray repair cross-complementing protein 1 (XRCC1) involved in the ligation step of both nucleotide and base excision repair. CSNK2A1 mediated phosphorylation of XRCC1 enhances the stability of

XRCC1-Ligase III complex [176, 177]. The involvement of CSNK2A1 in DNA repair pathways rendered it an important target for combinatorial therapies with adduct inducing agents like cisplatin. The damage induced by the latter, if not repaired by NER, gives rise to double stranded breaks at stalled replication forks and the accumulation of γ H2AX. In a study by Drygin et al., the treatment with CX-4945, CSNK2A1 inhibitor, induced formation of tails in the course of alkaline comet assay and the accumulation of phosphorylated γ H2AX. This thus confirms the role of CSNK2A1 in mediating repair of single strand breaks during the late stages of nucleotide excision repair [178]. In another study by Im and Nho on idiopathic pulmonary fibrosis fibroblasts, they discovered a reduction in expression of PUMA and caspase-3/7 following cisplatin treatment thus signifying a decrease in DNA-damage induced apoptosis. They also noted an increase in XRCC1 activity as a result of CSNK2A1 hyper-activation causing a drop in γ H2AX levels [179]. CSNK2A1 is also required for the phosphorylation of XPC at serine 94, as mentioned previously promoting the CPD and 6-4 PP repair[113].

3.2. CHEMICAL COMPOUNDS

Much effort is focused, nowadays, on identifying components that can modulate NER activity. During the last years, several distinct chemical compounds have been characterized for their ability to modulate NER activity in either a positive or negative manner.

3.2.1. NICOTINAMIDE

Nicotinamide (vitamin B3) is a precursor for NAD (Nicotinamide adenine dinucleotide), a coenzyme for ATP production. The supplementation of Nicotinamide can reverse the ATP depletion that occurs during chromatin remodeling and DNA repair [180]. This chemical does not prevent the formation of CPD or 8-oxo-guanine, but it enhances their removal. It favors the increase of unscheduled DNA synthesis after UV radiation and reduces UV-induced immunosuppression [181]. In addition, it prevents UV-induced glycolytic blockade and restores the ATP and NAD levels [182, 183]. Nicotinamide can have a potential role in the chemoprevention of arsenic-induced skin cancer. Arsenic is a UV radiation co-carcinogen found in contaminated water and it mediates DNA damage. The administration of nicotinamide prior to arsenic treatment combined with UV irradiation decreases the levels of CPDs and 8-oxo-guanines [184]. Nonetheless, nicotinamide supplementation also rescues the mitochondrial phenotype in XPA cells. The latter are characterized with reduced mitochondrial autophagy and increased membrane potential speculated to be the cause of neurodegeneration in XPA patients. The treatment of XPA cells with either nicotinamide riboside or nicotinamide mono-nucleotide promotes the NAD^+-SIRT1-PGC-1α axis attenuating PARP effect and reversing the mitochondrial dysfunction[185].

3.2.2. NOX1 INHIBITOR

NADPH oxidase (NOX) allows the generation of ROS following UVB radiation. Several NOX isoforms (NOX1 to NOX5, DUOX1, DUOX2) exist. These proteins differ in their tissue distribution and they are involved in regulating different biological processes such as cellular signaling, differentiation and regulation of gene expression. NOX proteins' activation requires

their assembly with others which in case of Nox1 are NOXA1, NOXO1, $p22^{phox}$, and small Rac GTPase [186]. NOX1 activation in XPC keratinocytes via DNA-PK/AKT1 axis elicits their neoplastic transformation [187]. Therefore, the inhibition of NOX1 might have a positive effect on NER. This blockade can be mediated by the utilization of peptide inhibitors that target either the proline-rich region of NOXO1 or SH3 domain of NOXA1 that are necessary for NOX1 function. Their utilization enhances CPD and (6-4) PP repair and decreases apoptosis by reducing activation of caspase 3, 8, and 9 [188]. Moreover, the same study revealed that CDK4, CDK6, cyclin (B, D1, E) and CDC25C were increased following NOX inhibition while CDKN2A and CDKN1A were reduced enabling cell cycle progression. On the other hand, NOX inhibition can also be mediated by syringic acid that blocks the NOX/PTP-κ /EGFR axis [189].

3.2.3. SILIBININ

It is a bioactive flavonolignan present in milk thistle. It has been reported that upon human dermal fibroblasts' exposure to UVB radiation, the treatment with silibinin increased TP53 and GADD45α expression and reduced the formation of CPDs. The same study also showed that silibinin increases the protein levels of XPA, in a TP53 dependent manner, together with XPG and XPF. At the mRNA level, only XPA but neither XPG nor XPF levels were increased, indicating that the increase in their protein levels can be mediated by silibinin's regulation at translational levels rather than its role in the enhancement of transcription [190]. Furthermore, Silymarin, whose major active ingredient is silibinin, has been shown to inhibit photocarcinogenesis via the inhibition of UV induced ROS, inflammation and immunosuppression. These flavonolignans accelerate the repair of CPDs and increase the expression of XPC and XPA despite lack of a UVB radiation filtering effect [191].

3.2.4. NAC

N acetylcysteine (NAC) is a nontoxic analog of cysteine with antioxidant activity that detoxifies mutagens. It can be deacetylated to produce cysteine, a precursor of GSH. NAC decreases the formation of DNA adducts and its intracellular metabolites are scavengers of ROS [192]. The administration of NAC to UVB irradiated normal human epidermal keratinocytes can partially inhibit the production of UVB-induced cytokine IL6 and TNFα [156]. NAC has also been demonstrated to reduce the formation of 8-oxoguanines and lipid peroxidation in rats treated with sodium fluoride. This suggested a possible role of NAC in antagonizing the damage induced by sodium fluoride [193]. In addition, the combination of NAC treatment with Acetyl-L-Carnitine prior to irradiation causes an increase in DNA damage related factors including XPC [194].

3.2.5 ACQ

ACQ is an alanine cysteine glutamine tripeptide with antioxidant activity compared to that of glutathione. Its activity was tested in keratinocytes and fibroblasts treated with hydrogen peroxide. The administration of ACQ decreased the positive staining with H_2DCFA signifying a decrease in the levels of reactive oxygen species. Hence, it can protect cells against H_2O_2 treatment [195]. This capacity was proven to reduce NER activity. However, the use of ACQ to enhance NER activity

has not been established so far. Therefore, it would of great importance to check this correlation in future studies [116].

3.2.6. ASCORBIC ACID

Ascorbic acid (ASA) is an antioxidant that protects DNA from damage [196]. It has also an anti-inflammatory potential as it suppresses NFKβ [197]. It has been established that in keratinocytes subjected to UVA radiation, the pretreatment with ASA prevents the changes in ROS, GSH, and lipid peroxidation levels thus it counteracts the UVA-induced oxidative stress. Since the change of GSH levels can modulate the expression level of XPC, and lipid peroxidation hinders NER, the use of ASA for NER enhancement should be further explored [118, 152]. Moreover, it has also been reported that Ascorbic acid decreases the phosphorylation of MAPK14 and MAPKAPK2 inhibiting UVA-induced MAPK activation together with the reduction of apoptosis through a decrease in caspase 3 activations [198].

3.2.7 RESVERATROL

Resveratrol (RSV) has a para-hydroxyl group conveying a scavenging activity of free radicals [199]. As proven by various *in vitro* studies, it can prevent H_2O_2 and UV induced oxidative damage [200]. RSV activates NFE2L2 pathway and induces the transcription and translation of glutamyl-cysteinyl ligase, glutathione peroxidase 2 (GPX2) and increases GSH levels. This NFE2L2 activation and increase in GSH levels render this molecule of interest for NER enhancement even though such role has not been explored yet. RSV does not induce the synthesis of NFE2L2 but it enhances its stability and nuclear accumulation. The NFE2L2 activation is mediated by the MAPK pathway mainly by MAPK1 [11].

3.2.8. SELENIUM

Selenium is a micronutrient that can be potentially used in cancer prevention. This potential role was examined in a study done on men with elevated risk of prostate cancer in New Zealand in 2004. Those individuals were provided with either a placebo or selenium supplementation in the form of selenised yeast for 6 months and DNA damage was assessed by comet assay. The results show an inverse correlation between DNA damage and selenium status [201]. A different study also reported a role of selenium in the repair of CPD adducts. A chloramphenicol acyltransferase reporter in a plasmid was inactivated by CPDs and then transfected into fibroblasts supplemented with selenium. The reporter activity was restored signifying the repair of the induced CPD adducts [202]. Selenium is also involved in enhancing the repair of oxidative DNA damage like 8-oxoguanine. These lesions are mainly repaired by 8-oxoguanine glycosylase (OGG1) where the oxidation of its redox-sensitive residues leads to the attenuation of OGG1's activity. Selenium induces antioxidant selenoproteins that help maintain OGG1 in a reduced active form. The effects of selenium can be due to (i) selenium metabolites that are not associated with proteins or (ii) selenoproteins with selenium in the form of selenocysteine [203].

3.2.9. POLYPHENOLS

Polyphenols can be found in a variety of plants including green tea leaves and grapes' seeds. Nowadays, various studies are focusing on the use of polyphenols in skin cancer prevention due to their potential role in photocarcinogenesis inhibition. Green tea polyphenols (GTP) were found to prevent UV induced immunosuppression while also decreasing the amount of CPDs. The latter effect was speculated to be the result of GTPs' enhancement of XPA, XPC, and RPA1's mRNA expression [204]. Green tea polyphenols are also effective in the reduction of inflammation markers (COX2, PGH2, PCNA and Cyclin D) and pro-inflammatory cytokines (TNFα, IL6, and IL1β) [205]. GSP (grape seeds proanthocyanidins) mediates similar effects as GTP concerning the repair of CPD as well as enhanced XPA, XPC, RPA11 and DDB2 expression. In addition, it favors the nuclear translocation of XPA and augments its interaction with ERCC1 [206].

3.2.10. VITAMIN E

The exposure of the skin to UV radiation causes depletion of vitamin E that quenches ROS[207]. One study revealed that the treatment with the antioxidant α-tocopherol, vitamin E, leads to both direct and indirect protections. The first is mediated by the quenching of free radicals while the latter is via the increased epidermal thickness[208]. Krol et al. also revealed that the topical - application of alpha tocopherol on mice skin inhibits the formation of cyclobutane pyrimidine dimers. This suggests a role of vitamin E in the protection against UV induced skin photo-damage. However, the applied vitamin E is rapidly depleted in a dose-dependent manner following UV radiation[209].

3.2.11 ACETOHEXAMIDE

This compound is an anti-diabetic drug targeting ATP-sensitive potassium channels and it belongs to the family of sulfonylureas regulating insulin secretions. However, a new function was attributed to acetohexamide following a chemical screen performed on BRCA1 mutated cells. These cells are deficient in base excision repair (BER) and hence accumulate oxidative stress. The screen consisted of treating the cells with a chemical library then transfecting them with GFP plasmid containing oxidized bases. Acetohexamide was then identified as a chemical molecule that enabled the repair of the oxidized bases in BER deficient cells and that was signified by the increase in GFP expression [210]. Another chemical screen-based study also proved the importance of such compound in enhancing DNA repair but of pyrimidine dimers rather than oxidized bases. They proved that acetohexamide enhances the removal of pyrimidine dimers in cells deficient in both the global and transcription-coupled nucleotide excision repair. The actual mechanism is still not clear but it involves the downregulation of MUTYH protein as knock out of this BER protein gave similar results compared to the drug treatment [211].

3.2.12. VITAMIN D

The active form of vitamin D is 1,25-hydroxy-cholecalciferol that can either be provided through diet or through the conversion of 7-dehydrocholesterol in the skin mediated by the exposure to UV light. It was reported that keratinocytes with intact vitamin D receptors (VDR) show accelerated repair of CPDs compared to counterparts with knocked out VDR [212]. Treatment of cells with 1,25 dihydroxyvitamin D3 increases the expression of XPC and DDB2 [213].

3.2.13. ECTEINASCIDIN 743 (ET743)

Also known as Trabectedin or Yondelis is an FDA approved antitumor chemotherapy drug. It binds to and alkylates guanine residues at the N^2 position in the minor groove bending the DNA towards the major groove opposite to the adduct. The mechanism of inhibition occurs at the TC-NER. Treatment of TC-NER proficient cells with Et743 generates more single strand breaks compared to cells with mutations in TC-NER involved proteins. The proposed mechanism based on bacterial homologs is that this drug traps endonucleases after the cleavage step preventing the ligation of the DNA [214].

3.2.14. F11782

The reported mechanism of action of F11782 is the inhibition of topoisomerases I and II. It is a 2',3'-bis-0pentafluorophenoxyacetyl-4',6'-ethylidene-β-D-glucoside of 4'-phosphate-4'-dimethylpipodophylloyoxin 2-N-methyl glucamine salt. However, in a DNA damage detection (3D) assay, Barret et al. reported the role of F11782 in the inhibition of NER using UVC damaged plasmid incubated with cell extract and biotinylated dNTPs. F11782 was found to inhibit the incision step of NER rather than the repair synthesis stage. Despite that, the actual target of drug mediating such inhibition is still unknown [215].

3.2.15. FLUDARABINE

Fludarabine or Fludara is a purine nucleoside analog used as chemotherapeutic medication for the treatment of leukemia and lymphoma [216, 217]. The effect of this drug on NER was reported by Yamauchi T. et al. using an alkaline comet assay to measure the amount of DNA strand breaks at the incision step and monitoring the re-joining of the DNA after repair via the incorporation of tritiated thymidine. The pre-treatment with Fludarabine inhibited thymidine incorporation and allowed the preservation of the comet tail up to 4 hours post UV with no sign of repair[218].

3.2.16. UCN-01

UCN-01 is known to block cell cycle checkpoints and inhibit protein kinase C [219]. Jiang and Yang tested the effects of this drug on cisplatin induced DNA damage normally repaired by NER. UCN-01 was found to inhibit repair as tested by repair synthesis assay and host cell reactivation. This is probably mediated by the hindrance of XPA-ERCC1 interaction despite the fact that no direct interaction between the drug and NER proteins was reported. They speculated that UCN-

01's effect might be through the regulation of signaling pathways enabling post-translational modifications of NER proteins [220].

3.3. BIOLOGICAL MOLECULES

Micro RNAs (miRNAs) are small non-coding RNA molecules with a seed region in their 5'end that interacts with the 3'UTR of mRNA leading to the latter's degradation or block of translation. They can also interact with 5'UTR and coding regions. miRNAs are involved in regulating a broad range of biological processes including DNA damage and repair genes [221]. For instance, miR-192 whose expression is induced by HBV infection can bind and inhibit mRNA of ERCC3 and ERCC4 [117]. Moreover, hypoxia can induce the down-regulation of RAD23B via the up-regulation of miR-373. The utilization of anti-miR-373 was able to reverse the hypoxia-induced Rad23B reduction [222]. CSA which is part of the TC-NER recognition was also proven to be suppressed by miR-521 [223]. In addition, a study conducted by Shin et al. utilizing irradiated NSCLC A549 cells showed the up-regulation of miR-34b that targets ERCC5 in addition to miR-192 and miR-215 that both target ERCC3, ERCC4 and XPA [221]. Furthermore, Crosby et al. showed that forced overexpression of miR-210 leads to the suppression of RAD52 [117]. On the other hand, Friboulet et al. revealed that miR-375 was reduced in ERCC1 positive cancers and its predicted targets are PARP4, ERCC3, TP53, and USP1 [224] (table 1). Since a wide range of miRNAs can control the expression of DNA repair genes, summarized in the following table, it would be of great interest to analyze the miRNA profile of NER-deficient cells. This analysis will enable the pinpointing of miRNAs with possible roles in the persistence of lesions by down regulating repair enzymes paving a road for the utilization of anti-miR to counteract their effects.

Table 1 miRNAs that regulate NER genes

miRNA	Target mRNA	Target mRNA alternative name
miR-373	RAD23B	
miR-521	CSA	ERCC8
miR-34b	XPG	ERCC5
miR-192	XPB XPF XPA	ERCC3 ERCC4
miR-215	XPB XPF XPA	ERCC3 ERCC4
miR-210	RAD52	
miR-375	PARP4 XPB TP53 USP1	ERCC3

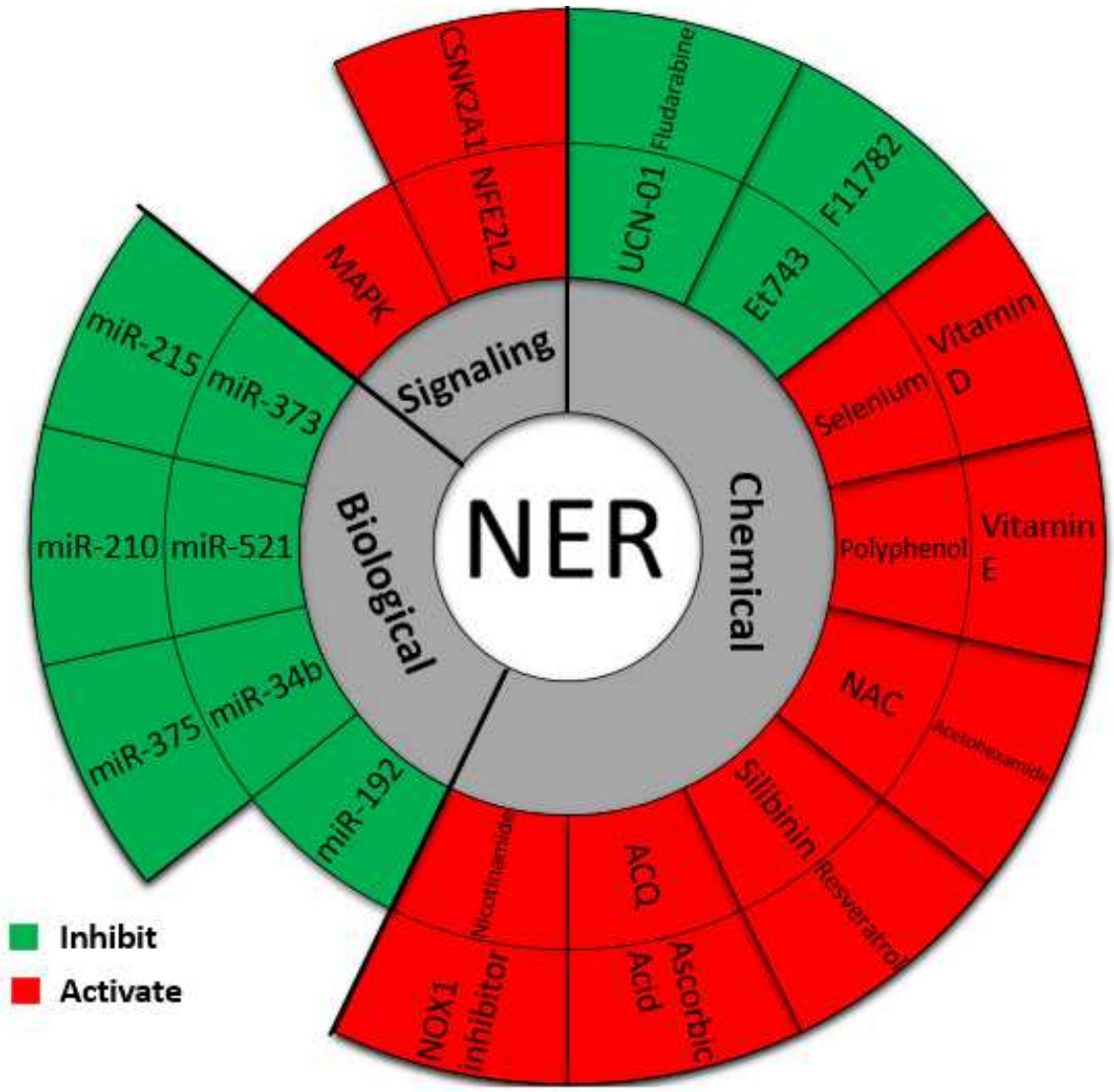

Figure 13 Method for the modulation of Nucleotide Excision Repair

Nucleotide Excision Repair is modulated by various signaling pathways that enhance its activity including CSNK2A1, Nrf2 and MAPK. This enhancement can also be mediated by several chemical molecules. On the other hand, the inhibition of NER can be mediated by either miRNAs that target NER genes or by chemical drugs normally used in combination with chemotherapies.

CHAPTER 3. XERODERMA PIGMENTOSUM (XP)

Xeroderma Pigmentosum originates from mutations in one of the several proteins involved in the NER pathway. It is an autosomal recessive genetic disease that is manifested mainly in children suffering from early onset of skin cancers and neurological abnormalities. Therefore, since our study is based in this disease it is important to first classify the different subgroups of XP focusing mainly on the XP-C complementation group and the different roles that XPC protein possess in

pathways other than that of nucleotide excision repair. Some treatments possibilities have emerged for XP-C which will also be explored here despite them being not yet FDA approved.

1. GENERALITIES AND COMPLEMENTATION GROUPS

XP is a rare autosomal disease characterized by high sunlight sensitivity. Patients exhibit freckle-like pigmentation in sun-exposed areas that can give rise to precancerous lesions. If kept unprotected, they can develop into skin cancer. Moreover, XP patients have an increased incidence of both melanoma and non-melanoma skin cancers with 2,000 and 10,000-fold increase respectively before the age of 20. In addition to the development of tumours patients also exhibit several neurological problems. Till date, eight XP complementation groups have been identified that correspond to mutations in eight genes involved in repair of UV induced DNA damage. Genes XPA through G is essential for the removal of UV photoproducts while XPV is involved in the replication of unrepaired DNA [225] (table 2). XP is characterized by the accumulation of mutations in either proto-oncogene (BRAF, NRAS, MYC…) or tumour suppressor genes (P53, PTCH1…) that persist due to a defect in NER [226].

1.1 XPC

XPC gene is located on chromosome 3 and codes for a 940 amino acid protein. Together with XPE, it acts as a damage detector in GGR. XPC recognizes the non-hydrogen-bonded bases of the undamaged strand to provide a platform for TFIIH [80]. As mentioned earlier, XPC is a heterotrimeric complex including hRAD23B and centrin 2 (CETN2). The first stabilizes XPC while the second enhances XPC damage recognition [227]. The gene coding for XPC is located on 3P25.1 [225] and the most frequent mutation is a homozygous frameshift mutation c.1643_1644delTG (p.Val548AlafsX25) which was reported in several XPC patients [228] in addition to a homozygous -9T>A mutation in intron 3 of XPC gene leading to a mRNA with exon 4 deleted [229]. XPC patients exhibit only skin disorders mainly in sun-exposed areas. They have a deficiency in the global genome repair but an active TCR. XPC cells are more resistant to killing by UV light than are XPA or XPD cells [230].

1.2 XPE

XPE or DDB2 binds UV damaged DNA and is part of GGR damage recognition step. By interacting with E2F1, DDB2 acts as a transcriptional activator. It also controls UV irradiation P53-dependent apoptosis [227]. XPE patients have only a slightly reduced rate of repair and are not highly sensitive to UV. It is presumed that XPE cells lack DDB2 involved in GGR and whose expression is controlled by P53 [231, 232]. XPE patients show slow excision of photoproducts accompanied with mild symptoms [233].

1.3 XPA

XPA gene encodes a 273 amino acid protein that is part of the pre-incision complex together with RPA and XPG and it controls its proper assembly in both GGR and TCR. XPA binds both NER substrates and oxidative DNA lesions through interacting with various proteins including the NER proteins: RPA, ERCC1, TFIIH, XPC as well as ataxia telangiectasia and Rad 3 related (ATR) protein regulating XPA's nuclear import after UV radiation. Moreover, its interaction with

deacetylase sirtuin 1 (SIRT1) favours its deacetylation which enhances XPA-RPA interaction [80]. XPA gene is located on 9q22.33 [228] where patients have mutations in the DNA binding regions of the protein but other mutations outside such regions may also exist. One of these mutations is a nonsense homozygous p.Arg228X mutation. XPA patients exhibit both skin cancer and neurodegeneration and are characterized by a severe deficiency in the repair process [234].

1.4 XPD AND XPB

XPD is part of Cdk activating complex (CAK) component of TFIIH; it's a 5'to 3' ATP dependent helicase. On the other hand, XPB is a 3'to 5' ATP hydrolysis-driven helicase though weaker than XPD [235]. Both unwind the damaged DNA in GGR and TCR to favour the assembly of the pre-incision complex [236]. However, the interaction between XPD, XPB and p53 apoptosis factor inhibits their helicase activity while reducing the instance of apoptosis [237]. Mutations in XPB genes include a heterozygous T>C transversion resulting in a phenylalanine -99-to serine missense mutation [229]. XPB and XPD patients show both neurodegeneration and cancer development. They manifest the most complicated clinical symptoms. XPB mutations occur outside the DNA/DNA helicase domain while XPD mutations occur within or outside the DNA/DNA or DNA/RNA helicase boxes [238].

1.5 XPG

XPG is a 133KDa nuclease that is recruited to the site of damage by XPA/RPA and TFIIH complexes. It cleaves at the 3' end at the single-stranded/ double-stranded DNA junction [239]. It interacts with a wide range of proteins. Its nuclease activity is dependent on its interaction with XPB helicase. XPG was also shown to interact with BER proteins in particular Nth1, DNA glycosylase-AP lyase, increasing its affinity to the damaged base [240]. Finally, Gadd45, growth arrest and DNA damage Inducible, interacts with XPG to mediate the demethylation of DNA hence stimulating DNA repair [241]. One of the mutations in the XPG gene is a single base pair deletion in a 2170-2172 AAA triplet nucleotide leading to a frameshift [229]. Patients show severe symptoms of neurological abnormalities, cancers, retardation, etc… Mutation of XPG affects both NER as well as BER [242].

1.6 XPF

It is a 103kDa nuclease, which similar to XPG, can recognize the single-strand/double-strand junction but at the 5’ end of the damaged bases and mediates cleavage at that site [243]. Its recruitment and positioning require that both XPA and XPG are bound to their substrates [244]. XPF mainly interacts with ERCC1 forming a dimer [236]. XPF patients exhibit a slow rate of excision.

1.7 XPV

It is a 79kDa Y family DNA polymerase that is not part of the NER pathway. However, its deficiency leads to XP even though NER is active. It is a translesion polymerase that bypasses the damage [245]. Mutation in XPV includes a nonsense mutation at nucleotide 378 [229] leading

patients to have deficiency in the Pol H involved in translesion synthesis. Other damage-binding include frameshifts and missense mutations. XPV like XPC has no neuropathologies but increased risk of skin cancer [246].

Table 2 Characteristics of NER genes

NER Gene	Chromosomal Location	Protein Size (aa)	Function	Notes
XPA	9q22.33	273	Damage Verification	Part of pre-incision complex
XPB/ERCC3	2q14.3	782	Helicase	Part of TFIIH complex
XPC	3p25.1	940	Damage Recognition (GGR)	Interacts with HR23B & CETN2
XPD/ERCC2	19q13.32	760	Helicase	Part of TFIIH complex
XPE/DDB2	11p11.2	427	Damage Recognition (GGR)	Interacts with DDB1
XPF/ERCC4	16p13.12	916	Incision	Interacts with ERCC1
XPG/ERCC5	13q33.1	1186	Incision	Part of pre-incision complex
XPV/POLH	6p21.1	713	Polymerase	Mediates Trans-Lesion Synthesis

2. XPC AND ITS ROLES

As mentioned earlier, XPC patients mainly exhibit skin tumours. Therefore, they provide a great model for UV induced skin tumours as the effect of such irradiation is not repaired and can ultimately lead to a faster rate of skin cells' malignant transformation. XPC is involved in the detection of DNA damage in GGR [80]. However, over the years several additional roles have been attributed to XPC which explains its divergent tumour profile. These roles include its interplay with base excision repair (BER), its role in redox homeostasis, cell cycle regulation and transcriptional regulation.

2.1 XPC AND BER

BER is another DNA repair pathway of base modifications caused by the spontaneous decay of DNA bases, ROS, or even alkylating agents. The first step is the recognition of the damaged base. In most cases, this base can be either a deaminated, depurinated or 8 oxoguanine bases. Poly-ADP-ribose polymerase 1 (PARP1) recognizes the altered base and activates the BER pathway [15]. In case of deamination of cytosine, the uracil base will be removed by the action of uracil DNA glycosylase that breaks the N-glycosidic bond between the sugar and carbon 1 of deoxy ribose. While in case of 8-oxoguanine it is mediated by glycosylase OGG1. This allows the generation of an apyrimidinic site (AP site). AP endonuclease creates a nick upstream to the AP site to create a 5' abasic deoxyribose phosphate (SRP). The exonuclease activity of DNA polymerase beta will mediate the removal of the dRP and the addition of a dNTP due to its 5' to 3' polymerase activity

while using the second strand as a template. The final step is the ligation of 3'OH of the newly added nucleotide to the 5'P of the upcoming one using DNA ligase1/3 [247]. XPC has been shown to participate in the initial phase of BER especially in the removal of oxidative DNA damage as XPC deficient cells show great sensitivity to the latter [79]. OGG1 activity is stimulated by XPC-HR23B that acts as a co-factor in BER. This heterodimer enhances the binding of OGG1 to the DNA but no stable ternary complex between the heterodimer and OGG1- DNA duplex was observed [79]. One of the proposed mechanisms of this action is that XPC-HR23B favours the change in DNA conformation at the damage site favouring OGG1 binding and allowing the excision to occur. After that, the competition between heterodimer XPC-HR23B and OGG1 in the binding to the generated AP site favours the turnover of OGG1 that can now go and cleave another site [248]. Another study also showed that XPC interacts with the endonuclease APE 1 [249]. In conclusion, it is postulated that XPC-HR23B bends DNA at damage sites enabling the loading and turnover of DNA glycosylases [82] thus explaining a novel role of XPC in BER and the removal of lesions created by oxidative damage like the 8-oxoguanines (figure 14).

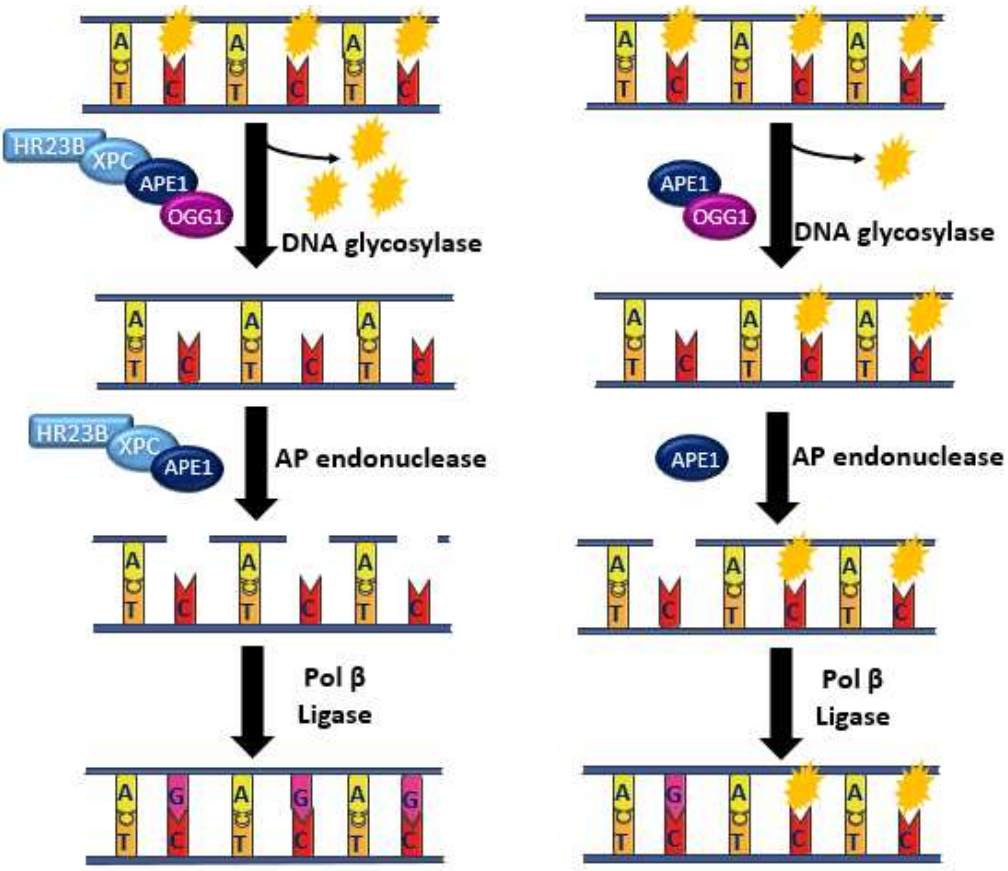

Figure 14 Interplay between NER and BER

Nucleotide Excision Repair (NER) protein XPC that is in complex with HR23B (RAD 23 homolog B) interact with APE1, endonuclease. XPC-HR23B enhances the role of OGG1 which is a glycosylase that catalyzes the removal of 8 oxoguanine damages (left panel). The result is a higher rate of repair of DNA damage when BER and NER pathways

are interconnected. On the other hand, a lower rate of repair is observed when BER pathway is utilized in the absence of NER proteins (right panel). XPC: Xeroderma Pigmentosum Protein C; HR23B: RAD 23 homolog B; APE1: Apurinic/apyrimidinic (AP) endonuclease 1; OGG1: Oxo Guanine Glycosylase.

2.2 XPC AND REDOX HOMEOSTASIS

Disrupted redox homeostasis in XPC deficient cells provided evidence for a role of XPC in this pathway. Silencing of XPC leads to a decrease in catalase activity leading to an increase in the levels of reactive oxygen species [250]. In addition, another study demonstrated that the accumulation of damage due to XPC deficiency increases the activation of DNA dependent protein kinases ultimately leading to the activation of AKT1 [251]. The latter leads to the activation of NADPH oxidase1 (NOX1) that produces ROS [188]. Finally, the combination of XPC and Apex deficiency leads to increased risk of cancer predisposition, where Apex is required for the activation of transcription factors like P53 by redox-dependent and independent mechanisms [252].

2.3 XPC AND CELL CYCLE

XPC was shown to deacetylase HR23B in order to form an HR23B-P53 complex thus preventing P53 degradation and enabling its function in cell cycle arrest [253]. In addition, damage recognition and XPC binding aids in the recruitment of ataxia telangiectasia mutated protein (ATM) and its association with the DNA [254]. This recruitment is mediated by the interaction between XPC and chromatin remodeling protein SNF5 following UV radiation [255]. ATM will then allow the phosphorylation and activation of downstream substrates including P53 that mediates cell cycle arrest due to its induction of P21 expression [256].

2.4 XPC AND TRANSCRIPTION

XPC was also reported to be involved in the regulation of transcription. In the absence of exogenous genotoxic stress, NER factors assemble sequentially with RNA polymerase II transcription machinery at promoters of activated genes in an XPC dependent manner. This triggers the achievement of optimal DNA demethylation and post translational modification of histones allowing efficient RNA synthesis. NER factors sequential assembly enabled by XPC starts with the recruitment of CSB, XPA/RPA followed by XPG/XPF/Gadd45α. This assembly occurs post the formation of the transcription initiation complex [257]. Moreover, Bidon et al. demonstrated that XPC, in the absence of damage as well, interacts with E2F1 favoring the recruitment of ATAC (histone acetyl transferase) complex to promoters conveying to XPC the title of RNA polymerase II cofactor [258].

3. POTENTIAL TREATMENTS FOR XP-C

Some approaches for potential treatments in XP-C includes the utilization of gene therapy methods for the introduction of non-mutated XPC genes or the utilization of repair machinery of non-human species to bypass the deficient repair pathways. Genetic therapy in patients is still a topic of debate ethically and in regards to its safety due to possible random integration of transgenes as well as

off-target regulation. Another alternative involves the isolation of patient's cells following their genetic manipulation to then be grafted back in the patients. Several studies have attempted to reverse the phenotype of XP-C cells via the re-introduction of non-mutated genes into XP-C cells. The latter was mediated by the utilization of recombinant adenoviruses to transfer a functional copy of XPC ameliorating photo-sensitivity and enabling DNA repair[259]. Adenoviruses can only mediate transient expression of the delivered gene as they lack the machinery required for the integration in the targeted cell genome. However, such vectors can allow the transfection of both dividing and non-dividing cells. Another group utilized a similar approach by using retroviral vectors for the delivery of XPC gene. This enabled a more stable expression due to gene integration however accompanied with lower transduction efficiency. XPC transduced cells showed correction of the XP defects. Transduced keratinocytes and fibroblasts were further on used to create in vitro skin reconstructions[260, 261]. Caution should be given when utilizing such approaches due to two main risk factors. The first being the possibility of transgene silencing via epigenetic regulation. The other more dangerous aspect is possible genotoxicity arising from the integration of the transgene in random position that can disrupt host genes[262]. The latter can be addressed via the use of more advanced genetic therapy techniques including CRIPSR-Cas9 to specifically introduce the normal gene replacing the mutated one but still off-target regulation is an issue. Another approach for XP-C treatment involves the introduction of repair enzymes to help bypass the deficiency in XPC. T4 endonuclease V is a repair enzyme utilized by bacteriophages to recognize CPD and thus creating a nick 5' of the dimer. Exonucleases will be further on recruited to degrade the area surrounding the single strand break to remove the damage and polymerases will then fill the gap. Dimericine is a T4 endonuclease V lotion under clinical trial phase 3 for its use in repair CPDs. It is based on the liposomal delivery of the enzyme to the skin showing no adverse effects and leading to fewer CPD damages. This lotion is still not FDA approved[262]. T4 endonuclease V was shown to exclusively repair CPD while UVSE (UV DNA damage endonuclease) expressed in *Deinococcus Radiodurans* was shown to allow the repair of both CPD and 6-4 PP lesions. The transfection of recombinant UVSE in HEK193T cells enables faster repair showing 80% repair of CPD and 85% repair of 6-4 PP one hour post irradiation as detected by ELISA. UVSE recognizes pyrimidine dimers and cleave phosphodiester bonds immedaitly at the 5'end of the lesion where the damage can be further on repaired by the BER machinery[263]. Finally, direct reversal of damage can be mediated by photolyases found in bacteria, plants and lower vertebrates. Such proteins are said to be dependent on blue light reactivation[264]. However, the introduction of these exogenous proteins can give rise to immune responses that need to be addressed as well causing further delay in the possible use of these methods in XP-C therapy.

CHAPTER 4. SUPPRESSOR MUTATIONS AND THEIR CLASSIFICATIONS

Genetic information encoded by the DNA should be preserved and faithfully transmitted across generations. This process is essential for determining the genetic composition of a species. Therefore, any mutation can alter the life of the affected species. Mutations range from nonsense, missense or frameshifts. These alterations' outcomes can change the functionality of encoded proteins or block their translation generating a diseased phenotype[265].

However, mutation is a double-edged sword. First, random mutations are the basis of evolution and organism adaptation to the environment, an aspect not discussed here[266]. Second, deleterious mutations have a counterpart: suppressor mutations. Assuming a primary mutation creates a diseased phenotype, a new mutation(s) can reverse its effect to generate a wild-type or less severe phenotype and thus is defined as synthetic rescue[267]. Synthetic lethality, on the contrary, involves cell death arising from the combination of loss of function mutations in at least two genes where the loss of function in any gene individually does not contribute on its own to cell death. This can be beneficial in identifying tumor vulnerabilities. Suppressor mutations have been found by genetic screening in yeast, flies and worms, enabling the understanding of genetic interactions occurring during development[268, 269]. The existence of secondary mutations may explain how some individuals appear healthy despite harboring disease-causing mutations[270] while, on the other hand, some patients show resistance to treatments[271]. For example, a secondary mutation in fetal globin genes can ameliorate the effects of β globin gene mutation, modifying the severity of sickle cell anemia[272]. In addition, a mutation in solute carrier family 30 member 8 (*SLC30A8*), which encodes an islet zinc transporter, decreases the risk of diabetes by 65% even in the presence of risk factors such as obesity[273]. The discovery of human suppressor mutations is still an emerging field with little documentation. Suppressor mutations are classified according to whether they are located in the same gene as the primary mutation to be intragenic or not hence extragenic.

In the course of this study, the screening of the two different libraries is an attempt to modify the expression of various genes in an attempt to mimic suppressor mutations identifying one that can reverse the detrimental effect of the primary mutation in XPC gene. For that, this chapter will focus on summarizing the different types of suppressor mutations discovered till date to aid later on in the possible characterization of any identified suppressor mutation in the course of our screen.

With the growth of genome-wide association studies (GWAS), characterization of synthetic rescue mutations in humans would be valuable to comprehend phenotypic outcomes in patients and create new therapeutic strategies based on synthetic rescue. Moreover, due to recent advances in cell phenotype-based screening it is only logical that such approaches are used for the identification of suppressor mutations. The screening methods rely on CRISPR-Cas9, RNAi, insertional mutagenesis and chemical screens combined with cell phenotype quantification methods[274-277].

1. INTRAGENIC SUPPRESSION

Intragenic suppression refers to the counteraction of an altered phenotype by a suppressor mutation located in the same gene as the primary mutation[278]. The classification is divided into true and pseudo revertant mutations.

1.1 TRUE REVERTANT

A single base modification caused by a primary mutation is completely reversed to the wild-type sequence due to a suppressor mutation at the same position[279] (figure 15a)that restores the wild-type amino acid sequence. However, suppressor mutation does not necessarily restore the same DNA due to the redundancy of the genetic codon (figure 15b). This was reported in *Caenorhabditis elegans* by Novelli et al., who found that a glutamine to proline mutation in the collagen processing protease (*dpy-31)* was reverted back to the wild-type phenotype[280].

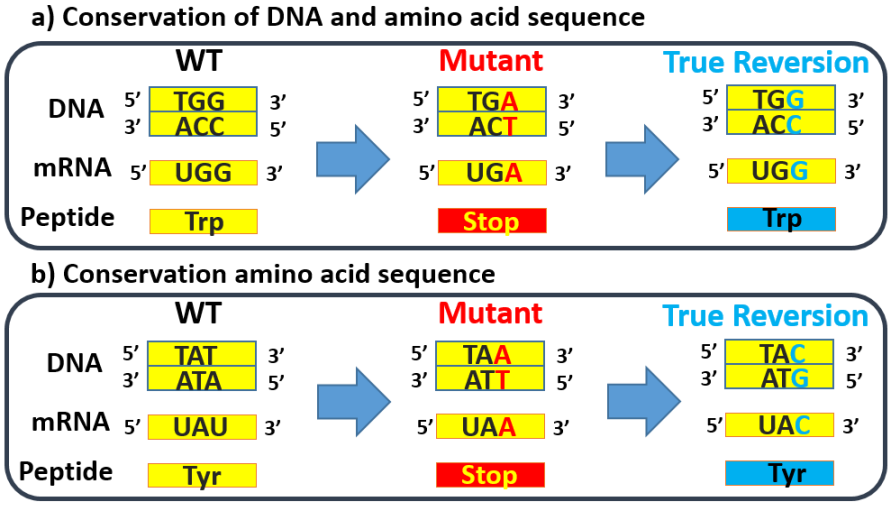

Figure 15 True Revertant Intragenic Suppression.

The primary and secondary mutation occur in the same codon and at the same level, the nucleotide level. a) A mutation that changes a guanine nucleotide into an adenine nucleotide can lead to the conversion of an encoded amino acid from tryptophan to a stop codon. A true reversion mutation can change the sequence back to tryptophan with an adenine mutated to guanine such that tryptophan replaces the stop codon. Thus, the DNA and amino acid sequences are conserved. b) In another scenario, a mutation of thymine to adenine changes the tyrosine amino acid to yield a stop codon. A true reversion mutation that changes the adenine to cytosine will enable the conversion of the stop codon back to tyrosine, thereby conserving the amino acid sequence alone. WT: wild type, Trp: tryptophan, Tyr: tyrosine

1.2 PSEUDO REVERTANT

The function of the gene product will be partially or fully restored even if the wild-type sequence is not restored. The suppressor mutation produces a modified DNA or amino acid sequence that

can still carry on the functional or structural characteristics of the wild-type gene[278]. Pseudo reversion is achieved through various mechanisms.

1.2.1 Base modification:

A single base change created can be corrected by another base modification either in the same codon or nearby. This modified gene codes for a different amino acid, but the resulting product can still restore the functionality of the original protein. The different base modifications can occur either in the same codon and the same or different nucleotide or at different codons in the same gene[269] (figure 16a). Examples from C. *elegans* include the conversion to proline amino acids created by a primary mutation that changed a glutamine to serine in the *dpy-31* gene. This reversion prevents the lethality induced by loss of function mutation of the latter gene[280]. Furthermore, several second-site missense mutations in the cell interaction *glp-1* gene promote the reversion of the primary temperature-sensitive missense mutation[281].

1.2.2 Frameshift mutation:

They involve changes in the reading frame due to the insertion or deletion of nucleotides. Addition of a nucleotide that results in a detrimental change to the reading frame can be restored by a deletion mutation nearby that restores the reading frame[282] (figure 16b).

1.2.3 Altered splicing:

Multiple splice variant genes demonstrate altered splicing where a mutation in one of the alternatively spliced exons can be suppressed by a mutation to the acceptor site near said exon omitting it (figure 16c). The perlecan-encoding gene *unc-52* exhibits altered splicing that reverts the effect of the primary mutation causing defects in myofilament assembly and in the attachment of the myofilament lattice to the muscle cell membrane.[283]. This mechanism is utilized for the treatment of Duchenne Muscular Dystrophy in which antisense oligonucleotides mimic altered splicing suppressor mutation by biding to the site of mutation and induce the skipping of the mutated exon[284].

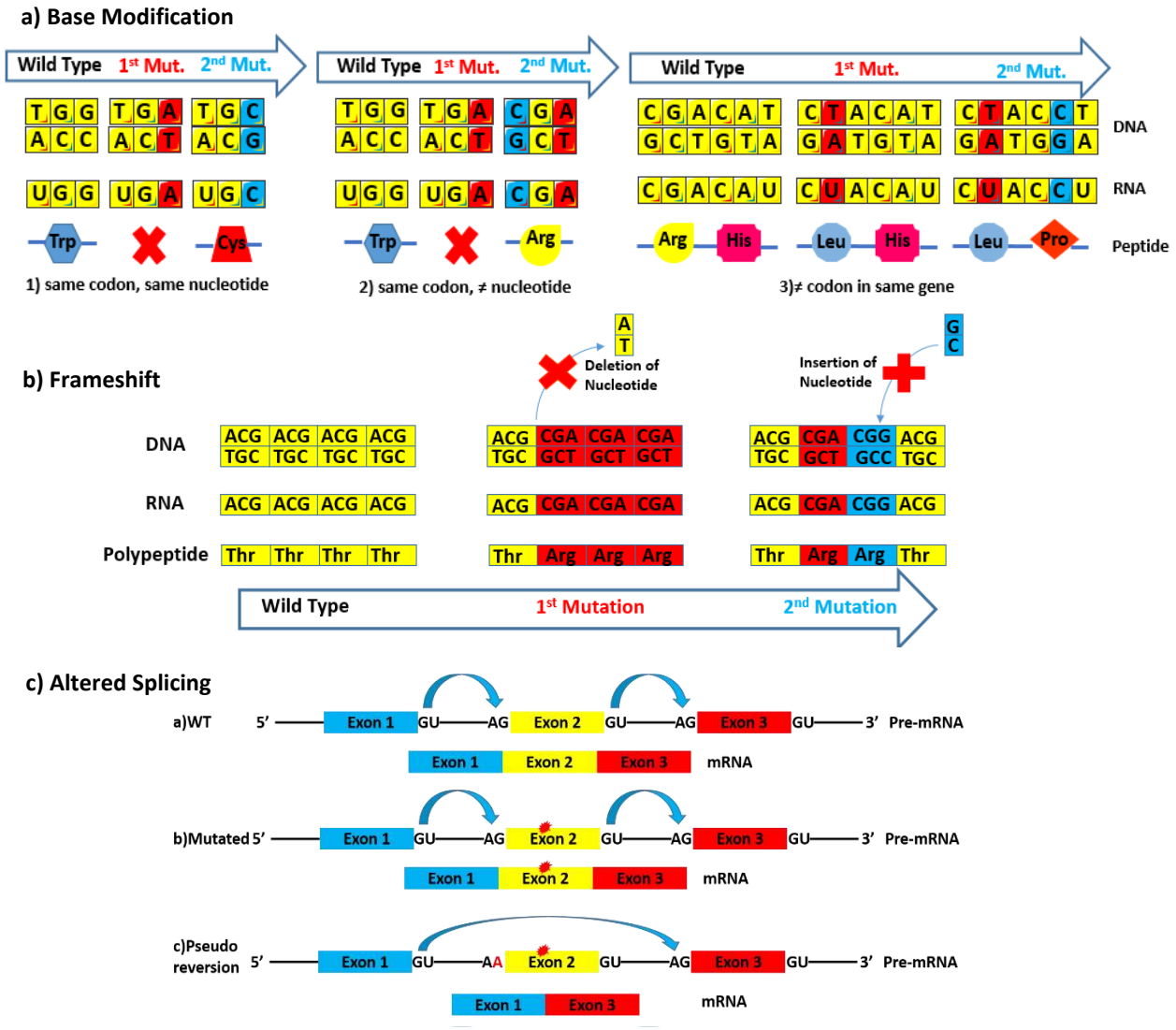

Figure 16 Different Forms of Intragenic Pseudo Reversion

Pseudo reversion of primary mutation can occur by various types of secondary suppressor mutation. The first is a) base modification further classified depending on the position of both mutations that can be in the 1) same codon and same nucleotide as the primary mutation resulting in a different translation output, from stop codon to cysteine for example, or 2) same codon but in a different nucleotide to produce arginine instead of a stop codon. In contrast, genes can be mutated at 3) different codons in the same gene to yield the amino acid proline near the mutated leucine. b) A frameshift secondary mutation can partially restore the reading frame if the primary deletion mutation is counteracted by a suppressor insertion mutation. c) Finally, altered splicing may mean that exons carrying mutations are skipped. This skipping can occur due to suppressor mutations altering the splice acceptor sites near the mutated exon that enable skipping and hence eliminate the effect of the primary mutation. WT: wild-type, Trp: tryptophan, Cys: cysteine, Arg: arginine, Leu: leucine, His: histidine, Pro: proline

2. EXTRAGENIC SUPPRESSION

The rescue of the mutant phenotype by a suppressor mutation located in a different gene is termed extragenic suppression. This involves either informational or functional suppression.

2.1 INFORMATIONAL SUPPRESSION

Informational suppression is allele-specific and gene-nonspecific[285] mutations involved in the transmission of genetic information from DNA to protein. They involve mutations that alter the machinery of DNA transcription, RNA processing, or protein translation. The genes responsible for stabilizing mRNAs or proteins can also influence the mutations that fall into this category: this stabilization may compensate for the poor functionality of a mutated product. The two genes involved in information suppression do not share a close functional relationship in a given developmental or pathological process.

2.1.1 NONSENSE SUPPRESSOR TRNA: TRANSLATIONAL SUPPRESSION

Nonsense mutations result from base modifications creating any of the three nonsense codons: UAA (ochre), UAG (amber), or UGA (opal) leading to termination of translation hence partial or complete loss of gene function. However, suppression of this mechanism is enabled by nonsense suppressor tRNAs with anticodons that recognize stop codons and adds amino acids at such sites to partially or fully restore protein function (figure 17a). A nonsense suppressor tRNA class with a mutation in the anticodon loop exists for the recognition of each type of the three stop codons [286]. For example, tRNA with a 3'AUG5' anticodon carries a tyrosine amino acid that is added to the growing polypeptide when it encounters the 5'UAC3' codon. Mutation in this anticodon from 3'AUG5' to 3'AUC5' results in a tRNA that still carries tyrosine but can now recognize the amber stop codon 5'UAG3' and add this tyrosine to the growing polypeptide chain instead of terminating translation (figure 17a). One downside of these mutated tRNAs is that they can no longer recognize their wild-type codons. However, tRNA genes are available in multiple copies across the genome; therefore, other copies can still code for the unmutated tRNA[287]. O'Neill et al. showed the presence of mutated tRNA genes by screening a human DNA library cloned in a bacteriophage with an opal suppressor tRNA probe[288].

2.1.2 LOSS OF NMD

NMD refers to "nonsense mRNA decay" initiated by the presence of a premature termination codon (PTC) 50 to 55 nucleotides upstream of the final exon-exon junction and leads to the downregulation of the transcript via its degradation[289]. However, the absence of NMD ensures a longer half-life for the transcripts carrying this PTC, increasing the chance that they will be translated. This loss can be mediated by mutations at the NMD level, including mutations in mRNA decay associated *SMG* kinase genes, enabling the translation of the mutated mRNA and thus suppressing the effects of the primary nonsense mutation[269] (figure 17b). It should be noted that increasing the translation of disease-associated mRNA is utilized for the treatment of certain

genetic disorders, including Duchenne muscular dystrophy, rendering the loss of NMD an appealing suppressor mechanism[290]. Loss of NDM was first identified in *C. elegans* following the creation of nonsense mutations by forward mutagenesis screens that yielded mutations in genes associated with NMD[291].

2.1.3 MODIFIED SPLICING

Unlike the altered splicing in pseudo revertant mutations, the effect of the primary mutation is suppressed by mutations at the level of the splicing machinery (figure 17c). In *C. elegans*, loss-of-function mutations in *smu* genes encoding proteins homologous to mammalian spliceosome-associated factors lead to enhanced exons skipping, including the skipping of exons with primary mutations[292]. The mutated perlecan gene *unc-52* is reportedly suppressed by loss-of-function mutations in the *smu-1 and smu-2* genes in addition to its suppression by altered splicing.

2.1.4 INFORMATIONAL DOSAGE SUPPRESSION

Dosage suppression involves elevated gene expression rather than a gene mutation to suppress the altered phenotype (figure 17d).

I. OVEREXPRESSION OF RIBOSOMAL SUBUNITS

The overexpression of ribosomal subunits has counterbalancing outcomes. Certain studies found a correlation between genetic fitness and ribosomal composition, suggesting a role for ribosomal subunit stoichiometry in regulating translation or affecting the progression of the cell cycle[293]. However, another study attributed a different role for these proteins, suggesting that they are possible chaperones that increase the stability of the proteins harboring mutations and shielding them from degradation[294].

II. PROTEIN TURNOVER

The overexpression of transcription factors leads to increased transcription of mutated genes. This increased gene expression increases the likelihood that the upregulated RNA will be translated[295].

III. MODULATING PROTEIN STABILITY OR DEGRADATION

Mutated mRNA can be translated to yield unstable proteins prone to degradation. Interfering with this degradation or stabilization of proteins can increase their half-lives, which may enable them to partially function, depending on the severity of the original mutation. J. Van Leeuwen et al. demonstrated that a genetic mutation in ubiquitin protein kinase *san1* annuls its role in targeting proteins' hydrophobic residues for proteasomal degradation[270]. In addition, overexpression of chaperones that stabilize the mutant protein increases the pool of active mutated proteins[295].

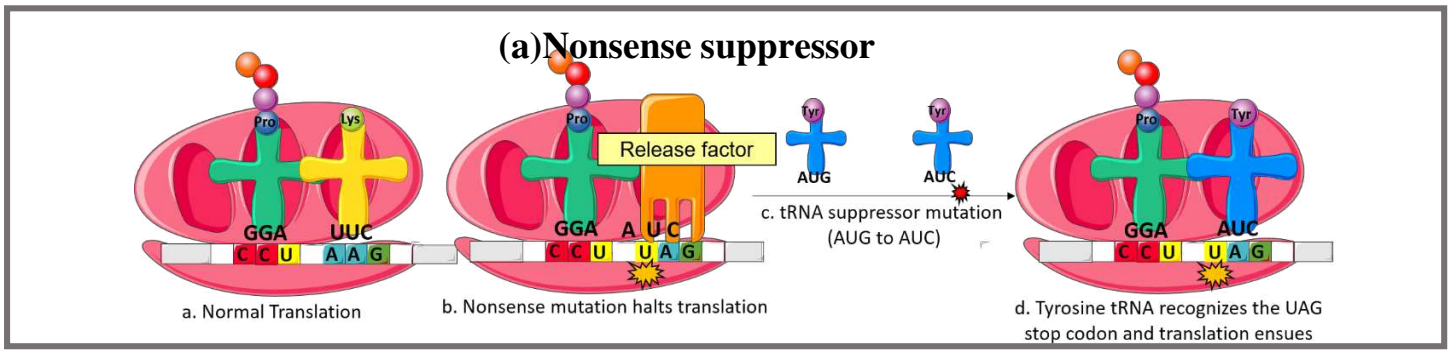
(a)Nonsense suppressor
Pro
Lys
GGA
UUC
C C U
A A G
a. Normal Translation
Release factor
Pro
GGA
A U C
C C U
U A G
b. Nonsense mutation halts translation
Tyr
AUG
Tyr
AUC
c. tRNA suppressor mutation
(AUG to AUC)
Pro
Tyr
GGA
AUC
C C U
U A G
d. Tyrosine tRNA recognizes the UAG
stop codon and translation ensues

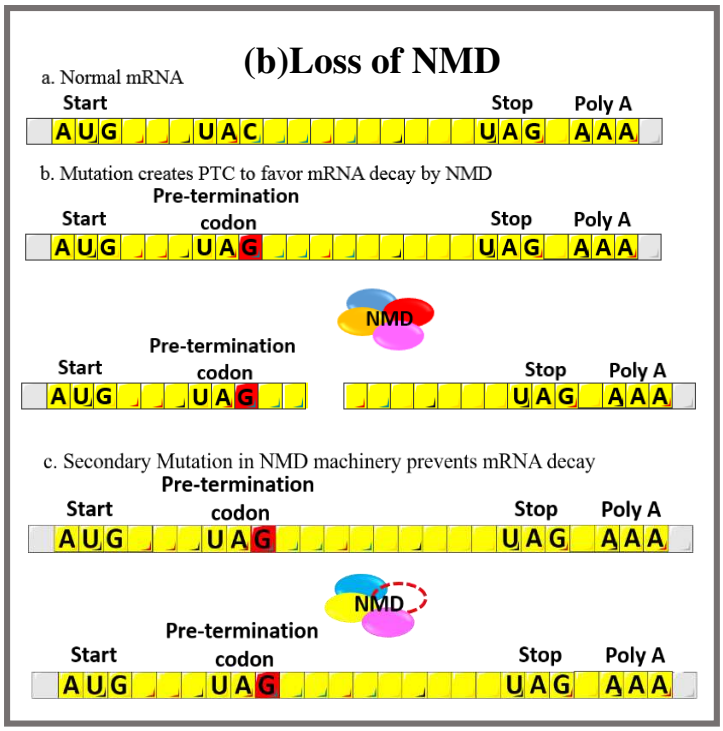
(b)Loss of NMD
a. Normal mRNA
Start
Stop
Poly A
A U G
U A C
U A G
A A A
b. Mutation creates PTC to favor mRNA decay by NMD
Pre-termination
codon
Start
Stop
Poly A
A U G
U A G
U A G
A A A
NMD
Pre-termination
codon
Start
Stop
Poly A
A U G
U A G
U A G
A A A
c. Secondary Mutation in NMD machinery prevents mRNA decay
Pre-termination
codon
Start
Stop
Poly A
A U G
U A G
U A G
A A A
NMD
Pre-termination
codon
Start
Stop
Poly A
A U G
U A G
U A G
A A A

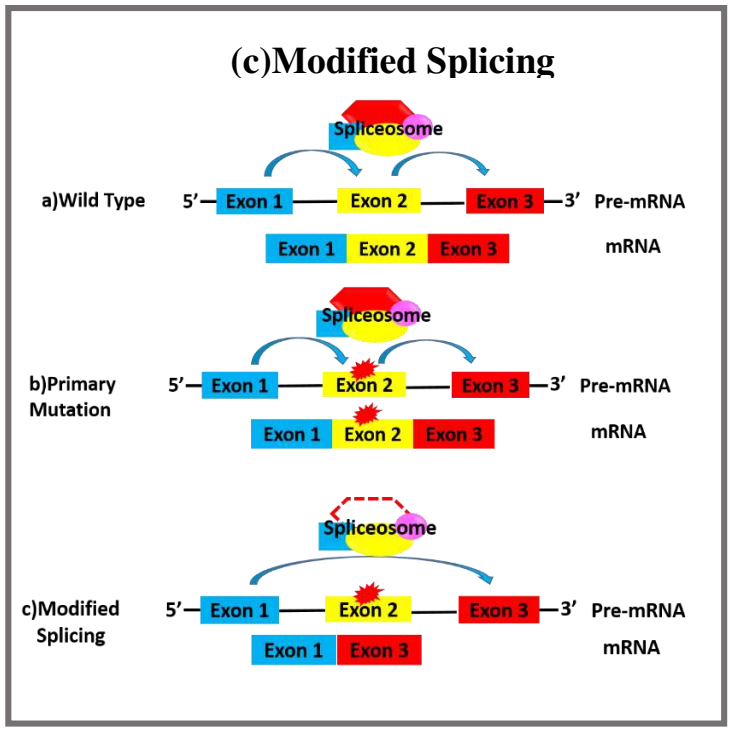
(c)Modified Splicing
Spliceosome
a)Wild Type
5'
Exon 1
Exon 2
Exon 3
3'
Pre-mRNA
Exon 1
Exon 2
Exon 3
mRNA
Spliceosome
b)Primary
Mutation
5'
Exon 1
Exon 2
Exon 3
3'
Pre-mRNA
Exon 1
Exon 2
Exon 3
mRNA
Spliceosome
c)Modified
Splicing
5'
Exon 1
Exon 2
Exon 3
3'
Pre-mRNA
Exon 1
Exon 3
mRNA

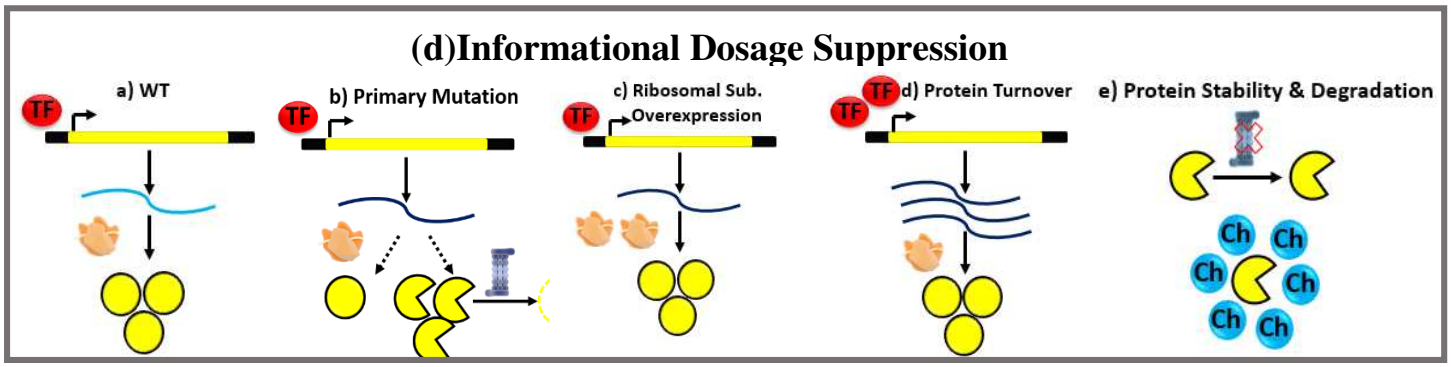
(d)Informational Dosage Suppression
TF
a) WT
TF
b) Primary Mutation
TF
c) Ribosomal Sub.
Overexpression
TF
d) Protein Turnover
e) Protein Stability & Degradation
Ch
Ch
Ch
Ch
Ch
Ch

Figure 17 Extragenic Informational Suppression.

Informational suppression deals with any suppressor mutations that alter the transmission of genetic information form DNA to protein. (a) Nonsense suppressor tRNA. tRNA with the anticodon 3'UUC 5' carries a lysine amino acid to add to the growing polypeptide when it encounters the codon 5'AAG3'. Mutation of this codon from 5'AAG3' to 5'UAG3' results in a stop codon. However, a tRNA suppressor mutation that mutates a 3'AUG5' anticodon to 3'AUC5' results in a tRNA that still carries the same amino acid tyrosine but can recognize the 5'UAG3' stop codon and prevent the termination of translation. (b) Loss of NMD. A nonsense mutation can cause the mRNA to carry a premature termination codon (PTC) that targets it for degradation by NMD. However, a suppressor mutation in the NMD machinery can block degradation and prevent protein loss. (c) Modified splicing involves skipping the exons that carry mutations. This phenomenon occurs due to suppressor mutations that altering the spliceosome, which enables the mutated exon to be skipped, thus eliminating the effect of the primary mutation. (d) Informational dosage suppression. Primary mutations can either decrease the expression or code for modified proteins that are subjected to proteasomal degradation. Suppressor mutations can increase the expression of the mutated protein by overexpressing either ribosomal subunits or transcription factors. Another mechanism deals with protein stability and degradation whereby a mutation in proteasomes can protect the mutated protein from degradation, or the protein can be rescued by overexpressed chaperone proteins that stabilize the mutated protein. tRNA: transfer RNA, Pro: proline, Lys: lysine, Tyr: tyrosine, NMD: nonsense mediated mRNA decay, PTC: premature termination codon, TF: transcription factor, CH: chaperon

2.2 FUNCTIONAL SUPPRESSION

Mutations can modulate the function of gene products by affecting their posttranslational modifications, localization or their interaction with either activators or inhibitors. Functional suppressors can help substitute or restore this modulated function via the alteration of proteins functionally related to the primary proteins[296]. Different classes of functional suppressors exist, and they are all gene-specific.

2.2.1 EPISTASIS

Signal transduction requires sequential steps initiated by receptor activation, second messengers, effectors and transcription factors. The modulation of one-step can hinder message transmission. Epistasis involves additional mutations in a different step upstream or downstream, but in the same pathway, that can restore protein functionality[297]. This occurs in regulatory switch pathways alternating between "on" and "off" state where the primary and suppressor mutation often have antagonistic effects. For example, in the sequential pathway of signal→ protein 1⊣ protein 2⊣ protein 3, the signal activates protein 1, which in turn inhibits protein 2 to abolish its effect in the inhibition of protein 3, thus rendering protein 3 active. A primary mutation that disrupts the function of protein 1 will block this pathway due to the constitutive activation of protein 2. However, an additional suppressor mutation to protein 2 enables the activation of protein 3, although in a constitutive manner. The two mutations in this example scenario are loss-of-function mutations. Another possible mechanism for epistatic suppression in the example pathway is the combination of a primary loss-of-function mutation in protein 1 and a simultaneous gain-of-function suppressor mutation in protein 3, reestablishing the pathway. Mutation in yeast cdc25, which encodes the guanine nucleotide exchange factor, prevents downstream Ras activation but

can be suppressed either by a secondary loss of function mutation in GTPase activating protein Ira1, a known inhibitor of Ras activation, or by a gain-of-function mutation in Ras itself (figure 18a). Dosage suppression was also recorded where Ras overexpression suppresses cdc25 mutation[298]. In mice, the functional loss of Mdm2, a TP53 negative regulator, can be suppressed by the functional loss of P53[299].

2.2.2 BYPASS SUPPRESSION

Bypass suppression genes belong to different pathways biochemically or genetically parallel. Here, the alteration of protein activity in a pathway is compensated by one of two modifications of an alternative protein in a related but different pathway[300]. The first involves bypassing of protein 1 loss of functionality by the alteration of the specificity of protein 2 such that the alternate pathway is rewired to perform the function of protein 1. In *E. coli*, mutations the alter the specificity of lactose permease permit the transport of maltose despite the presence of a mutated maltose permease[301](figure 18b).

Moreover, in yeast, the reduction of the mitochondrial membrane potential caused by the absence of mitochondrial ribosomal protein Mrpl3 is restored by the gain-of-function mutation in Atp1, an ATP synthase subunit[270]. The other model can be classified as both bypass and dosage suppressor because the amount of the alternate protein is the factor responsible for the compensation of the modified activity. The overexpression of protein 3 can overcome protein 1 mutation despite being of low constitutive activity at normal expression rate[302]. For instance, the overexpression of BRL1 involved in changing the nuclear membrane composition can suppress the inhibited nuclear protein import caused by a mutation in NUP116[303] (figure 18b).

2.2.3 INTERACTION SUPPRESSION

Interaction suppression affects proteins belonging to the same complex and it is allele- and gene-specific[278]. Mutations that change the shape or binding site of one protein prevent its complexation abrogating the complex's function. However, a suppressor mutation that creates a compensatory shape change in the second protein can help restore the lock-and-key interaction[304]. Another mechanism relies on the overexpression of another complex subunit that increases the recruitment ability of the mutated component without a compensatory change in the shape of the secondary protein[305]. The overexpression mass action will kinetically drive the formation of the complex regardless of the decreased binding constant. Moreover, overexpression of a paralog can also compensate for this loss[306]. Finally, a gain-of-function mutation in one of the remaining complex subunits can reinstate the complex function by either stabilizing it or completely substituting the function of the originally mutated component[307]. In yeast, mutation in the DNA polymerase delta subunit Pol31 is suppressed by either the mutation in the catalytic subunit Pol3 of the DNA polymerase or by its overexpression[308](figure 18c). Another example from yeast involves both Cdc2 kinase and Cdc13 cyclin, for which a suppressor mutation that

introduces an additional contact surface between the two proteins helps reestablish complex formation[309, 310].

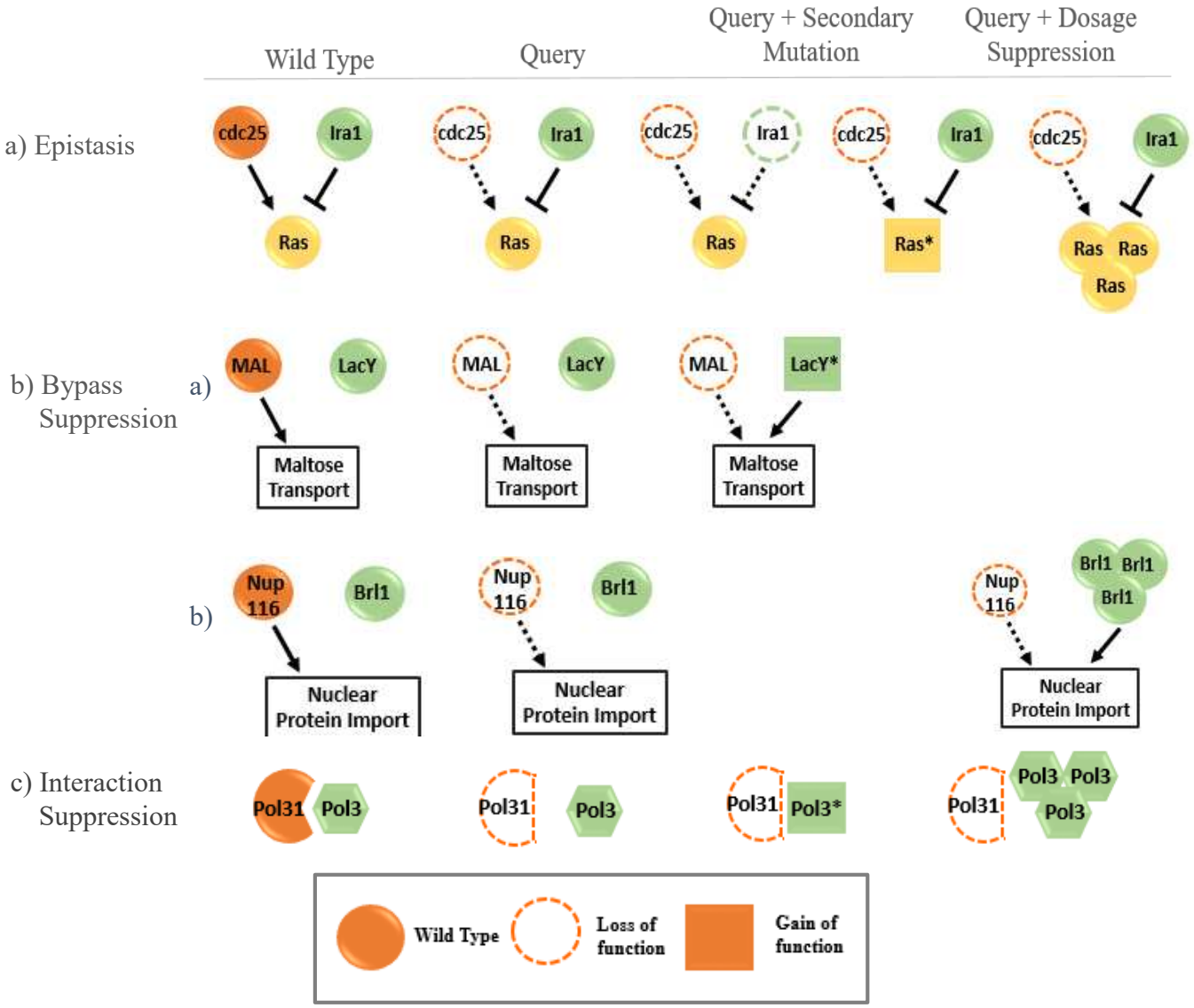

Figure 18 Functional Suppression: Epistasis, Bypass and Interaction Suppression.

(*a) Epistasis describes a suppressor mutation in a protein belonging to the same pathway as the protein that was primarily mutated. For example, a mutation in cdc25, a guanine nucleotide exchange factor, prevents downstream Ras activation but can be suppressed by either a secondary mutation in GTPase activating protein Ira1, a known inhibitor of Ras activation, or by a gain-of-function mutation in Ras itself. Dosage suppression was also recorded in which Ras overexpression can suppress the mutation of cdc25. (b) Bypass suppression involves two mutated genes that belong to different pathways that are functionally related. Mutations altering the specificity of lactose permease (LacY) permits the transport of maltose despite the mutation to maltose permease (MAL). Another example is that of the overexpressed BRL1 involvement in changing the nuclear membrane composition to suppress the inhibited nuclear protein import that was induced by a mutation in Nup116. The latter mechanism can be categorized as dosage suppression. (c) Interaction suppression involves mutations in proteins that belonging to the same complex. For instance, the mutation in the DNA polymerase delta subunit Pol31 is suppressed by either the mutation in the catalytic subunit Pol3 of DNA polymerase or by its overexpression. Cdc25: guanine nucleotide exchange factor, Ira1: GTPase activating protein, LacY: lactose permease, MAL: maltose permease, BRL1: Nucleus export protein, NUP116: nucleoprotein 116*

CHAPTER 5. HIGH CONTENT SCREENING FOR SUPPRESSOR MUTATIONS

The relationship between genotype and phenotype has long been studied by genetic screens introducing genetic perturbation into cells or organisms to investigate their effects on phenotype. Suppressor screens go one step further to identify modulators of an altered phenotype with an inborn genetic abnormality in an attempt to overcome the outcome of primary mutation. Since our study involves the use of two different screening techniques for the identification of suppressor mutations in the course of XP-C we will here classify the different screening procedures to clarify our reasons for choosing these particular screening techniques as well as their pros and cons.

In silico suppressor screen was performed by Das Sahu et al. It aimed to identify synthetic rescue (SR) mediators of resistance to immunotherapy by analyzing tumor transcriptomics and survival data of cancer patients. Several SR interactions in cancer cells resistant to therapy have been reported, some of which are rescuers of DNA methyltransferase (DNMT), which renders the cells resistant to killing by the DNMT1 inhibitor decitabine[271]. Another algorithmic based screening was carried out by Motter et al. who predicted secondary mutations in metabolic pathways reversing the growth defect of a primary metabolic one[311]. The utilization of this same approach to compare transcriptomes from patients with similar primary mutations but differing symptoms can help identify secondary suppressor mutations and synthetic rescuers. Nonetheless, other conventional screening approaches include CRISPR-Cas9, RNAi, insertional mutagenesis and chemical-based screening (table 3).On one hand, RNAi screen in our case is convenient to specifically down regulate our target genes for a short duration enough for the measurement of our readout with no need for stable long term knock down mediated by other screening techniques. Chemical screen on the other hand can allow the identification of drugs that can be on the fast track for clinical testing especially with screens based on the use of approved drugs.

Table 3 Pros and Cons of the different mutagenesis/gene expression alteration methods

Screening Technique	Pros	Cons
CRISPR-Cas9	• Induces irreversible alteration into the DNA that is transmitted to progeny. • Enables alterations in transcribed and untranscribed regions • Engineers versatility in Cas protein	• PAM sequence restrictions • Low efficiency of HDR relative to NHEJ.
RNAi	• Target genes can be identified immediately • RNAi can be chemically modified • RNAi can be used as a therapeutic agent	• Can partially suppress genes such that they are limited to knocking them down • Exhibits off-target effects • Limited to transcribed regions
Insertional Mutagenesis	• No need for complex library design	• Random insertion • Sequencing is necessary
Chemical	• No need for complex delivery techniques	• Requires time-consuming target identification

1 CRISPR-BASED SCREENING

CRISPR-Cas9 screens can be conducted in either arrayed or pooled formats. In both cases, cells harboring a particular mutation are subjected to knockout of different genes to assess the desired phenotype. In the arrayed format, a single gene is deregulated in each well and different phenotypes can then be investigated, such as death versus survival, or phenotypical changes at the single cell level[312]. In contrast, a pooled screen offers more high-throughput characteristics and delivers a massive library to cells that are then sorted based on a particular phenotype of interest. This sorting can be either a positive selection in which the perturbations that enable survival are enriched, or negative sorting where targets deplete cells from the population. The effects of genetic perturbations are determined by comparing the sgRNA profile. The latter selection is more laborious as it requires a highly sensitive readout. Nonetheless, following both selection techniques, DNA is extracted and PCR amplification of the sgRNA encoding regions is performed to be further on sequenced and mapped. This process identifies either the enriched or depleted genes[313](figure 19a). It should be noted that CRISPR-Cas9 screens have recently evolved such that they can be used not only for knockdown screens but also for loss-of-function or even activation screens due to the different possible modifications to sgRNA or to Cas9, such as those that disable some of its activities and fuse it with various effectors [314]. Moder et al. aimed to find a suppressor mutation enhancing the viability of cells deficient in the Fanconi anemia pathway. They generated their own disease model by introducing a frame-shift mutation in

FANCC by CRISP-Cas9, which led to the loss of its protein expression[315]. Loss of FANCC renders the cells hypersensitive to cross-linking agents such as mitomycin C (MMC). The cells were transfected with a pooled genome-scale CRISPR-knockout library and then selected with MMC to identify suppressors that rescue ΔFANCC hypersensitive phenotype. Moder et al. successfully identified several members of the BLM complex that is part of a multienzyme DNA helicase and bridged to the FA complex by FANCM[316].

Similarly, MUTYH gene suppression was determined to alleviate photosensitivity in cells harboring mutations in the nucleotide excision repair gene XPA. This mechanism was discovered through the combined chemical and CRISPR-Cas9 effects on a CRISPR-Cas9-created XPA-deficient cell model[211].

2 RNAI-BASED SCREENING

Different forms of interfering RNAs are microRNA (miRNA), small interfering RNA (siRNA) or short hairpin RNA (shRNA). miRNAs are generally not used in screens due to their partial complementarity that permits them to target several transcripts[317]. siRNAs are synthetically produced and can be introduced to the cells directly or within a plasmid as shRNA.

When performing RNAi-based screens, one should first identify which type of interfering RNA best suits the screen. If short-term silencing is required, siRNA libraries are the right choice as they do not undergo replication and are diluted upon cell division. siRNA libraries are mainly delivered to cells by lipid particles[318]. Otherwise, for long-term and stable silencing, shRNA vectors that can be integrated into the genome and copied to the progeny are used. The utilized vectors could be either nonviral plasmids or retroviral, adenoviral, or lentiviral vectors[319].

Similar to CRISPR-Cas9-based screens, RNAi screens are performed in two formats. Both siRNA and shRNA vectors can be utilized in the arrayed format each targeting one gene per well[320]. Pooled format is carried out with shRNA transfected or transduced in a large cell population then selected according to a particular phenotype. This process is followed by PCR amplification and sequencing of the enriched shRNA. Additional DNA sequences can also be added to the vectors to act as barcodes easing the identification of hits. This technique can also be used in a microarray format in which normal and mutant cell populations are transduced with barcode-containing vectors that are linked to two distinct fluorochromes, each unique to a population. The hybridization of DNA to the barcode probes on a microarray will favor the comparison between the shRNA profile of the normal and mutant cells[321](figure 19b). Microarray is not only used for assessing the output but can also be a screening format on its own. siRNAs, shRNA plasmids or even shRNA viral vectors can be arrayed on slides as individual drops, each targeting a specific gene. Cells can then be plated directly. After identifying the positions where a preferred phenotype is located, it can be simply linked to the target gene[322].

Luo et al. utilized a pooled genome-wide retroviral shRNA screen. The barcode incorporated shRNA vectors were transfected into normal and colorectal cells with KRAS activating mutation followed by microarray based comparison of shRNA profiles. They obtained several shRNA with anti-proliferative activity depleted from the population[323].

3 INSERTIONAL MUTAGENESIS-BASED SCREENING (GENE TRAP)

A gene trap cassette contains a promoterless reporter expressed only when inserted in the correct orientation in a transcriptional unit. It also contains one or several splice acceptor sites that render their expression conditional to the insertion of such cassette into introns or exons. Splicing enables the fusion of splice donor sites with the reporter splice acceptor creating transcriptional fusion and thus a fusion protein. Some insertions render the protein nonfunctional[324]. The procedure for insertional mutagenesis screening starts with the transduction of gene trap viruses. Expression of a reporter gene in the cassette allows the identification of the transduced cells to be FACS isolated. Phenotypic sorting is then performed to enrich the mutations favoring survival. The mutagenesis position is then determined by sequencing[325] (figure 19c).

Moder et al. perfumed a gene trap screen in parallel with the CRISPR-Cas 9 screen described earlier. They identified the loss of NAD(P)H:quinone oxidoreductase 1 (NQO1) as a possible suppressor mutation that alleviated the hypersensitivity of ΔFANCC HAP1 to MMC. Furthermore, BLM loss identified by CRISPR-Cas9, was also identified in the insertional mutagenesis screen[315]. A similar screen by Velimezi et al. led to the identification of *USP48*, that has a synthetic rescue interaction with FA genes[326]. The loss of *USP48* enhanced the recruitment of homologous recombination proteins RAD51 and BRCA1 and reduced chromosomal instability.

4 CHEMICAL-BASED SCREENING

Chemical screens can be either phenotypic or target based. Phenotypic screening involves the treatment of cells with molecules that enable the identification of hits that mediate the formation of a desired phenotype. This methodology allows for selecting compounds directly active in the cells. In contrast, target-based screens are mostly focused on purified protein(s) and how the treatment with different compounds can affect its (their) functions or interactions. The limitation of the target-based method has to do with the fact that certain compounds may not be active within the cell or may interact with multiple targets depending on the cell context, thus abolishing the paradigm of one compound for one target [327]. Chemical screening consists of cell seeding followed by compound treatment and incubation (figure 19d). Screen variables include compound concentration and incubation duration. Screening is conducted in an arrayed format with different possible readouts[328].

The biggest drawback of cell-based chemical screening is target identification, especially for newly created active compounds. Several target deconvolution techniques have been developed

for phenotypic screens, including affinity chromatography, activity-based protein profiling, analysis *in silico* or expression cloning[329].

Alli et al. conducted a chemical screen on a BRCA1-mutated breast cancer cells deficient in base excision repair (BER). To visualize the reversal of the BER, the cells were transduced with an adenovirus coding for ODD and containing GFP. The expression of the reporter is only mediated if the damage is repaired due to treatment, signifying that the compound restored the repair process. The compounds identified were the FDA approved acetohexamide and benserazide[210] previously used in treatment of diabetes and Parkinson; therefore, rerouting their use to potentially generate a new outcome would be relatively easy. In another screen, CRISPR-Cas9 generated XPA deficient HAP1 cell lines were treated with a library of 290 FDA-approved drugs, and the hits corresponded to drugs that alleviate the photosensitivity and enable the repair of DNA damage following UV irradiation. Acetohexamide was identified for its NER repair enhancement capacity[211].

5 EXAMINING DRUG RESISTANCE BY FUNCTIONAL GENETIC SCREENS

The development of drug resistance in the course of treatment is a common issue that hinders patient recovery. For instance, pancreatic ductal adenocarcinoma with oncogenic KRAS mutation exhibits resistance to gemcitabine treatment mediated by the gain of function of DCLK1. The targeting of the latter protein with anti-DCLK1 antibody inhibits in vivo tumorigenesis[330]. Thus, the identification of resistance mechanisms and mediators is of great importance. The latter seems possible with advances in screening technologies, especially in the fields of RNAi and CRISPR-Cas9. The most robust of such screens are survival-based positive selection screens. They are mediated by the introduction of either pooled shRNA or gRNA followed by the treatment with the drug in question for which the effect is hindered due to resistance. The identification of enriched sh/gRNA in these resistant cells enables the determination of possible targets for inhibition[331]. It is worth noting that the arrayed format of these screens is also effective for identifying resistance targets. For example, in a synthetic lethal experiment, treatment with AKT kinase inhibitor combined with a kinome RNAi library screening helped identify kinases involved with AKT for the mediation of survival, including inositol polyphosphate multikinase (IPMK). The latter can be targeted in combination with inhibited AKT to favor synergistic synthetic lethality[332]. Moreover, the involvement of PRC2 complex suppression in the mediation of resistance to BET inhibitors in Acute Myeloid Leukemia was also discovered by carrying out a pooled shRNA library targeting 626 chromatin-associated murine genes. The effect was mediated indirectly via the remodeling of regulatory pathways favoring the transcription of genes like *Myc*[333]. CRISPR-Cas9-based genome-wide screen in melanoma cells co-cultured with cytotoxic T cells identified the inhibition of members of the SWI/SNF chromatin remodeling complex, as sensitizers for T cell-mediated tumor killing and reversion of immunotherapy resistance[334]. Moreover, gene trap screens have also been utilized in synergy with chemical treatment. JW Bigenzahn et al. reported, after introducing a gene trap cassette in BCR-ABL$^+$ leukemia cells, that the inactivation of LZTR1

enables resistance against several BCR-ABL inhibitors due to increased RAS activity[335]. One final approach for deciphering resistance mediators can be via the utilization of sequencing. RNA sequencing of prostate circulating cancer cells from patients treated with androgen receptor inhibitors compared to untreated counteracts revealed the involvement of noncanonical Wnt signaling in resistance facilitation[336].

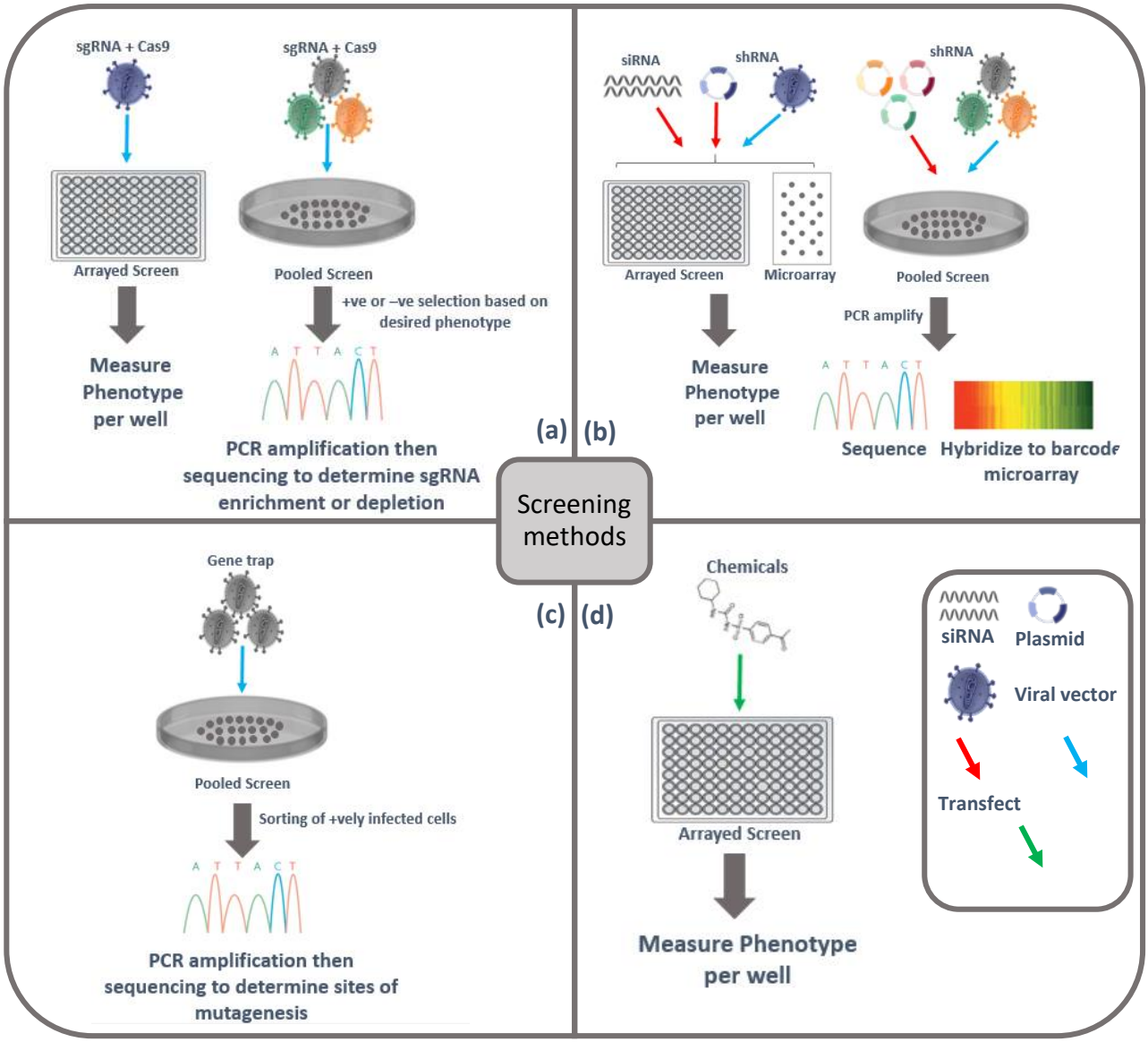

Figure 19 Screening Formats and Methods.

(a) CRISPR-Cas9 screening requires the delivery of the sgRNA and Cas-9 through viral vectors to infect cells in either an arrayed format, followed by the detection of phenotypic changes in each well or in a pooled format in which cells are positively or negatively selected based on the phenotype of interest, followed by PCR amplification and sequencing for the identification of the sgRNA that is enriched or depleted. (b) RNAi screening can be done by transfecting siRNA or shRNA plasmids or by transducing cells with shRNA viral vectors. These three forms can be used in the arrayed or micro arrayed format to target one gene per well/spot and measure readout. The pooled format utilizes shRNA in plasmids or viral vectors. The readout can be assessed by PCR amplification and sequencing of shRNA, or the barcode containing shRNA can be hybridized to the barcode microarray. (c) Insertional mutagenesis requires the transduction of cells in a pooled format with viral vectors carrying a gene trap cassette. Once the latter is inserted, the cells will be sorted if they are positively transduced and carry the phenotype of the insert. PCR amplification and sequencing will then enable the identification of sites of mutagenesis. (d) Chemical screens are initiated by treating cells in an arrayed format with one drug per well. The difficulty to track individually every drugs' effect and the possibility of interaction between drugs renders it impossible for this assay to be carried out in a pooled format. Different phenotypic outputs can be assessed after the arrayed format treatment. CRISPR: clustered regularly interspaced short palindromic repeats, sgRNA: single guide RNA, siRNA: short interfering RNA, shRNA: short hairpin RNA

MATERIALS AND METHODS

1. CELL CULTURE

1.1 CELL LINES

Wild type (AG10076) and XP-C (GM15983) immortalized patient derived-fibroblasts were purchased from Coriell Biorepository. XP-C fibroblasts possess a two-base pair shift mutation at codon 431 of the *XPC* gene. Primary XP-C cell line GM14867 (Coriell Institute) and FMA164 were also utilized for confirmation. The cells were cultured in DMEM high glucose, GlutaMAX™ media (Gibco^{tM}) supplemented with 10% FBS and 1% penicillin/streptomycin at 37°C in a 5% CO2 incubator.

1.2 CONFLUENCY ANALYSIS

Since specific cell confluencies are favored during the steps of chemical drug treatment, siRNA transfection and irradiation, the growth of the two cells was monitored as function of time. For that, different densities of each cell line (between 1000 to 20,000 cells/well) were seed in 96 well plates and monitored. Images of the cells were captured once per day at the same time point for 5 consecutive days using Zen Axio-observer then analyzed with PHANSTAT FIJI plugin with Halo correction for the automatic determination of cell confluency as function of time and seeding density.

2. IMMUNOFLUORESCENCE AND ASSOCIATED MICROSCOPY

For the characterization of cytoskeleton and XPC expression, both cell lines were seeded in 96 well microplates then fixed with 4% paraformaldehyde followed by permeabilization using 0.2% Triton X-100 and saturation with 3% FBS in PBS. Primary antibodies targeting XPC (mouse, santa cruz, sc-74410), Cytokeratin 14 (mouse, abcam, ab7800) and Vimentin (rabbit, abcam, ab92547) were utilized then incubate with 2ry Abs Alexa Fluor 488 (goat anti-mouse, Invitrogen) or Cy3 (goat anti-rabbit, Jackson). For YAP translocation, XP-C and WT cells were transfected with either siAS or siLAST1 then irradiated at dose 0.02J/cm^2. One hour post irradiation the cells were fixed then stained with YAP antibody (Santa Cruz). 2ry mouse-CY5 antibody (Jacksons Lab) was ten incubated together with FITC-Phaloidine (Thermofisher Scientific). Nuclear DNA was counter-stained with Hoechst (Sigma-Aldrich). Cell images were acquired by the Zen Axio-observer.

3. UVB DOSE RESPONSE

To examine the photosensitivity of XPC cells relative to WT in response to UVB irradiation both cells were seeded in 96 well plates until 80% confluency, washed with PBS then subjected to increasing doses of UVB. 24hrs post UV, the viability of the cells was recorded as a measurement

of the cells' reducing capacity by Presto Blue (Thermofisher Scientific) according to manufacturer's suggestion. The LD50 for each cell line was calculated.

4. QRT-PCR

Total RNA was isolated using RNeasy plus mini kit (Qiagen) then quantified using Nanodrop 1000. 1µg of RNA was reverse transcribed to cDNA using the Superscript vilo cDNA synthesis kit (Invitrogen). Next, 5µL of cDNA (5ng/µL) was used in qPCR reactions with gene-specific primers targeting XPC, PIK3C3, LAST1, FOXN1 and GAPDH (Qiagen). qPCR was performed by Platinum SYBER Green qPCR SuperMix-UDG (Invitrogen). Samples were run in triplicates through BioRad CFX96™ Real-time Sys (C1000 Touch™ Thermal Cycler). Melt curve analysis was conducted to ensure the specificity of the utilized primers by having a single melt-curve peak. Expression level of the target gene was normalized to the expression of glyceraldehyde-3-phosphate dehydrogenase (GAPDH) housekeeping gene. Relative expression levels were calculated based on the $2^{-\Delta\Delta CT}$ method reported Livak et al.[337].

5. PROTEIN EXTRACTION AND IMMUNOBLOTTING

Total proteins were extracted with REPA buffer (Sigma Aldrich) supplemented with protease and phosphatase inhibitor cocktail then dosage was carried out with BCA protein quantification kit (Life Technologies). Western blotting was performed as previously described [338]. Briefly, equal amounts of proteins were resolved by SDS-PAGE and transferred to nitrocellulose membrane (IBlot gel transfer, Life Technologies). The membrane was saturated with 5% lyophilized milk and primary antibodies were incubated at 4ºC overnight. Following the incubation with 2ry anti-HRP antibodies western lightening ECL Pro ECL (Perkin Elmer) was added and images were recorded using Biorad Molecular Imager® Chemi Doc™ XRS and analyzed using Image Lab™ software. For phosphorylation experiments, the membranes were stripped using ReBlot Plus Mild Antibody Stripping Solution (Merck), washed, blocked with 5%BSA then re-incubated with primary Ab following the previous protocol.

Table 4 Source of the utilized antibodies and their dilutions

Targeting Protein	Supplier	Dilution	Targeting Protein	Supplier	Dilution
P53	Sigma	1/6000	**PIK3C3**	Sigma	1/1000
p-P53 Ser15	Cell Technologies	1/2000	**LATS1**	Sigma	1/1000
AKT	Cell Technologies	1/2000	**GAPDH**	Santa Cruz	1/5000
p-AKT Ser473	Cell Technologies	1/2000	**XPC**	Santa Cruz	1/500
UVRAG	Cell Technologies	1/1000	**Yap**	Santa Cruz	1/1000

6. DNA LC-MS/MS

The quantification of pyrimidine dimers (CPD & 6-4PP) was carried out by LC-MS/MS according to previous protocol [339]. Briefly, both cell lines were seeded in 100mm dishes until sub-confluency where they were subjected to a UVB dose of 0.01J/cm^2. At different time points post UV (0, 2, 24 and 48h) the cells were collected and their DNA extracted with Qiagen DNEasy Kit (Courtaboeuf, France). Sample preparation was carried out in two steps, the first includes incubation of DNA for 2 hours at 37°C and pH 6 in the presence of nuclease P1, DNase II, and phosphodiesterase II. The pH was then raised to 8 by the addition of Tris. A second incubation period in the presence of phosphodiesterase I and alkaline phosphatase at 37°C for 2 hours yielded digested DNA with normal bases as nucleosides and photoproducts as dinucleoside monophosphates. Samples were then injected on an HPLC system (Agilent, Massy, France) connected to a reverse-phase HPLC column (150_2mm ID, 5 mm particle size, ODB, France). The detection was provided first by a UV detector aimed at quantifying normal nucleosides. Photoproducts were detected by a tandem mass spectrometer (API 3000, SCIEX, Thornill, Canada) used in the reaction-monitoring mode as previously described [340]. The four CPDs and the four 6-4PPs (TT, TC, CT, and CC derivatives) were quantified individually in the same HPLC run. Results were expressed in the number of lesions per million normal bases.

7. DNA REPAIR ICC AND SINGLE CELL ANALYSIS

For the quantification of DNA damage, cells were seeded and treated with the different conditions either drugs or siRNA. The cells were then further on subjected to UVB irradiation. 24h post UV, the cells were stained according to previous protocol [341] consisting first of cell fixation with 4% paraformaldehyde and permeabilized with 0.2% Triton X-100. Cells were further on treated with 2M HCL to denaturate the DNA and thus allow access to the DNA damage-targeting antibody. After saturation, the cells were incubated with 6-4PP antibody (64M-2 cosmo bio) followed by AF488 secondary antibody (Invitrogen) and the DNA was counterstained with Hoechst (Sigma Aldrich). Image acquisition and quantification were carried out by Cell-insight NXT high content screening platform at 10X magnification. Single-cell fluorescence was quantified for all the cells under each particular treatment condition.

8. CELL PROLIFERATION ASSAY

Cell health and genotoxicity can be assessed by staining the cells with ki67 antibody or by measuring the cell's ability to proliferate via the incorporation of the nucleoside analog EDU. For KI67 staining and single cell analysis, the cells were seeded until sub-confluency then subjected to UVB irradiation at a dose of 0.02J/cm^2. 24h post-irradiation the cells were fixed with 4% paraformaldehyde and permeabilized with 0.2% Triton X-100. After saturation, the cells were incubated with ki67 antibody (clone MIB-1, Clinisciences) followed by AF488 secondary

antibody (Invitrogen) and the DNA was counterstained with Hoechst (Sigma Aldrich). Image acquisition and quantification were carried out by Cell-insight NXT high content screening platform at 10X magnification. Single-cell fluorescence was quantified for all the cells under each particular treatment condition.

Cell proliferation can also be examined via the incorporation of the nucleoside analog EDU. The latter can be further on quantified by a click-it covalent reaction between an azide and alkyne catalyzed by copper. For that, both cell lines were seeded in 100mm dishes subjected to different forms of treatment followed by irradiation. Sham irradiated and sham-treated controls were also utilized. Two hours before the end of post UV incubation EDU was diluted in the cell media at different time points. The cells were then collected and stained according to the manufacturer's protocol. The samples were analyzed by flow cytometry (FACScan, BD LSRII flow cytometer, BD Biosciences). The post analysis was carried out using flowing software[342] (Turku Bioimaging, Finland).

9. APOPTOSIS-CELL EVENT QUANTIFICATION

To follow the effect of treatment on the induction of apoptosis post UV irradiation cell event (Thermofisher Scientific) was utilized that allows the measurement of caspase 3/7 activity. For that cells were seeded in 100mm dishes, treated with the molecules, irradiated them cells event was added post UV and incubated for 24hrs. The cells were then collected and PI was added before their analysis by flow cytometer (FACScan, BD LSRII flow cytometer, BD Biosciences). The post analysis was carried using flowing software[342] (Turko Bioimaging, Finland).

10. COMET ASSAY FOR THE QUANTIFICATION OF OXIDIZED PURINES

Comet assay is a single-cell gel electrophoresis assay that is used to measure the DNA lesions of cell extracts, and consequently, can monitor the excision repair capacity when it is employed at various time points post-treatment of cells. More specifically, upon adding FormamidoPyrimidine [fapy]-DNA Glycosylase (FPG) enzyme, we were able to detect 8-oxoguanine excision activity. Hydrogen peroxide (H_2O_2, 400µM) was used as an internal positive control. Cells were plated in 6 well plates as triplicates, transfected with siAS, siPIK3C3 or siLATS1 then irradiated with 0.02J/cm² UVB-irradiation to be collected after 0, 2 and 24 hours. Cells were harvested, counted and suspended at a concentration of 200 000 cells in 100 µL freezing buffer. Samples were stored at -80°C until use. Slides were prepared with normal agarose coating 219 one day in advance. On the day of the experiment, cells were deposited on the slides with 0.6 % solution of low-melting agarose followed by adding a coverslip, immersing in lysis buffer, and incubation for 1 hour after which a 3 times wash with Tris-HCL 0.4 M (neutralizing buffer) was done. FPG 0.05 u/µL (1.25 µL/slide) was then prepared in which 100 µL FPG solution with or without FPG enzyme was deposited on the slides and covered with coverslips. The slides were set on a humidified bed and added in a 37°C incubator for 40 minutes. The reaction was stopped by incubation for few minutes on ice. After digestion, the slides were transferred to an electrophoresis tank filled with electrophoresis buffer pre-chilled at 4 °C. The slides were left at room temperature for 30 min and electrophoresis was subsequently done for 30 min at 25 V and 300 mA. The slides were then rinsed

3 times with Tris-HCL 0.4M. 50 µL of Gel Red was added per slide and a coverslip was added for reading on next day. We read the slides using a 10X objective microscope and Comet Assay IV software (Perceptive Instruments, Suffolk, UK). 50 randomly selected nuclei were scored in each slide and triplicate slides were processed for each experimental point. The extent of damage was evaluated by the Tail DNA value defined as the percentage of DNA in the tail of the comet.

11. IMMUNO-PRECIPITATION

For the detection of autophagy protein interaction modulation following PIK3C3 knockdown, XP-C cells were transfected with either siAS or siPIK3C3 then irradiated at 0.02J/cm^2. Proteins were further on extracted using RIPA buffer supplemented with protease inhibitors. 1mg/ml of protein was incubated with either an IgG isotype or Beclin antibody (Cell Technologies) together with protein G Magne Beads (Promega). The complexes were incubated overnight at 4 degrees after which the beads were washed with the lysis buffer and the proteins and antibodies were eluted from the beads using LDS loading buffer and reducing agent (Invitrogen). The elutes as well as the input protein were resolved on SDS page and blotted with UVRAG antibody (Cell Technologies) to analyze the UVRAG-Beclin interaction.

12. 3D RECONSTRUCTED DERMAL EQUIVALENT

For the construction of dermal equivalent, 0.4 million XP-C fibroblasts were added to a hydrogel consisting of fibrinogen, aprotinine, thrombin, $CaCL_2$ and $NaCl_2$. The mixture was seeded in an insert and placed in the incubator for 30min to allow polymerization then was supplemented with Glutamax DMEME high glucose media supplemented with EGF, vitamin C, amphotericin, P/S and SVF. The dermal equivalent was cultured for 14 days to allow maturation. Three days prior to the end of culture the dermis was transfected with either siAS or siPIK3C3 using lipid particles. The dermal equivalents were then irradiated at the end of culture time with UVB at a dose of 0.01J/cm^2. Post irradiation the dermis was cultured in the presence of cell event for twenty four hours after which the dermis was dehydrated by a sucrose gradient and frozen with OCT. Samples were then sliced with cryotome then fixed with 4% PFA. Staining for both 6-4PP and PIK3C3 expression was carried out according to the protocol discussed earlier. Hoechst was used for counterstaining the nuclei. Image acquisition was carried out using Zeiss microscopy at 10X magnification.

13. STATISTICAL AND BIOINFORMATICS ANALYSIS

Screening hit selection and single cell analysis were carried out by R software[343]. GraphPad Prism v.8 was used for statistical analysis, data normalization and quantification of normality to allow the downstream selection of the respective statistical test (parametric or non-parametric) for each particular set of experiments. Functional annotation of pathways related to the siRNA hits was conducted using enricher bioinformatics tool. Protein interaction for siRNA hits was conducted using string bioinformatics tool.

AIM OF THE PROJECT

Mutations in DNA damage recognition protein, Xeroderma Pigmentosum protein C (XPC), hinders repair of UV induced photoproducts and increases skin cancer incidence. XP-C patients' cells are characterized with increased photosensitivity and accumulation of DNA damage post UV. Till date, there is no approved treatment for XP-C with only preventative measures at action. However, despite the diseased phenotype caused by XPC mutation, not all mutations are deleterious. This lead to the concept of suppressor mutations defined as secondary mutations in the genome that can help reverse the effect of a primary mutation. Therefore, based on the concept of suppressor mutations, our aim is to identify molecules that can reverse the phenotype of XP-C cells. We screened libraries of approved chemical drugs and kinase targeting siRNAs to mimic suppressor mutations and identify potential therapeutic targets in XP-C. The screening of approved drugs can allow for the possible drug re-purposing enabling a swift switch in the mode of action of the selected drugs toward a new purpose. The potential use of siRNAs in therapy can be possible via identifying the appropriate and selective delivery method. Also the possibility of substituting the siRNAs with kinase targeting drugs exhaustively explored in the literature provides another alternative for the feasibility of such therapy.

RESULTS AND DISCUSSION

CHAPTER 1. CHARACTERIZATION OF THE CELL LINES

1. IMMUNOCYTOCHEMISTRY OF XPC AND CYTOSKELETON

It is imperative, prior to the screening procedure, to characterize the cells' XPC expression ensuring that it's differentially regulated between the WT and XPC mutated fibroblasts. For that, both cell lines were immune-stained with antibody targeting XPC. XPC cells showed the absence of this protein compared to the normal cells. In addition, due to the difference in cell morphology between the two cell lines additional markers were utilized including vimentin, a fibroblast intermediate filament that revealed the equal wide spreading of cytoskeleton in the normal cells compared to the peri-nuclear localization in XPC cells. Moreover, XPC cells were also stained with cytokeratin 14, a keratinocyte intermediate filament, to ensure that they are indeed fibroblasts despite their keratinocytes like morphology (small and round morphology) (figure 20).

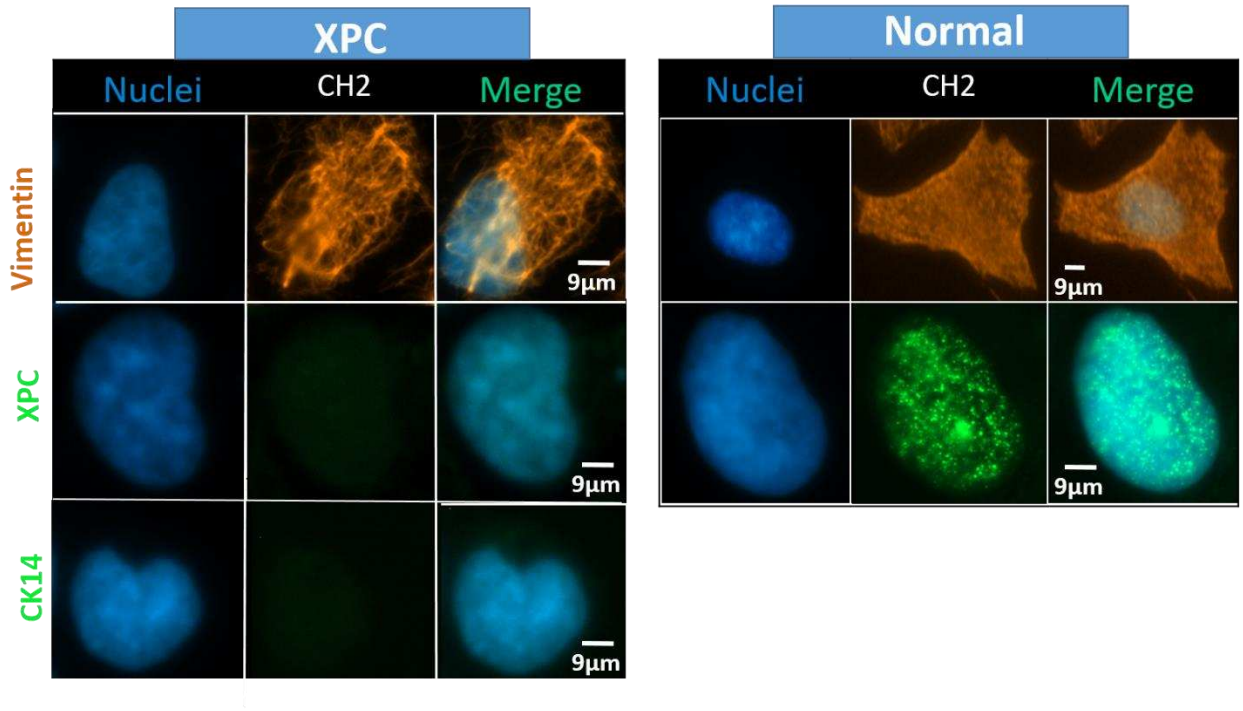

Figure 20 Characterization of the WT and XP-C cell lines by immunustaining.

XP-C and WT cell were seeded in 96 well plates then fixed and stained with different Antibodies for the analysis of XPC expression as well as the cytoskeleton.. XP-C cells show absence of XP-C protein compared to WT cells detected via the incubation with XPC antibody. Both cell lines are positively stained with vimentin, a marker for fibroblast. XP-C cells despite having a keratinocyte like round phenotype stain negatively with CK14 confirming their fibroblast nature.

2. ASSESSING XPC EXPRESSION AT THE RNA AND PROTEIN LEVEL

The expression of XPC mRNA and protein was examined in both WT and XP-C cells immortalized from patient primary fibroblasts. RT-PCR quantification of XPC mRNA revealed a highly significant five-fold decrease in XPC mRNA in XP-C cells compared to WT (p-value<0.0001). At the protein level, western blot analysis revealed the total absence of XPC protein expression in XP-C cells unlike the WT cells (p-value<0.001). Since the cells were both immortalized with SV40, the P53 expression at the protein level was also examined by western blot where both cells showed P53 expression. XP-C cells displayed a significant 1.5 increase in P53 expression compared to WT cells (p-value<0.01) (figure 21).

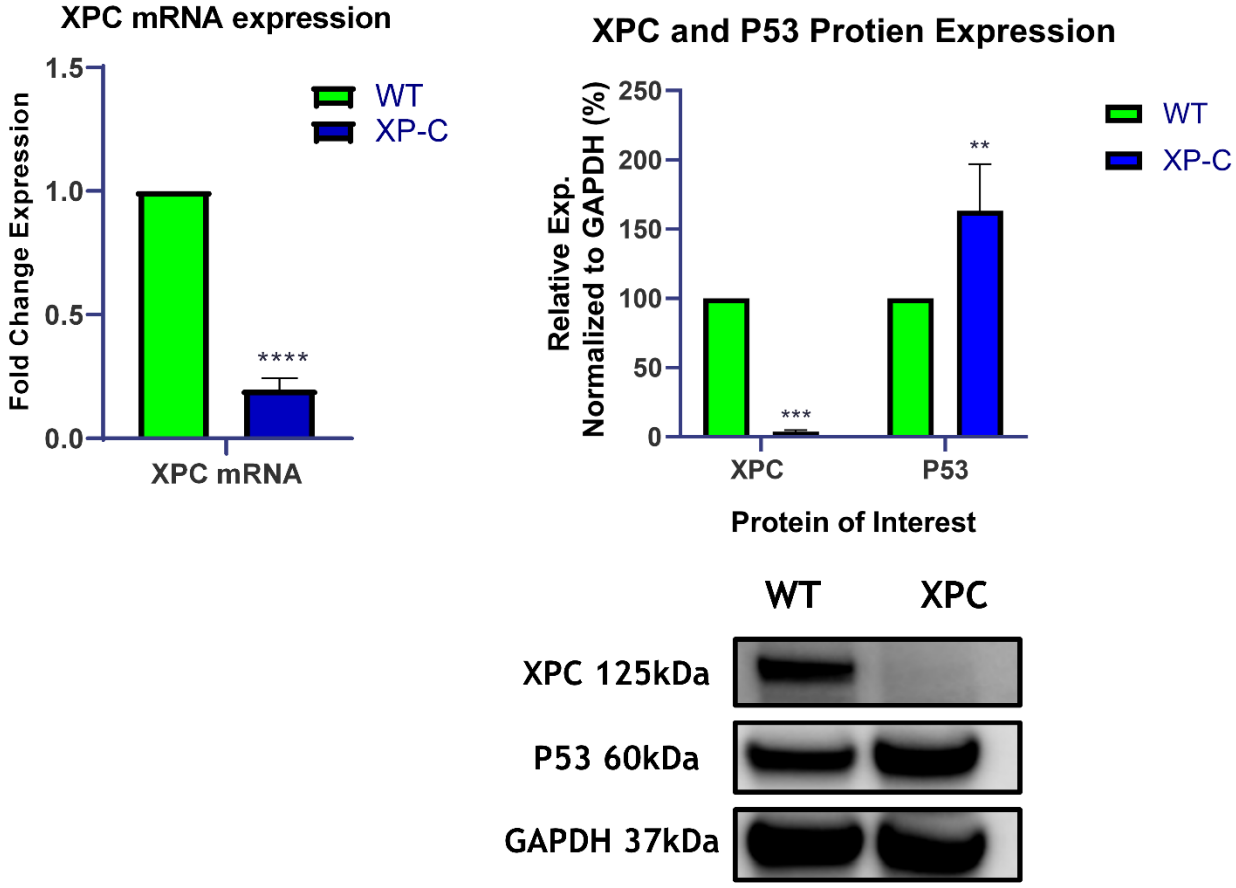

Figure 21 Downregulated expression of XPC mRNA and protein in XP-C cells with upregulated P53 expression compared to WT.

*RNA and protein extraction was carried out for both XP-C and WT cells to analyze the expression of XPC using RT-PCR and western blot. XP-C show significantly downregulated expression of XPC mRNA with total loss of XPC protein compared to WT cells. XP-C cells also show higher levels of P53 expression compared to WT cells. Unpaired t-test *** p-value <0.001, **** p-value<0.0001*

3. UVB PHOTOSENSITIVITY

To examine the photosensitivity of XP-C cells relative to WT, both cell lines were seeded until 80% confluency then subjected to increasing doses of UVB. After 24 hours, cells' viability was recorded as a measurement of the cells' reducing capacity by Presto Blue. Viability was normalized based on the percent of control calculation[344] with non-irradiated sample defined as controls and set as 100% viability. The LD50 of UVB was determined for both cell lines. Both cell lines showed a decrease in viability as a function of increased UVB doses. XP-C cells were more photosensitive showing a sharper significant ($p<0.001$) decrease in viability compared to the WT ones at each UVB dose. XP-C cells also showed a lower LD50 (about 0.02j/cm^2) compared to WT cells that required a considerably higher dose (about 0.19j/cm^2) to mediate an equal lethality of 50% (figure 22).

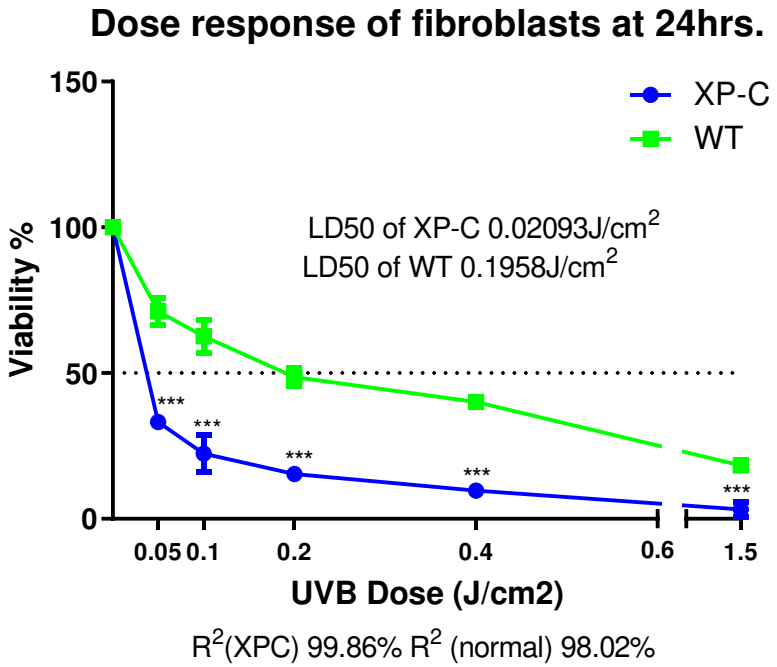

Figure 22. XP-C cells manifest increased sensitivity to UVB irradiation

*Viability of fibroblasts 24h post UVB. XP-C cells manifest significantly increased photosensitivity compared to WT cells. Both XP-C and WT cells were seeded in 96-well plates to be irradiated at 80% confluency with increasing UVB doses then their viability was quantified 24hours later by the incubation with PrestoBlue. XP-C cells show a sharper significant decrease in viability as a function of increased UVB dose compared to WT cells. Viability was calculated by means of percent of control with 100% control being non-irradiated cells. *** p< 0.001, unpaired t-test. Results presented are the mean of three technical replicates.*

4. DNA REPAIR KINETICS BY LC-MS/MS

XPC protein is essential for lesion recognition step of GGR[80]. For that, we aimed to determine the effect of *XPC* mutation on the repair of lesions. The two major photoproducts generated after UVB exposure are CPDs and 6-4PPs that are formed between pyrimidine dimers either TT, TC, CT, or CC. Quantification of these lesions was carried out by LC-MS/MS. The cells were seeded until 80% confluency then irradiated at 0.01 j/cm^2 then collected post UV at different time points. Following that, DNA was extracted and digested to be analyzed by LC-MS/MS. For CPDs, the 4 different lesion types were quantified. WT cells showed a decrease in different CPDs lesions' amounts as a function of time to reach a minimum after 48hrs signifying repair of DNA damage compared to XP-C cells who showed elevated amounts of lesions as a function of time. It should be noted that not all lesions were present in the DNA in the same quantities where the majority of CPD lesions were of TT-CPD nature to be followed by TC-CPD, CT-CPD where the least abundant lesion was CC-CPD. In addition, the repair kinetics differed between lesion types with the fastest repair for the CT-CPD in normal cells. Only the TT and TC lesions could be detected for the 6-4PPs, as the two remaining lesions were less frequent. 6-4 PPs were repaired faster than CPD with total repair 24hrs post UV in WT cells compared to the higher amounts of lesions in XP-C cells. There were no discrepancies in the repair kinetics between the TT and TC 6-4PP lesions in normal cells (figure 23).

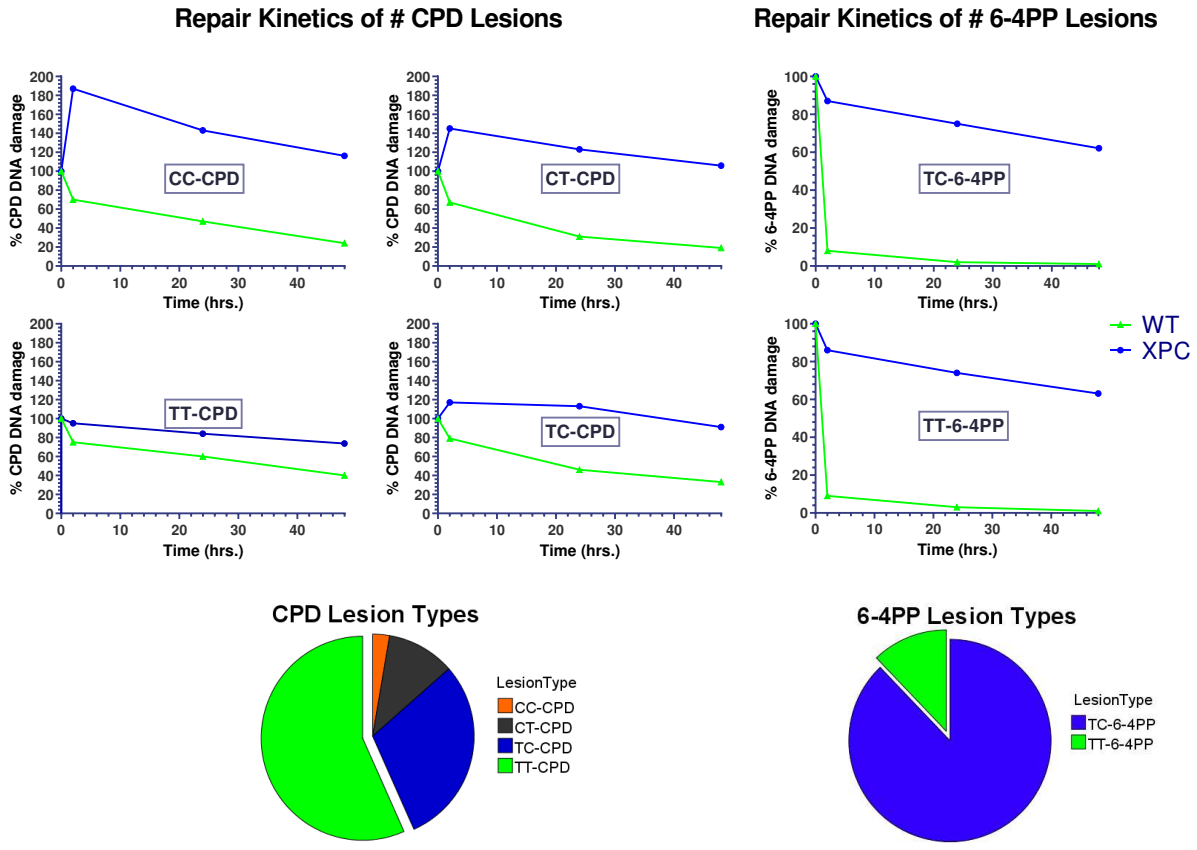

Figure 23 XP-C cells show decreased pyrimidine dimer repair kinetics compared to WT cells.

WT cells manifest faster repair kinetics of both CPD and 6-4PP lesions post UV compared to impaired repair in XP-C cells. Both cell lines were subjected to UVB then incubated for different time points post UV (0, 2, 24 and 48hours). At each time point, cells were collected, their DNA extracted and digested to be then analyzed by LC-MS/MS. Four different CPD lesion types (TT, TC, CT, CC) were quantified with TT-CPD being the most frequent. Normal cells show a decrease in the % of CPD lesions as a function of time signifying repair with different kinetics per lesion time. XP-C cells, however, manifest an increase in CPD lesion at 2h post UV and continue to have a large amount of lesion % as time elapses, a sign of impaired repair. Two lesion types were quantified for 6-4PP with TC-6-4PP being more abundant. Similar to CPD, impaired repair is visualized in XP-C cells manifested by a slow decrease in lesion % as a function of time compared to the normal cells which in contrast to CPD lesions show even faster repair for 6-4PP.CPD: cyclobutane pyrimidine dimer, 6-4PP: 6-4 photoproducts, WT: wild type, XP-C: Xeroderma Pigmentosum C

CHAPTER 2. SCREENING METHOD DESIGN AND VALIDATION

1. CELL CONTRACTION

One of the most crucial steps of the screening procedure is irradiation for the induction of DNA damage to be followed by the analysis of photosensitivity and damage repair. The latter requires aspiration of the media, washing of the cells with PBS, irradiation in the presence of PBS to be followed by the addition of media back to the cells with 24hrs incubation. The washing steps allow the removal of all traces of molecules from the media that can either absorb UVB and become oxidized or block the delivery of the rays to the cells. Unfortunately, the XPC cells manifest weak adhesion to the culture plates resulting in detachment of the cells upon the different washing steps and the contraction of the cells from the edges of the well. The following phenomena are not due to irradiation step that renders the cells contracted but rather the washing step as even non-irradiated cells manifested the same phenomena when undergoing the same steps of washing.

To tackle this issue several parameters were modified (figure 24). The optimal parameters were the aspiration of only 60-80% of volume in the well to prevent cell drying and contraction from the well edges. The use of reduced serum media Opti-MEM at 37° C decreased cell detachment but it was impossible to determine the effector of such result due to the undisclosed composition of this media. The latter also did not have any UVB shielding properties. Only one wash was carried out at extremely low speed (10µl/sec) and low Z position compared to the surface of the

well. The selected parameters, particularly the low speed, were not applicable for both screening platform: chemical screen platform at CMBA with lowest speed 30µl/sec which necessitates the coating of the culture plate with collagen to enable attachment.

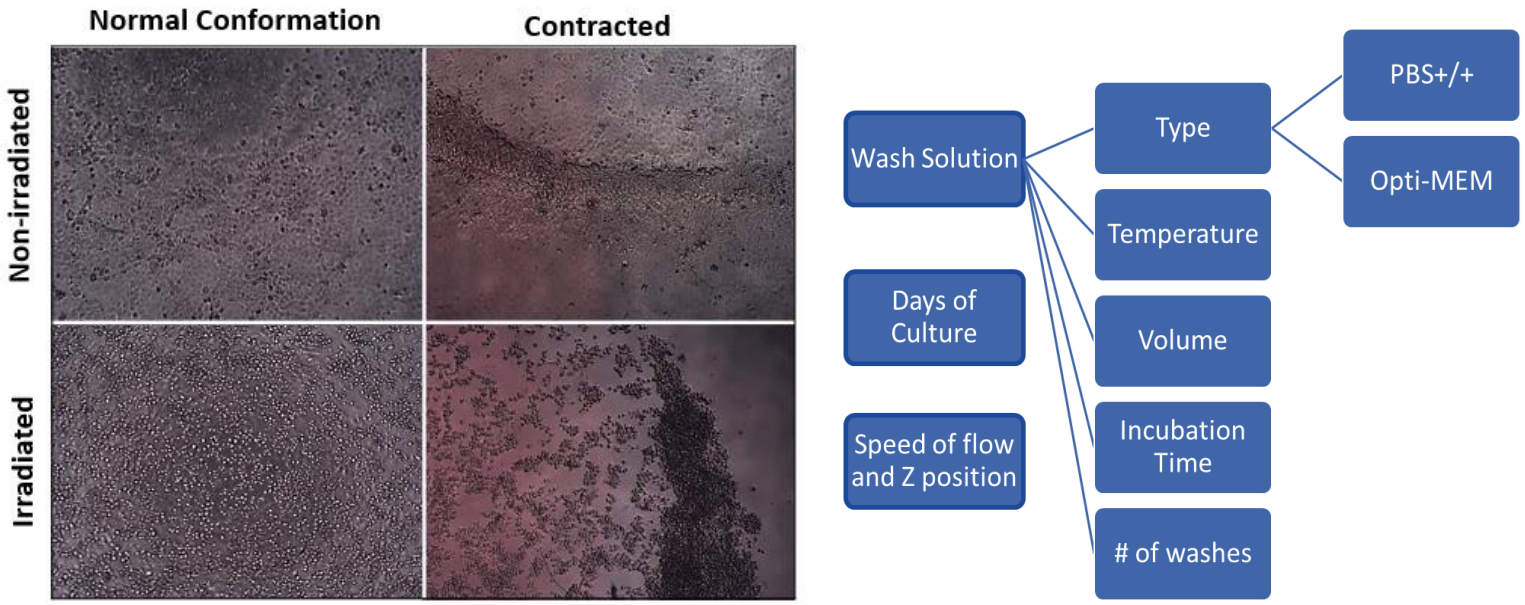

Figure 24 Optimization of cell adhesion and washing condition for the screening procedure.

Due to the fragility of the XPC cells several parameters where modified to ensure the proper adhesion of the cells during the screening procedure. Different washing solution were utilized of which optimem was found ideal. Temperature of the wash solution was kept at all times at 37°C with the shortest incubation time possible and least number of washes of one wash. The cells were kept in culture three days prior to irradiation to ensure proper amount of extracellular matrix secretion. Lowest possible Z position was utilized for the aspiration and washing of the cells at around 10-30µl/sec flow speed.

2. DESIGN OF THE CONTROLS

The aim of the study is to identify molecules that can reverse the phenotype of XPC cells. The study is novel with no known drug or siRNA in literature to serve as positive control enabling viability increase and repair. For that, concerning the chemical screen, the controls will be DMSO treated cells that are either irradiated to act as negative control or non-irradiated to act as positive control. For the siRNA screen, the cells will be transfected with non-targeting siRNA (siAS) to be either irradiated or sham treated. For the sake of elimination of between plate variation, it was important to have both controls in the same plate. However, since the whole plates will be irradiated at a time placing the positive non-irradiated controls in the same plates was not possible without modifying the plate cover to protect several wells from UV irradiation. These covers

effectively protected the cells from UV showing same viability as the non-irradiated ones even at high doses of UV for both cell lines (figure 25).

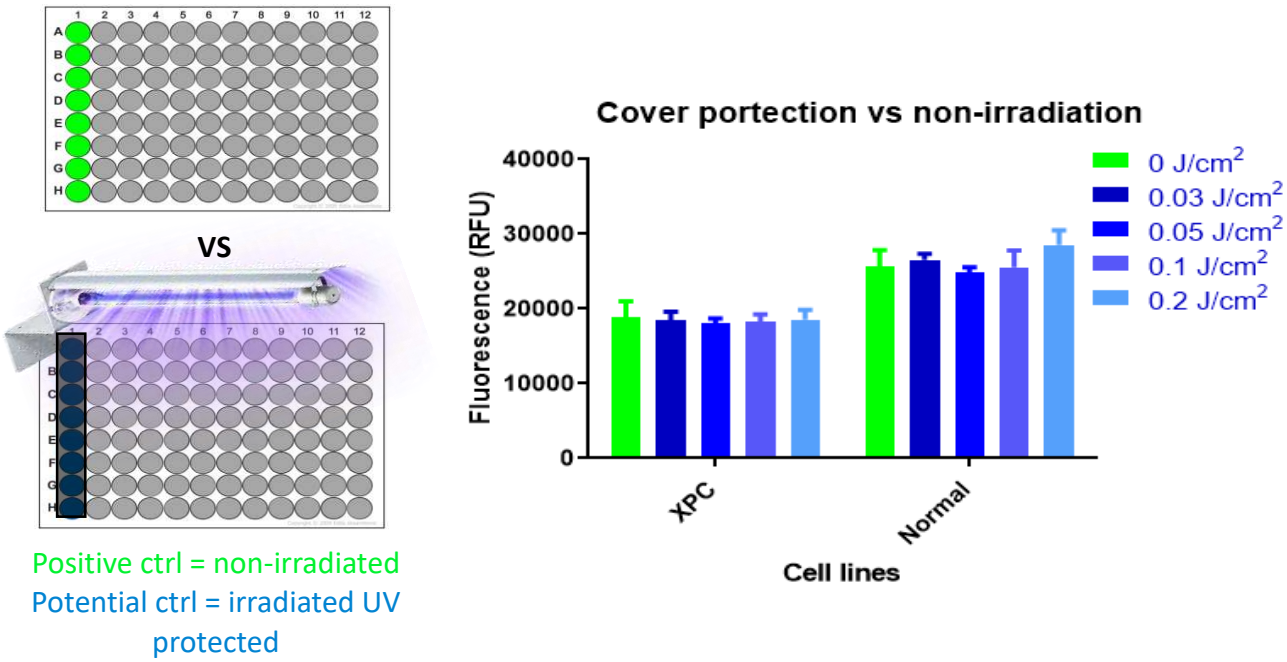

Figure 25 Validation of UV protection of control wells during the screening procedure.

For the sake of analysis and the elimination of between plates variation it is imperative to have both irradiated and non-irradiated controls in the same plate. For that, we designed a plate cover that allows the shielding of the first column of each plate from UV. The efficacy for UV protection was tested post irradiation with increased doses where both cell types showed the same viability for the protected columns compared to non-irradiated cells regardless of the irradiation dose utilized.

3. SIRNA SCREEN

For the siRNA screen, the zephyr robot was utilized and programmed with maestro software for the different pipetting steps. After the optimization of the program, the screen was held with the controls to validate the applicability of the procedure. The layout is presented below. Cells are seeded then 24hrs later forward transfected with either non-targeting siAS, siCD or non-transfected. siCD is a death inducing siRNA upon its entry in the cells hence it gives information on transfection efficiency by decreasing viability. 48hrs. post transfection cells were washed with opti-MEM, irradiated then the viability was recorded 24hrs. post UVB. The 48hrs transfection enables appropriate knockdown of the kinases as tested in our lab previously by means of kinetic analysis of knockdown post transfection. The results show good separation between the siAS irradiated vs UVB protected in both cell lines with good transfection efficiency manifested in low viability of siCD. Low toxicity exists for the transfection reagent when comparing cells incubated in presence of the reagent vs. non manipulated cells (figure 26).

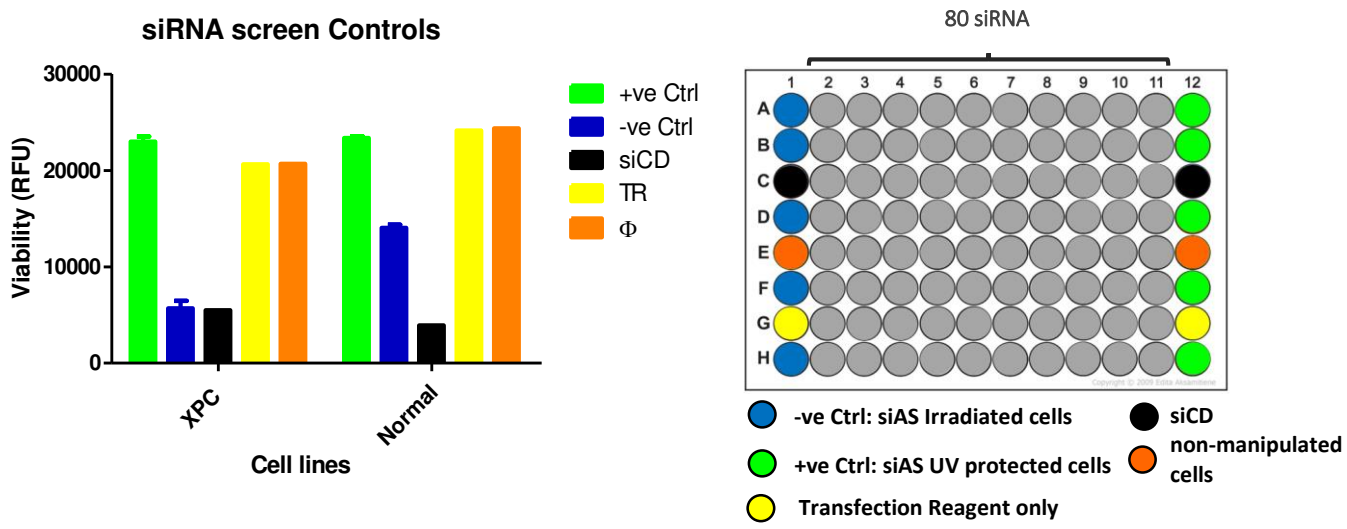

Figure 26 Design and validation of siRNA screen controls

The main controls of the siRNA screen are siAS irradiated cells (negative control), siAS non-irradiated cells (positive control), and siCD transfected cells used as control for transfection. A mock screen was carried out with these controls in both cell lines and viability was then measured via Presto Blue incubation. Good separation between the positive and negative controls was visualized in both cell lines depicted by the difference between the viabilities of irradiated vs. non-irradiated scramble transfected cell lines.

4. CHEMICAL SCREEN

For the chemical screen the robot Tecan-Freedom Evo was utilized for the different pipetting steps. After the optimization of the program the screen was held with the controls to validate the applicability of the procedure. The controls include DMSO treated UV irradiated or protected cells.

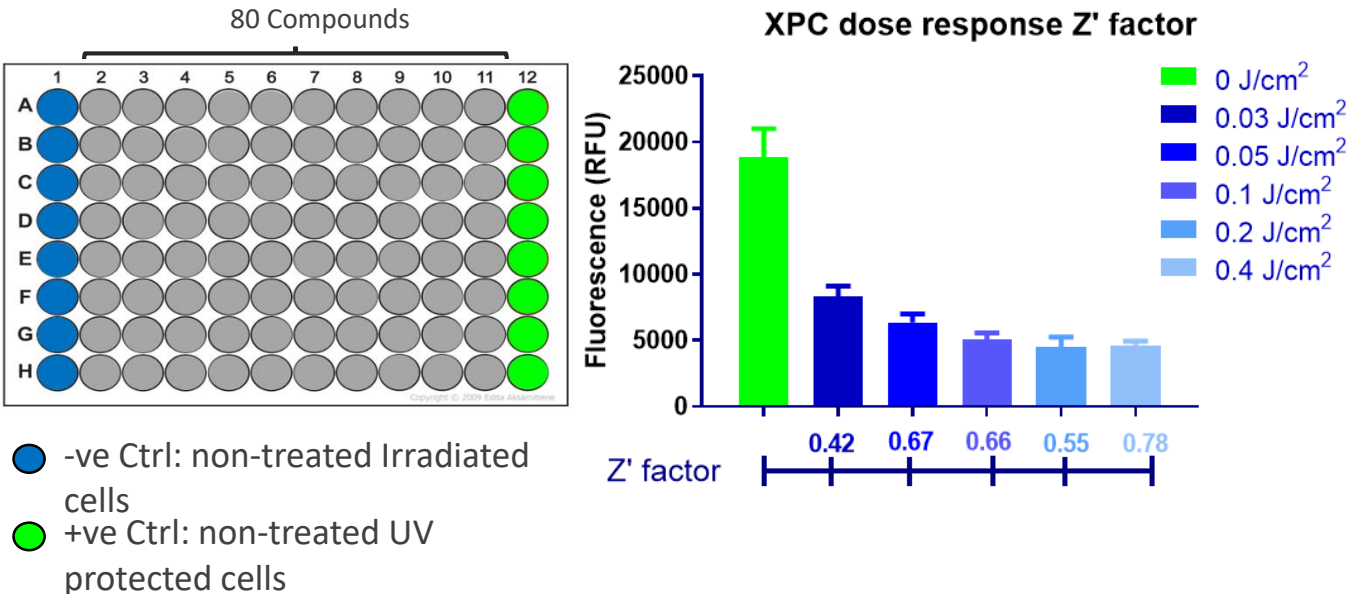

Figure 27 Chemical Screen UV dose optimization and reproducibility assessment.

To determine if the data collected from each plate meet the minimum quality requirements, quality control assessment was carried out with the controls. The latter include DMSO treated UV irradiated or protected cells. The calculation of the Z' factor was performed at the different doses to allow the selection of the appropriate dose giving a Z' factor above 0.5, without the induction of excessive cell death. This Z' factor signifies the applicability of the screen on large scale. Moreover, having a good separation between the positive and negative is a hallmark for cell reproducibility, for that several UV doses where tested. The dose 0.05j/cm^2 was chosen as it is the lowest lethal dose with a Z' factor above 0.5

Moreover, it is imperative to have good separation between the positive and negative control to have a reproducible assay, for that several UV doses were tested. The calculation of the Z' factor was performed at the different doses to allow the selection of the appropriate dose giving a Z' factor above 0.5, without the induction of excessive cell death, signifying the applicability of the screen on large scale. The dose 0.05j/cm^2 was chosen as it is lowest dose with a Z' factor above 0.5 (figure 27).

5. READOUTS

XPC phenotype comprises increased photosensitivity and accumulation of DNA damage. Therefore, for the reversal, the readouts should allow the measurement of cell viability and amount of residual DNA damage post UV to test whether either form of treatment can reverse the XPC phenotype.

5.1 VIABILITY

For the measurement of cell viability, a reproducible and fast assay is required therefore several products were considered. Presto Blue was utilized that measures the reducing capacity of cells. Its advantage is that it is a live cell assay that is not destructive to the cells like other viability reagents including MTT. It is also relatively more sensitive and requires low incubation time. Other than choice of reagents, the time point for the readout measurement was also optimized. The viability of both cell lines was measured post UVB irradiation with different doses and as function of different time points (24, 48, 72, 96hrs. post UV). The biggest separation between the viability of XPC and WT cells was observed with 24hrs. Having a good separation between the two cell lines aid in the identification of molecules that can increase the viability of XPC cells and render it close to that of WT when irradiated at the same dose. Beyond that, as the incubation time increases the gap between both cell lines decreased making it harder to use such time points for the screen. Therefore, 24hrs. post UV incubation was selected as readout time point for viability (figure 28).

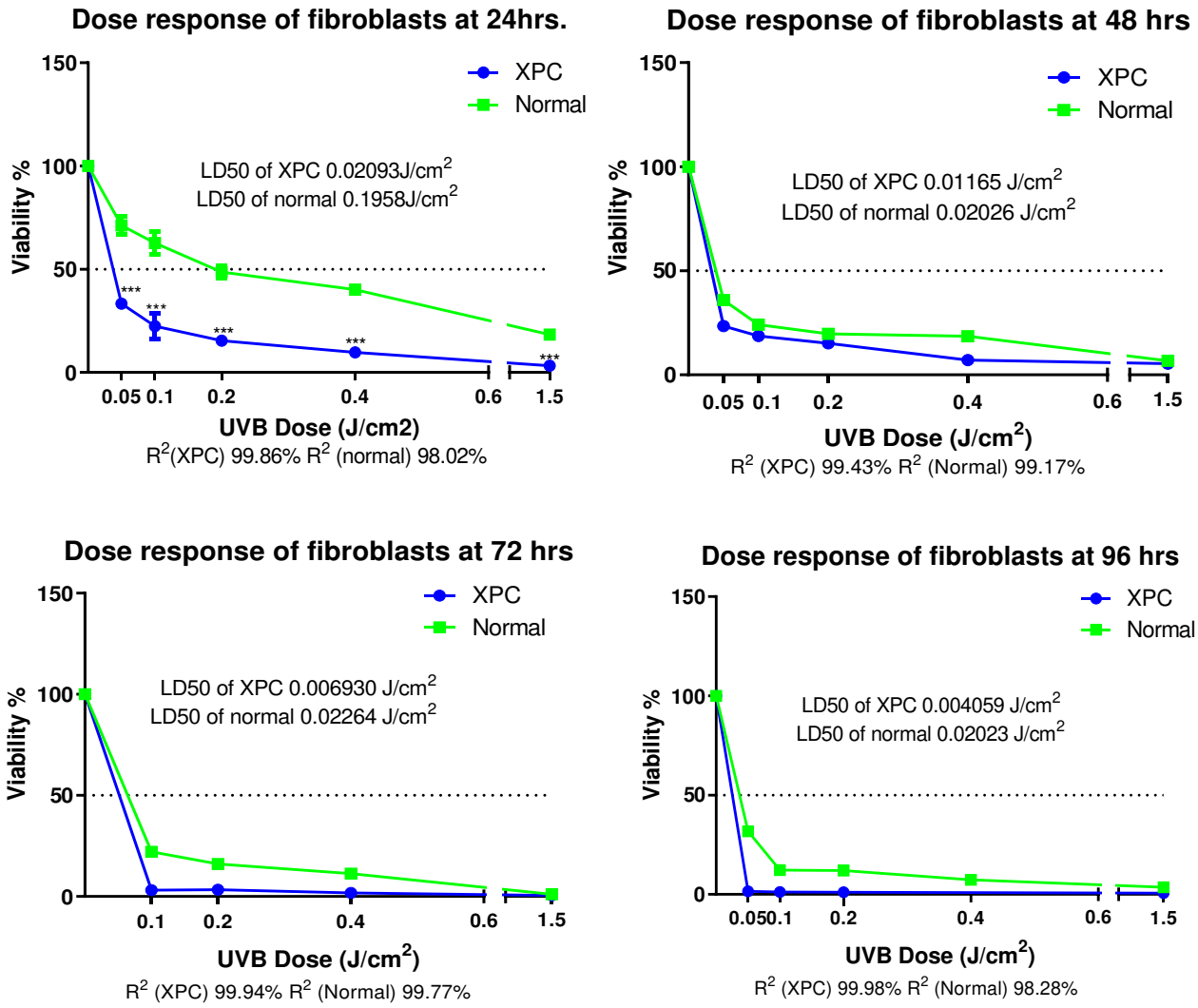

Figure 28 Optimization of the incubation time post UV for XP-C and WT cell lines.

For the carrying out the screening procedure, a readout based on viability was utilized. XP-C and WT cells were seeded in 96 well plates until 80% confluency then irradiated with different UVB doses. Several incubation times post UVB irradiation were tested including 24, 48, 72 and 96hours post UV. The incubation of 24hours post UV was the optimal one showing lowest toxicity range post UV still showing a good separation between XP-C and WT cells.

5.2 DNA DAMAGE

UVB induces the formation of two types of direct DNA damages that are the cyclobutane pyrimidine dimers (CPD) and the 6-4 pyrimidine pyrimidone photoproducts (6-4PP). The lesions require 48hrs and 24hrs, respectively, to be repaired in WT cells while they accumulate in XPC cells without repair. The quantification of DNA damage post treatment allows the identification of molecules that can decrease such damage in XPC cells. In the aim of extracting more data from

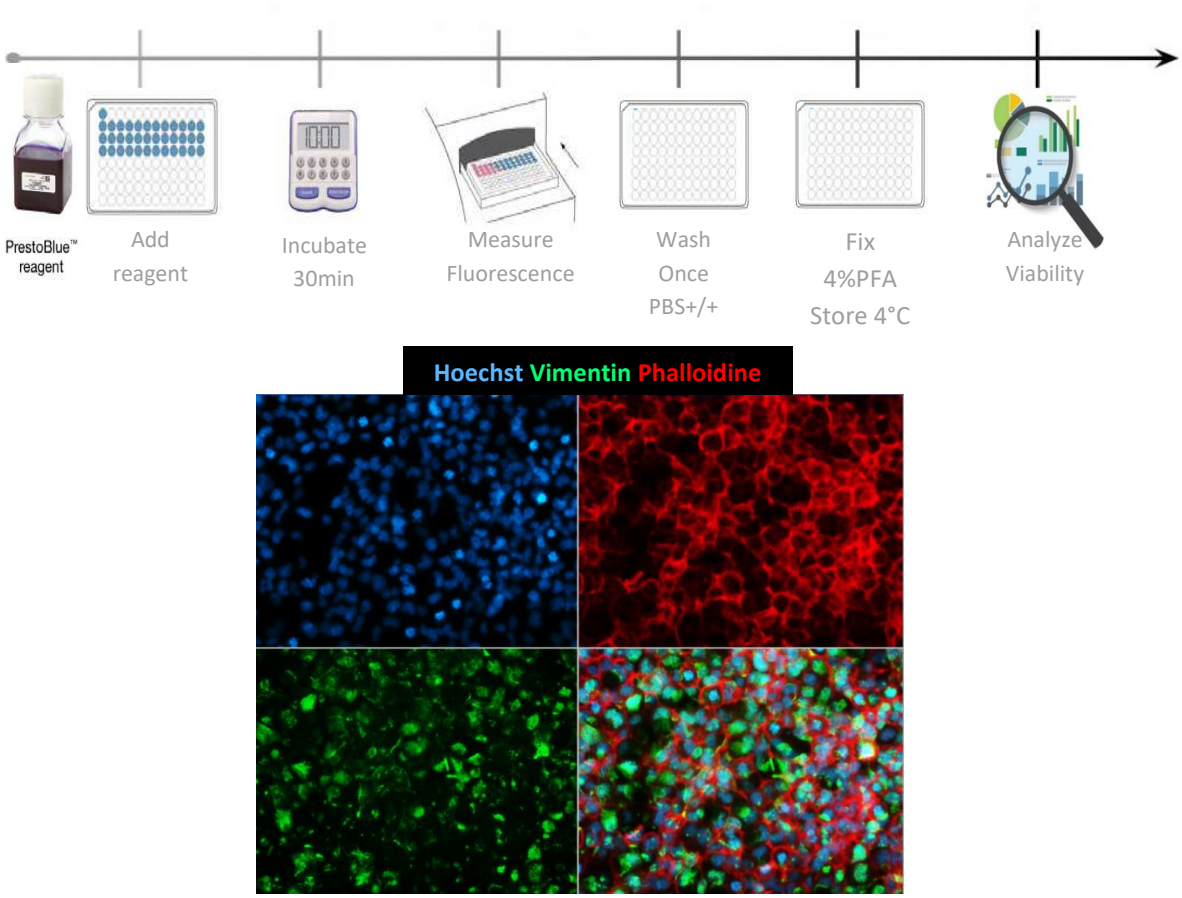

Figure 29 Multiplexing of Viability and Immunofluorescence readouts and the procedures followed.

For the sake of screening, it was imperative to test the possibility of performing both readout on the same plates. Presto Blue was said to be a live cell assay with limited toxicity on cells thus, we tested whether we can preserve cell integrity after Presto Blue incubation and washing steps then cell fixation. After testing several washing steps the cells were further on fixed and stained with vimentin, phalloidine and Hoechst. Indeed cells showed normal staining for intracellular matrix and nuclei.

each screen and to minimize the need to repeat each screen twice for the quantification of both readouts we tested the possibility of staining the cells that were previously incubated for the measurement of viability with presto blue assay. As a first step we tested whether the cell integrity was un-damaged post incubation with presto blue and whether any residual fluorescence will interfere with multiplexing of both assays. Cells incubated with the viability reagent were washed, fixed, permeabilized then stained with Hoechst for the visualization of their nuclei and with vimentin and phalloidine for the assessment of the cytoskeleton which were both intact. This signifies that the screen can be used for the assessment of both readouts successively. Moreover, since 24hrs. post UV was the chosen time point for the measurement of viability, 6-4 PP was the chosen damage to be detected as it possesses faster repair kinetics within the selected time point. 6-4 PP quantification was carried on non-treated irradiated or non-irradiated WT and XPC cells to confirm the validity of this protocol. XPC cells showed elevated levels of DNA damage 24hrs.

post UV while normal cells showed significant complete repair manifested with minimal DNA damage lesions detected at the same time point. The analysis is based on single cell quantification of the fluorescence signal within each nucleus for better statistical value. This is carried out by utilizing Hoechst staining for the identification of the nuclei that will be set as region of interest (ROI) for the quantification of DNA damage within the circumference of the nucleus of each individual cell (figure 29). We further on tested the applicability of this method on XP-C and WT cells. WT cells showed significant decrease in the amount of DNA damage 24 hours post UV while XP-C cells showed no repair (figure 30).

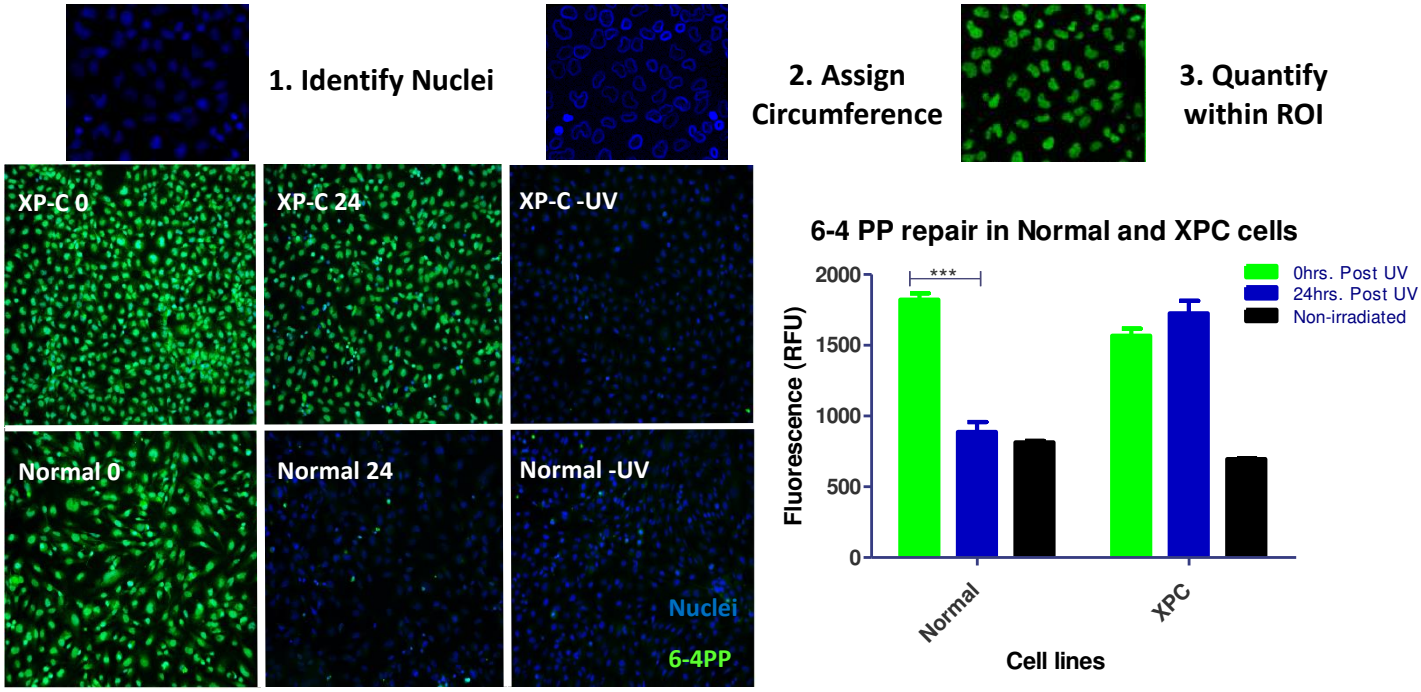

Figure 30 ***Single-cell analysis of nuclear DNA damage quantification.***

*UVB induces the formation of two types of direct DNA damages that are the cyclobutane pyrimidine dimers (CPD) and the 6-4 pyrimidine pyrimidone photoproducts (6-4PP). The lesions require 48hrs and 24hrs, respectively, to be repaired in WT cells while they accumulate in XP-C cells without repair. The quantification of DNA damage post-treatment allows the identification of molecules that can decrease such damage in XP-C cells. 6-4 PP quantification was carried on non-treated irradiated or non-irradiated WT and XP-C cells. XP-C cells show elevated levels of DNA damage 24hrs. post UV while normal cells show significant complete repair manifested with minimal DNA damage lesions detected after the same time point. The analysis is based on single-cell quantification of the fluorescence signal for better statistical value. This is carried out by utilizing Hoechst staining for the identification of the nuclei that will be set as the region of interest (ROI) for the quantification of DNA damage within the circumference of the nucleus of each individual cell.*** $p<0.001$ paired t test.*

6. CONFLUENCY ANALYSIS FOR SCREENING SCHEDULE

For the sake of having optimal conditions during transfection, drug treatment and irradiation, confluency analysis of both cell lines was carried out. For cell transfection the optimal cell confluency should be something between 30 to 50% confluent slightly lower than that of chemical treatment that requires 60% confluency. Irradiation on the other hand should be carried out at subconfluency corresponding to about > 80% confluency. For that, different cell densities were seeded in 96 well plates and incubated for 5 days where well images were taken daily and analyzed with ImageJ plugin PHANTAST with the application of HALO correction. The optimal cell density for having subconfluent cells after 5 days was 6000 cells for XPC cells and 5000 for the WT cells. The designed treatment protocol for the chemical treatment consists of seeding cells at day 1 followed with pre-treatment with drugs on day 3 then irradiation and post-treatment on day 4 to be completed with readout on day 5 (figure 31). The reason for the pre and post treatment is that the drug can either have a preventative effect if administered prior to UV radiation or therapeutic effect post irradiation so we would like to examine both conditions. As for the siRNA screen the seeding will be on day 1 followed by transfection on day 2 to be incubated for 48hrs prior to irradiation on day 4 and readout on day 5.

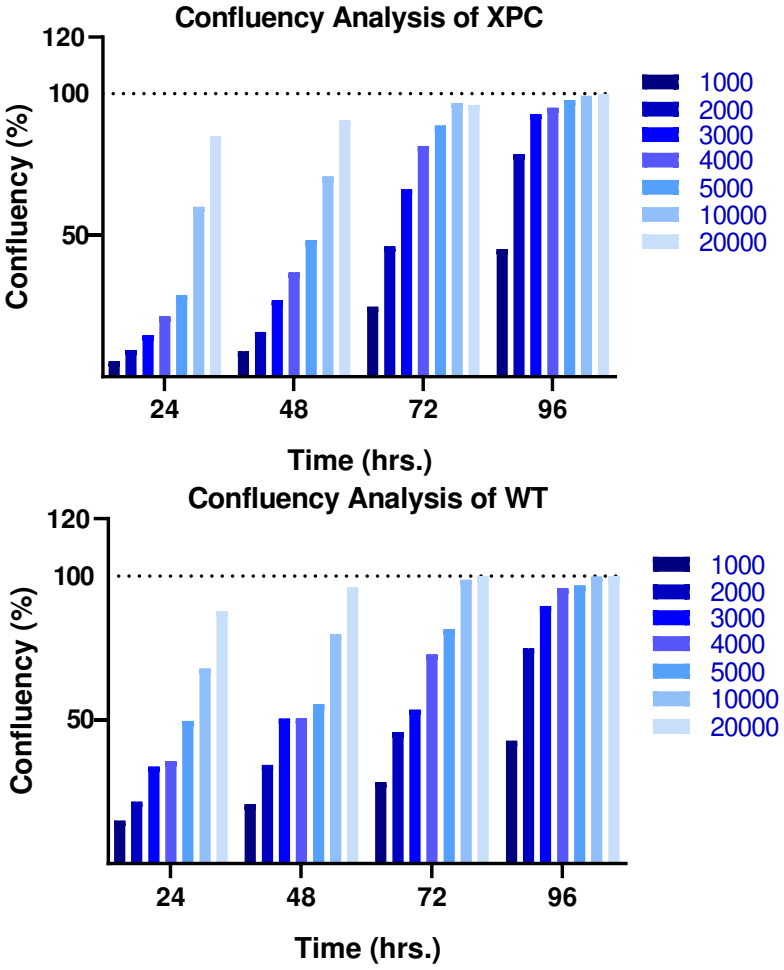

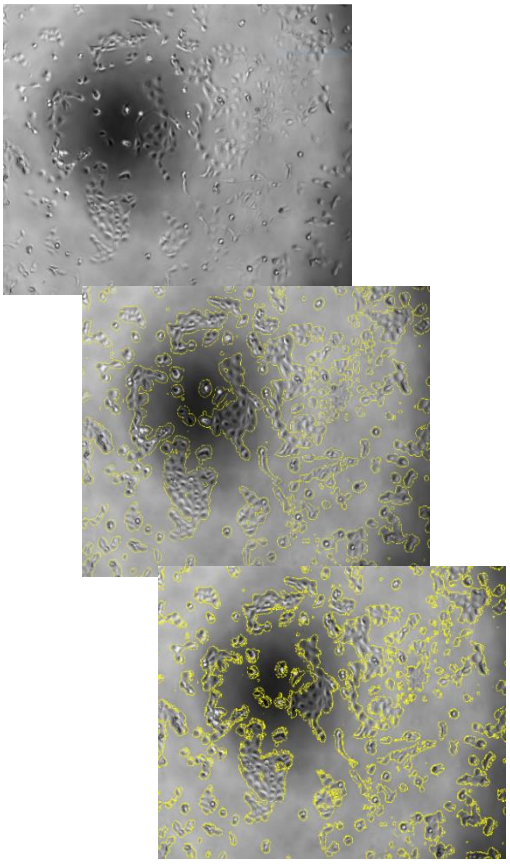

Figure 31 Quantification of XP-C and WT cell confluency.

Both XP-C and WT cells were seeded at different amounts per well (from 1000 to 20000 cells per well) and they were incubated for different times (24-96 hours). At each time point images of the cells were acquired in bright field then analyzed by imageJ plugin PHANTAST for the quantification of cell confluency. Based on that, specific cell count was used for seeding in both screens for the attaining of the desired cell confluency during the different treatments.

CHAPTER 3. CHEMICAL SCREEN

1. PRIMARY SCREEN

1.1 SCREEN LAYOUT AND CONTROLS

The utilized library is the Prestwick library of 1280 FDA approved drugs distributed over 16 daughter plates and placed in the inner wells while columns 1 and 12 are for both controls the sham treated irradiated negative control and the non-irradiated positive control. The concentration utilized is 10μM. The effect of the treatment can either be therapeutic or preventative to the UVB induced damage depending on the treatment time point pre or post UV that is why for the sake of this screen we will carry out both treatment protocols simultaneously. The plates will be first treated for 24hrs. with the drug to check the molecules' preventative effect. They will be then irradiated at 0.05 j/cm^2 then post treated to check the therapeutic effects. This course of treatment will be further on separated into pre and post treatment after hit identification to decipher whether pre, post or both treatment course is the main player for phenotype reversal. The drug treatment was done in duplicate with two test plates for each one daughter drug plate with 80 drugs per plate. An additional well per plate was added with no cells to allow the removal of the background fluorescence. The readout will be the measurement of cell viability by Presto Blue (figure 32).

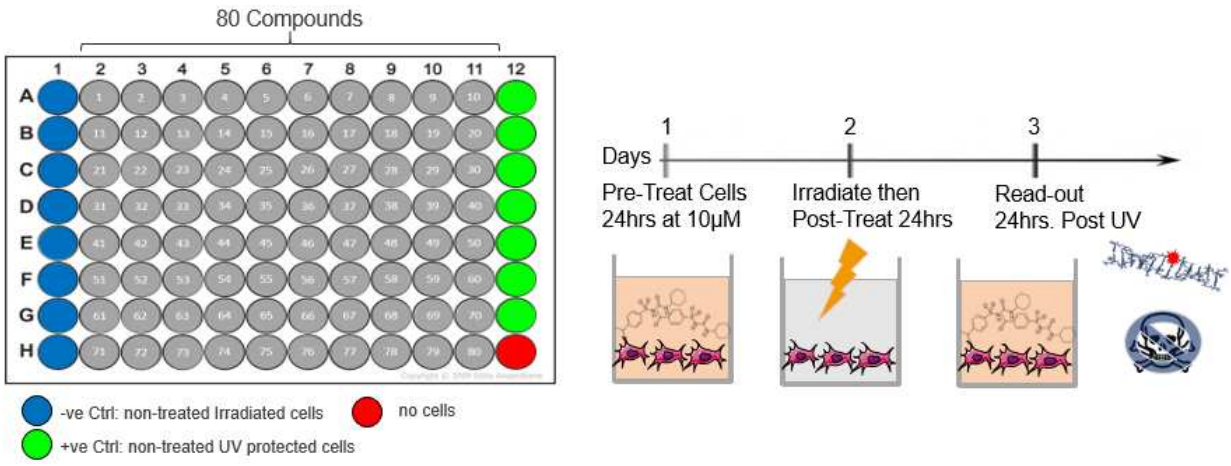

Figure 32 Layout of the Chemical primary screen

The general layout of the chemical screen consists of the screening of 80 compounds per plate at 10μM for twenty four hours after which the cells will be irradiated at 0.05J/cm^2 and incubated for an additional twenty-four hours with the same drugs. The readouts will be based on the quantification of both viability and DNA repair. The utilized controls are DMSO treated cells that will be either irradiated to serve as negative controls or non-irradiated serving as positive control. No cells well will be utilized for the subtraction of background Presto Blue noise.

1.2 HITS' SELECTION CRITERIA

To identify compounds that can improve the photosensitive phenotype of XP-C cells, Prestwick library of 1280 FDA and EMA approved drugs was screened on XP-C cells at 10μM for 24hrs in

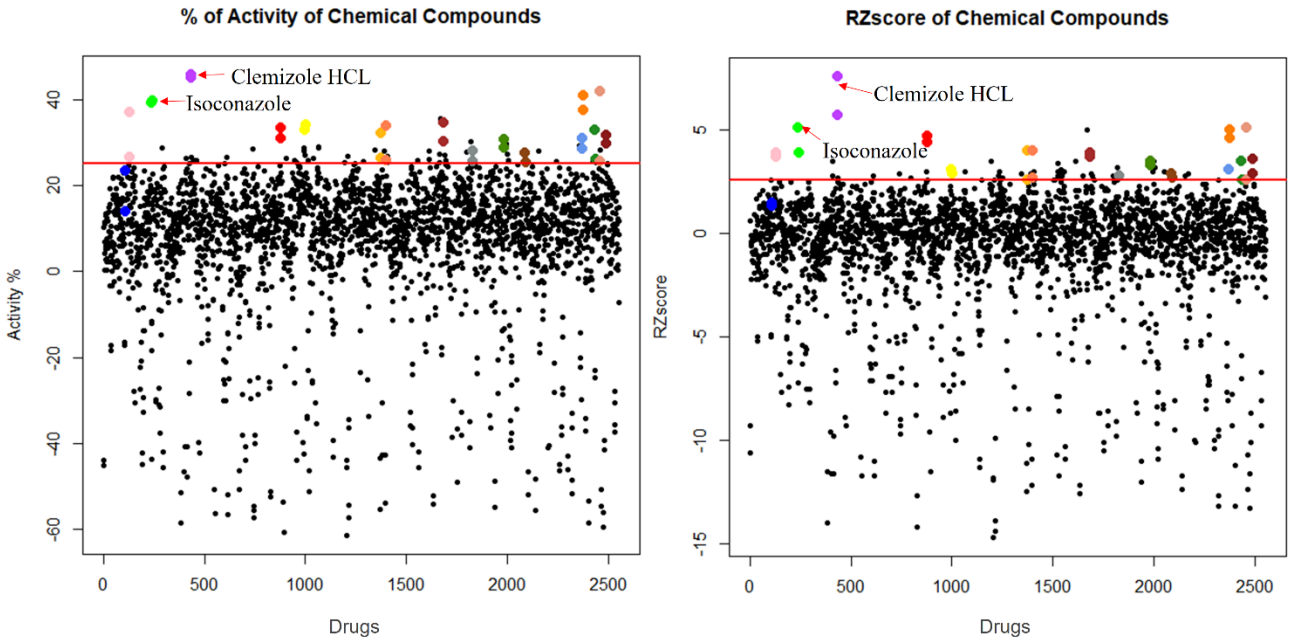

Figure 33 Identification of 16 compounds reversing XP-C photo-sensitivity upon UVB irradiation.

Prestwick library of chemical drugs was screened on XP-C cells. The cells were treated with the library at 10μM for 24 hours then further on irradiated at 0.05J/cm^2. Post Irradiation the cells were then incubated with the library for an additional 24h prior to having their viability assessed 24 hours post UV via the addition of PrestoBlue reagent and the recording of the fluorescent values. Based on two different normalization criteria, control based % of activity and non-control based RZscore, 16 compounds were selected manifesting >25% increase or >2.5 value for both % of activity and RZscore respectively. % Activity was calculated by normalizing the obtained values between the interval of 100% donated to non-irradiated DMSO treated cells and 0% that donated irradiated DMSO treated cells. RZscore was measured by normalizing the fluorescence values to the median and median absolute deviation. RZscore: Robust Z score

duplicates. Following the incubation, the cells were UVB irradiated at 0.05j/cm^2 based on Z' Factor calculation then post-treated with the same drugs for an additional 24hrs before the measurement of viability. The effect of the treatment can be either preventive or therapeutic to the UVB-induced damage depending on the treatment time point. The readout was the measurement of cell viability by Presto Blue. The bioactivity of the test compounds, signifying the drugs' beneficial effects on photo-resistance, was calculated from the fluorescence values by determining its relative percentage with respect to non-irradiated DMSO treated wells set as 100% and irradiated DMSO treated wells set as 0%. The robust Z score was also calculated per plate as an additional non-control based normalization technique. The hit selection was based on two criteria. Hits are test compounds that possess a bioactivity ≥ 25% and robust Z score ≥ 2.6. Sixteen molecules were identified on this basis (figure 33 and the table 5). An additional drug was added to the list which is acetohexamide as it was reported to have a positive effect on increasing XP-A cells' viability in response to UV irradiation [211].

Table 5 Raw data of the primary chemical screen hits

Compound ID	Formula	Bioactivity (%)	RZscore	Chemical Name
227	C19H21Cl2N3	45.5	6.6	Clemizole hydrochloride
127	C18H14Cl4N2O	39.6	4.5	Isoconazole
1704	C24H32O6	39.2	4.8	Desonide
1750	C21H25N	33.7	3.8	Terbinafine
546	C21H32O2	33.5	3.0	Pregnenolone
955	C12H14Cl2FNO4S	32.5	3.8	Florfenicol
477	C21H30O2	32.2	4.6	Progesterone
67	C18H14Cl4N2O	31.7	3.8	Miconazole

1770	C23H30N4O2S	30.8	3.3	Perospirone
792	C27H34I2N4	29.9	3.4	Propidium Iodide
1241	C22H18N2	29.8	3.4	Bifonazole
1700	C5H11Cl2N3	29.7	3.1	Histamine dihydrochloride
1735	C24H29N5O3	29.4	3.1	Valsartan
781	C25H32ClFO5	29.2	3.3	Clobetasol propionate
1117	C19H22FN3O	26.9	2.8	Azaperone
1334	C14H22N2O2	26.4	2.8	Rivatimine

2. SECONDARY SCREEN

2.1 SCREEN LAYOUT AND CONTROLS

To exclude the possibility of having false positives among the hits of the primary screen, a secondary screen of the 16 hit drugs was carried out. One additional drug was added which is acetohexamide as it was reported to have a protective effect on XPA cells in an NER independent manner [211] so it was included in the secondary screen to test its effect on XPC. Additional conditions were included together with the initial screen's conditions. The drugs were screened at three different concentrations: 1, 5 and the initial 10µM. The reason for that is to test whether the increased drug concentration may induce cytotoxicity. Moreover, the treated plates were irradiated at doses of 0.02j/cm^2, 0.05j/cm^2 or non-irradiated. Each drug was screened in triplicate in each of the different irradiation conditions and concentrations. The same viability readout will be measured.

2.2 HITS' SELECTION CRITERIA

Drug bioactivity was calculated by control based normalization of the fluorescence values with irradiated DMSO treated cells set at 0% bioactivity versus non-irradiated set at 100%. For each drug, a dose-response curve of bioactivity as a function of [drug] was plotted for the three different doses. The drugs that showed the highest bioactivity were isoconazole, clemizole hydrochloride, and bifonazole. Acetohexamide only mediated a slight increase in viability as a function of drug concentration and UV doses compared to the two other ones (figure 34).

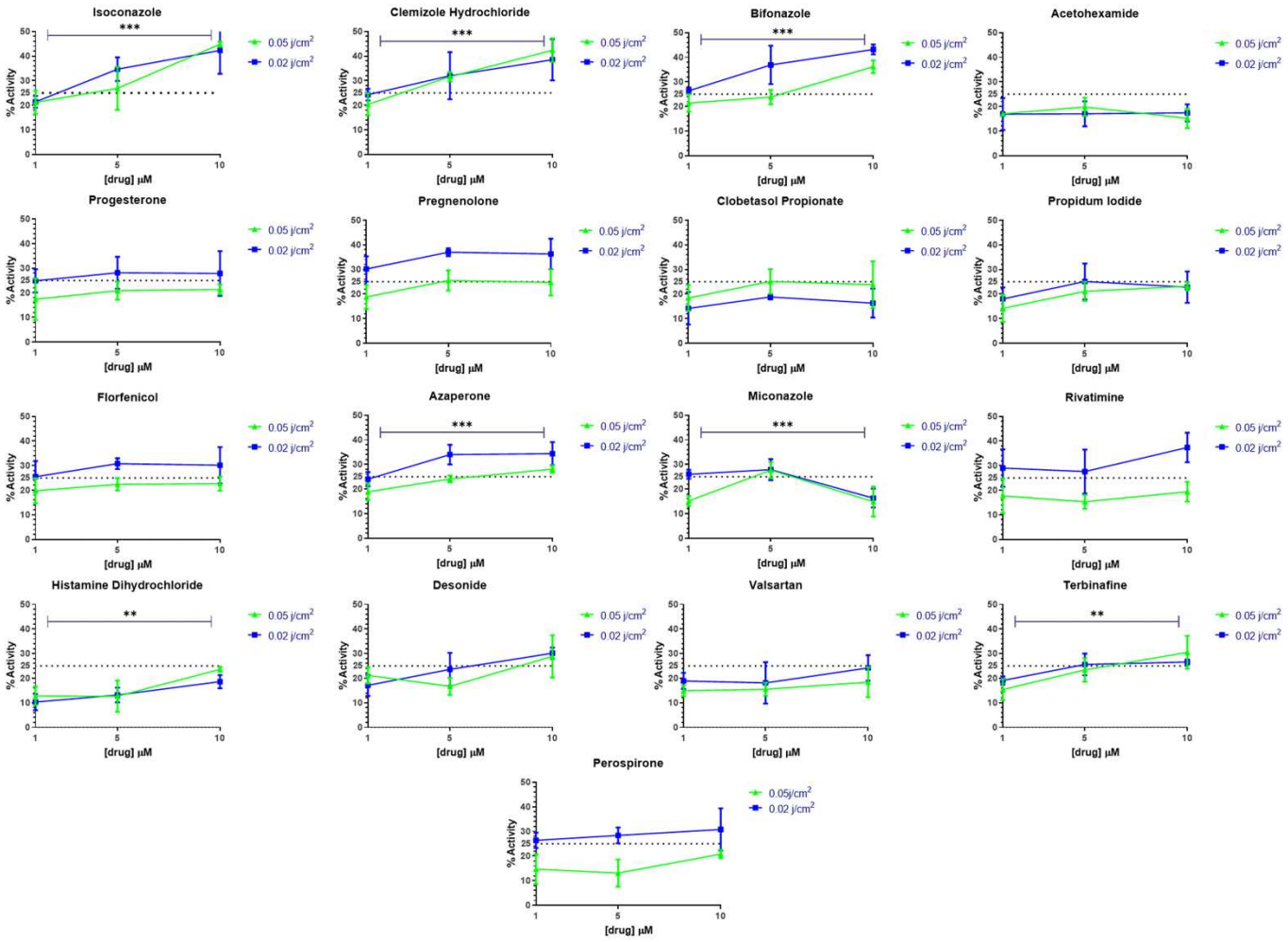

Figure 34 Confirmation of primary screen hits and the identification of the 3 most effective compounds.

*XP-C cells were treated with the different primary screen candidate compounds at three different concentrations (1, 5 & 10µM) then subjected to two UVB doses (0.02 & 0.05 j/cm^2) after which their viability was measured 24 hours later by the addition of PrestoBlue. It should be noted that pre and post-irradiation treatment with the drugs was carried out. The three compounds showing the increased drug bioactivity as a function of increased concentrations are isoconazole, clemizole hydrochloride and bifonazole showing the highest protection against UV irradiation. % Activity was calculated by determining the relative % of fluorescence with respect to non-irradiated DMSO treated cells set as 100% and irradiated DMSO treated cells set as 0%. The dotted line represents a threshold of 25% Activity. The statistical significance of the effect of two UVB doses and the three drug concentration on the % activity was conducted by using 2-way anova ** p<0.01, *** p<0.001.*

2.3 DNA DAMAGE ANALYSIS

After the assessment of drug bioactivity, it was also imperative to determine whether the identified drugs could reverse the impaired DNA repair activity in XP-C cells. For that, DNA damage analysis was carried out on the 17 drugs used in the secondary screen and irradiated at a dose of 0.05j/cm2. After the measurement of bioactivity, the plates were fixed and immunostained with an anti-6-4PP antibody for the quantification of the amount of DNA damage following drug treatment. The positive control showing maximal DNA damage was the DMSO treated irradiated cells while the negative control with minimal damage is the non-irradiated DMSO treated ones. The treatment with either isoconazole or clemizole hydrochloride showed a decrease in the amount of 6-4 PP at the single-cell level compared to untreated controls indicating an induced repair due to treatment. This decrease in DNA damage was significant ($p<0.001$) only when 5µM of both drugs was utilized (figure 35).

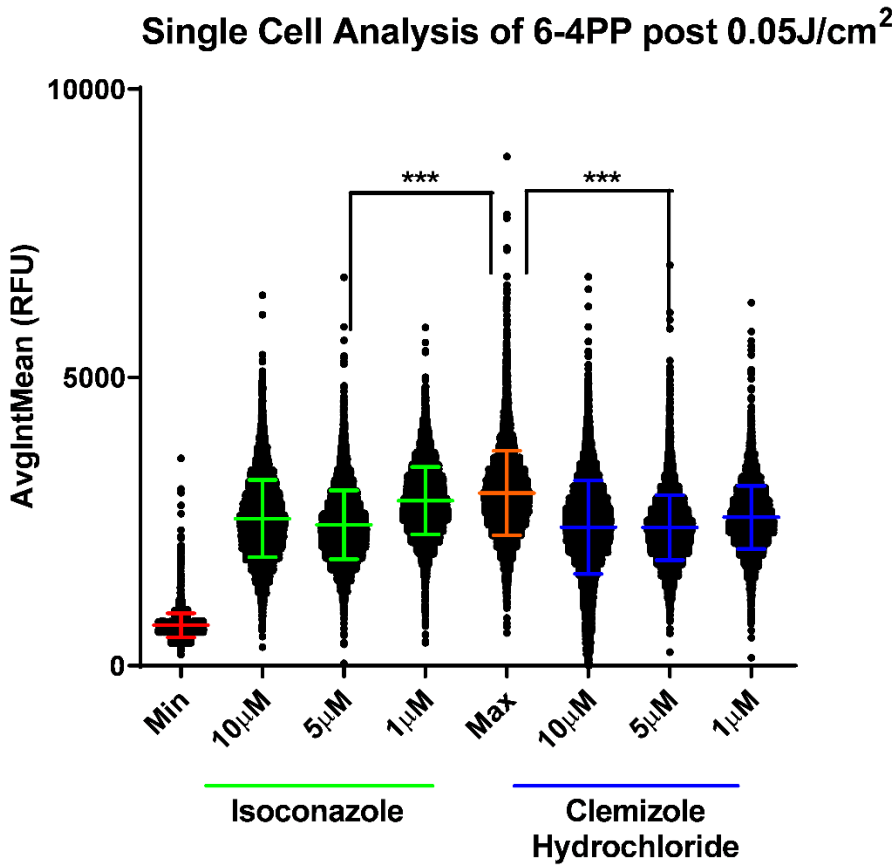

Figure 35 Identification of compounds enabling repair of 6-4PP in XP-C cells.

XP-C cells were treated with the 16 primary screen candidate hits at three different concentrations (1, 5 & 10µM) with pre and post-irradiation treatments. Irradiation was carried out at a dose of 0.05j/cm^2. 24 hours post UV the cells were fixed and stained with 6-4 PP antibodies for the quantification of DNA damage. Fluorescence intensities of individual cells for each condition were quantified and more than 1000 cells per condition were analyzed. Among the 16 hits, only isoconazole and Clemizole hydrochloride enabled a decrease in the amount of DNA damage post UV

*shown here. Almost 20% repair of 6-4PP DNA damage was recorded for both drugs at a concentration of 5µM which was found to be significant. DNA damage quantification in DMSO treated irradiated cells was used as positive control showing the maximum amount of DNA damage while quantification of 6-4PP in DMSO treated non-irradiated cells was taken as a negative control with the minimum amount of detected damage. *** p<0.001, freedman non-parametric test with dun's post hoc analysis.*

2.4 DRUG UV DOSE RESPONSE

To further characterize the effect of the two selected drugs on viability enhancement, UV dose-response experiments were carried out. In contrast to the previous experiments, the dose-response analysis here was performed on both the XP-C and WT cell lines and viability was calculated based on percent of control normalization to non-irradiated cells only. This aim was to decipher whether the effect is specific to XP-C cells or also valid in WT cells. The two cell lines were treated with either isoconazole, clemizole hydrochloride or DMSO then subjected to increasing UVB doses. Both drugs enabled enhanced photo-resistance to the increasing UVB doses in XP-C and WT compared to DMSO treated cells (figure 36). Such photo-resistance was significant for both drugs in XP-C cells with p-value <0.05. However, in WT cells, the treatment with isoconazole showed significant photo-resistance against increased UV doses irradiation (p-value <0.05), unlike clemizole hydrochloride whose increase in viability was not significant. Of note this protective effect does not seem to be specific to XP-C cells as a similar protective effect was also shown for the WT cells.

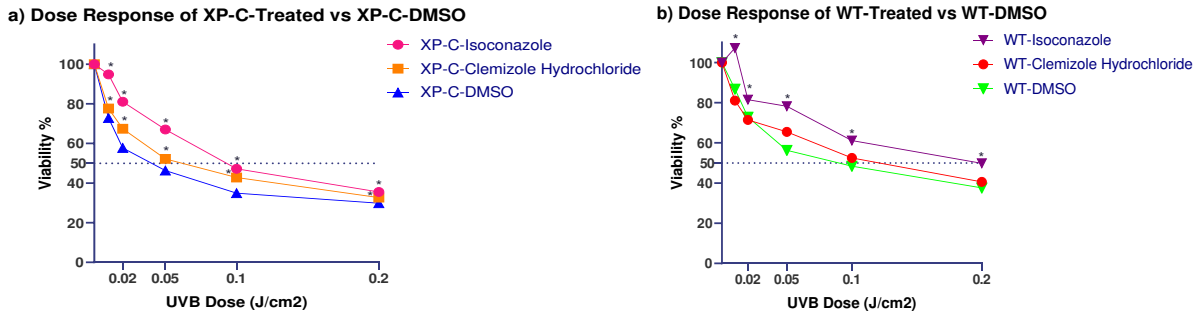

Figure 36 Isoconazole and Clemizole Hydrochloride viability analysis post UVB in both XP-C and WT cell lines.

XP-C and WT cells were treated with either drugs or DMSO (pre ad post-irradiation treatment) then subjected to increased UVB doses. Their viability was further on assessed 24hours post UV by the incubation with PrestoBlue. ***a)*** *Viability of XP-C treated cells vs DMSO. Both drugs enabled significant (p value<0.05) protection of XP-C cells from UVB induced death with isoconazole having a more protective effect.* ***b)*** *Viability of WT treated cells vs DMSO. Drug mediated protection against UVB irradiation was also evident in treated WT cells and not unique to XP-C cells. Only isoconazole mediated protection was significant with p value<0.05. Viability was calculated by determining the*

*percent of control with respect to non-irradiated DMSO treated cells taken as 100% viable. * p-value <0.05, Repeated Measure one way ANOVA with Dunnett's multiple comparison test.*

2.5 DRUG TREATMENT REGIMEN SEPERATION

As mentioned above, the chemical treatment consisted of two phases a pre-irradiation treatment to test the preventative effect of the drug and a post-irradiation treatment to examine its therapeutic effect. In order to determine which treatment phase had a more essential role in the phenotypic normalization, the two phases were separated and their effects were compared to that of the combined treatment regimen. For isoconazole, the pre-irradiation treatment had no effect compared to either the post-irradiation treatment or the combined pre and post-treatment that gave similar kinetics (figure 37). The increase in drug bioactivity % mediated by both treatment regimens combined at 5µM was significant with p-value <0.05. At 10µM the difference in bioactivity was significant between pre and post-treatment as well as between the pre and both treatments with p-value <0.01, signifying that both treatment regimens share significant protection compared to pretreatment. Thus isoconazole mostly serves as a therapeutic remedy post UVB irradiation. As for clemizole hydrochloride, the pre-irradiation treatment showed higher bioactivity than that of isoconazole but again the most effective regime is the both pre- and post-irradiation treatment showing the highest bioactivity. However, a significant difference in bioactivity only exists between pretreatment and both treatments together with p-value <0.05 at both 5 and 10µM. It should be noted that bioactivity is defined by the ability of the drugs to impose an effect on living matter which in this case is its ability to increase photo-resistance of the cells between non-irradiated cells set at 100% and irradiated non-treated cells set at 0% (figure 37).

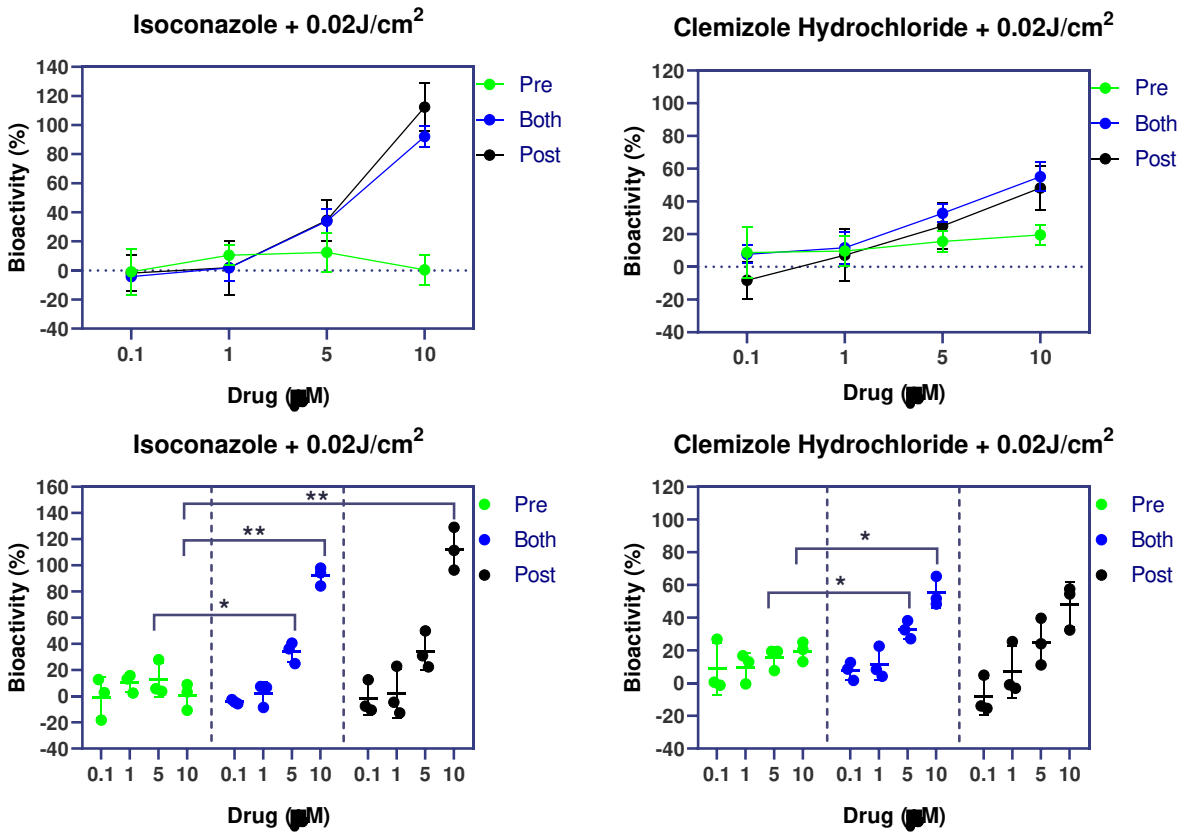

Figure 37 Drug treatment regimen separation.

*To determine which treatment regimen was more effective, XP-C cells were treated with the drugs either pre-irradiation, post-irradiation or both pre and post-irradiation. Drug Bioactivity % was then calculated 24 hours post UV. Such calculation is based on determining the relative percentage considering non-irradiated DMSO treated samples as 100% and irradiated ones as 0%. Thus the obtained fluorescence values normalized to these two controls. Isoconazole post-irradiation or both treatments showed a significant p value<0.01 increase in bioactivity at 10µM while only both treatments showed significant enhancement of bioactivity at 5µM compared to pre-treatment procedure. Clemizole hydrochloride, however, seems to have better bioactivity when both pre and post-irradiation regime was used where the increase of bioactivity was significant p value<0.0.5 for both 5µM and 10µM treatment compared to pre-treatment at each concentration respectively. *p value<0.05, **p value<0.01, 2-way ANOVA with Tukey's multiple comparison test.*

2.6 DOUBLE DRUG TREATMENT HAS NO SYNERGISTIC NOR ADDITIVE EFFECT

Both of the hits have an azole ring in their structure. We, therefore, examined whether the combined treatment with both drugs at 10µM could improve further the acquired photo-resistance compared to single-drug treatment. Accordingly, XP-C cells were treated with either drug alone or with both and then subjected to irradiation at a dose of 0.02j/cm^2. The double treatment had the

same bioactivity as the single treatment with isoconazole with no benefit (figure 38). Hence no synergetic effect was obtained upon double drug treatment.

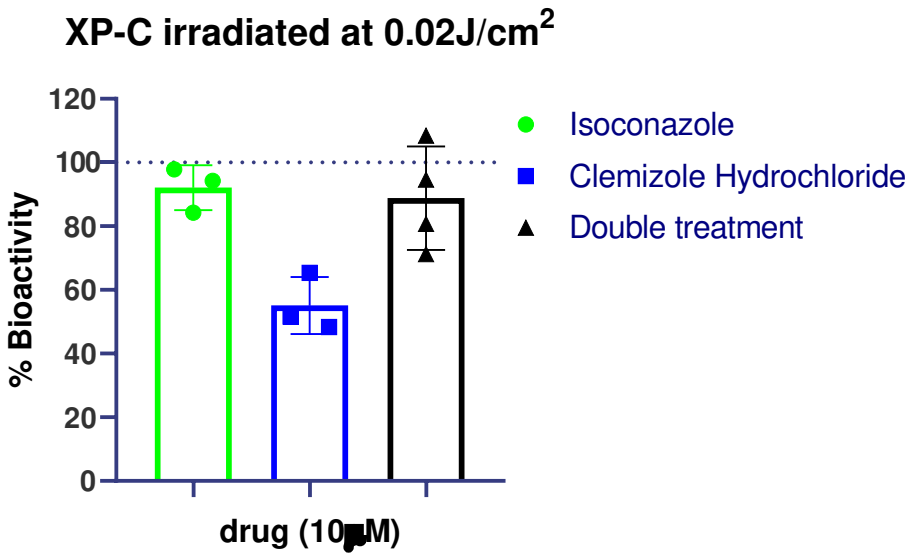

Figure 38 Double Drug Treatment

Double drug treatment was carried out to test whether both drugs possess synergistic or additive effects. XP-C cells were treated with either Isoconazole, clemizole hydrochloride or double treated at 10µM then irradiated at 0.02j/cm^2. % of drug bioactivity was measured 24 hours later. Double treatment showed the same protective profile as isoconazole with no added protection against UVB irradiation.

3. TREATMENT PHYSIOLOGICAL CONSEQUENCE

3.1 APOPTOSIS

In an attempt to decipher the cellular mechanisms of photo-resistance of the drug treatment, different cell phenotypes were analyzed. Apoptosis was therefore quantified using Cell Event which allows the indirect measurement of caspase 3/7 activity, key downstream players in the apoptosis activation cascade. XP-C cells were therefore treated with either drug or DMSO followed by UVB irradiation then staining with Cell event and PI 24hrs post UV. The samples were analyzed by flow cytometry. Out of the two drugs, Isoconazole showed a decrease in cell event % cells reaching 23.35% as well as lower PI-positive population percentage (9.57%) compared to DMSO treated cells showing higher population percentages of 41.23% and 11.57%, respectively. On the other hand, clemizole hydrochloride did not show any decrease in both quantified parameters. These results suggest that unlike isoconazole, it is probably not via the

reduction of apoptosis that the clemizole hydrochloride mediates its protective role (figure 39). Similar outputs were also detected in WT cells (figure 40).

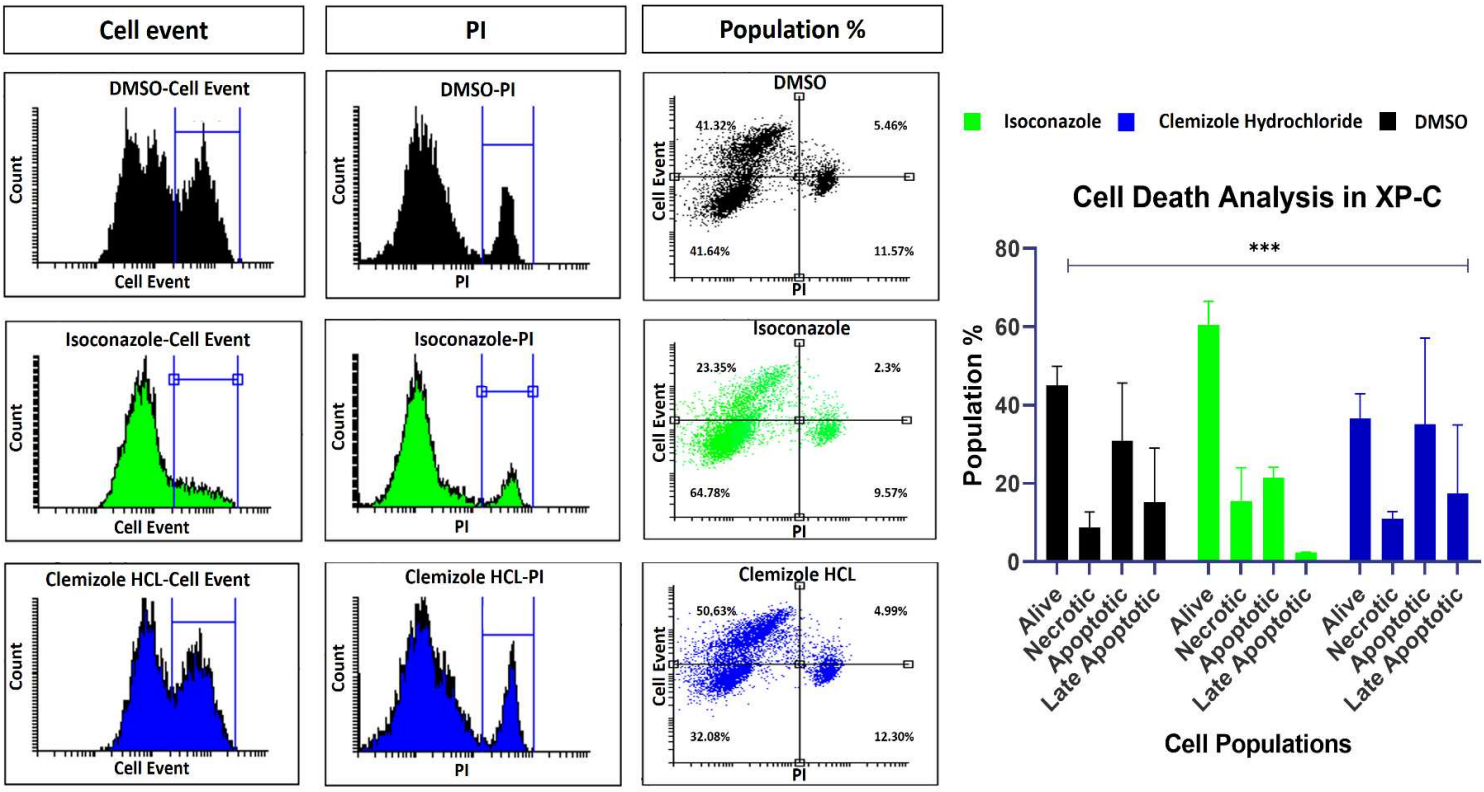

Figure 39 Isoconazole but not clemizole hydrochloride decreases the population % of apoptotic XP-C cells post UV.

*XP-C cells were treated with the different drugs or DMSO then irradiated. CellEvent caspase 3/7 marker was added post UV to quantify apoptosis. Cells were collected and PI was added just before analysis on flow cytometer. Isoconazole treatment decreased the percentage of apoptotic cells (23.35%) post UV compared to DMSO treated cells (41.32%) evident also by the increase in the live cell population. Clemizole hydrochloride, however, had no effect in increasing the live cell population with respect to DMSO treated cells (32.08% vs. 41.64%) and only a slight decrease in the apoptotic cell fraction so it is perhaps via another mechanism that this drug mediates its mode of action s it showed no further decrease in apoptotic cell population compared to DMSO treated cells. Two way anova was used to compare between the two independent variables (type of cell death or stain and nature of the drug treatment) and the dependent variable which is the population %, ***p<0.01.*

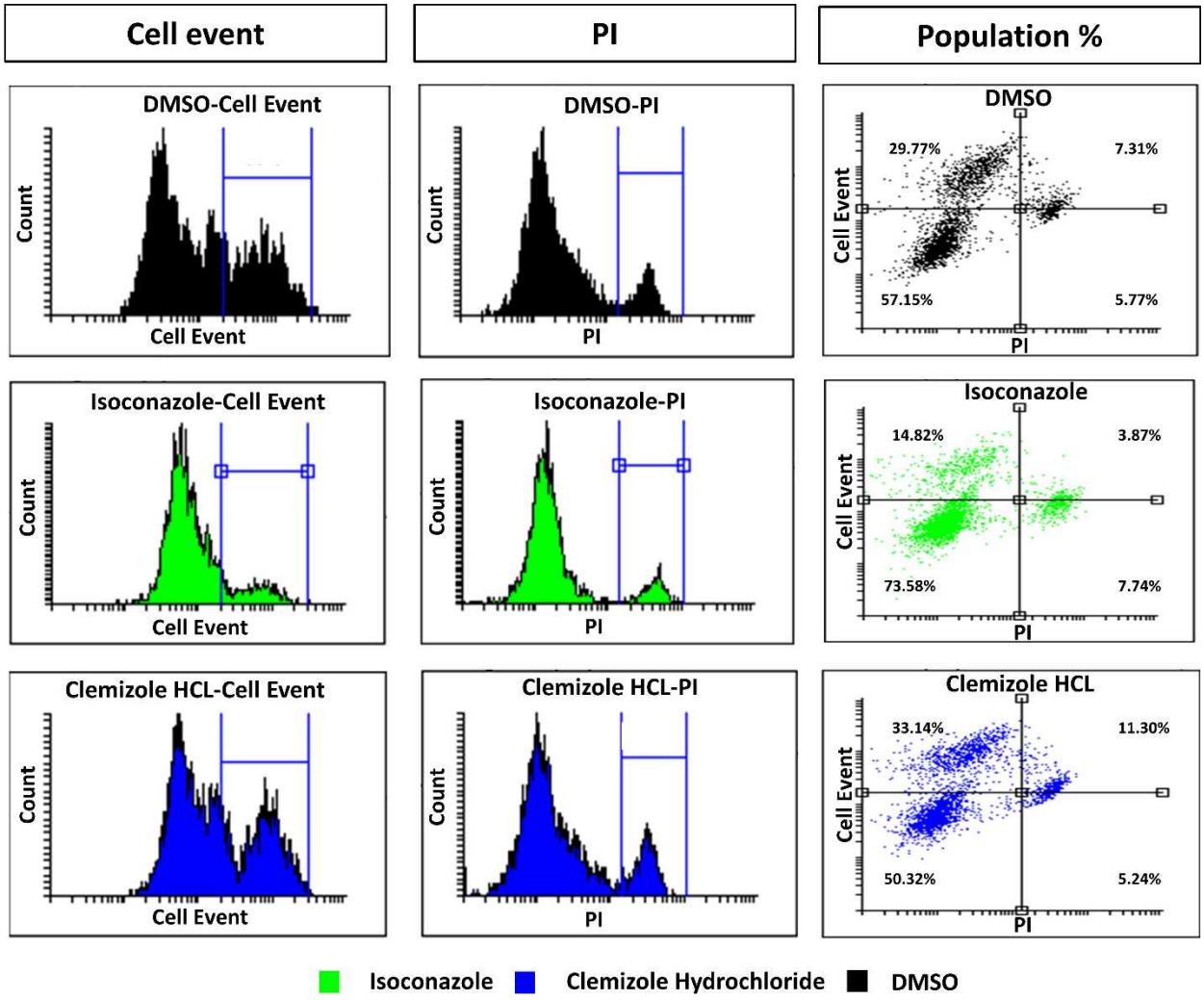

Figure 40 Isoconazole and not clemizole hydrochloride decreases the population % of apoptotic WT cells post UV.

WT cells were treated with the different drugs or DMSO then irradiated. Cell event caspase 3/7 marker was added post UV then cells were collected. PI was added just before analysis on flow cytometer. Isoconzaole treatment decreased the percentage of apoptotic cells post UV (14.82%) compared to DMSO treated cells (29.77%). Clemizole hydrochloride, however, had no effect so it is perhaps via another mechanism that this drug mediates its mode of action.

3.2 PROLIFERATION

3.3.1 KI67 STAINING

In a first step, and in order to analyze the proliferative state of the irradiated cells and whether the different treatments can modify this profile, cells were stained with Ki67 antibodies and analysis was carried out at the single-cell level. Ki67 antigen was expressed during all phases of the cell cycle (G1, S, G2, M) but not in quiescent cells. Both XP-C and WT cell lines were positive to

KI67 signifying that the cells are not in quiescent state post UV. Cells treated with either DMSO, isoconazole, clemizole hydrochloride, or both drugs showed no difference in the Ki67 expression profile (figure 41).

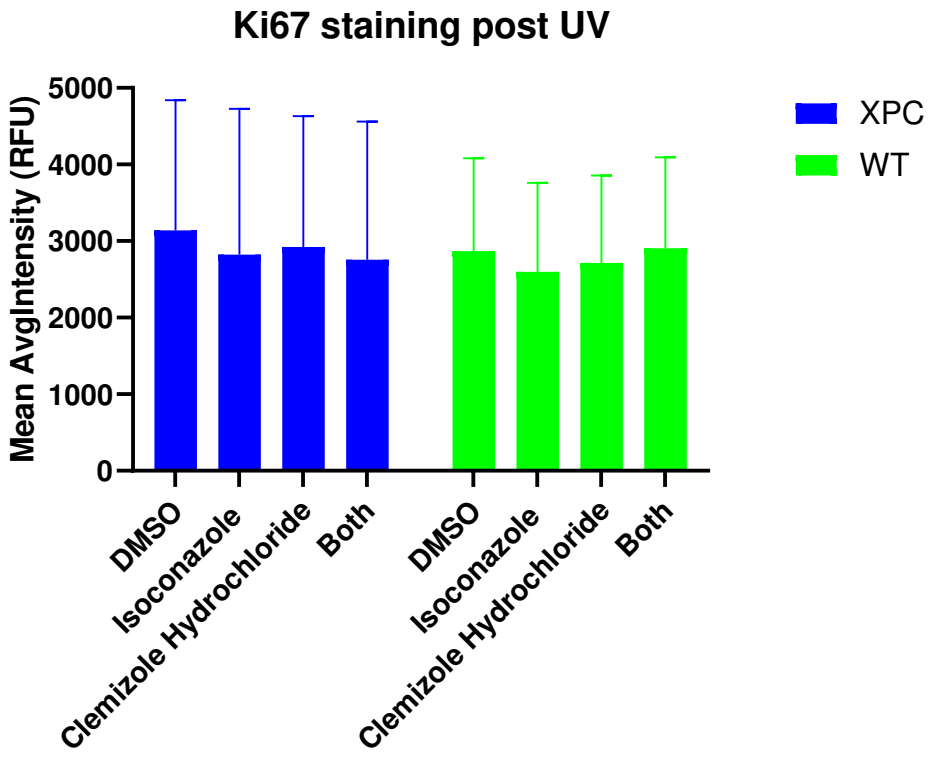

Figure 41 Drug treatment has no effect on ki67 proliferation marker expression.

XP-C and WT cells were treated with isoconazole, clemizole hydrochloride, both drugs or with DMSO then irradiated. 24 hours post UB the cells were fixed and stained with ki67 Ab. The staining profile of the proliferative marker ki67 was the same for all treatment conditions in both XP-C and WT cells.

3.3.2 EDU

Ki67 stains cells in various stages of the cell cycle, and it was previously reported that some non-proliferating cells tend to test positive for Ki67 due to antigen retention[345]. Moreover, bulky adducts generated by UV tend to block the progression of replication forks decreasing DNA replication. Therefore, in a second step, EDU incorporation assay was performed to clarify whether this positive staining was due to antigen retention or rather the cells were capable of recovering from the DNA replication blockade following different treatment. It should be noted that EDU insertion into DNA allows the identification of cells that have progressed through the S phase. XP-C cells were treated with either DMSO, isoconazole or clemizole hydrochloride in a pre and post-treatment regime and then irradiated with UV to be finally cultured in the presence of EDU at different time points (2hrs. or 4hrs. post UV). Cells were then collected and stained to be analyzed by flow cytometry. When comparing the course of EDU incorporation in DMSO treated cells over

the different time points post UV, it was clear that the intensity of EDU decreases as a function of time till becoming null at 24hrs. post UV. This signifies that the cells were no longer able to undergo DNA replication at 24hrs. post UV. Isoconazole had a slight effect on increasing EDU positive population at 2hrs. post UV, but both drugs failed to increase DNA replication beyond that showing similar effects to DMSO (figure 42). These results indicate that cell proliferation does not seem to be the major mechanism underlying the protective effect induced by these drugs.

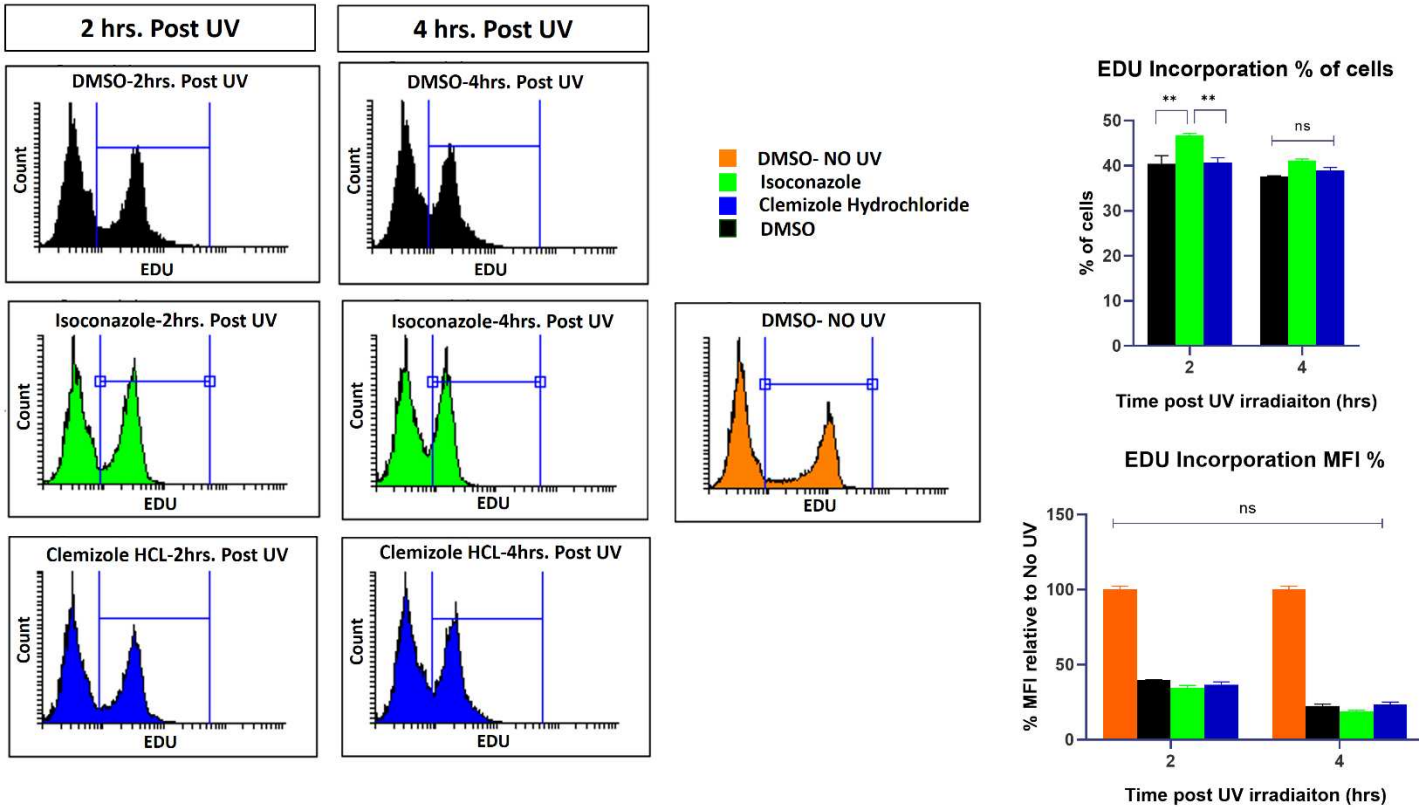

Figure 42 Same EDU incorporation profile is evident between drugs or DMSO treated XP-C cells.

*XP-C cells were treated with the different drugs or DMSO then irradiated. Prior to the end of the post UVB incubation, the cells were incubated in the presence of EDU. Cells were further on collected, stained and analyzed by flow cytometry. No difference is seen between the mean fluorescence intensity of the EDU positive populations between the different treatment condition at either 2 or 4 hours post UV. It should be noted that as incubation time post UV increases, the mean fluorescence intensity of EDU positive population decreases. Quantification of both the mean fluorescence intensity (MFI) and EDU positive population percentage were carried out. Two way anova was used to compare between the two independent variables (time post UV and nature of the drug treatment) and the dependent variable of either EDU population percentage or MFI, **p<0.01.*

CHAPTER 4. siRNA SCREEN

1. PRIMARY SCREEN

1.1 SCREEN LAYOUT AND CONTROLS

We used the Qiagen human siRNA kinase library targeting the total 646 kinases with 2 different siRNAs each (Qiagen siRNA libraries (V1.0)). A total of 1292 different sequences of siRNAs were placed in the inner wells of 17 different mother plates with controls on the edges as depicted. The final concentration of the siRNA utilized is 5 nM and the transfection was carried out for 48 hours to allow proper knockdown of mRNA expression. Plates were further on UVB irradiated at 0.03 J/cm^2 and 24hrs later viability was assessed using presto blue. It should be noted that the two siRNA targeting the same kinase were placed in the same plate in different wells as shown in the plate format where they were designated by the same number. The positive control that shows highest viability is the siAS transfected non-irradiated while the negative control is the siAS transfected irradiated cells. SiCD is used to analyze the transfection efficiency as their proper delivery allows the induction of cell death in the cells allowing a notable decrease in viability (figure 43). This screening procedure was carried out on both cell lines simultaneously.

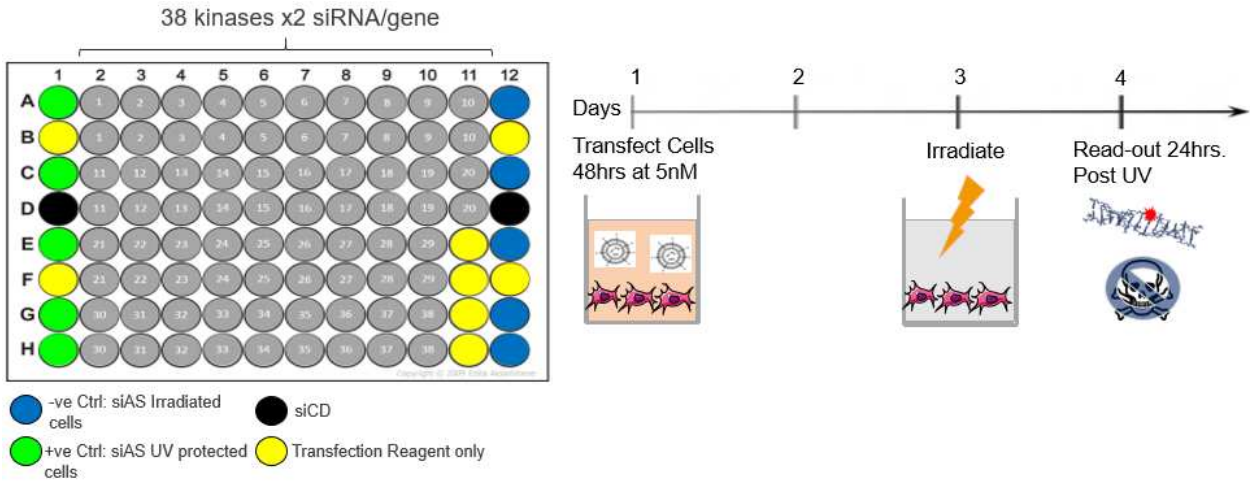

Figure 43 Layout of the siRNA primary screen

The general layout of the siRNA screen consists of the screening of 76 siRNAs per plate with two different siRNAs targeting the same kinase. The transfection will be carried out at 5nM for forty-eight hours after which the cells will be irradiated and incubated for an additional twenty-four hours. The readouts will be based on the quantification of both viability and DNA repair. The utilized controls are siAS transfected cells that will be either irradiated to serve as negative controls or non-irradiated serving as positive control. siCD was used as a control for transfection. AS: All Star, CD: cell death

1.2 HITS' SELECTION CRITERIA

After the performance of the actual screen, the readout is in the form of fluorescence value for each well where the latter requires normalization to eliminate the variation that arises between the plates. There are three causes for such variation. The first is the difference in transfection efficiency between plates that was evident in the values recorded by the siCD. The second is the variation in the irradiation that is not homogenous throughout the totality of the wells per plate and between the different plates as the controls varied within and between plates. Finally, the two utilized siRNAs per kinase have different sequences which signify a difference in knock-down efficiency. Therefore, different normalization techniques were utilized to identify the most appropriate method (figure 44).

Normalization techniques can be either control or non-control based. The first attempt was via the utilization of the non-control based Z score or robust Z score. The advantage of the use of the non-control based robust Z score is that it is less sensitive to outliers compared to the Z score.

$$Z\ score = \frac{Xi - mean\ (ASR)}{SD(ASR)}$$

$$robust\ Z\ score = \frac{Xi - median(Xall)}{MAD(Xall)} = \frac{Xi - median(Xall)}{1.4826 * median|Xi - median(Xall)\ |}$$

After the performance of both normalizations, the positive control values in both cases differed between plates which requires additional normalization. For that two attempts were done. The first involves the multiplication of the score with siCD of each plate then dividing it by the median of siCD for all the plates to normalize for the difference in the transfection efficiency.

$$modified\ robust\ Z\ score = \frac{robust\ Z\ score * siCDi}{median(siCD)}$$

However, since siCD is based on inducing the death of the cells to allow the visualization of the transfection efficiency then the output will be based of the viability measurement of the few cells remaining due to the proper transfection of the cell death inducing siRNA in the siCD wells excluding the possibility of using such normalization technique. The next option is to use the siAS wells for the normalization using the median of irradiated siAS per plate and the median of irradiated siAS calculated from all the plates combined. The latter proved to be not helpful as some plates show a negative median for the irradiated siAS transfected wells rendering it impossible for hit identification due to the negative sign.

Therefore, we utilized percent of control for hit identification taking the siAS non-irradiated median as 100% viability and the median of the irradiated ones as 0%. After the normalization, hits were identified as siRNA enabling an increase in viability of ≥ 25% compared to the siAS

irradiated wells. In addition, additional selection criteria were utilized to include the siRNAs that manifest a RZ score ≥ 1.8

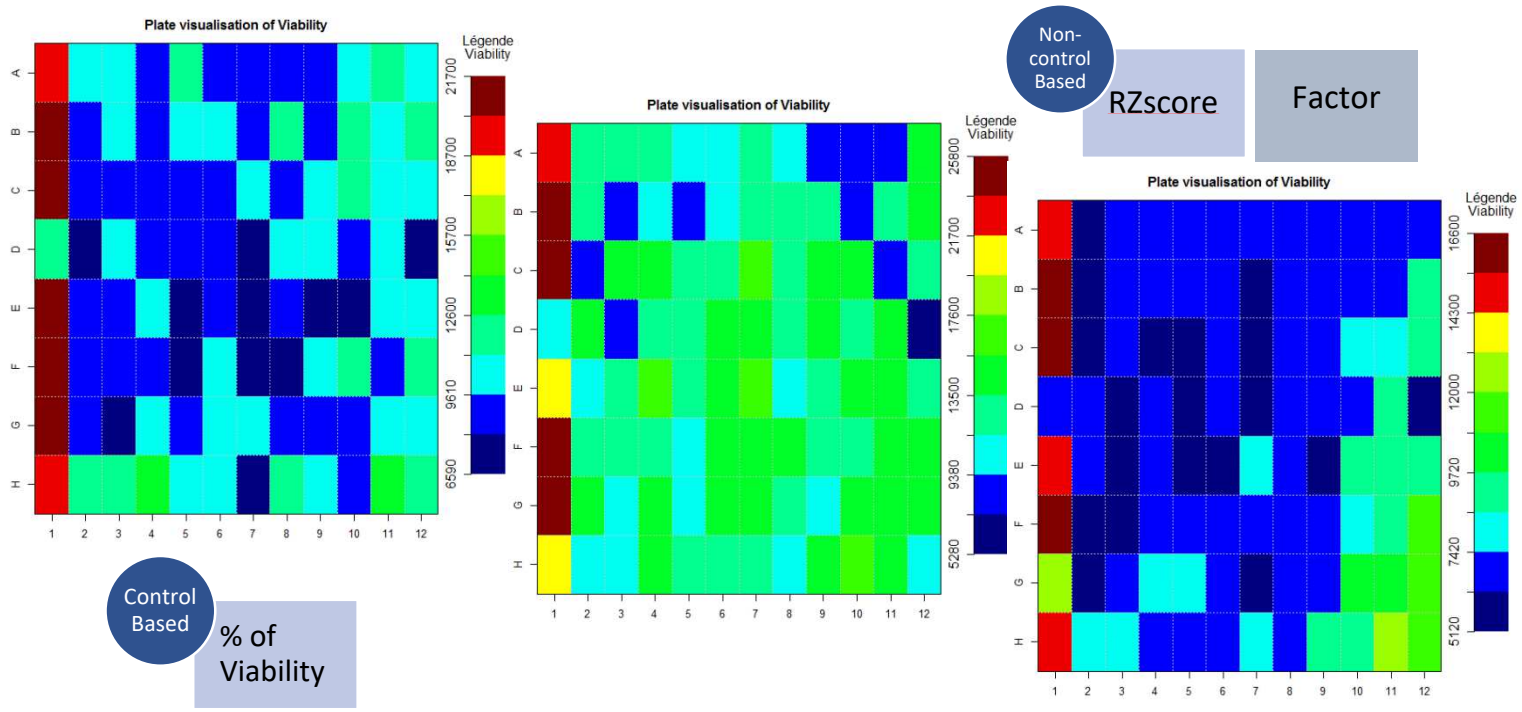

Figure 44 Raw viability data heatmap of transfected plates and normalization techniques

The heat map shows the distribution of viability values among the well of different plates. The 3 utilized normalization techniques to limit the inter-plate variation are the control based percentage of viability and the non-control based RZscore and correction factor normalization. Hits that are found positive in the majority of the normalization techniques were considered for further analysis.

The final normalization was based on the utilization of the geometric mean for the calculation of correction factor for each plate. This method starts with the calculation of the geometric mean of the raw viability values for all the plates combined. Then for each plate, the raw viability of each well will be divided by this geometric mean to allow the calculation of well correction factor. Finally, per plate, the median of the well correction factors will be calculated. This median will act as plate correction factor to allow the normalization of the between plate variation. So from that, we obtain one correction factor per plate so that all the raw viability values will be divided by their respective plate correction factor. This is a non-control based normalization. Combining all three normalization techniques, 28 kinases were selected for the secondary screening procedure (figure 45). These kinases were selected from the data of the XP-C cells screening. Some of these siRNA increase the viability of XPC exclusively while some have effects of both WT and XPC cells (table 6) after the comparison of these 28 hits of XP-C with the hits of the WT screen.

$$geometric\ mean = \sqrt[n]{X1_{plate\ a} * X2_{plate\ a} * X1_{plate\ b} \dots Xth_{plate\ z}}$$

$$FW_{th_{plate}a} = well\ correction\ factor_{plate\ a} = \frac{Xth_{plate\ a}}{geometric\ mean}$$

$$plate\ correction\ factor_a = median\ (FW_{th_{plate}a})$$

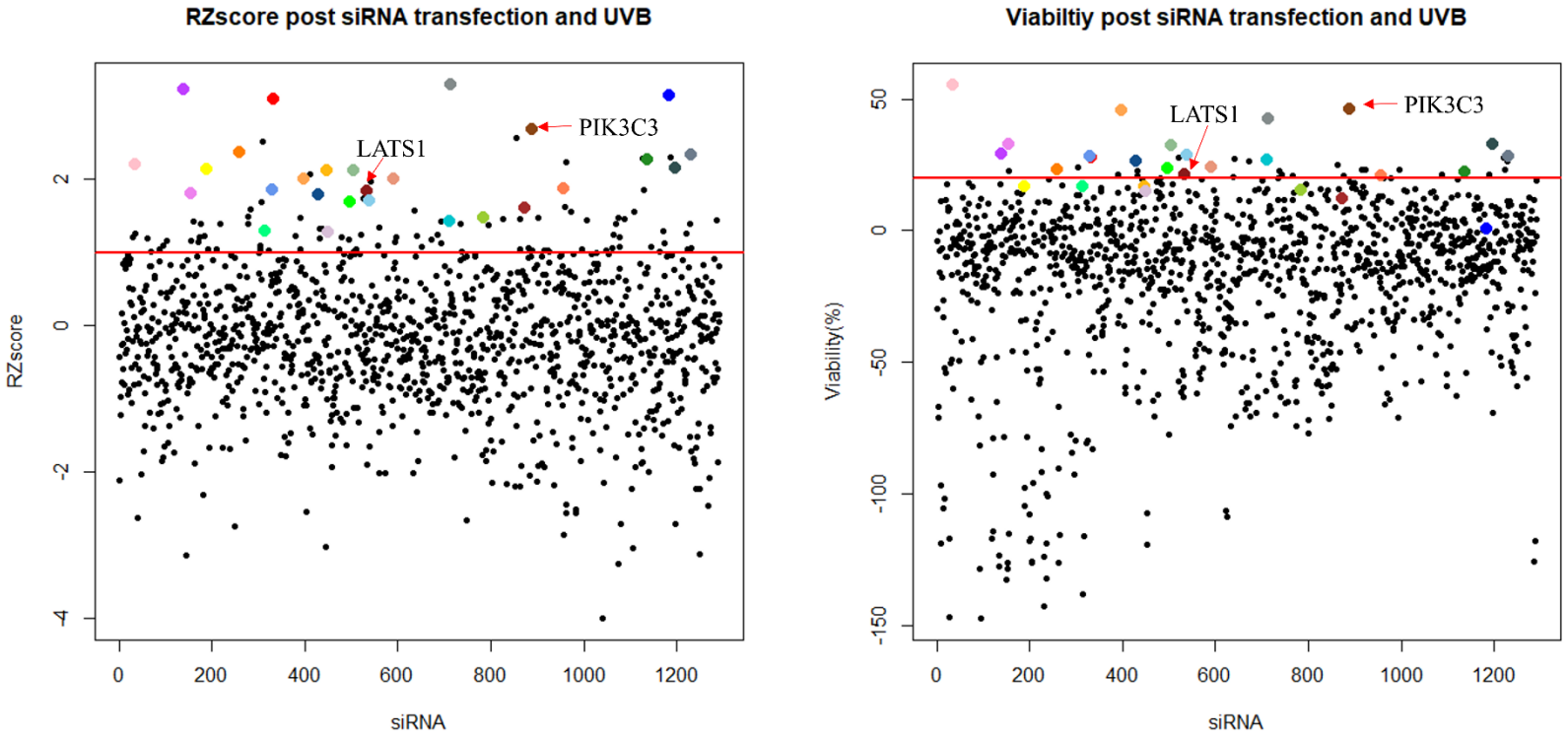

Figure 45 Identification of 28 kinases decreasing XP-C photo-sensitivity upon UVB irradiation.

Kinome targeting siRNA human library was screened on both XP-C and WT cells. Both cell lines were transfected with the library and controls at 5nM and incubated for forty-eight hours. The cells were further on irradiated at 0.03J/cm^2 UVB dose and their viability was measured twenty-four hours post irradiation via the addition of Presto Blue. Based on the different normalization techniques, mainly the control based % of activity and non-control based RZscore, 28 kinases were identified whose knock down enabled a >25% increase or >1.8 value for both % of activity and RZscore respectively. Control based % of activity was calculated by the normalization of the presto Blue data to the interval of 100% corresponding to siAS transfected non-irradiated cells and 0% attributed to siAS transfected irradiated cells. RZscore was calculated using the median and median absolute deviation per plate. RZscore: Robust Z score.

Table 6 Data of the primary siRNA screen hits after the different normalization techniques

% of Control Normalization		RZscore Normalization			Plate Factor Normalization	
Gene	XPC Viability	Gene	Rzscore XPC	Rzscore WT	Gene	XPC/Factor
AK2	55.45	NEK4	3.3	0.79	AK2	15971.66728
PIK3R3	46.28	CALM2	3.23	-0.68	NEK4	15297.84373
FASTK	45.74	TEK	3.14	-0.24	IRAK1	14537.11188
NEK4	42.67	DGUOK	3.1	0.23	CALM2	14233.83013
CAMK2G	33.03	PIK3R3	2.69	0.54	DGUOK	14027.24962
TIE1	32.82	CLK1	2.36	1.22	PIK3R3	13341.60173
ITK	32.263	TSSK6	2.34	1.19	TEK	13138.67661
CALM2	29.34	STK17B	2.27	1.43	TIE1	13114.0164
LATS2	28.72	AK2	2.2	1.13	ITK	13054.04914
DGKZ	28.27072	TIE1	2.16	0.41	PRKACG	12902.45329
TSSK6	28.14	CDK2	2.14	-0.25	CLK1	12674.00691
DGUOK	27.84	ITK	2.12	-0.02	FASTK	12604.87486
NEK3	27.09	GRK6	2.11	0.74	STK17B	12554.80524
GAK	26.64	FASTK	2.01	1.15	CDK2	12534.95829
MAP3K6	24.049	MAP3K6	2	0.06	GRK6	12490.1751
IRAK1	23.76587	PRKACG	1.88	0.54	GAK	12444.96992
CLK1	23.39498	DGKZ	1.85	0.13	MAP3K6	12386.07954
STK17B	22.24702	LATS1	1.83	-0.15	PIK3C3	12378.92896
LATS1	21.42016	CAMK2G	1.8	0.65	LATS1	12126.9889
PRKACG	20.90685	GAK	1.79	1.28	DGKZ	12047.15746
CDK2	16.98371	LATS2	1.71	1.46	RPS6KB1	12008.47428
GRK6	16.65791	IRAK1	1.69	1.28	TSSK6	11637.3345
DDR2	16.6161	PIK3C3	1.6	1.74	LATS2	11183.26259
PANK2	15.60773	RPS6KB1	1.48	0.91	CAMK2G	11131.84962
GSK3A	15.0651	PANK2	1.48	-0.49	DDR2	10851.78081
PIK3C3	12.29368	NEK3	1.43	1.25	PANK2	10730.46429
RPS6KB1	2.546046	DDR2	1.29	0.58	NEK3	10724.17409
TEK	0.781111	GSK3A	1.27	1.04	GSK3A	10291.37009

1.3 GO ENRICHMENT OF HITS

To figure out whether there is a relationship between the selected 28 kinases or if they belong to a common pathway, gene ontology and pathway analysis were conducted using Enrichr. It should be noted that these 28 kinases were selected based on the data of photo-protection in XP-C cells regardless whether some also have protective effects in WT cells as well or are exclusive to XP-C cells. This database allows the identification of the top ontologies or pathways that most genes in a particular hit list belong to. The output is in ranks where the highest rank is the pathway that most genes belong to. The scoring can be based on p value, rank-Z score, or a combination of the

(a) Panther-Pathway Analysis

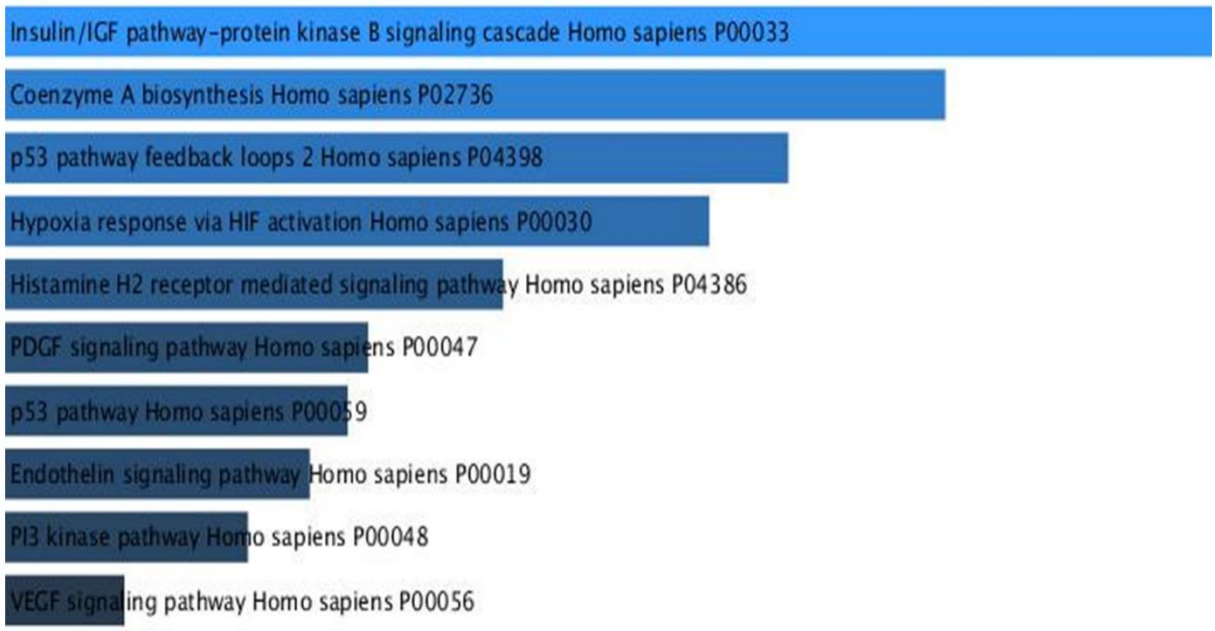

(b) GO-Biological Process

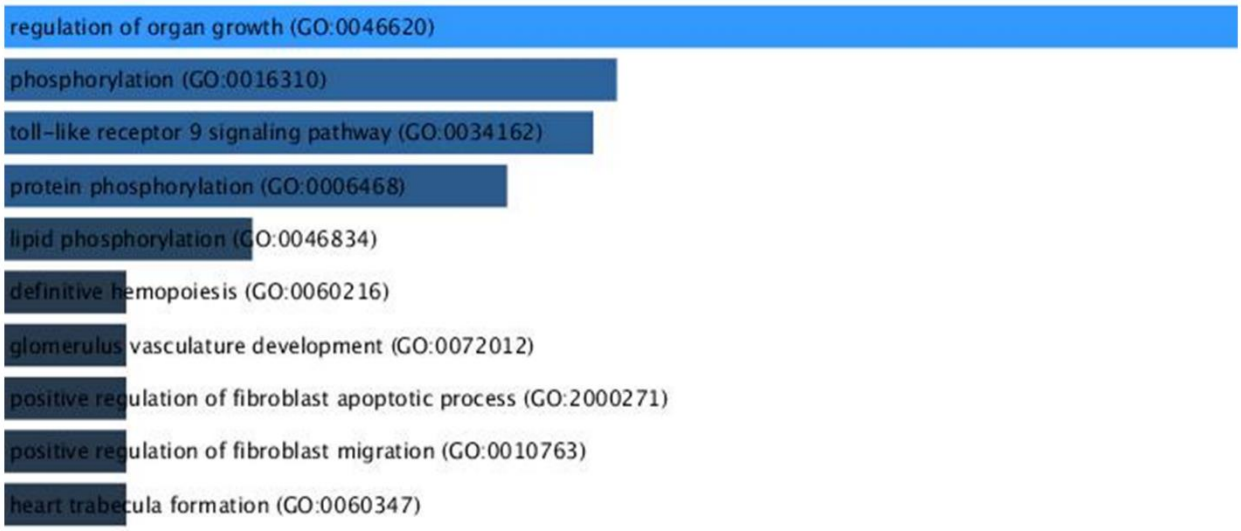

Figure 46 Biological Pathways enriched among the siRNA primary screen hits

The identified deregulated genes of the primary siRNA screen were run in the enricher software to allow the clustering of the different genes into common biological pathways based on the data provided by panther analysis and GO biological processes. One pathway of interest involves the regulation of the apoptotic process.

two. When conducting pathway analysis based on data from panther database and the combined score ten pathways were obtained. One pathway of interest is the P53 signaling pathway that might explain the increased survival of cells once such genes are deregulated leading to the inhibition of this pathway. However, when exploring the GO enrichment for common biological processes the top enriched processes are related to protein phosphorylation which is expected given the kinase nature of the used library. One of the enriched GO is the regulation of the apoptotic process (GO:004298) involving the genes: LATS1, LATS2, IRAK1, MEK4, RPS6KB1, TIE1, TEK, and DDR2 (figure 46).

2. SECONDARY SCREEN

2.1 SCREEN LAYOUT AND CONTROLS

A secondary screen with the 28 selected kinases was carried out on the XPC and WT cells. The aim of this secondary screen is to eliminate any false positives that might have been selected among the possible hits of the primary screen. Two siRNAs per kinase were utilized to have a total of 56 siRNAs utilized which correspond to the same siRNA sequences used in the primary screen. The positive control that shows highest viability is the siAS transfected non-irradiated cells while the negative control is the siAS transfected irradiated cells. SiCD is used to analyze the transfection efficiency as their proper delivery allows the induction of cell death in the cells allowing a notable decrease in viability. An additional control was added designated by EG5, an siRNA that induces mitotic arrest due to the depletion of KIF11 (Eg5) encoding a motor protein that belongs to the kinesin-like protein family involved in chromosome positioning and bipolar spindle formation during cell mitosis. This control can act as a marker for transfection efficiency as well and it was either irradiated or non-irradiated. The same siRNA concentration of 5nM was utilized with 48hrs transfection. The screening was carried out in triplicate.

2.2 HITS' SELECTION CRITERIA

Secondary screen hit selection was similar to the criteria utilized for the primary screen where the results of controls based normalization designated by % of control as well as non-control based normalization designated by Zscore were utilized. The confirmed hits were the ones showing a viability higher than 20% and a Zscore above 1.8. Twenty-eight different siRNAs were selected from the fifty-six ones that were tested (table 7). Some siRNAs selected target the same kinase with different sequences for a total of 23 kinases targeted (figure 47).

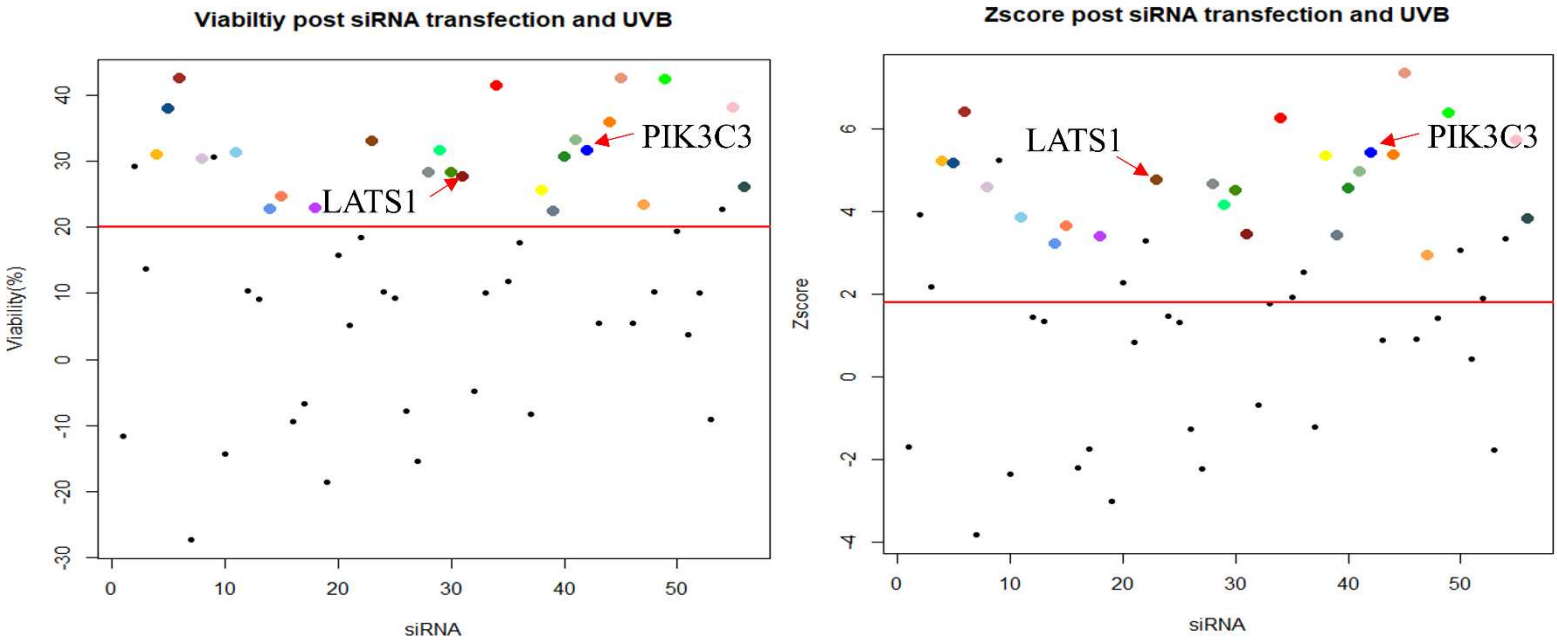

Figure 47 Secondary siRNA screen hits validation on XP-C cells

The primary screen selected hits were screened again on XP-C cells in a secondary screen for hit validation and the elimination of false positives. Same procedure of transfection at 5nM for 48 hours followed by irradiation at 0.03J/cm^2 then measurement of viability was carried out. After normalization based on % of control (>20%) and Z score (>1.8), twenty eight siRNA were selected where some target the same kinases with 2 different sequences. The total amount of targeted kinases is 23 different genes.

Table 7 Confirmed hits of the secondary siRNA screen on XP-C cells

Gene	Zscore	% of Control	Gene	Zscore	% of Control
AK2_5	3.927062	29.11726	LATS2_1	3.429556	27.60679
CALM2_7	5.21025	30.89495	MAP3K6_6	6.249729	41.37262
CAMK2G_2	5.150012	37.9231	NEK4_6	5.323561	25.50276
CAMK2G_3	6.392244	42.4956	PANK2_5	3.412649	22.46257
CDK2_8	4.56631	30.34379	PANK2_6	4.551301	30.56283
CLK1_2	5.220535	30.68944	PIK3C3_5	4.949462	33.14366
DDR2_2	3.841227	31.17385	PIK3C3_6	5.411534	31.48701
DGKZ_5	3.214304	22.75285	PIK3R3_5	5.358642	35.79591
DGUOK_10	3.644053	24.68216	PRKACG_5	7.333284	42.4458
FASTK_8	3.374449	22.93462	RPS6KB1_4	2.937697	23.34491
GSK3A_1	4.742301	32.96922	STK17B_1	6.36139	42.2956
ITK_6	4.64827	28.32118	TIE1_3	3.335515	22.68225
LATS1_5	4.132616	31.60858	TSSK6_1	5.71493	38.10533
LATS1_6	4.505755	28.17822	TSSK6_2	3.807859	25.96305

2.3 DNA DAMAGE ANALYSIS

The capacity of the knockdown of a particular kinase in enabling increase of XPC cells' photo-resistance post UVB is not enough as it should be coupled with enhanced repair of the created DNA damage. The lack of the latter leads to accumulation of DNA damage that with increased cell survival can give rise to mutation and ultimately cancer. Therefore, an additional readout was carried out to assess the ability to knock down particular kinases to decrease DNA damage. For that, XP-C cells were transfected with the siRNA library then UVB irradiated and incubated. Twenty-four hours post incubation the cells were fixed and stained with anti-6-4PP antibody to quantify the residual amount of DNA damage. The DNA damage analysis was carried out by quantifying the median fluorescence average intensity further on normalized such as 100% DNA damage was attribute to cells transfected with siAS and irradiated while 0% damage corresponds to cells transfected with siAS but in the absence of irradiation.

Out of the selected siRNA only a few enabled a slight decrease in DNA damage amount with the most prominent ones being the siRNAs targeting the genes LATS1 and PIK3C3 enabling a 20% repair of DNA damage when compared to siAS transfected irradiated cells (figure 48). The single cell representation of the selected kinases is portrayed as well where the difference between the siAS transfected irradiated cells and the kinase knocked down cells were found to be significant (figure 49).

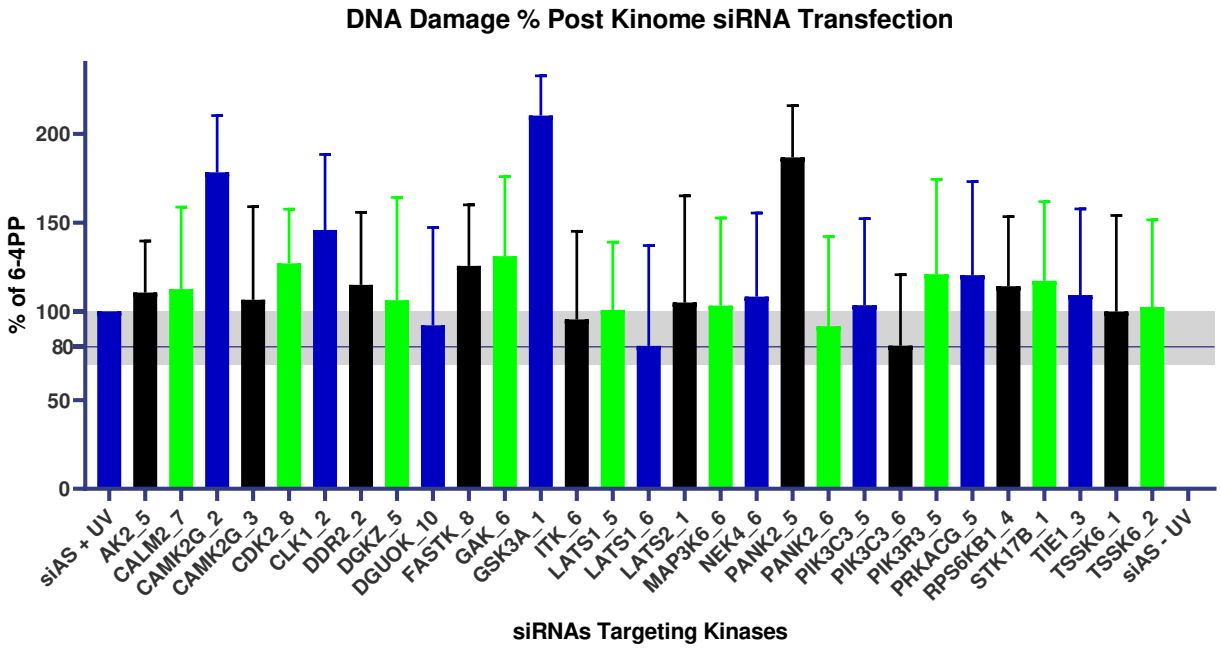

Figure 48 identification of siRNAs partially decreasing % of DNA damage in XP-C cells.

XP-C cells were transfected at 5nM with the 28 siRNAs hits of the secondary screen then irradiated at 0.03J/cm^2. The cells were further on fixed twenty four hours later and stained with 6-4 PP antibody and Hoechst. The fluorescence intensity of individual cells was calculated per condition then normalized to that of siAS transfected irradiated cells set as 100% and siAS non-irradiated cells set as 0%. Kinases whose knockdown enabled a 20% decrease in DNA damage were selected which are LAST1 and PIK3C3.

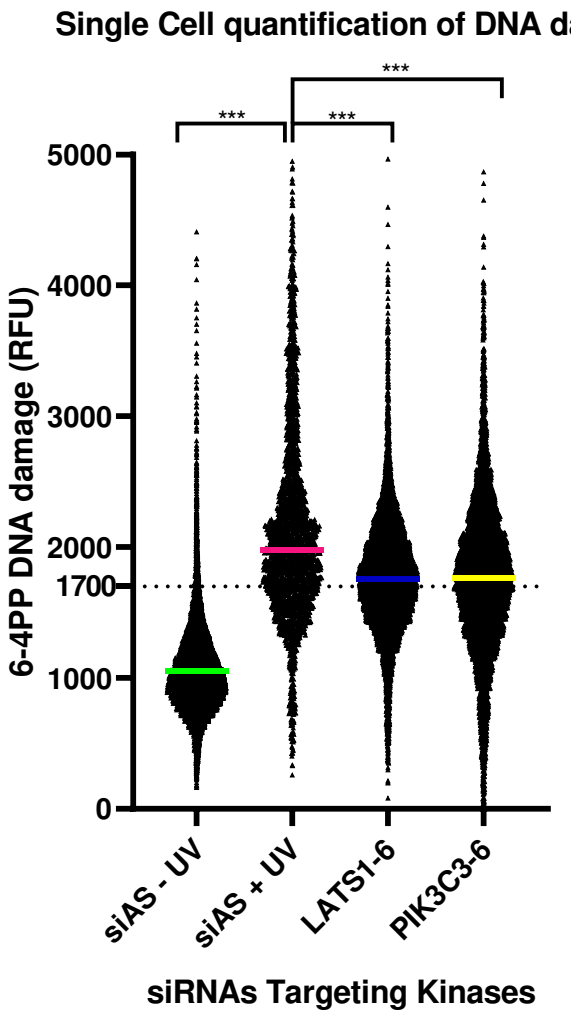

Figure 49 Single cell analysis of LATS1 and PIK3C3 mediated decrease in DNA damage levels.

*Following transfection with secondary screen hits and irradiation, XP-C cells were stained with 6-4PP antibodies followed by DNA counterstain with Hoechst. More than 1000 cells per condition were selected based on DNA stain and their DNA damage was quantified. Mean average intensity per cell is presented here in a violin plot that shows a decrease in DNA damage for cells transfected with either LATS1 or PIK3C3 compared to siAS transfected irradiated cells. This decrease was found to be significant. *** p<0.001, freedman non-parametric test with dun's post hoc analysis.*

2.4 KNOCKDOWN VALIDATION AT RNA AND PROTEIN LEVEL

To validate the effect of the selected siRNAs in down-regulating their targets, the expression levels of both LATS1 and PIK3C3 were investigated at mRNA and protein levels. WT and XP-C cells were transfected with either AS, siLATS1 or siPIK3C3 to be followed by both RNA and protein extraction. RT-qPCR revealed at ten-fold significant decrease in PIK3C3 mRNA in both WT and XP-C cells (p-value<0.001 and p-value<0.01 respectively). Fourfold decrease in expression of LATS1 was shown upon transfection with siLATS1 siRNA (p-value<0.05). This is also reflected

at the protein level with the absence of protein expression for both PIK3C3 and LATS1 in transfected cells compared to siAS transfected cells (figure 50).

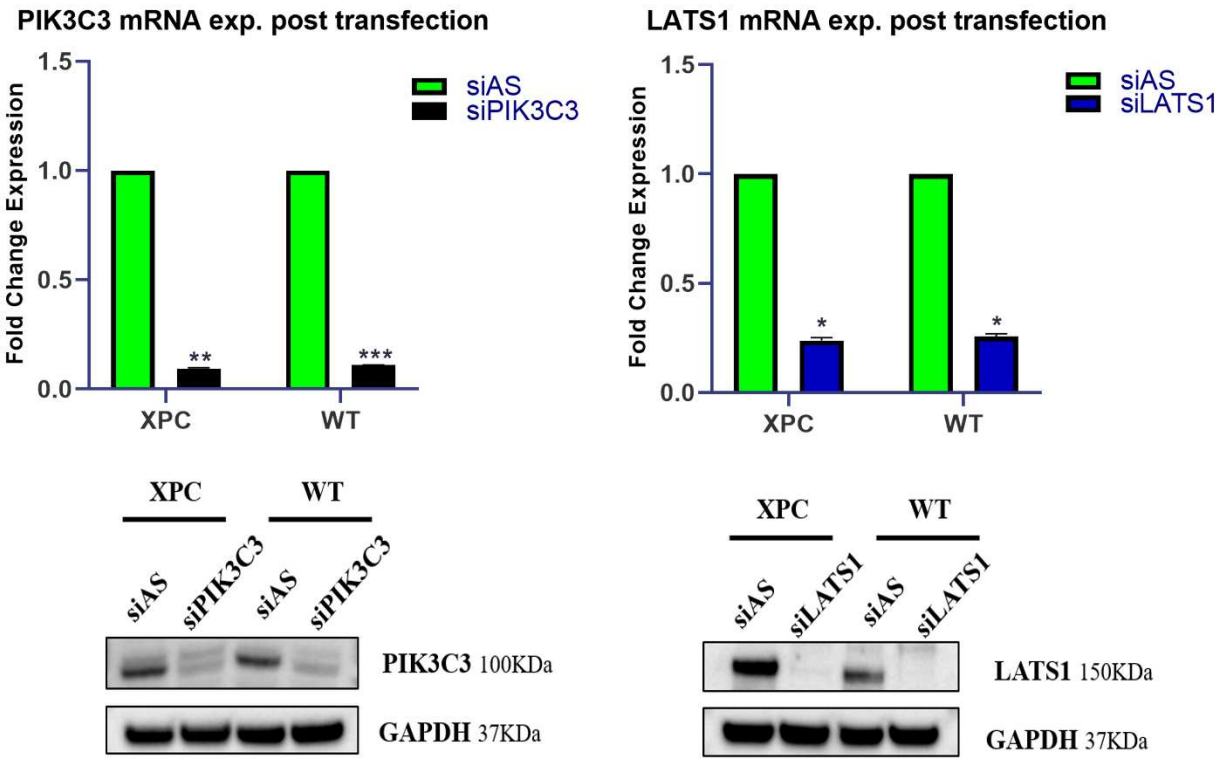

Figure 50 Validation of siRNA mediated knockdown at the mRNA and protein level

*To ensure that both siPIK3C3 and siLATS1 specifically knockdown the expression of their targets, XP-C and WT cells were transfected with either these siRNAs or siAS. After forty eight hours of incubation RNA and protein extraction was carried out. Both siPIK3C3 and siLATS1 were able to significantly decrease the expression of PIK3C3 and LATS1 respectively at the mRNA level in both XP-C and WT detected by RT-PCR. This knockdown was validated at the level of protein expression via western blot where transfected cells manifest absence of protein bands at the level of each target protein compared to siAS transfected samples. N =3 paired t-test *p-value<0.05, **p-value<0.01, ***p-value<0.001*

2.6 BIOINFORMATICS ANALYSIS OF OFF-TARGET EFFECTS

siRNAs mediate the knockdown of a particular gene via the degradation of its mRNA. This action is completed via the perfect complementarity between the mRNA and the siRNA incorporated in the RISC complex favoring the cleavage and thus degradation of the messenger RNA. However, siRNAs possess off target effects due to their miRNA like activity where only a seed region of around 7 bases and not the whole siRNA sequence has to have perfect complementarity with the mRNA for the deregulation to occur. Therefore, according to the sequence of the siRNA different possible miRNA like effects can exist allowing the downregulation of genes other than the intended target.

In the course of our study it is important to identify any possible off target effect to unravel the gene whose knockdown is really enabling the phenotypic reversal of the XP-C cells. For that, the two siRNAs that were validated to have an effect in this reversal were blasted against the whole genomic transcripts to determine on which other mRNA they can exert a miRNA like effect on. It was central to determine the mRNA as the two siRNA had similar effects so it is perhaps via the off-target regulation of the same gene that they exert their action. This was carried out with the **Genome-wide enrichment of seed sequence matches: GESS bioinformatics method.** One identified off-target deregulated gene is FOXN3 which has a role in repression of transcription and cell cycle arrest due to DNA damage. One can hypothesize that perhaps the knockdown of this gene prevents the cell cycle arrest and allows cells to go further and undergo mitosis. However, such possible role mediated by off-target downregulation needs to be confirmed by quantifying FPXN3 expression in transfected cells hence determining if the phenotypic reversal is due to off-target or on-target regulation of the hits identified. Expression profile of FOXN3 mRNA was analyzed by RT-PCR in XP-C and WT cells transfected with either siLATS1, siPIK3C3 or siAS. No significant down-regulation of FOXN3 expression was observed in siLATS1 or siPIK3C3 transfected XP-C and WT cells compared to siAS transfected cells eliminating the possibility that the reversal may have been due to a downstream effect of the deregulation of the off-target FOXN3 (figure 51).

Transcript ID	Gene	Rank	Role
NM_025059.3	CCDC170	62114	Golgi-associated microtubules' organization and stabilization
NM_001085471.1	FOXN3	63305	Transcriptional repressor that may be involved in DNA damage-inducible cell cycle arrests
NM_005197.3	FOXN3	63306	
XM_005267288.1	FOXN3	63307	
XM_005267289.1	FOXN3	63308	
XM_005267290.1	FOXN3	63309	
XM_005267291.1	FOXN3	63310	
NM_001145442.1	POTEM	65896	Unknown function, part of the cytoskeleton
NM_001013659.2	ZNF793	68431	May be involved in transcriptional regulation

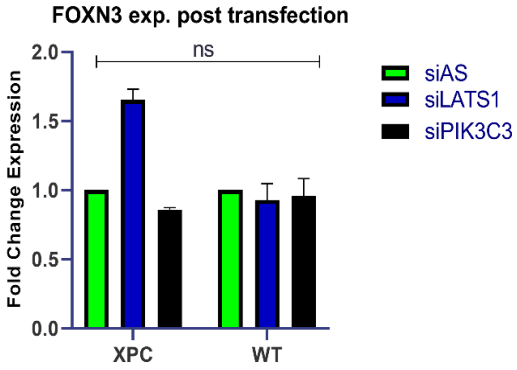

Figure 51 GESS analysis of off-target siRNA effects and RT-PCR mediated confirmation of the main hit

siRNAs can possess miRNA like effects on downregulating genes other than their targets based on incomplete complementarity. For that we utilized the GESS bioinformatics tool to identify possible off-target effects of the two siRNAs based only on seed complementarity of each siRNA sequence with the whole transcriptome. The mRNA that are potentially downregulated via a miRNA effect by both siRNAs were determined. A list of potential hits was generated among which FOXN3 deregulation was of interest due to its role in DNA damage-inducible cell cycle arrest. RT-PCR analysis negated the potential downregulation of this mRNA whose expression was not diminished in neither WT nor XP-C cells transfected with siLATS1 or siPIK3C3 compared to siAS.

2.7 siRNA SECONDARY SCREEN ON WT CELLS

Among the hits selected in the primary screen, some siRNAs showed increase in viability of both WT cells as well as XP-C as a consequence of the knockdown of their respective kinases. Therefore, screening hits on WT cells will allow us to check whether the effect is XP-C dependent or not. Also, identifying potential kinase knockdowns that can help protect WT cells is of great interest. The selected primary screen siRNAs were screened in WT cells at a higher dose of 0.1j/cm^2 and hit selection was based on the Zscore and % of control as discussed earlier. Ten kinases were selected whose knockdown enhances viability of WT cells to UVB irradiation (figure

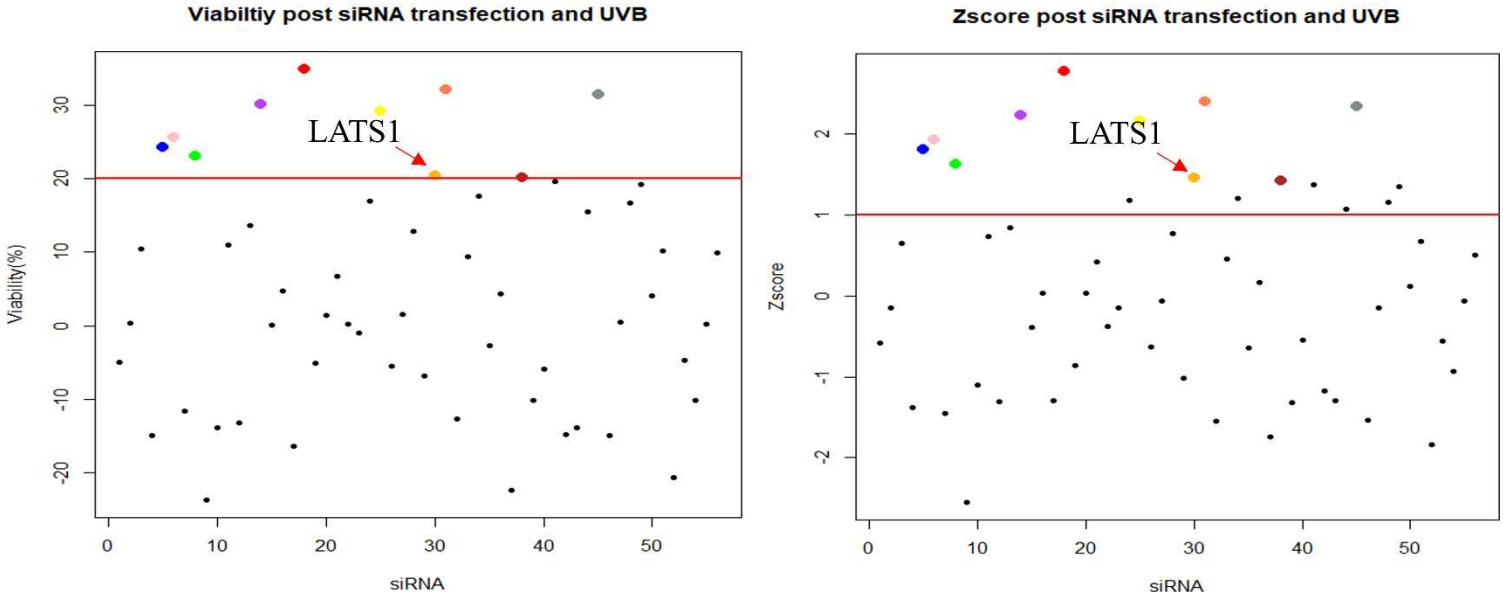

Figure 52 Secondary siRNAs screen hits validation on WT cells

The primary screen selected hits were screened again on WT cells in a secondary screen for hit validation and the elimination of false positives. Same procedure of transfection at 5nM followed by irradiation at 0.1J/cm^2 then measurement of viability was carried out. After normalization based on % of control (>20%) and Z score (>1.8), ten siRNAs were selected where some target the same kinases with 2 different sequences. This allows the identification of hits with exclusive effect on XP-C cells like PIK3C3 only found protective for XP-C cells or hits with common protective response in both cell lines.liek LATS1.

52, table 8). All the genes selected also enabled an increase in XPC viability except for IRAK1 gene that had an exclusive effect in WT cells rather than XPC.

Table 8 Confirmed hits of the secondary siRNA screen on WT cells

Gene	Zscore	% of Control
CAMK2G_2	1.812826	24.28381
CAMK2G_3	1.93524	25.63021
CDK2_8	1.633119	23.07316
DGKZ_5	2.238294	30.14579
FASTK_8	2.78004	34.92197
IRAK1_5	2.158327	29.14894
LATS1_6	1.456052	20.39447

LATS2_1	2.397941	32.13593
NEK4_6	1.419124	20.18567
PRKACG_5	2.347105	31.50222

2.8 UVB DOSE RESPONSE AANALYSIS POST TRANSECTION IN XP-C AND WT CELLS

To further characterize the effect of PIK3C3 and LATS1 knockdown on the enhancement of viability, both XP-C and WT were transfected with either siAS, siPIK3C3 or siLAT1 then subjected to increasing doses of UVB. Viability was measured twenty four hours later and normalized to that of non-irradiated cells (viability 100%). This can help decipher whether the effect of the knockdown of these particular kinases is specific to XP-C or is a general protection phenomenon for both cell lines. SiPIK3C3 transfection in XP-C conveyed a significant protection against increased UVB doses compared to siAS transfected cells (p-value<0.05). Such effect was not evident for WT cells where only siLATS1 transfection enhanced the viability of WT cells post UVB (p-value<0.05). LATS1 knockdown also mediated photo-protection in XP-C cells but was not significant (figure 53). In conclusion, the protective effect of PIK3C3 knockdown was specific to XP-C cells while LATS1 knockdown mediated photo-resistance in both XP-C and WT cells.

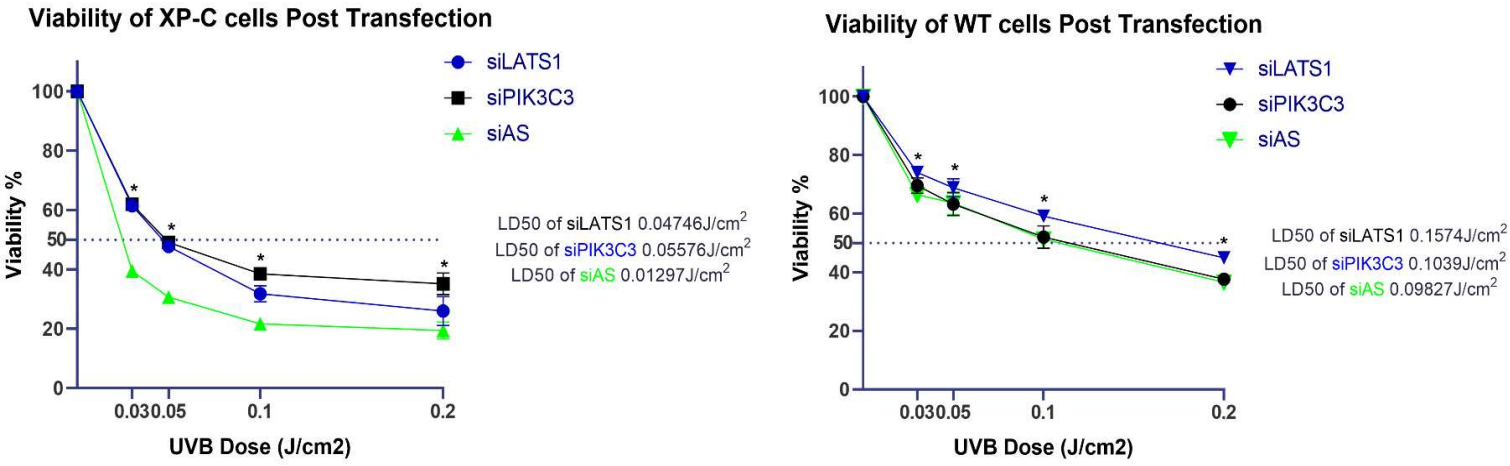

Figure 53 Consequence of PIK3C3 and LATS1 knock down on cell viability in UVB dose response analysis

*XP-C and WT cells were transfected with either siLATS1, siPIK3C3 or siAS then subjected to increased UVB doses. Their viability was further on assessed 24hours post UV by the incubation with PrestoBlue. Both siRNAs showed UV-protection in XP-C cells with siPIK3C3 having a higher and significant increase in XP-C viability compared to siAS (p-value<0.05) with LD50 of 0.05576J/cm² compared to 0.01297J/cm² for siAS transfected cells. WT cells UVB-protection was evident in cells with LATS1 knockdown (p-value<0.05) showing increase in LD50 to reach 0.1574J/cm² while siPIK3C3 transfection had no effect. Viability was calculated by determining the percent of control with respect to non-irradiated siAS transfected cells taken as 100% viable. * p-value <0.05, For WT cells: Repeated Measure one way ANOVA with Dunnett's multiple comparison test and for XP-C cells Freedman test with Dunn's multiple comparison.*

3. KNOCKDOWN PHYSIOLOGICAL CONSEQUENCE

3.1 REDUCTION OF APOPTOSIS BY PIK3C3 AND LATS1 KD IN XP-C AND WT CELLS RESPECTIVELY

To examine the cellular mechanisms of photo-resistance mediated via the depletion of the two hit kinases LATS1 and PIK3C3, we assessed cell death. Quantification of apoptosis using Cell Event, indirect measurement of caspase 3/7 activity, and PI staining were carried out. XP-C or WT cells were transfected with either siAS, siLATS1 or siPIK3C3 then irradiated at doses 0.03J/cm^2 and 0.1J/cm^2 respectively for XP-C and WT cells. Twenty hours post UV the cells were collected and analyzed by flow cytometry. Both siLATS1 and siPIK3C3 transfection enabled a significant increase in XP-C live cell population compared to siAS transfected cells (p-value<0.001). The photo-resistance mediated by PIK3C3 knockdown in XP-C cells was greater than that of LATS1 knockdown. The opposite is visualized in WT cells, where LATS1 knockdown induced a higher increase in live cell population compared to a lower increase induced by PIK3C3 knockdown (p-value<0.001) (figure 54). This suggests that PIK3C3 knockdown in XP-C cells and LATS1 knockdown in WT cells decrease the level of apoptosis in these cells post UVB irradiation.

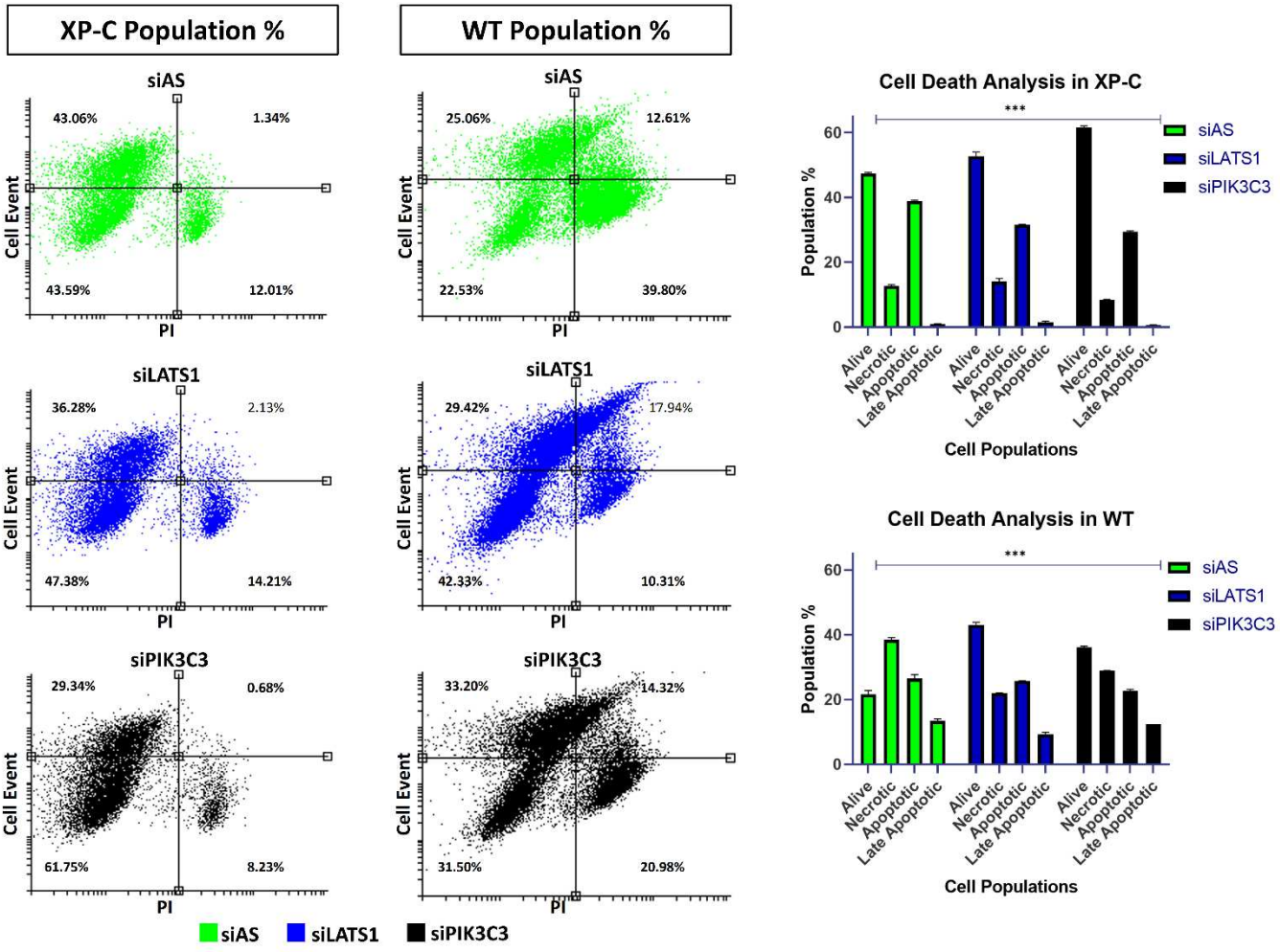

Figure 54 PIK3C3 and LAST1 knockdown and their consequences on apoptotic cell death in XP-C and WT cell lines.

*To decipher the effect of downregualtion on UVB induced apoptotic cell death, XP-C and WT cells were transfected with siAS,siPIK3C3 or siLAT1 then irradiated at 0.03 and 0.1J/cm^2 for the XP-C and WT cells respectively. CellEvent caspase 3/7 marker was added post UV then cells were collected. PI was added just before analysis on a flow cytometer. Both knock downs efficiently increased live cell populations in XP-C cells with siPIK3C3 mediating a higher increase (61.75% vs. 43% for siAS) accompanied with a decrease in apoptotic cell population (29% vs. 43% for siAS). For WT cell LATS1 knock down mediated a higher increase in live cell population compared to siPIK3C3 or siAS. Two way anova was used to compare between the two independent variables (type of cell death or stain and nature of the transfection) and the dependent variable which is the population %, ***p<0.01.*

3.2 NO CHANGE IN THE PROLIFERATION STATUS UPON TATGETED KINASES' DOWNREGULATION IN XP-C AND WT CELLS

To study the effect of the different siRNAs transfection on the proliferative capacity of the cells, XP-C and WT cells were transfected with the different siRNAs then subjected or not to UVB irradiation at 0.02J/cm^2. Two hours post UV and EDU incorporation, the cells were collected and stained. Analysis with flow cytometry revealed no significant difference in EDU incorporation at

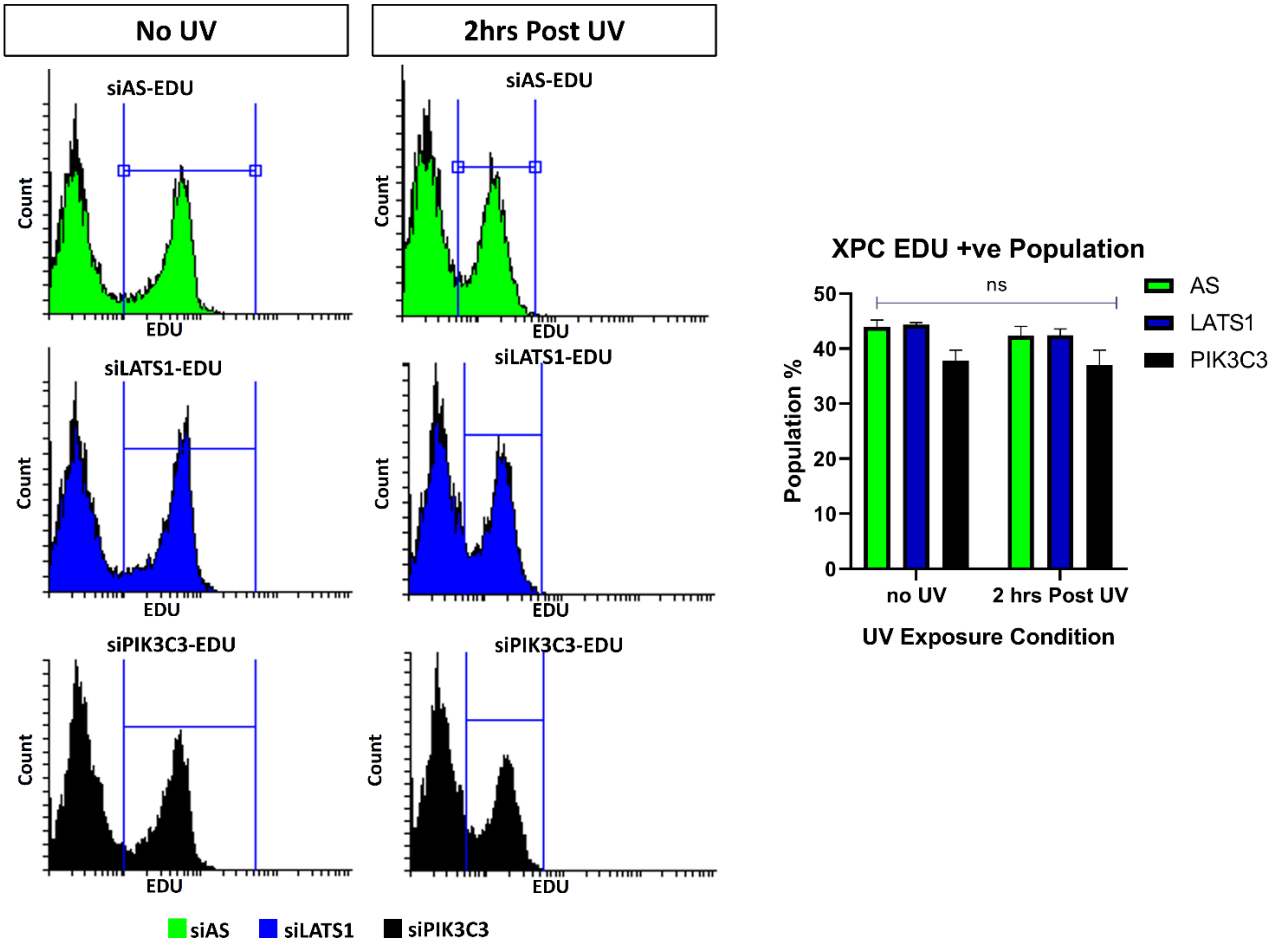

Figure 55 Same EDU incorporation is evident between siPIK3C3, siLLAST1 and siAS transfected XP-C cell line.

XP-C cells were transfected with the different siRNAs then irradiated. Prior to the end of the post UVB incubation, the cells were incubated in the presence of EDU. Cells were further on collected, stained and analyzed by flow cytometry. No difference is seen between the EDU positive populations in the different treatment condition at either 2 or 4 hours post UV. Two way anova was used to compare between the two independent variables (time post UV and nature of the siRNA transfected) and the dependent variable of EDU population percentage.

the basal non-irradiated level as well as two hours post UV for both XP-C and WT cells transfected with either siAS, siLATS1 or siPIK3C3. Hence, it is not via proliferation enhancement that the down regulated kinases exert their action in the enhancement of cell viability (figure 55 and figure

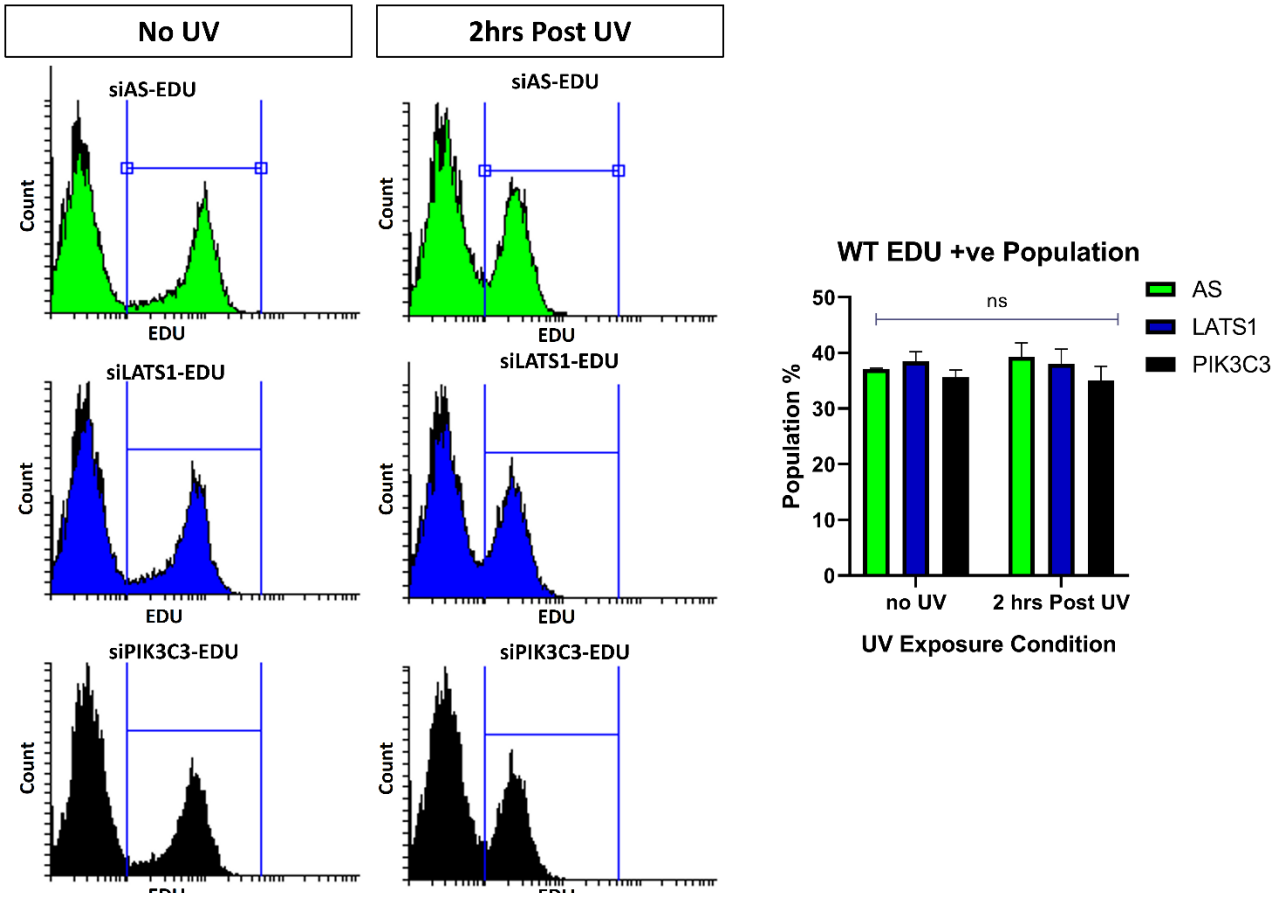

Figure 56 Same EDU incorporation is evident between siPIK3C3, siLLAST1 and siAS transfected WT cell line.

WT cells were transfected with the different siRNAs then irradiated. Prior to the end of the post UVB incubation, the cells were incubated in the presence of EDU. Cells were further on collected, stained and analyzed by flow cytometry. No difference is seen between the EDU positive populations in the different treatment condition at either 2 or 4 hours post UV. Two way anova was used to compare between the two independent variables (time post UV and nature of the siRNA transfected) and the dependent variable of EDU population percentage.

56) despite LATS1 knockdown showing a slight increase in EDU incorporation at basal level in both cell lines.

3.3 EFFECT OF TRANSFECTION ON OXIDIZED PURINE REPAIR

XPC cells are characterized by an increase in the production of reactive oxygen species due to a disrupted homeostasis. The latter favors the formation of oxidized purines[188]. Thus, to decipher the effect of transfection on the production and repair of oxidized purines, XP-C and WT cells were transfected with the different siRNAs, irradiated at dose 0.02J/cm^2 then collected at different times points post UV (0, 2 and 24 hours). The cells were then analyzed with modified alkaline assay with the addition of FPG that allows the conversion of oxidized purines into strand breaks permitting their quantification by the subtraction of the mean tail intensities in the presence of FPG from those in the absence of FPG. The speed of repair was determined via the quantification of the slope of decrease in damage as function of time. WT cells transfected with siLAT1 showed lower amount of oxidized purines at time zero post UV compared to siAS or siPIK3C3 transfected WT cells (p-value<0.001). Regardless of the downregulated kinase, all conditions manifest significant decrease in amount of oxidized purines as function of time post UVB irradiation. siAS and siPIK3C3 transfected WT cells show similar repair kinetics, with siAS samples manifesting slightly faster repair with slope of -0.2886 compared to -0.2148 for siPIK3C3. In XP-C cells little repair is visualized for XP-C cells transfected with siAS that show lower amount of oxidized purines at time zero compared to the other conditions despite not being significant. SiLATS1 transfected cells manifest greater oxidized purines at time zero but they were significantly decreased as function of increased incubation time post UV with a slope of -0.3626. Slower repair is visualized in PIK3C3 knocked down XP-C cells showing a slope of -0.23. It should be noted that the slope for the repair was calculated based on the linear regression for each condition (figure 57).

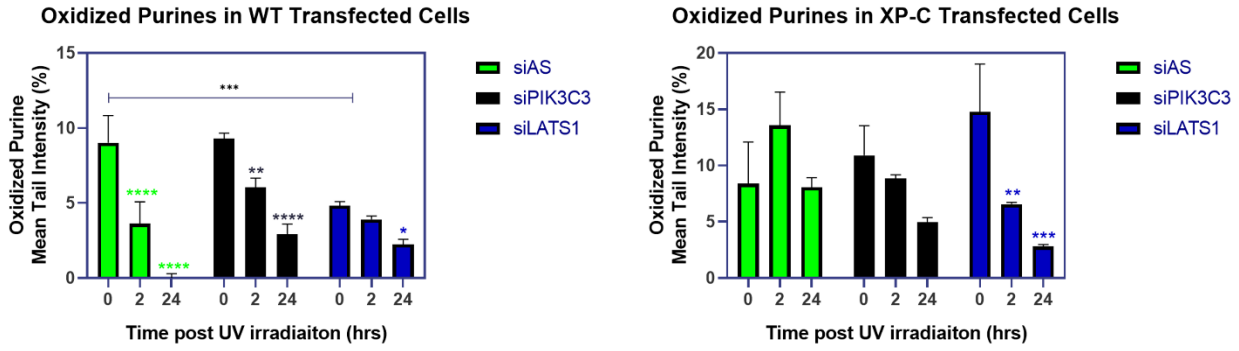

Figure 57 Repair of oxidized purines in WT and XP-C cells post transfection

The amounts of oxidized purines were quantified in the different transfection conditions with either siAS, siPIK3C, siLATS1 for both WT and XP-C cells using comet assay ± FPG. WT cells with downregulation of LATS1 manifest lower amounts of lesions at time zero compared to siAS or siPIK3C WT transfected cells. In all samples the amount of damage decreased as function of time with fastest repair for siAS transfected cells. XP-C cells, however, showed

*little repair for oxidized purines in siAS condition, while in both siPIK3C and siLATS1 repair was evident as function of time ad was more efficient for XP-C cells with LATS1 knockdown. Two-way anova with Tukey's multiple comparison and linear regression. *p-value<0.05, **p-value<0.01, ***p-value<0.001, ****p-value<0.0001.*

4. DECIPHERING REGULATION OF MOLECULAR MECHANISMS OF XPC SYNTHETIC RESCUE

4.1 EFFECT OF siPIK3C3 AND siLATS1 ON THE PHOSPHORYLATION PROFILE OF AKT AND P53.

In order to decipher the effect of LATS1 and PIK3C3 depletion then irradiation on the downstream effected signaling, we chose to quantify the phosphorylation level of both phospho-AKT Ser473 and phospho-P53 Ser15 as well as P53 and AKT expression. Phosphorylation of AKT Ser473 was shown to be mediated by UVB irradiation and leads to skin survival via the inhibition of apoptosis [346]. As for phosphorylation of P53 at Ser15, it is considered as an early step leading to downstream induction of apoptosis[347].

XP-C and WT cells were cultured in 6-well plates and transfected with either siAS, siLATS1 or siPIK3C3. Forty-eight hours later the cells were exposed or not to UVB of dose 0.02J/cm^2.The same dose was used for both cell lines. Thirty minutes post UV, the cells were collected and their proteins extracted to be resolved on SDS-PAGE.

XP-C cells transfected with PIK3C3 showed no change in P53 expression or P-P53 Ser15 phosphorylation at the basal level compared to siAS transfected cells. However, post irradiation siPIK3C3 XP-C cells manifested a significant (p-value<0.05) decrease in P53 expression as well as decrease in P53 Ser15 phosphorylation hence explaining the lower apoptotic levels manifested in XP-C siPIK3C3 transfected cells. As for AKT expression and phosphorylation, basal level expression of AKT was non-significantly higher in siPIK3C3 transfected cells. An inverse profile was displayed post irradiation with lower AKT expression for siPIK3C3 transfected XP-C cells combined with a significant (p-value<0.05) increase in AKT Ser473 phosphorylation compared to siAS controls (figure 58a). WT cells transfected with siPIK3C3 showed no change in the basal or post irradiation expression level of either P53 or AKT between siPIK3C3 transfected versus siAS cells. The phosphorylation levels of both proteins were as well unaltered (figure 58b). This lack of differential expression and phosphorylation validates the absence of effect of siPIK3C3 transfection on WT cells compared to their effects on XP-C cells.

a) Effect of PIK3C3 knock down on XP-C cells

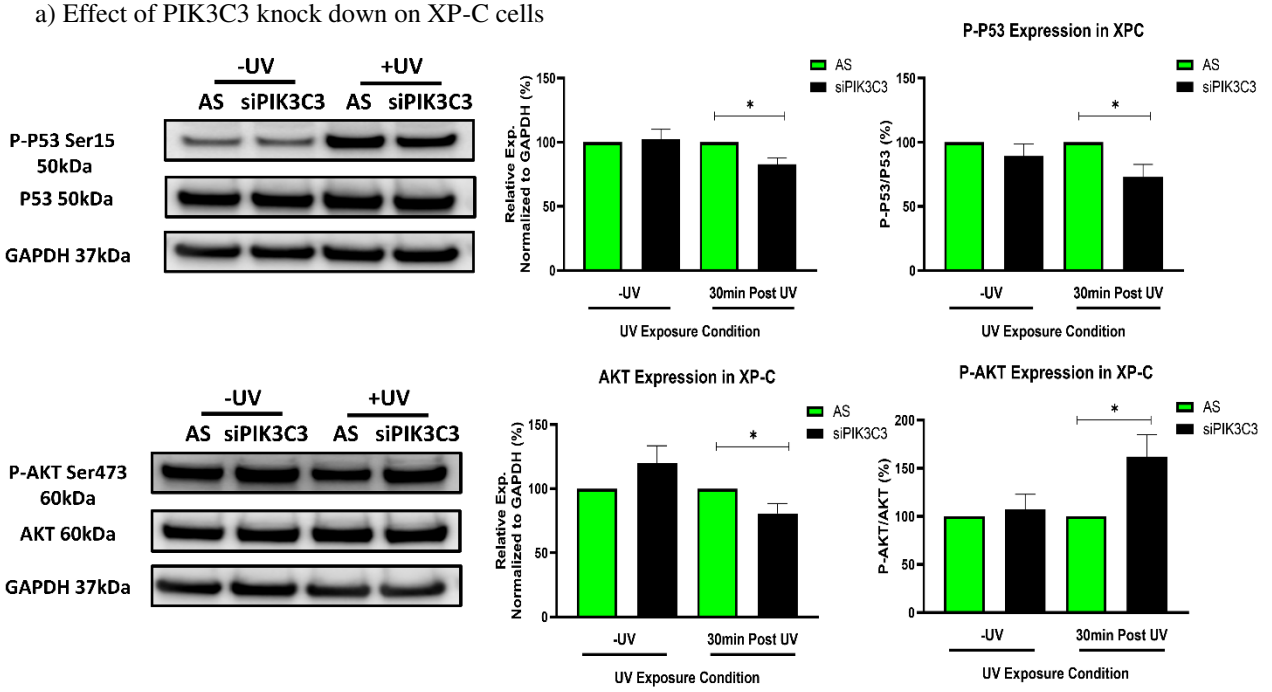

b) Effect of PIK3C3 knock down on WT cells

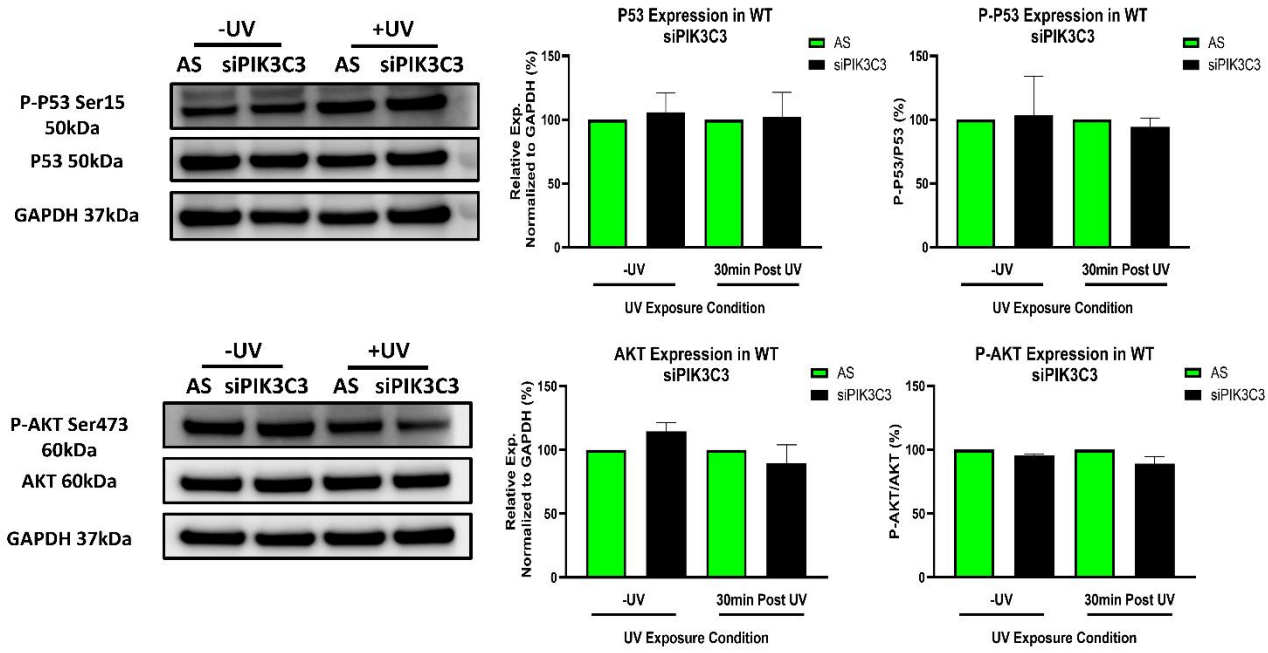

Figure 58 The effect of PIK3C3 knock down on the phosphorylation profile of P53 Ser15 and AKT Ser473 in XP-C and WT cells.

*XP-C and WT cells were transfected with either siAS or siPIK3C3 then irradiated. Protein extraction was then carried out to follow up the phosphorylation profile of both P53 and AKT. a)siPIK3C3 transfection lead to a decrease in the level s of P-P53 Ser15 while mediating an increase of P-AKT Ser473 (p-value<0.05) in XP-C cells. b) WT cells showed no significant difference for both phosphorylated proteins profile. Paired t-test *p-value<0.05*

SiLATS1 showed no significant changes in P53 expression or phosphorylation compared to siAS in transfected XP-C cells at both basal and post irradiation conditions. Although, this treatment was able to induce changes in AKT expression with an increase at basal level (p-value<0.05) and a non-significant decrease upon irradiation. P-AKT Ser473 was elevated in siLATS1 transfected cells with and without UV but was non-significant (figure 59a). Finally, LATS1 downregulation in WT cells showed similar effects as siPIK3C3 transfection in XP-C. siLATS1 transfection in WT cells enabled a non-significant decrease in both P53 and AKT levels while P-P53 Ser15 was significantly downregulated and P-AKT Ser473 significantly upregulated (p-value<0.05) in response to UV irradiation and compared to scrambled transfected WT cells. Thus LATS1 downregulation was more effective in WT cells altering both P53 and AKT phosphorylation compared to a lower effect manifested in XP-C cells (figure 59b).

a) Effect of LATS1 knock down on XP-C cells

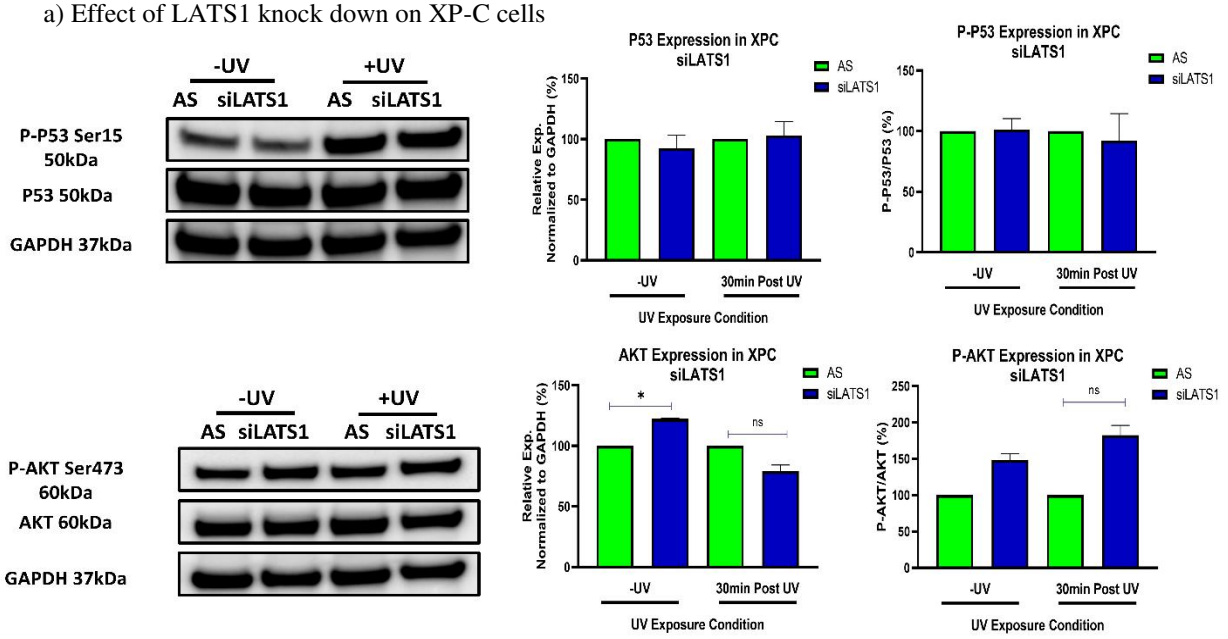

b) Effect of LATS1 knock down on WT cells

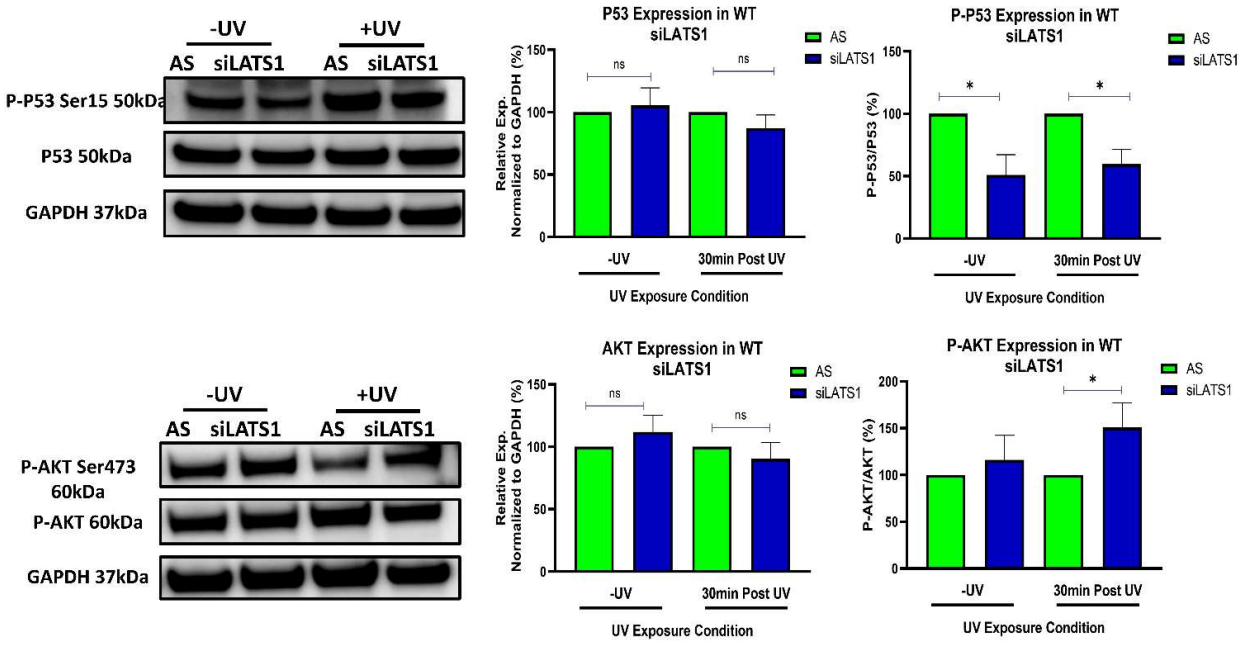

Figure 59The effect of LATS1 knock down on the phosphorylation profile of P53 Ser15 and AKT Ser473 in XP-C and WT cells.

*XP-C and WT cells were transfected with either siAS or siLATS1 then irradiated. Protein extraction was then carried out to follow up the phosphorylation profile of both P53 and AKT. a) siLATS1 transfection lead to an increase in the level s of P-P53 P-AKT Ser473 without affecting P-P53 Ser15 levels in XP-C cells. b) WT cells showed a decrease in P-P53 Ser15 with an increase in P-AKT Ser473 upon LATS1 knockdown. Paired t-test, *p-value<0.05*

4.2 EFFECT OF LATS1 DOWNREGULATION ON YAP EXPRESSION AND TRANSLOCATION

LATS1 is one of the proteins involved in the Hippo pathway (Supplementary figure 1). The latter negatively regulates the activity of the transcriptional co-activator with PDZ-binding motif (TAZ) and the Yes-associated protein 1 (YAP). The off-state of the Hippo pathway involves the translocation of the YAP/TAZ complex to the nuclei where it interacts with the TEA domain family member (TEAD) leading to the transcription of genes controlling cell proliferation, apoptosis and cell fate [348]. In the on-state, YAP/TAZ will be sequestered to the cytoplasm where they will be subjected to degradation. Therefore, we postulate that the knockdown of LATS1 might have an effect on the YAP expression. XPC and WT cells were transfected with either siAS or siLATS1 then irradiated at 0.02J/cm^2. The cells were further on collected 30 minutes post UV and had their proteins extracted to be resolved on SDS-PAGE. On one hand, YAP expression was unaltered upon LATS1 transfection in XP-C cells compared to siAS in both irradiated and sham irradiated samples. There was a slight but insignificant increase in YAP expression in LATS1 transfected WT cells post UV. On the other hand, LATS1 transfected WT non-irradiated cells manifested an increase in YAP expression compared to siAS transfected control. However, upon irradiation Yap expression was downregulated in WT LATS1 transfected cells. Both regulations in WT cells were not significant (figure 60).

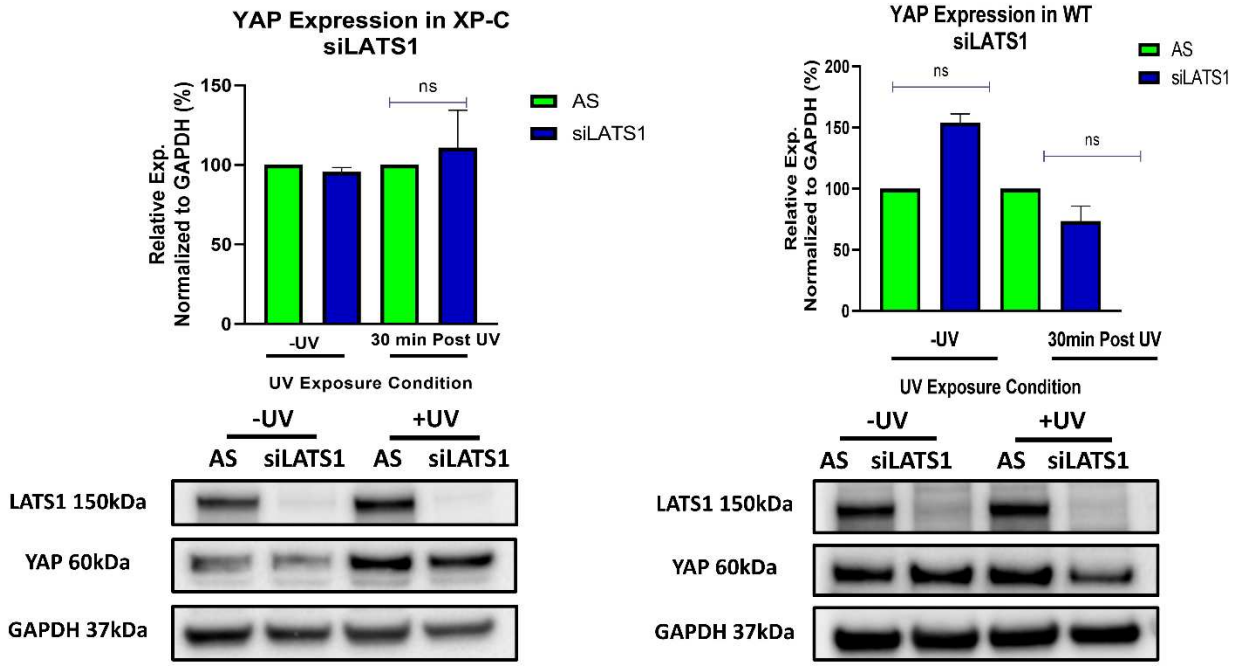

Figure 60 YAP expression profile in XP-C and WT cells upon LATS1 downregulation

YAP expression at the basal and post UV levels was analyzed in both XP-C and WT cells transfected with siAS or siLATS1. No difference was recorded for YAP expression in XP-C cells between siAS versus siLATS1 transfections. In WT cells basal YAP was upregulated upon LATS1 knockdown while post UV expression was decreased. However, both differential regulations were not significant. Paired t-test.

Due to the lack of significant differences in YAP expression in XP-C siLATS1 transfected cells, we then proceeded to quantify the translocation of YAP to the nuclei to further clarify the nature of the observed photo-protection. XP-C and WT cells were seeded in 96 well plates then transfected with either siAS or siLAST1. One hour post irradiation the cells were fixed. After permeabilization, the cells were incubated with an antibody against YAP. Phalloidin staining was used to delimit the circumference of the cell while Hoechst staining enabled the determination of the nuclear region. XP-C cells manifested vast translocation of YAP to the nuclei at the basal level upon the knockdown of LATS1 (p-value<0.001) which was lower upon irradiation but still significantly different than siAS transfected irradiated XP-C cells (p-value<0.01). WT cells showed slight increase in translocation of YAP to the nuclei at basal and irradiated states but were not significant (figure 61). However, these translocations had no effects on the proliferation capacity of both XP-C and WT cells as manifested earlier. So it perhaps via another pathway that YAP is exerting its protective in XP-C cells.

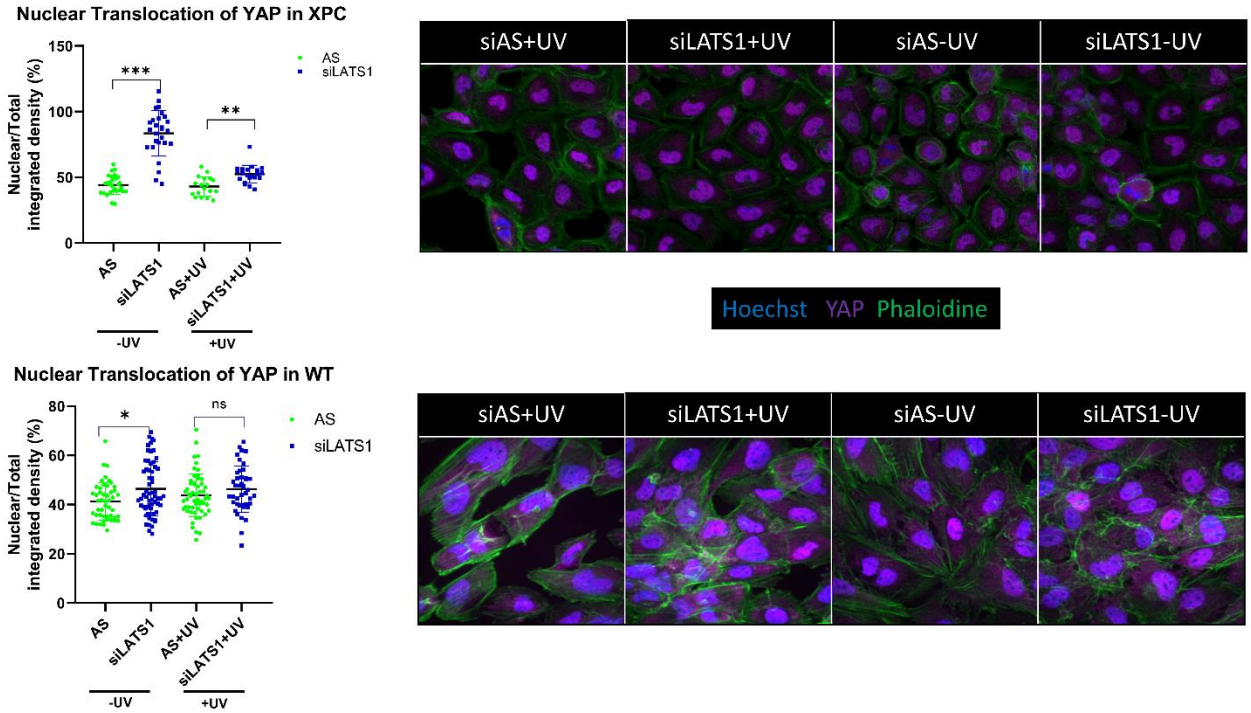

Figure 61 YAP translocation upon LATS1 downregulation in XP-C and WT cells.

The effect of siLATS1 transfection on YAP translocation to the nucleus was quantified in both XP-C and WT cells prior and post UVB irradiation. XPC and WT cells were seeded in 96 well plates and transfected with either siLATS1 or siAS for 48 hours. The cells were then irradiated and fixed one hour post UV. YAP Ab was utilized to follow the translocation of YAP protein while staining with both Hoechst and phalloidine were used to delimit both the nuclei

*and the cell circumference respectively. XP-C cells manifested increased translocation of YAP to nuclei prior and post UV upon LATS1 knockdown. WT showed as well YAP translocation at the basal no UV level that was less upon irradiation. Mixed effect analysis with Tukey's multiple comparison analysis. *p-value<0.05, **p-value<0.01, ***p-value<0.001.*

4.3 PIK3C3 KD MEDIATES SYNTHETIC RESCUE IN XPC CELLS

In order to understand better the downstream effects of PIK3C3 knockdown, we performed string protein analysis to find validated protein interactors with PIK3C3. The search was based on known interactions from databases or experimentally established interactions. In addition, other interactors based on gene neighborhood, fusion and co-occurrence, text mining, co-expression and protein homology were taken into consideration. Ten proteins were identified which mostly belong to the autophagy pathway (figure 62) including UVRAG, Beclin and ATG proteins. PIIK3C3 is an active mediator of autophagy via the formation of complexes with Beclin and UVRAG[349] . Therefore we wanted to examine the changes in UVRAG and Beclin interaction upon the depletion of PIK3C3. For that XP-C cells transfected with either siAS or siPIK3C3 were subjected to irradiation then their proteins were extracted. These proteins were then incubated with isotype or Beclin antibody coated protein G Magne beads to immune-precipitate Beclin interacting partners, mainly UVRAG, and decipher their differential interaction between siAS and siPIK3C3 transfected cells. Western blot of the eluted samples from the beads revealed decreased complex formation between UVRAG and Beclin as visualized by the lower intensity of UVRAG detected after immune-precipitation using Beclin antibody in siPIK3C3 transfected cells compared to siAS transfected cells (figure 63). This indicated that in the absence of PIK3C3 UVRAG interacts less with Beclin. It should be noted that the isotype controls did show a band for UVRAG of lower intensity relative to the immune-precipitation samples due to the need for more rigorous washing steps and the need for lysate pre-clearing to prevent non-specific binding to the beads.

Moreover, whole cell lysate (WCL) blotting revealed an up regulation of UVRAG expression in siPIK3C3 transfected samples that we investigated further (figure 63). XP-C and WT cells transfected with siPIK3C3 and siAS then irradiated were examined to quantify UVRAG expression. This confirmed the WCL results where UVRAG is significantly upregulated in XP-C cells lacking PIK3C3 (p-value<0.01). WT cells, however, did not show any upregulation in UVRAG expression (figure 64). This upregulation of UVRAG in XP-C cells and its reduced involvement in the autophagic complex signifies an alternative non-autophagy related function for UVRAG.

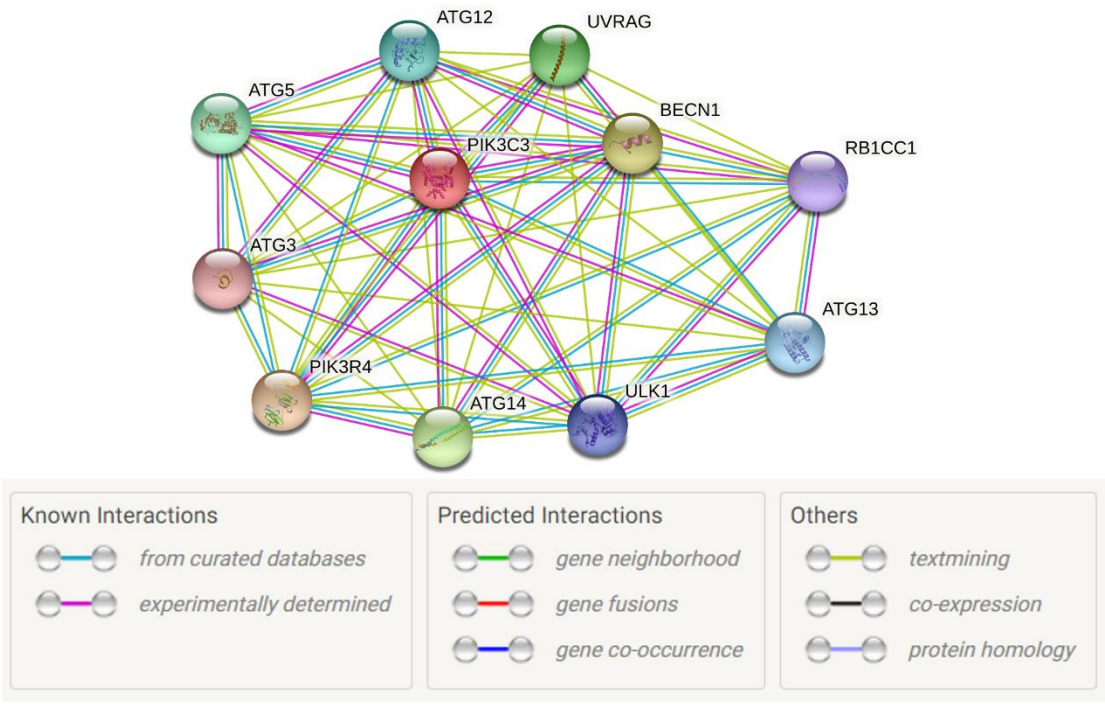

Figure 62 Direct Interactors In the network of PIK3C3.

For the determination of the possible downstream effectors of the PIK3C3 knock down string protein interaction analysis was carried out to identify potential and experimentally proven interactor with the PIK3C3 protein where the majority belonged to the autophagy pathway.

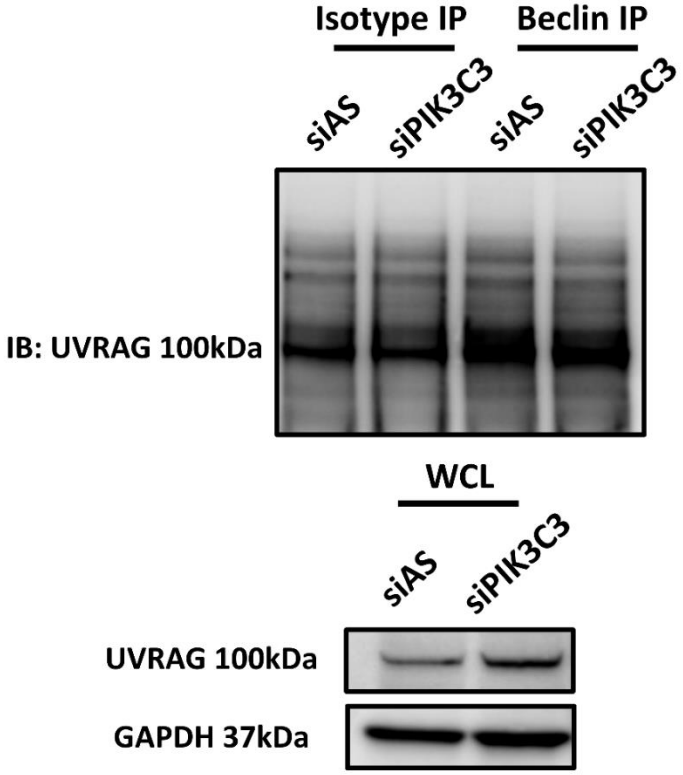

Figure 63 Co-Immunoprecipitation of UVRAG with Beclin in XP-C siPIK3C3 transfected and irradiated protein extract.

To visualize changes in Beclin-UVRAG interaction upon siPIK3C transfection, Beclin antibody was mobilized with protein G Magne beads to allow the immunoprecipitation of both Beclin and other interacting proteins. The resulting immunoprecipitated proteins were run on SDS page gel and immunoblotted for the detection of UVRAG comlexed with Beclin. PIK3C3 knockdown slightly decreased UVRAG association with Beclin compared to siAS transfected cells.

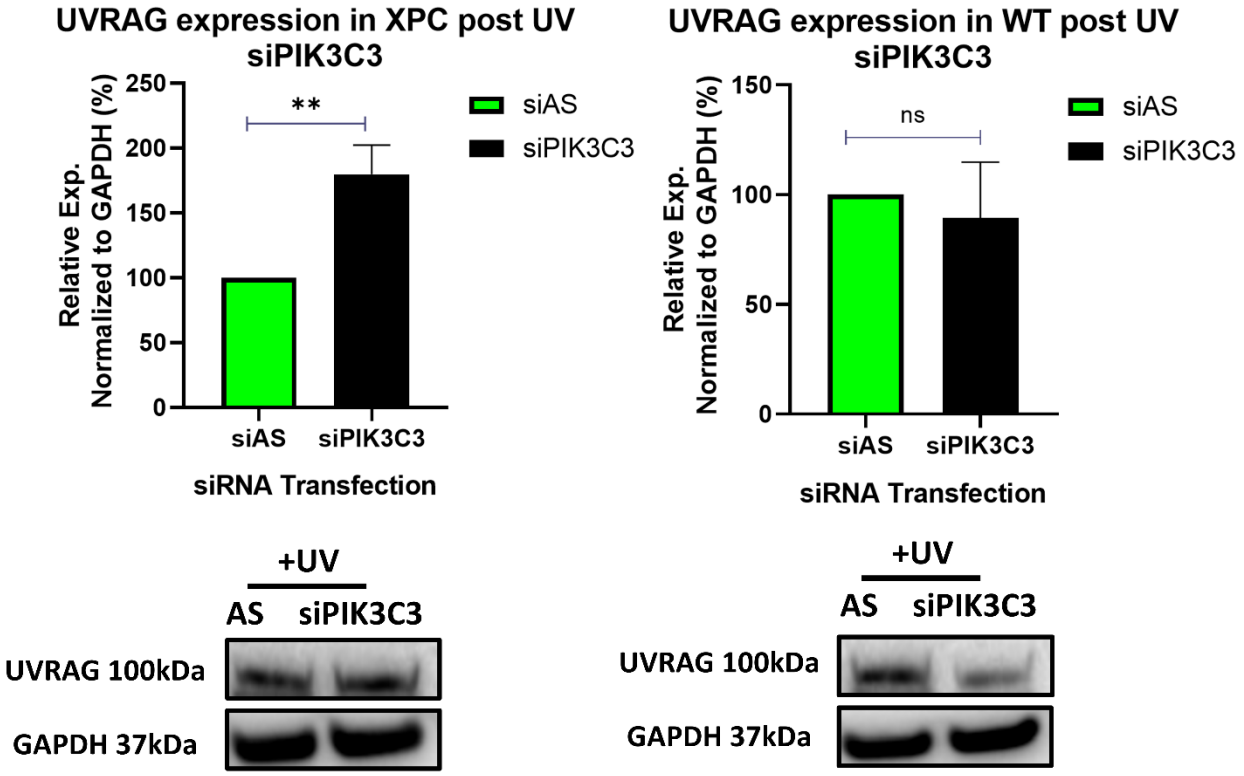

Figure 64 UVRAG expression levels differ between XP-C and WT cells with PIK3C3 downregulation.

*UVRAG expression was analyzed post siPIK3C3 transfection in XP-C and WT cells after UV irradiation. XP-C cells manifest a significant increase in UVRAG expression upon PIK3C3 deregulation that was not evident in WT cells. Paired t-test,**p-value<0.01.*

5. VALIDATION OF SIRNA MEDIATED PHOTO-RESISTANCE ON PRIMARY XP-C AND WT CELLS

The exclusive photo-protective effect of PIK3C3 knockdown on XP-C immortalized cells and the effect of LATS1 downregulation on both WT and XP-C immortalized cells were further on validated on primary cell lines. Primary XP-C and WT fibroblasts were transfected with either siAS, siPIK3C3 or siLATS1 for forty eight hours then irradiated at increasing UVB doses to have

their viability quantified twenty four hours post UV. siPIK3C3 transfection in primary XP-C cells enabled a significant (p-value<0.05) photo-protection upon increasing UVB doses compared to siAS transfected cells showing an LD50 of 0.08J/cm^2 matched by an LD50 of 0.02J/cm^2 for siAS. LATS1 downregulation did as well increase XP-C cells' viability mediating an LD50 of 0.045J/cm^2 but was not significantly varied from siAS. For WT cells, siPIK3C3 showed the same LD50 value as siAS transfected cells of 0.065J/cm^2 while siLATS1 manifested only a slight increase in protection with an LD50 of 0.069J/cm^2 which was not found significant (figure 65). In conclusion, this confirms the XP-C exclusive effect of PIK3C3 knockdown.

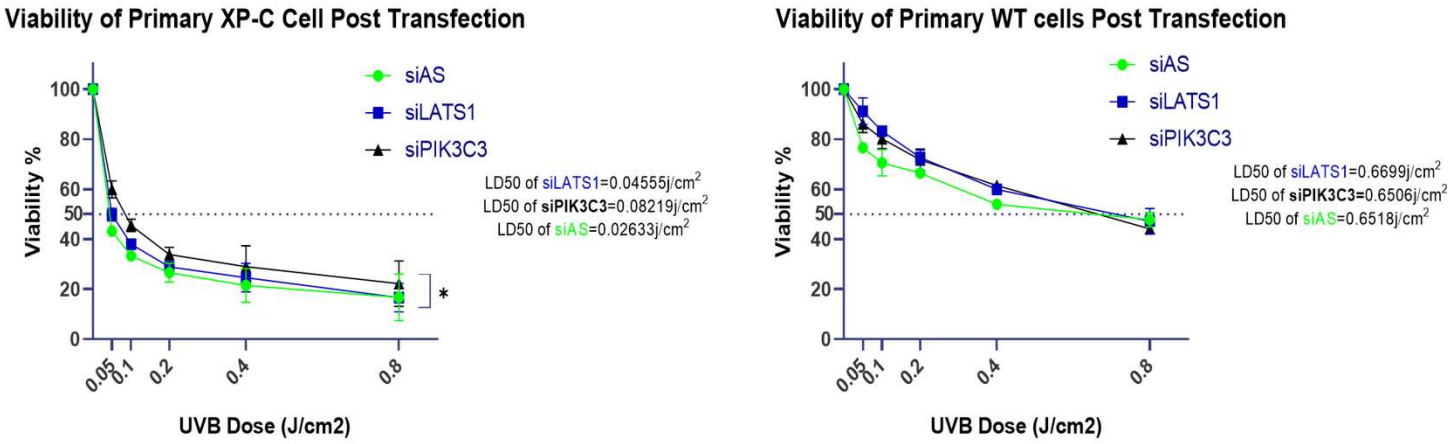

Figure 65 PIK3C3 and LATS1 knock down's consequence on cell viability in primary XP-C and WT cells

*XP-C and WT primary cells were transfected with either siLATS1, siPIK3C3 or siAS then subjected to increased UVB doses. Their viability was further on assessed 24hours post UV by the incubation with PrestoBlue. Both siRNAs showed UV-protection in XP-C cells with siPIK3C3 having a higher and significant increase in XP-C viability compared to siAS giving higher LD50 of 0.08J/cm^2 for siPIK3C3 transfected cells (p-value<0.05). WT cells UVB-protection was not highly enhanced after transfection with only slight variation in LD50 values compared to siAS. Viability was calculated by determining the percent of control with respect to non-irradiated siAS transfected cells taken as 100% viable. Freedman test with Dunn's multiple comparison * p-value <0.05.*

6. 3D DERMAL CONSTRUCTS

Experimentation on cells in 2D culture is imperative yet limited by the fact that it does not resemble the physiological conditions in the human body. Since XP-C is a rare disease it is quite difficult to obtain skin samples from patients. For that, the alternative is to reconstruct 3D XP-C skin equivalents in the lab from amplified 2D cultured XP-C patient cells thus providing access to a model closer to the physiological one with possibility of having more constructs for experimentation. The protocol consists of seeding XP-C fibroblast, embedded in fibrin hydrogel, in an insert to allow dermal equivalent formation. This is then followed by the seeding of WT keratinocytes on top of the dermis that will further on differentiate by placing the construct in air/liquid interface. As an attempt to visualize the difference posed by PIK3C3 knockdown, XP-C

dermal equivalents were constructed then transfected with siPIK3C or siAS for three days prior to their irradiation with UVB at 0.01J/cm2. Cell apoptosis will be monitored via staining with cell event for 24 hours post irradiation. Twenty four hours post UVB, the samples were frozen then sliced for staining. Part of the dermis was used for protein extraction for western blot. The dermis will be stained with PIK3C antibody, 6-4PP DNA damage recognition antibody, and Hoechst. We were able to construct the dermal equivalent and monitor the different markers of apoptosis and DNA damage yet the transfection of the cells was not efficient as PIK3C was still visualized by both immune-fluorescent staining and western blot (figure 66). The other possibility was to transfect the cells with the siRNA prior to their seeding however due to the minimal 2 weeks' time required for dermal maturation the siRNA mediated knockdown will not be stable for that long duration. Therefore, the final alternative is to create PIK3C3 knock out XP-C cells via CRISPR-Cas 9 technology to ensure a longer duration of knockdown. In conclusion, despite the fact that the transfection of inserts in 3D was not possible due to lack of access for the siRNA in the dense construct we still managed to optimize the different readouts to be carried out including the monitoring of apoptosis and DNA damage post irradiation on the dermal equivalent to be created by PIK3C3 knocked out XP-C cells. It would be of interest after that to continue till the formation of the full XP-C skin construct and study whether PIK3C3 deregulation can have an effect on keratinocytes' invasion in XP-C dermis.

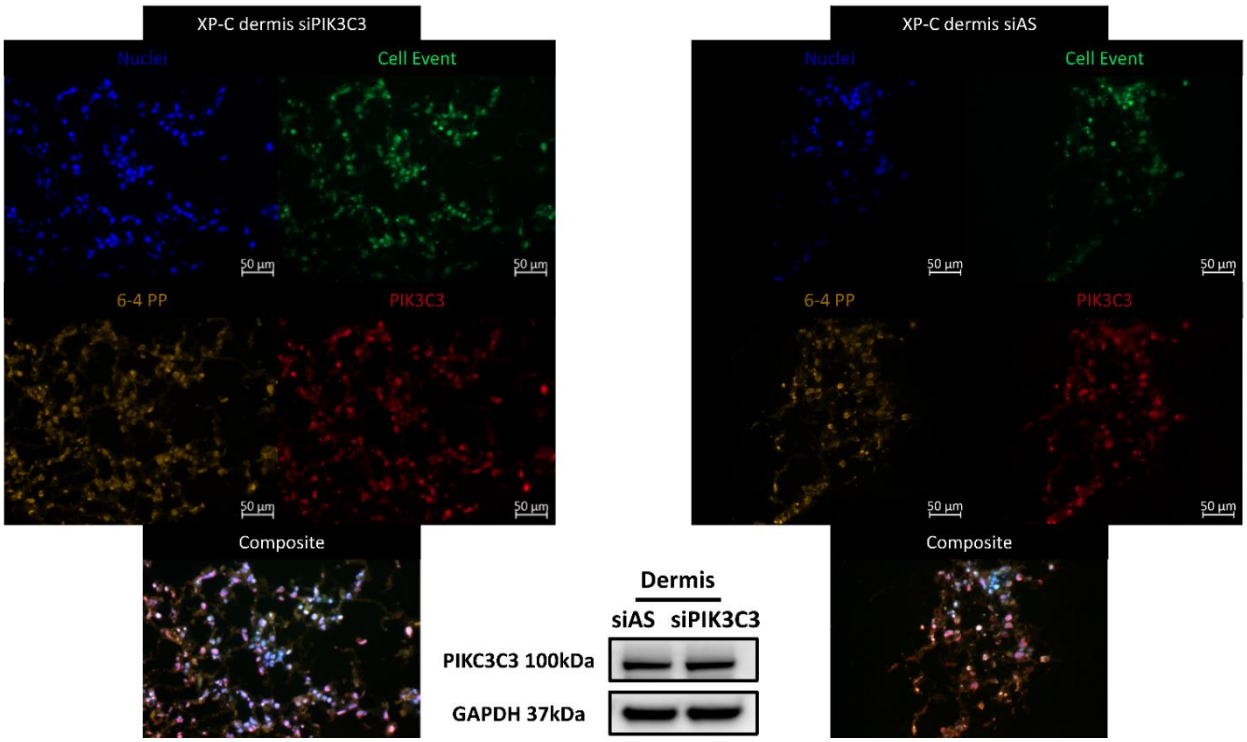

Figure 66 XP-C dermal equivalent immune-stained for the quantification of apoptosis, 6-4PP and PIK3C3 expression with western blot validation of the latter.

3D re-constructed dermal equivalents were constructed using XP-C cells then subjected to both siRNA transfection and UV irradiation. Transfection of siPIK3C3 was not efficient in decreasing PIK3C3 expression detected by both immune-fluorescence as well as western blot. Similar levels of apoptosis and 6-4 PP were detected that can be explained by the lack of differential regulation of PIK3C3.

GENERAL DISCUSSION

CHEMICAL SCREEN DISCUSSION

The presented work identified two drugs, isoconazole and clemizole hydrochloride that could partially reverse the XP-C characteristic phenotype: increased photosensitivity and absence of DNA damage repair of photoproducts. In addition, both drugs also enabled photo-protection in WT cells exposed to high doses of UVB irradiation.

XP-C patient cells carry a mutation in the *XPC* gene required for the recognition of DNA damage. This mutation renders the cells photosensitive[350] and unable to repair UVB induced DNA damage. Here we confirmed the photosensitive profile of XP-C as they show a significantly (p-value<0.001) reduced viability compared to WT cells as a function of increased UV doses (figure 22). Such cells lack the XPC proteins, as confirmed by immunostaining signifying that such mutation leads to the complete loss of the XPC protein (figure 20). Moreover, upon the quantification of the different UVB induced DNA lesions by LC-MS/MS is was evident that XP-C cells manifest slower repair kinetics compared to WT cells. UVB induced lesions include either CPD or 6-4PP that are formed between two adjacent pyrimidines giving four possible lesions T-T, C-C, C-T and T-C[351]. The most abundantly formed lesions are the T-T and T-C lesions for both the CPD and the 6-4PP. In WT cells both lesion types of 6-4PP are readily repaired by the cells few hours post irradiation while CPDs require more time with lesion dependent repair kinetics the slowest repair being for T-T, T-C, C-C then C-T CPD showing the fastest repair confirmed by us and others[352]. XP-C cells show no or reduced repair for both CPD and 6-4PP different lesion types as a function of time (figure 23).

Drug repurposing is the process of testing previously approved drugs, used for a particular therapeutic purpose, for their potential use in the treatment of other common or rare diseases. This cuts down drug discovery costs and the long process of toxicity and pharmacokinetics testing[353]. For that, our aim was to test a library of 1280 approved drugs for their potential use in normalizing the XP-C phenotype. XP-C cells were treated with the compounds at 10µM for 24h then irradiated with UVB and then treated again with the same compounds at the same concentration for an additional period of 24h. The overall viability of the treated cells, proportional to the amount of metabolically active cells, was then measured via incubation with PrestoBlue. The fluorescent values obtained were normalized via either the calculation of drug activity %, control based with 100% for non-irradiated DMSO treated cells and 0% for irradiated ones or via the calculation of the non-control based RZscore. Drugs that showed an activity ≥25% with an RZscore above 2.6 were selected as primary hits to be confirmed via a secondary screening which were 16 drugs (figure 33). Acitohexamide was added to the secondary screen drug list due to its previously described photo-protective effect on XPA cells via the enabling of damage repair[211]. Isoconazole, clemizole hydrochloride and bifonazole manifested the highest bioactivity after secondary screening enabling photo-protection in XP-C cells compared to DMSO treated controls

with a range of 20 to 40% increase of cell viability depending on the conditions (figure 34). However, the enabling of photo-resistance is not sufficient by itself for a satisfying curative outcome. The persistence of cells with accumulated DNA damage can lead to the conversion of such lesions into mutations which depending on their localizations can lead to carcinogenesis[354]. The main lesion in XP cells mediating the UV signature mutation is the C-C lesion where the slow repair of such lesion in XP cells compared to its fast repair in WT cells favors the deamination and induction of mutations[351]. Therefore, photo-resistance should be associated with increased DNA damage repair in the perspective of therapeutic treatment. Indeed, we tested the capacity of the 16 primary hits and acetohexamide in mediating the decrease of DNA damage post UVB irradiation. Out of this collection, two compounds, isoconazole and clemizole hydrochloride decreased the amount of DNA damage post UV in XP-C cells by about 20% (p-value<0.001 at 5µM) (figure 35).

Isoconazole is an azole antifungal drug with no reported data on its effect in sun-shielding upon its use on the skin while clemizole hydrochloride is a Histamine H1 antagonist. Other documented functions for clemizole hydrochloride include its role in the treatment of HCV infection [355] and its blocking effect on TRPC5 ion channels [356]. These functions fail to explain these drugs' effect on XP-C cells suggesting possible alternative mode(s) of action than the ones documented that needs to be further on explored.

One similar approach to ours was conducted on XP-A cells where the anti-diabetic drug acetohexamide was found to be effective in reducing the cells' photosensitivity and enabling damage repair [211] mediating the identification of an additional mode of action for this drug not related to its documented effect. Acetohexamide had minimal effect in the reversal of XP-C phenotype when tested in our screen, yet we managed to identify other drugs that can aid in this phenotypic partial reversal. Acetohexamide enabled the degradation of MUTYH, a protein involved in the removal of adenine residues mispaired with 8-oxo-guanine residues after oxidative stress[357]. The authors hypothesized that the degradation of such protein might be enabling spatial access of the lesions to other repair machinery independent of nucleotide excision repair[211] which was not yet further explored to date. It is therefore possible that the hit drugs identified in this study might similarly impose spatial access effect or that they interfere with on one or several mediators of DNA repair, a hypothesis which needs to be further on examined.

Collectively, our data show that isoconazole and clemizole hydrochloride mediated an increase in cell viability post UV irradiation and enabled to a lower extinct the repair of accumulated DNA damage in the form of UVB-induced 6-4PP. Isoconazole, on one hand, mediated a curative effect post UV irradiation by enabling the decrease of apoptotic cells' population as measured by flow cytometry with cell event caspase 3/7 activity staining (figure 39). Clemizole hydrochloride's effect, on the other hand, was both preventative pre UV and curative post UV irradiation showing a p-value<0.05 while the difference between the post-irradiation alone and the pre-irradiation treatment was not significant (figure 37) . Such effect is mediated via a yet unknown mechanism. The simultaneous double treatment with both drugs revealed no synergistic nor additive effect

(figure 38). This suggests that both drugs interfere with a similar biological process or target which is consistent with the fact that they share similar chemical scaffold (azole ring). Moreover, both drugs were shown not to affect the cells' proliferation rate (figure 42). The photoprotective effect of the drugs was also evident in WT cells post UV irradiation signifying the involvement of a protective pathway indirectly related to the mutated *XPC* gene (figure 36). This work will mark the first attempt in discovering compounds for the amelioration of the XP-C phenotype yet the exact regulated target needs to be further on explored to allow the identification of the effectors aiding in this phenotypic reversal and thus paving a way for a potential therapy for this yet untreatable genodermatosis.

SIRNA SCREEN DISCUSSION

This work allowed the identification of two kinases whose knockdown can partially reverse the phenotype of XP-C cells enabling an increase in photo-resistance and decrease in the accumulation of DNA damage following UVB irradiation. The two kinases are LATS1, an integral player in the Hippo pathway, and PIK3C3, involved in autophagy. The effect of LATS1 knockdown was evident in both WT and XP-C cells whereas downregulation of PIK3C3 mediated a photo-protection exclusive to XP-C cells.

UVB irradiation generates a plethora of damage in our DNA including mainly pyrimidine dimers. These dimers are repaired by the Nucleotide Excision Repair machinery to maintain genomic integrity. NER is further on sub-classified into global genome-NER (GG-NER) repairing damages throughout the genome and transcription coupled-NER (TC-NER) mainly designated for repair in actively transcribed genes. Mutations in one of the associated NER machinery can lead to de-regulation of this orchestrated repair process and the development of numerous pathologies. Xeroderma Pigmentosum C is a complementation group of the NER-deficient disease, Xeroderma Pigmentosum, with a mutation in GG-NER damage recognition protein XPC[350]. XP-C patients manifest sensitivity to UV irradiation and accumulation of DNA damages. We confirmed the latter profile in our XP-C cell lines. XP-C patient derived cells used in this study manifest a downregulation of XP-C mRNA expression (p-value<0.0001) and absence of protein expression (p-value<0.001) (figure 21). Upon UVB irradiation, XP-C cells manifest decreased viability as function of increased UVB dose compared to WT cells showing higher photo-resistance (p-value<0.05) (figure 22). Finally, LC-MS/MS quantification of 6-4 PP and CPD in XP-C versus WT cells as function of incubation time post UVB revealed that WT cells indeed can efficiently repair pyrimidine dimers compared to XPC deficient cells as shown earlier[351] (figure 23).

XPC mutation increases the risk of cancer in patients, who need to be shielded from UV light at all times. However, not all mutations are deleterious. Suppressor mutations can reverse the effect of a primary mutation via a second one. This secondary mutation might take place in a gene belonging to the same pathway or a distinct one. Although not extensively studied in humans,

suppressor mutations can help explain how some individuals appear to be normal despite carrying a disease causing mutation that is counteracted by a suppressive one[358]. Therefore, our aim was to utilize the concept of suppressive alteration in the course of XP-C. XP-C and WT cells were transfected with an siRNA library targeting all human kinases followed by irradiation to allow DNA damage induction. After recovery time, readouts were quantified to identify hit siRNAs mediating photo-resistance and damage repair. Primary screening allowed the identification of twenty eight different kinases whose knockdown enabled increase in post UVB viability (figure 45) . Hit confirmation was then carried by secondary screening that allowed the elimination of false positives (figure 47). Finally, staining the cells transfected with secondary screen hits allowed the identification of siLATS1 and siPIK3C3 that in addition to their photo-protective effect also enable decrease in the amount of UVB-induced 6-4 PP by 20% compared to siAS transfected irradiated cells (p-value<0.001) (figure 49).This is critical as increasing cell viability alone without repair can further on allow the accumulation of cells harboring lesions and ultimately lead to carcinogenesis[354]. Moreover, the simultaneous screening of WT cells can be advantageous in detecting kinases' deregulation with exclusive effects on either XP-C or WT cells (figure 52). siRNAs mainly function via the degradation of target mRNA due to perfect complementarity between their sequences. That being said, incomplete complementarity of siRNAs can lead to secondary off-target effects. For that we conducted bioinformatics based identification of commonly deregulated off-targets of the two identified siRNAs. This search yielded FOXN3 further on confirmed not to be deregulated in either siPIK3C3 or siLATS1 transfected XP-C and WT cells (figure 51). Moreover, the knock down of the intended targets, LATS1 and PIK3C3, post transfection was validated at the mRNA level by RT-PCR and protein level by western blot (figure 50). Finally, UVB dose response analysis on WT and XP-C cells transfected with siAS, siPIK3C or siLATS1 then irradiated at increasing doses revealed that the knock down of LATS1 despite increasing XP-C cell viability also had similar effect on WT cells (p-value<0.05). The knock down of PIK3C3, however, mediated an increase in XP-C cells' viability compared to siAS control (p-value<0.05) without having a protective effect on WT cells (figure 53).

Phenotypic reversal especially at the level of increased viability post UV can rise from either modulation of apoptosis, cell proliferation or the indirect effects of reactive oxygen species. For that, monitoring of cell event caspase activity marker and PI incorporation was utilized to visualize the effect of downregulation on the apoptotic profile of WT and XP-C cells. In compliance with viability measurements, siPIK3C3 indeed showed significant upregulation in the live cell population (61.75%) in XP-C cells followed by siLATS1 with 47.38% compared to siAS transfected XP-C cells with 43.49%. WT cells' highest live cell population % was mediated by siLATS1 transfection (figure 54). This means that siLATS1 was able to increase live cell population in both XP-C and WT cells while siPIK3C3 was only effective in decreasing apoptosis in XP-C cells and not WT. Nonetheless, both siRNAs failed to exhibit any change in EDU incorporation signifying that their mediated effects is not via the modulation of the proliferative capacity of cells (figure 55 , figure 56). Moreover, ROS production can alter cell homeostasis and lead to damages at the level of the DNA including the formation of oxidized purines[359].

Therefore, we wanted to test whether the different transfections can alter the amount of produced ROS or if they can modify the repair of ROS generated DNA damages in both WT and XP-C cells using comet assay. LATS1 downregulation in WT cells resulted in initial lower amount of oxidized purines at time zero post UV that can be linked to having lower ROS generated upon irradiation. As for siAS and siPIK3C3 transfected cells they show similar amount of lesions and display similar repair kinetics of the damage as function of increased time post UV with slightly faster repair shown in siAS cells. XP-C cells showed non-significant lower damage in siAS transfected cells compared to remaining conditions. However, the repair of the lesions was not evident in siAS transfected cells compared to siPIK3C3 and siLATS1 showing repair with faster kinetics for LAST1 knockdown. This signifies that despite the fact the different knockdowns did not alter the amount of the damage induced in the DNA at time zero they still mediated better repair compared to scrambled controls (figure 57).

P53 is activated post damage induction and can determine cell fate by stalling cell cycle progression to allow repair or by committing cells with irreparable damage to apoptotic cell death. The phosphorylation of P53 at Ser15 is one marker for P53 activation and commitment to the induction of apoptosis [347]. Therefore, we quantified the levels of P-P53 Ser15 phosphorylation in XP-C and WT cells subjected to the different siRNAs to follow the anti-apoptotic effect these treatments have on the cell lines. The decrease in PIK3C3 expression in XP-C cells on one hand leads to a decrease in P-P53 Ser15 levels post UV (p-value<0.05) as well as decreasing the expression of P53 (figure 58). On the other hand, this PIK3C downregulation in WT cells had no differential effect. The opposite is visualized in siLATS1 transfection where no difference in both P-P53 Ser15 or P53 was recorded for XP-C cells while WT cells demonstrated decreased levels of both P53 and P-P53 Ser15 (p-value<0.05) (figure 59).

AKT is a critical effector of the PI3K/AKT/mTOR pathway that controls several functions from anti-apoptosis, proliferation and DNA repair among others. Its activation is mediated by the phosphorylation of Thr308 by PDK1[360] and Ser473 by mechanistic target of rapamycin complex 2 (mTORC2)[361] and DNA-dependent protein kinase (DNA-PK)[362]. Upon activation AKT translocates to various cellular compartments following its dissociation from the membrane. Moreover, Ser473 phosphorylation was shown to be upregulated post UVB irradiation and leads to skin survival[346]. For that, we also examined the levels of this phosphorylation in siLATS1 and siPIK3C transfected cells to try and further explain the cause of survival post irradiation. An increase in P-AKT Ser473 was detected post UV in XP-C cells transfected with either siPIK3C3 or siLATS1 while only in WT cells transfected with siLATS1 and not siPIK3C3 (figure 58, figure 59). A study by Tu et al revealed that the phosphorylation of AKT Ser473 requires the association of DNA-PKcs- mTORC2 upon UVB irradiation and is attenuated by the depletion of either. This UVB induced association reduced UVB-induced cell death and apoptosis[346]. This could be one possible mechanism by which the different transfections mediate anti-apoptotic effect via the upregulation of AKT Ser473 phosphorylation. Another possible mechanism involves the P300 histone acetyltransferase activated by AKT thus facilitating chromatin remodeling and recruitment

of repair complexes decreasing the need to commit cells toward cell death[363]. It should be noted that the phosphorylation of AKT at Ser473 as mentioned earlier is mediated by either mTORC2 or DNA-PK which explains the fact that despite the knockdown of PIK3C3 this residue was still being phosphorylated. On the contrary it is the Thr308 phosphorylated via PDK1 whose activation necessitates the formation of PIP3 via class I PI3K. PIK3C3 is not directly involved in AKT phosphorylation being a class III PI3K.

The actual link between LATS1 or PIK3C3 downregulation and increased viability accompanied with reduced damage still needs to be further on investigated. Concerning LATS1, YAP expression and translocation is the most straightforward downstream mechanism to investigate. Despite not showing changes in YAP expression (figure 60), XP-C cells manifested increased nuclear translocation upon siLATS1 transfection (p-value<0.01) which is present to a lower extent in WT cells (figure 61). This translocation was not accompanied, however, with changes in proliferative capacity of XP-C cells signifying the involvement of yet another downstream effector whose expression was favored by YAP nuclear translocation (figure 55). Concerning PIK3C, autophagy is the most relevant pathway associated with this protein. Autophagy requires the formation of complexes between several partners including PIK3C3, Beclin and UVRAG among others[349]. For that we wanted to examine the effect of PIK3C downregulation on complex formation between Beclin and UVRAG. Co-immunoprecipitation on XP-C siPIK3C3 vs. siAS irradiated cells revealed lower degree of complex formation upon siPIK3C3 transfection (figure 63). Of interest is the fact that these cells also manifested upregulation of UVRAG expression that we confirmed with western blot (p-value<0.01) (figure 64). This signifies that UVRAG overexpressed in siPIK3C3 XP-C cells might be mediating a photo-protective effect independent from its role in autophagy. In fact, UVRAG was first isolated as cDNA that can partially complement UV sensitivity in Xeroderma Pigmentosum C cells[364]. Further investigation of the link between UVRAG and DNA repair revealed that the former is required for GG-NER as it accumulates at lesion and associates with DDB1 to promote the assembly and activity of $CRL4^{DDB2}$ complex (DDB2-DDB1-CuL4A-Roc1). $CRL4^{DDB2}$ complex ubiquitinates several downstream NER factors and histones allowing the destabilization of damage containing nucleosomes facilitating recruitment of downstream effectors[365]. UVRAG was also said to be involved in centrosome stability and DNA-PK regulation[366]. Further investigation of UVRAG accumulation at damage sites should be carried out to try and understand how the autophagy independent role of UVRAG fits in the XPC deficient model of GG-NER.

Finally since the study was based on the screening on immortalized cell lines, the validation of the results on primary cell lines as well is imperative. For that, primary XP-C and WT fibroblast were transfected with either siLATS1, siPIK3C3 or siAS then subjected to increased UVB doses. PIK3C3 knockdown was able to partially rescue (p-value< 0.05) XP-C cells compared to a lower extent of photoprotection mediated via siLATS1with respect to siAS transfected cells (figure 65). The effect of siLATS1 was less evident in WT cells showing only slight protection. Still the

quantification of DNA damage levels is essential to eliminate the possibility of damage accumulation in surviving cells escaping cell death without repair which is a perspective.

CONCLUSION AND PERSPECTIVES

XP-C is a genetic disease characterized by increased sensitivity to ultraviolet irradiation and the accumulation of DNA damage. It originates from mutations in the *XPC* gene leading to deficiency in the protein required for damage recognition. XP-C is mainly manifested in children who are called children of the moon and should be shielded from sun rays at all times. Skin cancer incidence is elevated in XP-C with around 2,000 and 10,000 fold increase in incidence of NMSC and melanoma respectively. There is no effective treatment for XP-C. Therefore the aim of our study was to screen libraries of biological and chemical molecules to identify hits that can partially reverse the phenotype of XPC cells.

The screening of approved chemical drug library allowed the identification of two drugs with general UVB protective roles in both XP-C and WT cells. Both isoconazole and clemizole hydrochloride allowed the enhancement of cell viability in response to UVB irradiation accompanied with 20% decrease in the amount of generated DNA damage. Isoconazole was effective in decreasing cellular apoptosis in XP-C cells without showing any effect on the proliferative capacity of the cells. The validation of these two effects is necessary on other XP-C cell lines. Furthermore, to determine the particular downstream affected mechanism of such treatments, proteomics analysis of treated vs. sham treated cells is imperative to identify the downstream deregulated pathway in response to such treatments. The fact that both drugs are approved and readily used in clinics can ease the transition in the utilization of such drugs for another mode of action related to photo-protection.

The screening of kinase targeting RNAi library allowed the identification of two kinases capable upon downregulation of increasing the viability of XP-C cells and mediating slight repair. Among the two kinases, PIK3C3 knockdown had an exclusive effect on XP-C cells and not WT cells mediating a decrease in apoptotic cell death, phosphorylated P-P53 Ser15 and decreased association between beclin and UVRAG. This knockdown also enabled an increase in phosphorylated AKT Ser473 and UVRAG expression which we hypothesize might be the effector post PIK3C3 knockdown mediating the phenotypic reversal. The latter UVRAG overexpression was not shown in WT cells. Perspective work on the activity of UVRAG should be carried out including any detected differences in its recruitment to damaged lesions and how it affects the interactions among the DNA repair proteins in the course of XPC deficient cells model. The other identified kinase is LATS1 whose protective effect although visible in XP-C cells it is much more effective in WT cells. SiLATS1 transfection allowed a decrease in apoptotic cell death with lower P-P53 Ser15 in WT cells. It was also accompanied by an increase in phosphorylated AKT Ser 473 for both WT and XP-C cells. Knockdown of LATS1 favored the translocation of the downstream effector YAP to the nucleus to allow the expression of various genes whose expression needs to be analyzed to pinpoint the actual mechanism mediated via LATS1 knockdown. These two

candidate siRNAs can provide potential therapies for XP-C patients in particular the knock down of PIK3C3. One can imagaine the utilization of such siRNAs via their liposomal delivery into the effected tissue by topical application or injection. Other delivery options can also be envisioned inlcuidng adenoviral vectors. Due to the presence of chemical drugs also enabling inhibition of these kinases this can help the switch to treatments involving the chemical rather than siRNA inhibition of these kinases. Ofcourse further analysis of the involved mechanisms of such downregulation should be carried out together with RNAseq analysis of modulated mRNA expression as a result of transfection to eliminate off-target effects.

Finally, these results necessitate their validation on primary XP-C cell lines. Despite already confirming the photo-protective effect on primary cells it will be also necessary to decipher the downstream effects of knockdown on these primary cells in the same manner as conducted on the immortalized cells utilized in this study. A final step will be the testing of the effects of such knockdowns on 3D reconstructed XP-C skin model as it is more relevant in comparison to the physiological human condition.

FRENCH SUMMARY

Criblage à haut contenu à base d'ARNi et de produits chimiques pour la normalisation du phénotype XPC

Introduction

La Xeroderma Pigmentosium C (XP-C) est une génodermatose autosomique récessive rare. Les patients de cette pathologie sont porteurs d'une mutation dans la protéine XPC de reconnaissance des dommages de l'ADN appartenant à la voie de réparation par excision des nucléotides (NER)[338]. Cette mutation génère un phénotype pathologique caractérisé par une photosensibilité extrême et l'accumulation de dommages à l'ADN induits par les UV sans leur réparation. La persistance de ces dommages favorise leur conversion en mutation de transition C-T, signature des UV, qui conduit finalement au cancer de la peau. L'apparition de cette dernière est précoce chez les patients XPC et ils présentent un risque 2 000 et 10 000 fois plus élevé de mélanome et de cancer cutané non mélanique respectivement. Par conséquent, l'objectif de ce projet est de cribler des molécules chimiques et biologiques afin d'identifier les hits qui peuvent inverser ce phénotype malade.

Materials and Methods

Des cellules XP-C et normales dérivées de patients seront utilisées pour cribler une bibliothèque chimique de 1280 médicaments approuvés par la FDA ou une bibliothèque de siRNA visant à diminuer l'expression de toutes les kinases humaines, étant donné l'implication des kinases dans les différentes voies de réparation de l'ADN. Les cellules seront ensuite irradiées par des UVB pour induire des lésions de l'ADN, puis l'inversion phénotypique sera surveillée au niveau de la photosensibilité par le colorant bleu Presto pour cellules vivantes ou au niveau de la réparation des lésions de l'ADN via la quantification des lésions par immunocytochimie en marquant les lésions de l'ADN avec un anticorps pour visualiser quel traitement permet une diminution du niveau de lésions et donc une réparation (figure 67). Une caractérisation plus poussée de l'effet des hits a été effectuée sur la base de leur capacité à modifier l'apoptose, la prolifération cellulaire, la génération d'espèces réactives de l'oxygène et les dommages à l'ADN générés en aval. Pour les résultats des cribles de siRNA, une analyse en aval de l'expression de plusieurs protéines a été réalisée par western blot. Le choix des protéines analysées dépendait de la nature de la cible du hit et de la voie de signalisation dans laquelle elle est impliquée. Une analyse de la translocation des protéines a également été réalisée. La dernière étape consistera à tester ces molécules sur sur des cellules primaires et de la peau reconstruite en 3D en laboratoire, qui imite davantage les conditions physiologiques des patients.

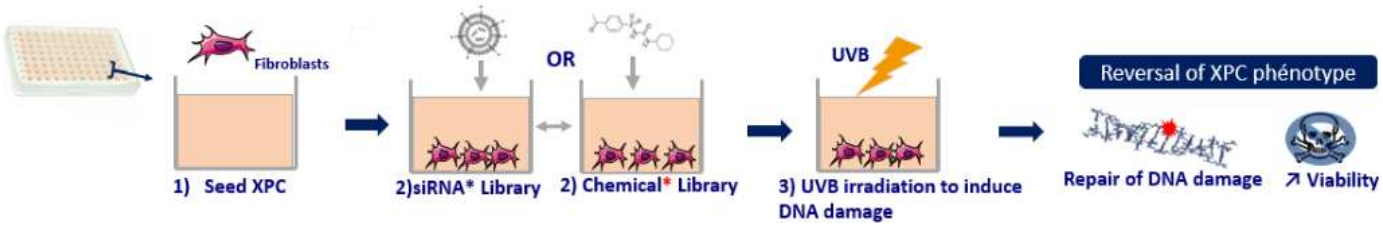

Figure 67 Aperçu de la procédure de criblage pour le siRNA et le criblage chimique

Résulte & Discussion

Dans cette étude, nous avons criblé des bibliothèques pour identifier des molécules qui peuvent inverser le phénotype des cellules XP-C, il était donc impératif de vérifier d'abord ce phénotype dans la lignée cellulaire utilisée. L'expression de la protéine XPC a été examinée dans les cellules WT et XP-C immortalisées à partir de fibroblastes primaires de patients. Contrairement aux cellules WT, les cellules XP-C ont montré une absence totale de protéine XPC (figure 68a). Le profil photosensible des cellules XP-C a également été confirmé par une analyse dose-réponse où la viabilité des cellules XP-C a diminué davantage en fonction de l'augmentation des doses d'UVB par rapport aux cellules WT (figure 68b). Enfin, l'accumulation et la réparation des dommages à l'ADN ont été quantifiées dans les cellules XP-C et WT par LC-MS/MS. Les cellules WT ont montré une diminution des quantités de lésions des différents CPDs en fonction du temps pour atteindre un minimum après 48h indiquant une réparation efficace des dommages à l'ADN alors qu'au contraire, les cellules XP-C ont montré des quantités élevées et constantes de lésions en fonction du temps. 6-4 Les PPs ont été réparés plus rapidement que les CPDs avec une réparation totale 24h après UV dans les cellules WT par rapport à la quantité plus élevée de lésions dans les cellules XP-C (figure 68c).

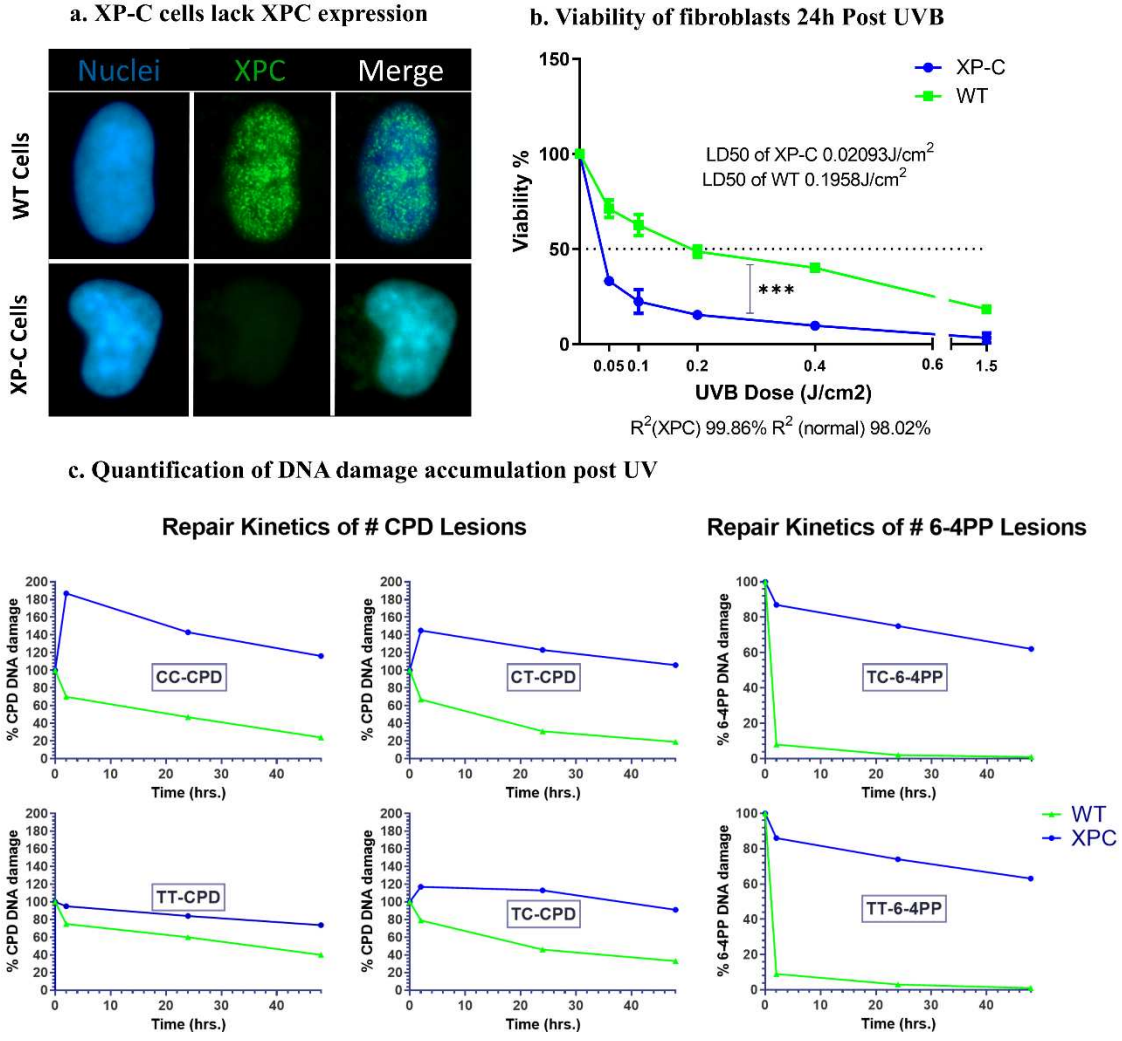

Figure 68 Caractérisation des cellules XP-C et WT.

*a) Les cellules XP-C n'expriment pas la protéine XPC. Les cellules XP-C et WT ont été fixées et colorées avec l'anticorps anti-XPC pour analyser son expression différentielle dans les deux lignées cellulaires. Les cellules XP-C, contrairement aux cellules WT, ne manifestent pas l'expression de la protéine XPC dans leurs noyaux. b) Viabilité des fibroblastes 24h après UVB. Les cellules XP-C manifestent une photosensibilité significativement accrue par rapport aux cellules WT. Les cellules XP-C et WT ont été ensemencées dans des plaques de 96 puits pour être irradiées à 80% de confluence avec des doses croissantes d'UVB, puis leur viabilité a été quantifiée 24h plus tard par l'incubation avec PrestoBlue. Les cellules XP-C montrent une diminution significative plus marquée de la viabilité en fonction de l'augmentation de la dose d'UVB par rapport aux cellules WT. La viabilité a été calculée en pourcentage du contrôle, le contrôle à 100% étant des cellules non irradiées. *** p< 0,001, test t non apparié. Les résultats présentés sont la moyenne de trois répétitions techniques. c) Quantification de l'accumulation des dommages à l'ADN après l'exposition aux UV. Les cellules WT présentent une cinétique de réparation plus rapide des lésions CPD et 6-4PP après l'exposition aux UV, alors que les cellules XP-C présentent une réparation déficiente. Les deux lignées cellulaires ont été soumises à des UVB puis incubées à différents moments après les UV. À chaque point de temps, les cellules ont été collectées, leur ADN extrait et digéré pour être ensuite analysé par LC-MS/MS. Quatre différents types de lésions de DPC ont été quantifiés, la DPC-TT étant la plus fréquente. Les cellules normales montrent une diminution du % de lésions CPD en fonction du temps signifiant une réparation avec des cinétiques différentes par temps de lésion. Les cellules XP-C, cependant, manifestent une augmentation des lésions CPD à 2h après UV et continuent à avoir une grande quantité de % de lésions au fur et à mesure que le temps s'écoule, un signe de réparation altérée. Deux types de lésions ont été quantifiés pour le 6-4PP, le TC-6-4PP étant plus abondant. Comme pour la DPC, l'altération de la réparation est visualisée dans les cellules XP-C par une lente diminution du pourcentage de lésions en fonction du temps, par rapport aux cellules normales qui, contrairement aux lésions de la DPC, présentent une réparation encore plus rapide pour le 6-4PP.DPC : dimère de cyclobutane pyrimidine, 6-4PP : photoproduits 6-4, WT : type sauvage, XP-C : Xeroderma Pigmentosum C, LD50 : dose létale 50, R2 : coefficient de détermination.*

Pour le criblage chimique, 1280 médicaments différents ont été utilisés pour prétraiter les cellules XP-C en double dans une plaque à 96 puits. Après l'induction de dommages à l'ADN, les cellules ont également été post-traitées avec les mêmes médicaments, puis incubées pendant vingt-quatre heures pour permettre leur récupération. La viabilité des cellules traitées a été mesurée et comparée au contrôle positif de cellules non traitées non irradiées et au contrôle négatif de cellules irradiées non traitées. Parmi les médicaments testés dans la bibliothèque, seize médicaments ont entraîné une augmentation de plus de 25 % de la viabilité cellulaire (figure 69a). Ensuite, après marquage et quantification des dommages à l'ADN, deux médicaments, l'isoconazole et le chlorhydrate de clemizole, ont diminué de 20% la quantité de dommages à l'ADN (figure 69b). Une caractérisation plus poussée de ces deux médicaments en séparant le traitement en traitement pré-irradiation ou post-irradiation a révélé que la post-irradiation était plus efficace pour induire la photo-résistance des cellules XPC sensibles à la lumière (figure 69d). L'un des deux médicaments, l'isoconazole, a réduit la mort apoptotique des cellules XPC (figure 69c) mais n'a eu aucun effet sur leur taux de prolifération. Le mode d'action connu des deux médicaments sélectionnés est un antifongique pour l'isoconazole et un antagoniste des récepteurs de l'histamine pour le chlorhydrate de clémizole. Cela n'explique pas leurs effets dans la protection des cellules XPC contre la mort induite par l'irradiation. Par conséquent, une étude plus approfondie du mécanisme d'action possible est nécessaire en comparant le profil d'expression des protéines des cellules traitées et non traitées afin d'identifier un nouveau mécanisme d'action possible pour ces deux médicaments. Des travaux similaires ont été réalisés sur une autre lignée cellulaire moins courante, la lignée XPA, qui présente une mutation de la protéine XPA nécessaire au contrôle des dommages. On a découvert que l'acétohexamide, un médicament antidiabétique, induit la photorésistance dans ces cellules par

un mécanisme d'action différent de celui rapporté. On a constaté que l'acétohexamide diminuait l'expression d'une protéine impliquée dans une autre voie de réparation de l'ADN[211].

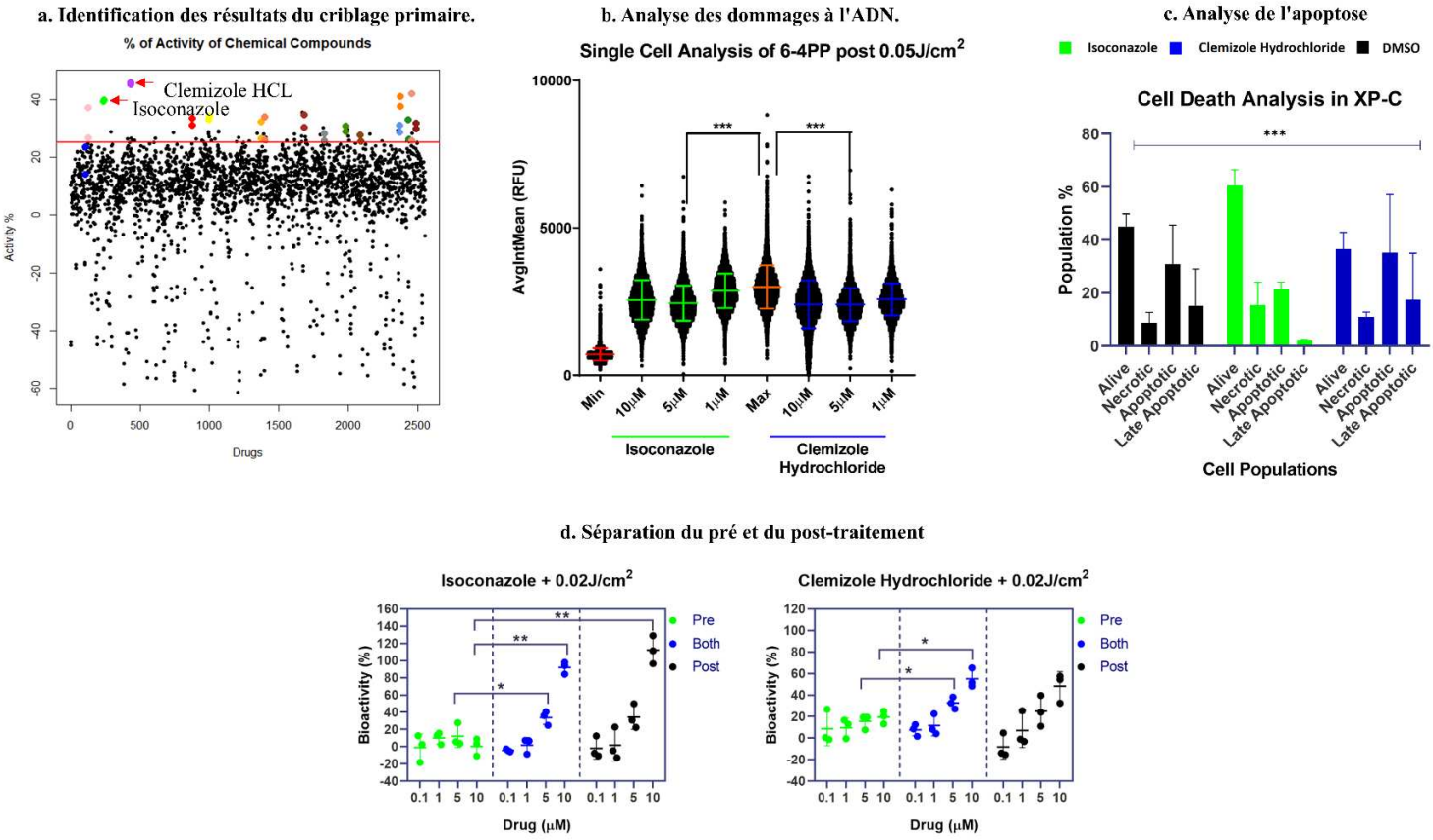

Figure 69 Résumé des résultats de l'analyse chimique.

a*) Identification des résultats de la criblage primaire. La bibliothèque de médicaments chimiques de Prestwick a été criblée sur des cellules XP-C. Les cellules ont été traitées avec la bibliothèque pendant 24 heures, puis irradiées. Les cellules ont été traitées avec la bibliothèque pendant 24 heures puis irradiées. Après l'irradiation, les cellules ont été incubées avec la bibliothèque pendant 24 heures supplémentaires avant que leur viabilité ne soit évaluée 24 heures après l'irradiation par l'ajout du réactif PrestoBlue et l'enregistrement des valeurs de fluorescence. En se basant sur le % d'activité du contrôle, 16 composés ont été sélectionnés, manifestant une augmentation de l'activité de plus de 25 %. b) Analyse des dommages à l'ADN. Les cellules XP-C ont été traitées avec les 16 candidats du dépistage primaire à trois concentrations différentes (1, 5 et 10µM) avec des traitements pré- et post-irradiation. L'irradiation a été effectuée à une dose de 0.05j/cm2. 24 heures après l'irradiation, les cellules ont été fixées et colorées avec des anticorps 6-4 PP pour la quantification des dommages à l'ADN. Les intensités de fluorescence des cellules individuelles pour chaque condition ont été quantifiées et plus de 1000 cellules par condition ont été analysées. Parmi les 16 résultats, seuls l'isoconazole et le chlorhydrate de clémizole ont permis une diminution de la quantité de dommages à l'ADN post-UV montrée ici. Près de 20% de réparation des dommages à l'ADN du 6-4PP a été enregistré pour les deux médicaments à une concentration de 5µM, ce qui a été jugé significatif. La quantification des dommages à l'ADN dans les cellules irradiées traitées au DMSO a été utilisée comme contrôle positif montrant la quantité maximale de dommages à l'ADN tandis que la quantification du 6-4PP dans les cellules non irradiées traitées au DMSO a été prise comme contrôle négatif avec la quantité minimale de dommages détectés. *** p<0,001, test non paramétrique de freedman avec analyse post hoc de dun. c) Analyse de l'apoptose. Les cellules XP-C ont été traitées avec les différents médicaments ou le DMSO puis irradiées. Le marqueur caspase 3/7 de CellEvent a été ajouté après l'irradiation puis les cellules ont été collectées. Le PI a été ajouté juste avant l'analyse sur un cytomètre en flux. Le traitement à l'isoconazole a diminué le pourcentage de cellules apoptotiques après les UV par rapport aux cellules traitées au DMSO. Le chlorhydrate de clémizole, cependant, n'a pas eu d'effet ; c'est donc peut-être par un autre mécanisme que ce médicament exerce son mode d'action. Une anova à deux voies a été utilisée pour comparer les deux variables indépendantes (type de mort cellulaire ou de coloration et nature du traitement médicamenteux) et la variable dépendante qui est le pourcentage de la population, ***p<0,01.d) Séparation du pré et du post traitement. Pour déterminer quel schéma de traitement était le plus efficace, les cellules XP-C ont été traitées avec les médicaments soit avant l'irradiation, soit après l'irradiation, soit avant et après l'irradiation. Le pourcentage de bioactivité du médicament a ensuite été calculé 24 heures après l'irradiation. Ce calcul est basé sur la détermination du pourcentage relatif en considérant les échantillons traités au DMSO non irradiés comme étant 100% et les échantillons irradiés comme étant 0%. Ainsi, les valeurs de fluorescence obtenues ont été normalisées par rapport à ces deux contrôles. a) Séparation du régime de traitement médicamenteux. L'isoconazole post-irradiation ou les deux traitements ont montré une augmentation significative de la bioactivité à 10µM, tandis que seuls les deux traitements ont montré une augmentation significative de la bioactivité à 5µM par rapport à la procédure de prétraitement. Le chlorhydrate de clémizole, cependant, semble avoir une meilleure bioactivité lorsque les deux régimes de pré- et post-irradiation ont été utilisés où l'augmentation de la bioactivité était significative avec une valeur p<0.0.5 pour les traitements de 5µM et 10µM par rapport au prétraitement à chaque concentration respectivement.*

En ce qui concerne le criblage biologique, une bibliothèque de siRNAs ciblant toutes les kinases humaines a été utilisée pour traiter les XPCs et les cellules normales, puis pour détecter si un renversement phénotypique se produit. 1292 siRNA différents ont été utilisés pour traiter des cellules XP-C qui ont ensuite été irradiées et laissées se rétablir pendant 24 heures avant de mesurer leur viabilité. Vingt-huit siRNA différents ont été sélectionnés sur la base de leur capacité à induire une augmentation de 25 % de la viabilité cellulaire par rapport aux contrôles transfectés avec des siRNA non ciblés (figure 70a). Parmi eux, le ciblage de deux kinases que sont PIK3C3 et LATS1

a permis une réparation de 20% des dommages induits à l'ADN (figure 70b). La spécificité des deux siRNA dans l'élimination des kinases cibles a été confirmée par western blot (figure 70c). Le knockdown de PIK3C3 en particulier a eu un effet exclusif sur la photoprotection des cellules XP-C et aucun effet sur les cellules normales, ce qui indique que la dérégulation de cette kinase peut aider à inverser partiellement l'effet de la mutation XPC. De plus, les effets photo-protecteurs de ces kinases knockdown dans les cellules XP-C et WT ont également été validés dans un test de réponse aux UVB où siPIK3C a été capable d'induire une viabilité plus élevée dans les cellules XP-C transfectées par rapport aux cellules non transfectées en fonction de l'augmentation des doses d'UVB. Par contre, l'effet de siLATS1 était plus évident dans l'augmentation de la viabilité des cellules WT en fonction de l'augmentation des doses d'UVB. Les effets des deux downregualtions ont été examinés au niveau de l'apoptose induite dans les cellules XP-C et WT. SiPIK3C a montré une réduction de la population de cellules apoptotiques dans les cellules XP-C tandis que siLATS1 a eu un effet similaire mais sur les cellules WT (figure 70d). La régulation de la signalisation en aval induite par le knockdown de ces kinases a également été étudiée par western blot. Parmi les effecteurs en aval de LATS1, nous avons identifié que YAP était fortement transloqué vers les noyaux lors du knockdown de LAST1 dans les deux lignées cellulaires (figure 71a). Comme pour PIK3C3, le knock down dans les cellules XP-C a conduit à une augmentation de l'expression d' UVRAG non visualisée dans les cellules WT (figure 71b). L'expression d'UVRAG est impliquée dans l'association du complexe $CRL4^{DDB2}$ au site de dommage, nous spéculons donc que cette propriété d'UVRAG pourrait être impliquée dans notre étude et que cela nécessite des études supplémentaires pour être validé. La dernière étape de validation consiste à tester l'efficacité de la photo-protection induite par le knock down de cette kinase sur une peau reconstruite en 3D. Cette peau sera fabriquée au laboratoire à partir de fibroblastes et de kératinocytes dérivés de patients XP-C afin de reconstruire la peau XP-C et de tester le knock down sur ce modèle, car il s'agit d'un modèle physiologique plus pertinent. Le XPC est un excellent modèle pour comprendre l'initiation

du cancer de la peau, car il est accéléré dans ces cellules. En améliorant ce phénotype, nous pouvons donc trouver des moyens de retarder ou de prévenir l'initiation du cancer.

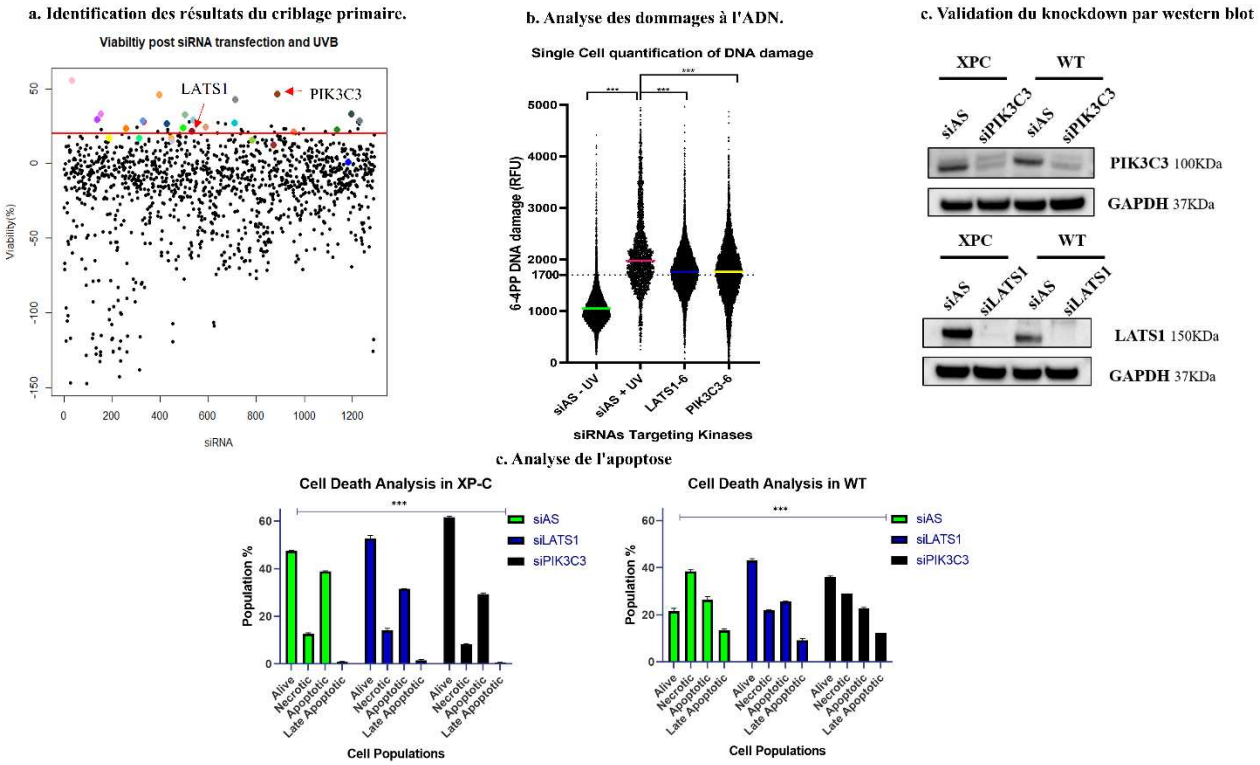

Figure 70 Résumé des résultats du siRNA

*a) Identification des résultats du criblage primaire. La librairie humaine de siRNA ciblant les kinomes a été criblée sur XP-C. Les cellules ont été transfectées avec la bibliothèque et les contrôles à 5nM et incubées pendant quarante-huit heures. Les cellules ont ensuite été irradiées à une dose d'UVB de 0,03J/cm2 et leur viabilité a été mesurée vingt-quatre heures après l'irradiation par l'ajout de bleu Presto. 28 kinases ont été identifiées dont le knock down a permis une augmentation de >25% du % d'activité. b) Analyse des dommages à l'ADN. Après transfection avec les hits secondaires et irradiation, les cellules XP-C ont été colorées avec l'anticorps 6-4 suivi d'une contre-coloration de l'ADN avec Hoechst. Plus de 1000 cellules par condition ont été sélectionnées sur la base de la coloration de l'ADN et leurs dommages à l'ADN ont été quantifiés. L'intensité moyenne par cellule est présentée ici dans un graphique en forme de violon qui montre une diminution des dommages à l'ADN pour les cellules transfectées avec LATS1 ou PIK3C3 par rapport aux cellules irradiées transfectées avec siAS. Cette diminution s'est avérée significative. *** p<0,001, test non paramétrique de freedman avec analyse post hoc de dun. c) Validation du knock down par western blot. Un western blot a été réalisé sur les cellules transfectées et les cellules XP-C et WT ont montré une diminution de l'expression des deux kinases après le knock down avec chaque siRNA respectif. d) Analyse de l'apoptose. Pour déchiffrer l'effet de la downregualtion sur la mort cellulaire apoptotique induite par les UVB, les cellules XP-C et WT ont été transfectées avec siAS, siPIK3C3 ou siLAT1 puis irradiées à 0,02 et 0,1J/cm2 pour les cellules XP-C et WT respectivement. Le marqueur caspase 3/7 de CellEvent a été ajouté après l'irradiation puis les cellules ont été collectées. Le PI a été ajouté juste avant l'analyse sur un cytomètre en flux. Les deux knock downs ont augmenté efficacement les populations de cellules vivantes dans les cellules XP-C, le siPIK3C3 ayant entraîné une augmentation plus importante. Pour les cellules WT, le knock down de LATS1 a entraîné une augmentation plus importante de la population de cellules vivantes par rapport au siPIK3C3 ou au siAS. Une anova à deux voies a été utilisée pour comparer les deux variables indépendantes (type de mort cellulaire ou de coloration et nature de la transfection) et la variable dépendante qui est le pourcentage de population, ***p<0,01*

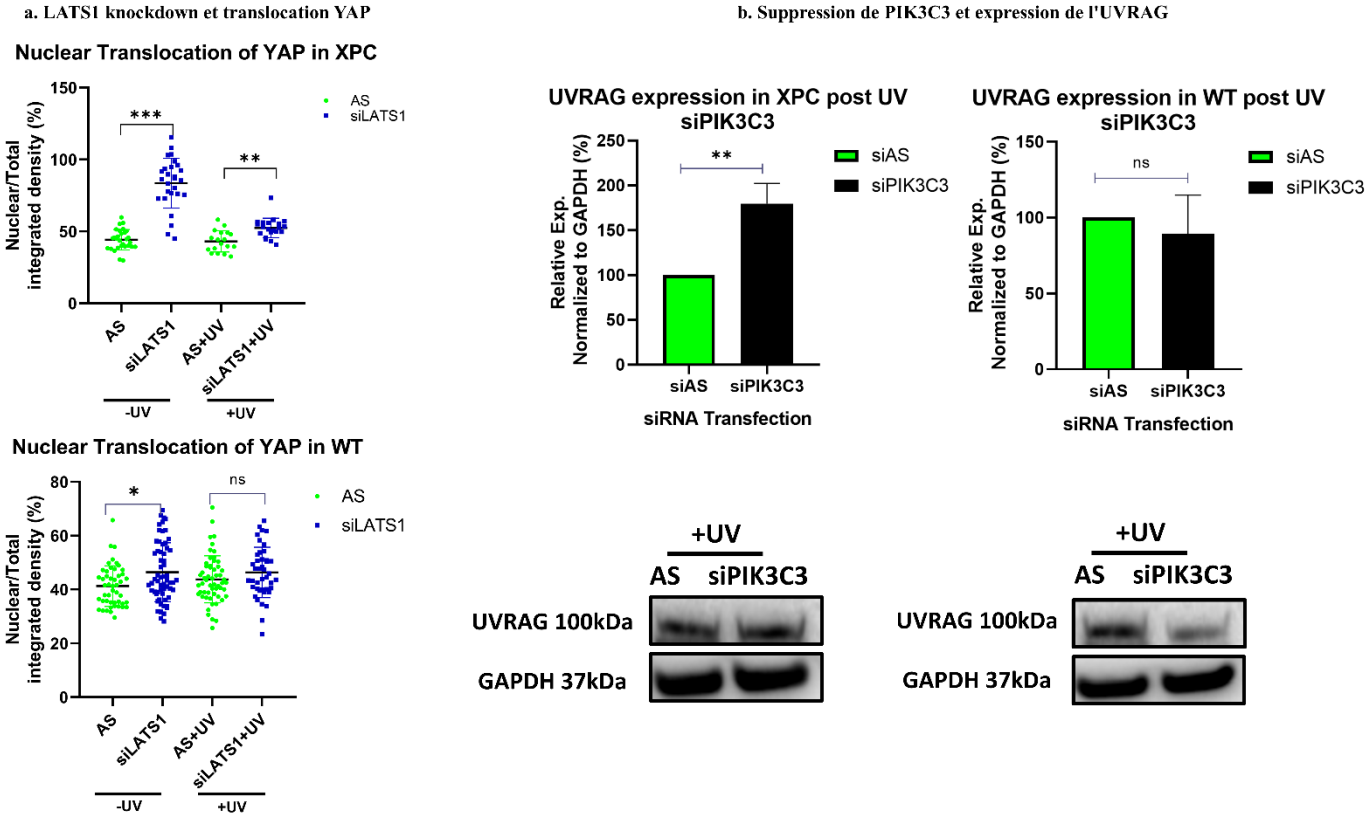

Figure 71 Analyse mécaniste des voies en aval des kinases kocked down

a*) Baisse de la régulation de LATS1 et translocation de YAP. L'effet de la transfection de siLATS1 sur la translocation de YAP vers le noyau a été quantifié dans les cellules XP-C et WT avant et après l'irradiation UVB. Les cellules XP-C ont montré une augmentation de la translocation de YAP vers les noyaux avant et après l'irradiation UVB, suite à l'élimination de LATS1. Les cellules WT ont également montré une translocation de YAP au niveau basal sans UV qui était moindre après irradiation. Analyse d'effet mixte avec analyse de comparaison multiple de Tukey. *valeur p<0,05, **valeur p<0,01, ***valeur p<0,001.b) Suppression de PIK3C3 et expression d'UVRAG. L'expression d'UVRAG a été analysée après transfection de siPIK3C3 dans les cellules XP-C et WT après irradiation UV. Les cellules XP-C manifestent une augmentation significative de l'expression d'UVRAG lors de la dérégulation de PIK3C3 qui n'était pas évidente dans les cellules WT. Test t apparié, **valeur p<0,01.*

REFERENCE LIST

1. Bode AM and Dong Z (2003) Mitogen-activated protein kinase activation in UV-induced signal transduction. Sci STKE 2003:Re2. doi: 10.1126/stke.2003.167.re2

2. Strozyk E and Kulms D (2013) The role of AKT/mTOR pathway in stress response to UV-irradiation: implication in skin carcinogenesis by regulation of apoptosis, autophagy and senescence. Int.J.Mol.Sci. 14:15260-15285.

3. Tan NS and Wahli W (2014) The emerging role of Nrf2 in dermatotoxicology. EMBO Mol.Med. 6:431-433.

4. Gegotek A and Skrzydlewska E (2015) The role of transcription factor Nrf2 in skin cells metabolism. Arch.Dermatol.Res. 307:385-396.

5. Choi HR, Shin JW, Na JI, Nam KM, Lee HS and Park KC (2015) Novel Antioxidant Tripeptide "ACQ" Can Prevent UV-Induced Cell Death and Preserve the Number of Epidermal Stem Cells. Oxid Med Cell Longev 2015:359740. doi: 10.1155/2015/359740

6. Watt FM and Fujiwara H (2011) Cell-extracellular matrix interactions in normal and diseased skin. Cold Spring Harb.Perspect.Biol. 3.

7. D'Errico M, Teson M, Calcagnile A, Nardo T, De LN, Lazzari C, Soddu S, Zambruno G, Stefanini M and Dogliotti E (2005) Differential role of transcription-coupled repair in UVB-induced response of human fibroblasts and keratinocytes. Cancer Res. 65:432-438.

8. Noonan FP, Zaidi MR, Wolnicka-Glubisz A, Anver MR, Bahn J, Wielgus A, Cadet J, Douki T, Mouret S, Tucker MA, Popratiloff A, Merlino G and De Fabo EC (2012) Melanoma induction by ultraviolet A but not ultraviolet B radiation requires melanin pigment. Nat.Commun. 3:884.

9. Frechet M, Warrick E, Vioux C, Chevallier O, Spatz A, Benhamou S, Sarasin A, Bernerd F and Magnaldo T (2008) Overexpression of matrix metalloproteinase 1 in dermal fibroblasts from DNA repair-deficient/cancer-prone xeroderma pigmentosum group C patients. Oncogene 27:5223-5232.

10. Nakad R and Schumacher B (2016) DNA Damage Response and Immune Defense: Links and Mechanisms. Front Genet. 7:147.

11. Soeur J, Eilstein J, Lereaux G, Jones C and Marrot L (2015) Skin resistance to oxidative stress induced by resveratrol: from Nrf2 activation to GSH biosynthesis. Free Radic.Biol.Med. 78:213-223.

12. Blanpain C, Mohrin M, Sotiropoulou PA and Passegue E (2011) DNA-damage response in tissue-specific and cancer stem cells. Cell Stem Cell 8:16-29.

13. Jackson SP and Bartek J (2009) The DNA-damage response in human biology and disease. Nature 461:1071-1078.

14. Pan MR, Li K, Lin SY and Hung WC (2016) Connecting the Dots: From DNA Damage and Repair to Aging. Int.J.Mol.Sci. 17.

15. Zhou BB and Elledge SJ (2000) The DNA damage response: putting checkpoints in perspective. Nature 408:433-439.

16. Ravanat JL, Douki T and Cadet J (2001) Direct and indirect effects of UV radiation on DNA and its components. J Photochem Photobiol B 63:88-102. doi: 10.1016/s1011-1344(01)00206-8

17. Seebode C, Lehmann J and Emmert S (2016) Photocarcinogenesis and Skin Cancer Prevention Strategies. Anticancer Res 36:1371-8.

18. Rastogi RP, Singh SP, Hader DP and Sinha RP (2010) Detection of reactive oxygen species (ROS) by the oxidant-sensing probe 2',7'-dichlorodihydrofluorescein diacetate in the cyanobacterium Anabaena variabilis PCC 7937. Biochem Biophys Res Commun 397:603-7. doi: 10.1016/j.bbrc.2010.06.006

19. Armstrong JD and Kunz BA (1990) Site and strand specificity of UVB mutagenesis in the SUP4-o gene of yeast. Proc Natl Acad Sci U S A 87:9005-9. doi: 10.1073/pnas.87.22.9005

20. Delinasios GJ, Karbaschi M, Cooke MS and Young AR (2018) Vitamin E inhibits the UVAI induction of "light" and "dark" cyclobutane pyrimidine dimers, and oxidatively generated DNA damage, in keratinocytes. Sci Rep 8:423. doi: 10.1038/s41598-017-18924-4

21. Lee CH, Wu SB, Hong CH, Yu HS and Wei YH (2013) Molecular Mechanisms of UV-Induced Apoptosis and Its Effects on Skin Residential Cells: The Implication in UV-Based Phototherapy. Int J Mol Sci 14:6414-35. doi: 10.3390/ijms14036414

22. Iordanov MS, Choi RJ, Ryabinina OP, Dinh TH, Bright RK and Magun BE (2002) The UV (Ribotoxic) stress response of human keratinocytes involves the unexpected uncoupling of the Ras-extracellular signal-regulated kinase signaling cascade from the activated epidermal growth factor receptor. Mol Cell Biol 22:5380-94. doi: 10.1128/mcb.22.15.5380-5394.2002

23. Yajima I, Kumasaka MY, Thang ND, Goto Y, Takeda K, Yamanoshita O, Iida M, Ohgami N, Tamura H, Kawamoto Y and Kato M (2012) RAS/RAF/MEK/ERK and PI3K/PTEN/AKT Signaling in Malignant Melanoma Progression and Therapy. Dermatol Res Pract 2012:354191. doi: 10.1155/2012/354191

24. Ming M, Han W, Maddox J, Soltani K, Shea CR, Freeman DM and He YY (2010) UVB-induced ERK/AKT-dependent PTEN suppression promotes survival of epidermal keratinocytes. Oncogene 29:492-502. doi: 10.1038/onc.2009.357

25. Gottlieb TM, Leal JF, Seger R, Taya Y and Oren M (2002) Cross-talk between Akt, p53 and Mdm2: possible implications for the regulation of apoptosis. Oncogene 21:1299-303. doi: 10.1038/sj.onc.1205181

26. Dijkers PF, Birkenkamp KU, Lam EW, Thomas NS, Lammers JW, Koenderman L and Coffer PJ (2002) FKHR-L1 can act as a critical effector of cell death induced by cytokine withdrawal: protein kinase B-enhanced cell survival through maintenance of mitochondrial integrity. J Cell Biol 156:531-42. doi: 10.1083/jcb.200108084

27. Datta SR, Dudek H, Tao X, Masters S, Fu H, Gotoh Y and Greenberg ME (1997) Akt phosphorylation of BAD couples survival signals to the cell-intrinsic death machinery. Cell 91:231-41. doi: 10.1016/s0092-8674(00)80405-5

28. Franke TF (2008) PI3K/Akt: getting it right matters. Oncogene 27:6473-6488.

29. Xu N, Lao Y, Zhang Y and Gillespie DA (2012) Akt: a double-edged sword in cell proliferation and genome stability. J.Oncol. 2012:951724.

30. Ma XM and Blenis J (2009) Molecular mechanisms of mTOR-mediated translational control. Nat Rev Mol Cell Biol 10:307-18. doi: 10.1038/nrm2672

31. Dufner A and Thomas G (1999) Ribosomal S6 kinase signaling and the control of translation. Exp Cell Res 253:100-9. doi: 10.1006/excr.1999.4683

32. Frodin M and Gammeltoft S (1999) Role and regulation of 90 kDa ribosomal S6 kinase (RSK) in signal transduction. Mol Cell Endocrinol 151:65-77. doi: 10.1016/s0303-7207(99)00061-1

33. Zhang Y, Dong Z, Nomura M, Zhong S, Chen N, Bode AM and Dong Z (2001) Signal transduction pathways involved in phosphorylation and activation of p70S6K following exposure to UVA irradiation. J Biol Chem 276:20913-23. doi: 10.1074/jbc.M009047200

34. Zhang Y, Zhong S, Dong Z, Chen N, Bode AM, Ma W and Dong Z (2001) UVA induces Ser381 phosphorylation of p90RSK/MAPKAP-K1 via ERK and JNK pathways. J Biol Chem 276:14572-80. doi: 10.1074/jbc.M004615200

35. Zhang Y, Dong Z, Bode AM, Ma WY, Chen N and Dong Z (2001) Induction of EGFR-dependent and EGFR-independent signaling pathways by ultraviolet A irradiation. DNA Cell Biol 20:769-79. doi: 10.1089/104454901753438589

36. Zhang Y, Ma WY, Kaji A, Bode AM and Dong Z (2002) Requirement of ATM in UVA-induced signaling and apoptosis. J Biol Chem 277:3124-31. doi: 10.1074/jbc.M110245200

37. Zhang Y, Mattjus P, Schmid PC, Dong Z, Zhong S, Ma WY, Brown RE, Bode AM, Schmid HH and Dong Z (2001) Involvement of the acid sphingomyelinase pathway in uva-induced apoptosis. J Biol Chem 276:11775-82. doi: 10.1074/jbc.M006000200

38. Chen N, Ma W, Huang C and Dong Z (1999) Translocation of protein kinase Cepsilon and protein kinase Cdelta to membrane is required for ultraviolet B-induced activation of mitogen-activated protein kinases and apoptosis. J Biol Chem 274:15389-94. doi: 10.1074/jbc.274.22.15389

39. Huang C, Li J, Chen N, Ma W, Bowden GT and Dong Z (2000) Inhibition of atypical PKC blocks ultraviolet-induced AP-1 activation by specifically inhibiting ERKs activation. Mol Carcinog 27:65-75.

40. Nakamura S, Takahashi H, Kinouchi M, Manabe A, Ishida-Yamamoto A, Hashimoto Y and Iizuka H (2001) Differential phosphorylation of mitogen-activated protein kinase families by epidermal growth factor and ultraviolet B irradiation in SV40-transformed human keratinocytes. J Dermatol Sci 25:139-49. doi: 10.1016/s0923-1811(00)00123-7

41. She QB, Ma WY and Dong Z (2002) Role of MAP kinases in UVB-induced phosphorylation of p53 at serine 20. Oncogene 21:1580-9. doi: 10.1038/sj.onc.1205239

42. She QB, Chen N and Dong Z (2000) ERKs and p38 kinase phosphorylate p53 protein at serine 15 in response to UV radiation. J Biol Chem 275:20444-9. doi: 10.1074/jbc.M001020200

43. She QB, Ma WY, Zhong S and Dong Z (2002) Activation of JNK1, RSK2, and MSK1 is involved in serine 112 phosphorylation of Bad by ultraviolet B radiation. J Biol Chem 277:24039-48. doi: 10.1074/jbc.M109907200

44. Zhong S, Zhang Y, Jansen C, Goto H, Inagaki M and Dong Z (2001) MAP kinases mediate UVB-induced phosphorylation of histone H3 at serine 28. J Biol Chem 276:12932-7. doi: 10.1074/jbc.M010931200

45. Zhong S, Jansen C, She QB, Goto H, Inagaki M, Bode AM, Ma WY and Dong Z (2001) Ultraviolet B-induced phosphorylation of histone H3 at serine 28 is mediated by MSK1. J Biol Chem 276:33213-9. doi: 10.1074/jbc.M103973200

46. Nomura M, Kaji A, He Z, Ma WY, Miyamoto K, Yang CS and Dong Z (2001) Inhibitory mechanisms of tea polyphenols on the ultraviolet B-activated phosphatidylinositol 3-kinase-dependent pathway. J Biol Chem 276:46624-31. doi: 10.1074/jbc.M107897200

47. Nomura M, Kaji A, Ma WY, Zhong S, Liu G, Bowden GT, Miyamoto KI and Dong Z (2001) Mitogen- and stress-activated protein kinase 1 mediates activation of Akt by ultraviolet B irradiation. J Biol Chem 276:25558-67. doi: 10.1074/jbc.M101164200

48. Liu G, Zhang Y, Bode AM, Ma WY and Dong Z (2002) Phosphorylation of 4E-BP1 is mediated by the p38/MSK1 pathway in response to UVB irradiation. J Biol Chem 277:8810-6. doi: 10.1074/jbc.M110477200

49. Kawasumi M, Lemos B, Bradner JE, Thibodeau R, Kim Y-s, Schmidt M, Higgins E, Koo S-w, Angle-Zahn A, Chen A, Levine D, Nguyen L, Heffernan TP, Longo I, Mandinova A, Lu Y-P, Conney AH and Nghiem P (2011) Protection from UV-induced skin carcinogenesis by genetic inhibition of the ataxia telangiectasia and Rad3-related (ATR) kinase. Proceedings of the National Academy of Sciences 108:13716-13721. doi: 10.1073/pnas.1111378108

50. Kumar R, Deep G and Agarwal R (2015) An Overview of Ultraviolet B Radiation-Induced Skin Cancer Chemoprevention by Silibinin. Curr Pharmacol Rep 1:206-215. doi: 10.1007/s40495-015-0027-9

51. Kindas-Mügge I, Riedler C, Fröhlich I, Micksche M and Trautinger F (2002) CHARACTERIZATION OF PROTEINS ASSOCIATED WITH HEAT SHOCK PROTEIN HSP27 IN THE SQUAMOUS CELL CARCINOMA CELL LINE A431. Cell Biology International 26:109-116. doi: https://doi.org/10.1006/cbir.2001.0822

52. Ming M, Feng L, Shea CR, Soltani K, Zhao B, Han W, Smart RC, Trempus CS and He YY (2011) PTEN positively regulates UVB-induced DNA damage repair. Cancer Res 71:5287-95. doi: 10.1158/0008-5472.can-10-4614

53. Shen WH, Balajee AS, Wang J, Wu H, Eng C, Pandolfi PP and Yin Y (2007) Essential role for nuclear PTEN in maintaining chromosomal integrity. Cell 128:157-70. doi: 10.1016/j.cell.2006.11.042

54. Carballo GB, Honorato JR, de Lopes GPF and Spohr T (2018) A highlight on Sonic hedgehog pathway. Cell Commun Signal 16:11. doi: 10.1186/s12964-018-0220-7

55. Jia Y, Wang Y and Xie J (2015) The Hedgehog pathway: role in cell differentiation, polarity and proliferation. Arch Toxicol 89:179-91. doi: 10.1007/s00204-014-1433-1

56. Rahnama F, Shimokawa T, Lauth M, Finta C, Kogerman P, Teglund S, Toftgård R and Zaphiropoulos PG (2006) Inhibition of GLI1 gene activation by Patched1. Biochem J 394:19-26. doi: 10.1042/bj20050941

57. Mizuno T, Tokuoka S, Kishikawa M, Nakashima E, Mabuchi K and Iwamoto KS (2006) Molecular basis of basal cell carcinogenesis in the atomic-bomb survivor population: p53 and PTCH gene alterations. Carcinogenesis 27:2286-94. doi: 10.1093/carcin/bgl107

58. Charazac A, Fayyad N, Beal D, Bourgoin-Voillard S, Seve M, Sauvaigo S, Lamartine J, Soularue P, Moratille S, Martin MT, Ravanat JL, Douki T and Rachidi W (2020) Impairment of Base Excision Repair in Dermal Fibroblasts Isolated From Nevoid Basal Cell Carcinoma Patients. Front Oncol 10:1551. doi: 10.3389/fonc.2020.01551

59. Dumaz N, Jouenne F, Delyon J, Mourah S, Bensussan A and Lebbé C (2019) Atypical BRAF and NRAS Mutations in Mucosal Melanoma. Cancers (Basel) 11. doi: 10.3390/cancers11081133

60. Brose MS, Volpe P, Feldman M, Kumar M, Rishi I, Gerrero R, Einhorn E, Herlyn M, Minna J, Nicholson A, Roth JA, Albelda SM, Davies H, Cox C, Brignell G, Stephens P, Futreal PA, Wooster R, Stratton MR and Weber BL (2002) BRAF and RAS mutations in human lung cancer and melanoma. Cancer Res 62:6997-7000.

61. Curtin JA, Fridlyand J, Kageshita T, Patel HN, Busam KJ, Kutzner H, Cho KH, Aiba S, Bröcker EB, LeBoit PE, Pinkel D and Bastian BC (2005) Distinct sets of genetic alterations in melanoma. N Engl J Med 353:2135-47. doi: 10.1056/NEJMoa050092

62. Omholt K, Platz A, Kanter L, Ringborg U and Hansson J (2003) NRAS and BRAF mutations arise early during melanoma pathogenesis and are preserved throughout tumor progression. Clin Cancer Res 9:6483-8.

63. Cheng KC, Cahill DS, Kasai H, Nishimura S and Loeb LA (1992) 8-Hydroxyguanine, an abundant form of oxidative DNA damage, causes G----T and A----C substitutions. J Biol Chem 267:166-72.

64. Fine B, Hodakoski C, Koujak S, Su T, Saal LH, Maurer M, Hopkins B, Keniry M, Sulis ML, Mense S, Hibshoosh H and Parsons R (2009) Activation of the PI3K pathway in cancer through inhibition of PTEN by exchange factor P-REX2a. Science 325:1261-5. doi: 10.1126/science.1173569

65. Mense SM, Barrows D, Hodakoski C, Steinbach N, Schoenfeld D, Su W, Hopkins BD, Su T, Fine B, Hibshoosh H and Parsons R (2015) PTEN inhibits PREX2-catalyzed activation of RAC1 to restrain tumor cell invasion. Sci Signal 8:ra32. doi: 10.1126/scisignal.2005840

66. Hodis E, Watson IR, Kryukov GV, Arold ST, Imielinski M, Theurillat JP, Nickerson E, Auclair D, Li L, Place C, Dicara D, Ramos AH, Lawrence MS, Cibulskis K, Sivachenko A, Voet D, Saksena G, Stransky N, Onofrio RC, Winckler W, Ardlie K, Wagle N, Wargo J, Chong K, Morton DL, Stemke-Hale K, Chen G, Noble M, Meyerson M, Ladbury JE, Davies MA, Gershenwald JE, Wagner SN, Hoon DS, Schadendorf D, Lander ES, Gabriel SB, Getz G, Garraway LA and Chin L (2012) A landscape of driver mutations in melanoma. Cell 150:251-63. doi: 10.1016/j.cell.2012.06.024

67. Berger MF, Hodis E, Heffernan TP, Deribe YL, Lawrence MS, Protopopov A, Ivanova E, Watson IR, Nickerson E, Ghosh P, Zhang H, Zeid R, Ren X, Cibulskis K, Sivachenko AY, Wagle N, Sucker A, Sougnez C, Onofrio R, Ambrogio L, Auclair D, Fennell T, Carter SL, Drier Y, Stojanov P, Singer MA, Voet D, Jing R, Saksena G, Barretina J, Ramos AH, Pugh TJ, Stransky N, Parkin M, Winckler W, Mahan S, Ardlie K, Baldwin J, Wargo J, Schadendorf D, Meyerson M, Gabriel SB, Golub TR, Wagner SN, Lander ES, Getz G, Chin L and Garraway LA (2012) Melanoma genome sequencing reveals frequent PREX2 mutations. Nature 485:502-506. doi: 10.1038/nature11071

68. Barrows D, Schoenfeld SM, Hodakoski C, Silkov A, Honig B, Couvillon A, Shymanets A, Nürnberg B, Asara JM and Parsons R (2015) p21-activated Kinases (PAKs) Mediate the Phosphorylation of PREX2 Protein to Initiate Feedback Inhibition of Rac1 GTPase. J Biol Chem 290:28915-31. doi: 10.1074/jbc.M115.668244

69. Halaban R (2015) RAC1 and melanoma. Clin Ther 37:682-5. doi: 10.1016/j.clinthera.2014.10.027

70. Isabelle C, Nicolas J, Christelle C, Marianne L, Anne D, Florent G, Philippe B, Christine C and Philippe B (2006) P16 is overexpressed in cutaneous carcinomas located on sun-exposed areas. European Journal of Dermatology 16:518-522. doi: 10.1684/ejd.2006.0024

71. Viros A, Sanchez-Laorden B, Pedersen M, Furney SJ, Rae J, Hogan K, Ejiama S, Girotti MR, Cook M, Dhomen N and Marais R (2014) Ultraviolet radiation accelerates BRAF-driven melanomagenesis by targeting TP53. Nature 511:478-482. doi: 10.1038/nature13298

72. Petit-Frère C, Clingen PH, Grewe M, Krutmann J, Roza L, Arlett CF and Green MH (1998) Induction of interleukin-6 production by ultraviolet radiation in normal human epidermal keratinocytes and in a human keratinocyte cell line is mediated by DNA damage. J Invest Dermatol 111:354-9. doi: 10.1038/sj.jid.5602962

73. Miyauchi-Hashimoto H, Sugihara A, Tanaka K and Horio T (2005) Ultraviolet radiation-induced impairment of tumor rejection is enhanced in xeroderma pigmentosum a gene-deficient mice. J Invest Dermatol 124:1313-7. doi: 10.1111/j.0022-202X.2005.23717.x

74. Athar M, An KP, Morel KD, Kim AL, Aszterbaum M, Longley J, Epstein EH, Jr. and Bickers DR (2001) Ultraviolet B(UVB)-induced cox-2 expression in murine skin: an immunohistochemical study. Biochem Biophys Res Commun 280:1042-7. doi: 10.1006/bbrc.2000.4201

75. De Fabo EC and Noonan FP (1983) Mechanism of immune suppression by ultraviolet irradiation in vivo. I. Evidence for the existence of a unique photoreceptor in skin and its role in photoimmunology. J Exp Med 158:84-98. doi: 10.1084/jem.158.1.84

76. Beissert S, Rühlemann D, Mohammad T, Grabbe S, El-Ghorr A, Norval M, Morrison H, Granstein RD and Schwarz T (2001) IL-12 prevents the inhibitory effects of cis-urocanic acid on tumor antigen presentation by Langerhans cells: implications for photocarcinogenesis. J Immunol 167:6232-8. doi: 10.4049/jimmunol.167.11.6232

77. Mareddy S, Reddy J, Babu S and Balan P (2013) Xeroderma pigmentosum: man deprived of his right to light. ScientificWorldJournal. 2013:534752.

78. Iyama T and Wilson DM, III (2013) DNA repair mechanisms in dividing and non-dividing cells. DNA Repair (Amst) 12:620-636.

79. D'Errico M, Parlanti E, Teson M, de Jesus BM, Degan P, Calcagnile A, Jaruga P, Bjoras M, Crescenzi M, Pedrini AM, Egly JM, Zambruno G, Stefanini M, Dizdaroglu M and Dogliotti E (2006) New functions of XPC in the protection of human skin cells from oxidative damage. EMBO J. 25:4305-4315.

80. Pascucci B, D'Errico M, Parlanti E, Giovannini S and Dogliotti E (2011) Role of nucleotide excision repair proteins in oxidative DNA damage repair: an updating. Biochemistry (Mosc.) 76:4-15.

81. Spivak G (2015) Nucleotide excision repair in humans. DNA Repair (Amst) 36:13-18.

82. Melis JP, van SH and Luijten M (2013) Oxidative DNA damage and nucleotide excision repair. Antioxid.Redox.Signal. 18:2409-2419.

83. Paques F and Haber JE (1999) Multiple pathways of recombination induced by double-strand breaks in Saccharomyces cerevisiae. Microbiol.Mol.Biol.Rev. 63:349-404.

84. Yun MH and Hiom K (2009) CtIP-BRCA1 modulates the choice of DNA double-strand-break repair pathway throughout the cell cycle. Nature 459:460-463.

85. Wang H, Li Y, Truong LN, Shi LZ, Hwang PY, He J, Do J, Cho MJ, Li H, Negrete A, Shiloach J, Berns MW, Shen B, Chen L and Wu X (2014) CtIP maintains stability at common fragile sites and inverted repeats by end resection-independent endonuclease activity. Mol.Cell 54:1012-1021.

86. Mitra S (2011) Does evening sun increase the risk of skin cancer? Proc.Natl.Acad.Sci.U.S.A 108:18857-18858.

87. Adair JE, Maloney SC, Dement GA, Wertzler KJ, Smerdon MJ and Reeves R (2007) High-mobility group A1 proteins inhibit expression of nucleotide excision repair factor xeroderma pigmentosum group A. Cancer Res. 67:6044-6052.

88. Liu Y, Bernauer AM, Yingling CM and Belinsky SA (2012) HIF1alpha regulated expression of XPA contributes to cisplatin resistance in lung cancer. Carcinogenesis 33:1187-1192.

89. Ma L, Weeda G, Jochemsen AG, Bootsma D, Hoeijmakers JH and van der Eb AJ (1992) Molecular and functional analysis of the XPBC/ERCC-3 promoter: transcription activity is dependent on the integrity of an Sp1-binding site. Nucleic Acids Res. 20:217-224.

90. Jaitovich-Groisman I, Benlimame N, Slagle BL, Perez MH, Alpert L, Song DJ, Fotouhi-Ardakani N, Galipeau J and Alaoui-Jamali MA (2001) Transcriptional regulation of the TFIIH transcription repair components XPB and XPD by the hepatitis B virus x protein in liver cells and transgenic liver tissue. J.Biol.Chem. 276:14124-14132.

91. Park JM and Kang TH (2016) Transcriptional and Posttranslational Regulation of Nucleotide Excision Repair: The Guardian of the Genome against Ultraviolet Radiation. Int.J.Mol.Sci. 17.

92. Rezvani HR, Mahfouf W, Ali N, Chemin C, Ged C, Kim AL, de Verneuil H, Taieb A, Bickers DR and Mazurier F (2010) Hypoxia-inducible factor-1alpha regulates the expression of nucleotide excision repair proteins in keratinocytes. Nucleic Acids Res 38:797-809. doi: 10.1093/nar/gkp1072

93. Merkel P, Khoury N, Bertolotto C and Perfetti R (2003) Insulin and glucose regulate the expression of the DNA repair enzyme XPD. Mol.Cell Endocrinol. 201:75-85.

94. Tan T and Chu G (2002) p53 Binds and activates the xeroderma pigmentosum DDB2 gene in humans but not mice. Mol.Cell Biol. 22:3247-3254.

95. Liu J, Lin M, Zhang C, Wang D, Feng Z and Hu W (2012) TAp63gamma enhances nucleotide excision repair through transcriptional regulation of DNA repair genes. DNA Repair (Amst) 11:167-176.

96. Hartman AR and Ford JM (2002) BRCA1 induces DNA damage recognition factors and enhances nucleotide excision repair. Nat.Genet. 32:180-184.

97. Mahfouf W, Hosseini M, Muzotte E, Serrano-Sanchez M, Dousset L, Moisan F, Rachidi W, Taieb A, Rudolf J and Rezvani HR (2019) Loss of epidermal hypoxia-inducible factor-1alpha blocks UVB-induced tumorigenesis by affecting DNA repair capacity and oxidative stress. J Invest Dermatol. doi: 10.1016/j.jid.2019.01.035

98. Dominguez-Brauer C, Chen YJ, Brauer PM, Pimkina J and Raychaudhuri P (2009) ARF stimulates XPC to trigger nucleotide excision repair by regulating the repressor complex of E2F4. EMBO Rep. 10:1036-1042.

99. Ming M, Shea CR, Guo X, Li X, Soltani K, Han W and He YY (2010) Regulation of global genome nucleotide excision repair by SIRT1 through xeroderma pigmentosum C. Proc.Natl.Acad.Sci.U.S.A 107:22623-22628.

100. Ming M, Soltani K, Shea CR, Li X and He YY (2015) Dual role of SIRT1 in UVB-induced skin tumorigenesis. Oncogene 34:357-63. doi: 10.1038/onc.2013.583

101. Christmann M, Tomicic MT, Origer J, Aasland D and Kaina B (2006) c-Fos is required for excision repair of UV-light induced DNA lesions by triggering the re-synthesis of XPF. Nucleic Acids Res. 34:6530-6539.

102. Crawford EL, Blomquist T, Mullins DN, Yoon Y, Hernandez DR, Al-Bagdhadi M, Ruiz J, Hammersley J and Willey JC (2007) CEBPG regulates ERCC5/XPG expression in human bronchial epithelial cells and this regulation is modified by E2F1/YY1 interactions. Carcinogenesis 28:2552-2559.

103. Nag A, Bondar T, Shiv S and Raychaudhuri P (2001) The xeroderma pigmentosum group E gene product DDB2 is a specific target of cullin 4A in mammalian cells. Mol.Cell Biol. 21:6738-6747.

104. Zhao Q, Barakat BM, Qin S, Ray A, El-Mahdy MA, Wani G, Arafa e, Mir SN, Wang QE and Wani AA (2008) The p38 mitogen-activated protein kinase augments nucleotide excision repair by mediating DDB2 degradation and chromatin relaxation. J.Biol.Chem. 283:32553-32561.

105. Sugasawa K, Okuda Y, Saijo M, Nishi R, Matsuda N, Chu G, Mori T, Iwai S, Tanaka K, Tanaka K and Hanaoka F (2005) UV-induced ubiquitylation of XPC protein mediated by UV-DDB-ubiquitin ligase complex. Cell 121:387-400.

106. Wang QE, Praetorius-Ibba M, Zhu Q, El-Mahdy MA, Wani G, Zhao Q, Qin S, Patnaik S and Wani AA (2007) Ubiquitylation-independent degradation of Xeroderma pigmentosum group C protein is required for efficient nucleotide excision repair. Nucleic Acids Res. 35:5338-5350.

107. Schwertman P, Lagarou A, Dekkers DH, Raams A, van der Hoek AC, Laffeber C, Hoeijmakers JH, Demmers JA, Fousteri M, Vermeulen W and Marteijn JA (2012) UV-sensitive syndrome protein UVSSA recruits USP7 to regulate transcription-coupled repair. Nat.Genet. 44:598-602.

108. Sin Y, Tanaka K and Saijo M (2016) The C-terminal Region and SUMOylation of Cockayne Syndrome Group B Protein Play Critical Roles in Transcription-coupled Nucleotide Excision Repair. J.Biol.Chem. 291:1387-1397.

109. Kang TH, Reardon JT and Sancar A (2011) Regulation of nucleotide excision repair activity by transcriptional and post-transcriptional control of the XPA protein. Nucleic Acids Res. 39:3176-3187.

110. Perez-Oliva AB, Lachaud C, Szyniarowski P, Munoz I, Macartney T, Hickson I, Rouse J and Alessi DR (2015) USP45 deubiquitylase controls ERCC1-XPF endonuclease-mediated DNA damage responses. EMBO J. 34:326-343.

111. Lee TH, Park JM, Leem SH and Kang TH (2014) Coordinated regulation of XPA stability by ATR and HERC2 during nucleotide excision repair. Oncogene 33:19-25.

112. Nguyen TA, Slattery SD, Moon SH, Darlington YF, Lu X and Donehower LA (2010) The oncogenic phosphatase WIP1 negatively regulates nucleotide excision repair. DNA Repair (Amst) 9:813-823.

113. Shah P, Zhao B, Qiang L and He YY (2018) Phosphorylation of xeroderma pigmentosum group C regulates ultraviolet-induced DNA damage repair. Nucleic Acids Res 46:5050-5060. doi: 10.1093/nar/gky239

114. Robu M, Shah RG, Petitclerc N, Brind'Amour J, Kandan-Kulangara F and Shah GM (2013) Role of poly(ADP-ribose) polymerase-1 in the removal of UV-induced DNA lesions by nucleotide excision repair. Proc.Natl.Acad.Sci.U.S.A 110:1658-1663.

115. Thorslund T, von KC, Harrigan JA, Indig FE, Christiansen M, Stevnsner T and Bohr VA (2005) Cooperation of the Cockayne syndrome group B protein and poly(ADP-ribose) polymerase 1 in the response to oxidative stress. Mol.Cell Biol. 25:7625-7636.

116. Langie SA, Knaapen AM, Houben JM, van Kempen FC, de Hoon JP, Gottschalk RW, Godschalk RW and van Schooten FJ (2007) The role of glutathione in the regulation of nucleotide excision repair during oxidative stress. Toxicol.Lett. 168:302-309.

117. Xie QH, He XX, Chang Y, Sun SZ, Jiang X, Li PY and Lin JS (2011) MiR-192 inhibits nucleotide excision repair by targeting ERCC3 and ERCC4 in HepG2.2.15 cells. Biochem.Biophys.Res.Commun. 410:440-445.

118. Langie SA, Kowalczyk P, Tudek B, Zabielski R, Dziaman T, Olinski R, van Schooten FJ and Godschalk RW (2010) The effect of oxidative stress on nucleotide-excision repair in colon tissue of newborn piglets. Mutat Res 695:75-80. doi: 10.1016/j.mrgentox.2009.12.005

119. Feng Z, Hu W and Tang MS (2004) Trans-4-hydroxy-2-nonenal inhibits nucleotide excision repair in human cells: a possible mechanism for lipid peroxidation-induced carcinogenesis. Proc Natl Acad Sci U S A 101:8598-602. doi: 10.1073/pnas.0402794101

120. Hiramatsu K, Ogino T, Ozaki M and Okada S (2006) Monochloramine inhibits ultraviolet B-induced p53 activation and DNA repair response in human fibroblasts. Biochim Biophys Acta 1763:188-96. doi: 10.1016/j.bbamcr.2005.11.009

121. Konstantinopoulos PA, Spentzos D, Fountzilas E, Francoeur N, Sanisetty S, Grammatikos AP, Hecht JL and Cannistra SA (2011) Keap1 mutations and Nrf2 pathway activation in epithelial ovarian cancer. Cancer Res. 71:5081-5089.

122. Kansanen E, Jyrkkanen HK and Levonen AL (2012) Activation of stress signaling pathways by electrophilic oxidized and nitrated lipids. Free Radic.Biol.Med. 52:973-982.

123. Kimura M, Yamamoto T, Zhang J, Itoh K, Kyo M, Kamiya T, Aburatani H, Katsuoka F, Kurokawa H, Tanaka T, Motohashi H and Yamamoto M (2007) Molecular basis distinguishing the DNA binding profile of Nrf2-Maf heterodimer from that of Maf homodimer. J.Biol.Chem. 282:33681-33690.

124. McMahon M, Itoh K, Yamamoto M, Chanas SA, Henderson CJ, McLellan LI, Wolf CR, Cavin C and Hayes JD (2001) The Cap'n'Collar basic leucine zipper transcription factor Nrf2 (NF-E2 p45-related factor 2) controls both

constitutive and inducible expression of intestinal detoxification and glutathione biosynthetic enzymes. Cancer Res. 61:3299-3307.

125. Reisman SA, Lee CY, Meyer CJ, Proksch JW and Ward KW (2014) Topical application of the synthetic triterpenoid RTA 408 activates Nrf2 and induces cytoprotective genes in rat skin. Arch.Dermatol.Res. 306:447-454.

126. Zhu H, Jia Z, Zhang L, Yamamoto M, Misra HP, Trush MA and Li Y (2008) Antioxidants and phase 2 enzymes in macrophages: regulation by Nrf2 signaling and protection against oxidative and electrophilic stress. Exp.Biol.Med.(Maywood.) 233:463-474.

127. Wu T, Wang XJ, Tian W, Jaramillo MC, Lau A and Zhang DD (2014) Poly(ADP-ribose) polymerase-1 modulates Nrf2-dependent transcription. Free Radic.Biol.Med. 67:69-80.

128. Sun Z, Chin YE and Zhang DD (2009) Acetylation of Nrf2 by p300/CBP augments promoter-specific DNA binding of Nrf2 during the antioxidant response. Mol.Cell Biol. 29:2658-2672.

129. Braun S, Hanselmann C, Gassmann MG, auf dem KU, Born-Berclaz C, Chan K, Kan YW and Werner S (2002) Nrf2 transcription factor, a novel target of keratinocyte growth factor action which regulates gene expression and inflammation in the healing skin wound. Mol.Cell Biol. 22:5492-5505.

130. Heath WR and Carbone FR (2013) The skin-resident and migratory immune system in steady state and memory: innate lymphocytes, dendritic cells and T cells. Nat.Immunol. 14:978-985.

131. van den Bogaard EH, Bergboer JG, Vonk-Bergers M, van Vlijmen-Willems IM, Hato SV, van der Valk PG, Schroder JM, Joosten I, Zeeuwen PL and Schalkwijk J (2013) Coal tar induces AHR-dependent skin barrier repair in atopic dermatitis. J.Clin.Invest 123:917-927.

132. Pi J, Diwan BA, Sun Y, Liu J, Qu W, He Y, Styblo M and Waalkes MP (2008) Arsenic-induced malignant transformation of human keratinocytes: involvement of Nrf2. Free Radic.Biol.Med. 45:651-658.

133. Chun KS, Kundu J, Kundu JK and Surh YJ (2014) Targeting Nrf2-Keap1 signaling for chemoprevention of skin carcinogenesis with bioactive phytochemicals. Toxicol.Lett. 229:73-84.

134. Aggarwal BB and Shishodia S (2006) Molecular targets of dietary agents for prevention and therapy of cancer. Biochem.Pharmacol. 71:1397-1421.

135. Li W, Liu H, Zhou JS, Cao JF, Zhou XB, Choi AM, Chen ZH and Shen HH (2012) Caveolin-1 inhibits expression of antioxidant enzymes through direct interaction with nuclear erythroid 2 p45-related factor-2 (Nrf2). J.Biol.Chem. 287:20922-20930.

136. Kang BY, Kim S, Lee KH, Lee YS, Hong I, Lee MO, Min D, Chang I, Hwang JS, Park JS, Kim DH and Kim BG (2008) Transcriptional profiling in human HaCaT keratinocytes in response to kaempferol and identification of potential transcription factors for regulating differential gene expression. Exp.Mol.Med. 40:208-219.

137. Wlaschek M, Tantcheva-Poor I, Naderi L, Ma W, Schneider LA, Razi-Wolf Z, Schuller J and Scharffetter-Kochanek K (2001) Solar UV irradiation and dermal photoaging. J.Photochem.Photobiol.B 63:41-51.

138. Kwak MK, Itoh K, Yamamoto M and Kensler TW (2002) Enhanced expression of the transcription factor Nrf2 by cancer chemopreventive agents: role of antioxidant response element-like sequences in the nrf2 promoter. Mol.Cell Biol. 22:2883-2892.

139. Kohle C and Bock KW (2007) Coordinate regulation of Phase I and II xenobiotic metabolisms by the Ah receptor and Nrf2. Biochem.Pharmacol. 73:1853-1862.

140. Schafer M, Willrodt AH, Kurinna S, Link AS, Farwanah H, Geusau A, Gruber F, Sorg O, Huebner AJ, Roop DR, Sandhoff K, Saurat JH, Tschachler E, Schneider MR, Langbein L, Bloch W, Beer HD and Werner S (2014) Activation of Nrf2 in keratinocytes causes chloracne (MADISH)-like skin disease in mice. EMBO Mol.Med. 6:442-457.

141. Tang L, Li J, Lin X, Wu W, Kang K and Fu W (2012) Oxidation levels differentially impact melanocytes: low versus high concentration of hydrogen peroxide promotes melanin synthesis and melanosome transfer. Dermatology 224:145-153.

142. Kokot A, Metze D, Mouchet N, Galibert MD, Schiller M, Luger TA and Bohm M (2009) Alpha-melanocyte-stimulating hormone counteracts the suppressive effect of UVB on Nrf2 and Nrf-dependent gene expression in human skin. Endocrinology 150:3197-3206.

143. Schafer M, Dutsch S, auf dem KU, Navid F, Schwarz A, Johnson DA, Johnson JA and Werner S (2010) Nrf2 establishes a glutathione-mediated gradient of UVB cytoprotection in the epidermis. Genes Dev. 24:1045-1058.

144. Lee DJ, Kang DH, Choi M, Choi YJ, Lee JY, Park JH, Park YJ, Lee KW and Kang SW (2013) Peroxiredoxin-2 represses melanoma metastasis by increasing E-Cadherin/beta-Catenin complexes in adherens junctions. Cancer Res. 73:4744-4757.

145. Natarajan VT, Singh A, Kumar AA, Sharma P, Kar HK, Marrot L, Meunier JR, Natarajan K, Rani R and Gokhale RS (2010) Transcriptional upregulation of Nrf2-dependent phase II detoxification genes in the involved epidermis of vitiligo vulgaris. J.Invest Dermatol. 130:2781-2789.

146. Kannan S and Jaiswal AK (2006) Low and high dose UVB regulation of transcription factor NF-E2-related factor 2. Cancer Res. 66:8421-8429.

147. Ernst IM, Wagner AE, Schuemann C, Storm N, Hoppner W, Doring F, Stocker A and Rimbach G (2011) Allyl-, butyl- and phenylethyl-isothiocyanate activate Nrf2 in cultured fibroblasts. Pharmacol.Res. 63:233-240.

148. Fourtounis J, Wang IM, Mathieu MC, Claveau D, Loo T, Jackson AL, Peters MA, Therien AG, Boie Y and Crackower MA (2012) Gene expression profiling following NRF2 and KEAP1 siRNA knockdown in human lung fibroblasts identifies CCL11/Eotaxin-1 as a novel NRF2 regulated gene. Respir.Res. 13:92.

149. Song K, Peng S, Sun Z, Li H and Yang R (2011) Curcumin suppresses TGF-beta signaling by inhibition of TGIF degradation in scleroderma fibroblasts. Biochem.Biophys.Res.Commun. 411:821-825.

150. Patterson AD, Carlson BA, Li F, Bonzo JA, Yoo MH, Krausz KW, Conrad M, Chen C, Gonzalez FJ and Hatfield DL (2013) Disruption of thioredoxin reductase 1 protects mice from acute acetaminophen-induced hepatotoxicity through enhanced NRF2 activity. Chem.Res.Toxicol. 26:1088-1096.

151. Hayashi A, Suzuki H, Itoh K, Yamamoto M and Sugiyama Y (2003) Transcription factor Nrf2 is required for the constitutive and inducible expression of multidrug resistance-associated protein 1 in mouse embryo fibroblasts. Biochem.Biophys.Res.Commun. 310:824-829.

152. Han W, Ming M, Zhao R, Pi J, Wu C and He YY (2012) Nrf1 CNC-bZIP protein promotes cell survival and nucleotide excision repair through maintaining glutathione homeostasis. J Biol Chem 287:18788-95. doi: 10.1074/jbc.M112.363614

153. Mimura J and Fujii-Kuriyama Y (2003) Functional role of AhR in the expression of toxic effects by TCDD. Biochim.Biophys.Acta 1619:263-268.

154. Pollet M, Shaik S, Mescher M, Frauenstein K, Tigges J, Braun SA, Sondenheimer K, Kaveh M, Bruhs A, Meller S, Homey B, Schwarz A, Esser C, Douki T, Vogel CFA, Krutmann J and Haarmann-Stemmann T (2018) The AHR represses nucleotide excision repair and apoptosis and contributes to UV-induced skin carcinogenesis. Cell Death & Differentiation 25:1823-1836. doi: 10.1038/s41418-018-0160-1

155. Kimura S, Warabi E, Yanagawa T, Ma D, Itoh K, Ishii Y, Kawachi Y and Ishii T (2009) Essential role of Nrf2 in keratinocyte protection from UVA by quercetin. Biochem.Biophys.Res.Commun. 387:109-114.

156. Takei K, Hashimoto-Hachiya A, Takahara M, Tsuji G, Nakahara T and Furue M (2015) Cynaropicrin attenuates UVB-induced oxidative stress via the AhR-Nrf2-Nqo1 pathway. Toxicol.Lett. 234:74-80.

157. Choi HK, Kim DH, Kim JW, Ngadiran S, Sarmidi MR and Park CS (2010) Labisia pumila extract protects skin cells from photoaging caused by UVB irradiation. J.Biosci.Bioeng. 109:291-296.

158. Grandjean-Laquerriere A, Gangloff SC, Le NR, Trentesaux C, Hornebeck W and Guenounou M (2002) Relative contribution of NF-kappaB and AP-1 in the modulation by curcumin and pyrrolidine dithiocarbamate of the UVB-induced cytokine expression by keratinocytes. Cytokine 18:168-177.

159. Svobodova A, Zdarilova A and Vostalova J (2009) Lonicera caerulea and Vaccinium myrtillus fruit polyphenols protect HaCaT keratinocytes against UVB-induced phototoxic stress and DNA damage. J.Dermatol.Sci. 56:196-204.

160. Gottlieb TM, Leal JF, Seger R, Taya Y and Oren M (2002) Cross-talk between Akt, p53 and Mdm2: possible implications for the regulation of apoptosis. Oncogene 21:1299-1303.

161. Ferguson-Yates BE, Li H, Dong TK, Hsiao JL and Oh DH (2008) Impaired repair of cyclobutane pyrimidine dimers in human keratinocytes deficient in p53 and p63. Carcinogenesis 29:70-75.

162. Manning BD and Cantley LC (2007) AKT/PKB signaling: navigating downstream. Cell 129:1261-1274.

163. Liu Q, Turner KM, Alfred Yung WK, Chen K and Zhang W (2014) Role of AKT signaling in DNA repair and clinical response to cancer therapy. Neuro.Oncol. 16:1313-1323.

164. Garrington TP and Johnson GL (1999) Organization and regulation of mitogen-activated protein kinase signaling pathways. Curr.Opin.Cell Biol. 11:211-218.

165. Lin YW, Chuang SM and Yang JL (2003) Persistent activation of ERK1/2 by lead acetate increases nucleotide excision repair synthesis and confers anti-cytotoxicity and anti-mutagenicity. Carcinogenesis 24:53-61.

166. Lewis TS, Hunt JB, Aveline LD, Jonscher KR, Louie DF, Yeh JM, Nahreini TS, Resing KA and Ahn NG (2000) Identification of novel MAP kinase pathway signaling targets by functional proteomics and mass spectrometry. Mol.Cell 6:1343-1354.

167. Wang QE, Han C, Zhao R, Wani G, Zhu Q, Gong L, Battu A, Racoma I, Sharma N and Wani AA (2013) p38. Nucleic Acids Res. 41:1722-1733.

168. Chaiprasongsuk A, Lohakul J, Soontrapa K, Sampattavanich S, Akarasereenont P and Panich U (2017) Activation of Nrf2 Reduces UVA-Mediated MMP-1 Upregulation via MAPK/AP-1 Signaling Cascades: The Photoprotective Effects of Sulforaphane and Hispidulin. J.Pharmacol.Exp.Ther. 360:388-398.

169. Guerra B and Issinger OG (2008) Protein kinase CK2 in human diseases. Curr Med Chem 15:1870-86.

170. Tawfic S, Yu S, Wang H, Faust R, Davis A and Ahmed K (2001) Protein kinase CK2 signal in neoplasia. Histol Histopathol 16:573-82. doi: 10.14670/hh-16.573

171. Miyata Y (2009) Protein kinase CK2 in health and disease: CK2: the kinase controlling the Hsp90 chaperone machinery. Cell Mol Life Sci 66:1840-9. doi: 10.1007/s00018-009-9152-0

172. Piazza FA, Ruzzene M, Gurrieri C, Montini B, Bonanni L, Chioetto G, Di Maira G, Barbon F, Cabrelle A, Zambello R, Adami F, Trentin L, Pinna LA and Semenzato G (2006) Multiple myeloma cell survival relies on high activity of protein kinase CK2. Blood 108:1698-707. doi: 10.1182/blood-2005-11-013672

173. Duncan JS, Turowec JP, Duncan KE, Vilk G, Wu C, Luscher B, Li SS, Gloor GB and Litchfield DW (2011) A peptide-based target screen implicates the protein kinase CK2 in the global regulation of caspase signaling. Sci Signal 4:ra30. doi: 10.1126/scisignal.2001682

174. Mottet D, Ruys SP, Demazy C, Raes M and Michiels C (2005) Role for casein kinase 2 in the regulation of HIF-1 activity. Int J Cancer 117:764-74. doi: 10.1002/ijc.21268

175. Becherel OJ, Jakob B, Cherry AL, Gueven N, Fusser M, Kijas AW, Peng C, Katyal S, McKinnon PJ, Chen J, Epe B, Smerdon SJ, Taucher-Scholz G and Lavin MF (2010) CK2 phosphorylation-dependent interaction between aprataxin and MDC1 in the DNA damage response. Nucleic Acids Res 38:1489-503. doi: 10.1093/nar/gkp1149

176. Loizou JI, El-Khamisy SF, Zlatanou A, Moore DJ, Chan DW, Qin J, Sarno S, Meggio F, Pinna LA and Caldecott KW (2004) The protein kinase CK2 facilitates repair of chromosomal DNA single-strand breaks. Cell 117:17-28.

177. Parsons JL, Dianova, II, Finch D, Tait PS, Strom CE, Helleday T and Dianov GL (2010) XRCC1 phosphorylation by CK2 is required for its stability and efficient DNA repair. DNA Repair (Amst) 9:835-41. doi: 10.1016/j.dnarep.2010.04.008

178. Siddiqui-Jain A, Bliesath J, Macalino D, Omori M, Huser N, Streiner N, Ho CB, Anderes K, Proffitt C, O'Brien SE, Lim JK, Von Hoff DD, Ryckman DM, Rice WG and Drygin D (2012) CK2 inhibitor CX-4945 suppresses DNA repair

response triggered by DNA-targeted anticancer drugs and augments efficacy: mechanistic rationale for drug combination therapy. Mol Cancer Ther 11:994-1005. doi: 10.1158/1535-7163.mct-11-0613

179. Im J and Nho RS (2019) Fibroblasts from patients with idiopathic pulmonary fibrosis are resistant to cisplatin-induced cell death via enhanced CK2-dependent XRCC1 activity. Apoptosis. doi: 10.1007/s10495-019-01529-9

180. Halliday GM, Bock VL, Moloney FJ and Lyons JG (2009) SWI/SNF: a chromatin-remodelling complex with a role in carcinogenesis. Int.J.Biochem.Cell Biol. 41:725-728.

181. Thompson BC, Surjana D, Halliday GM and Damian DL (2014) Nicotinamide enhances repair of ultraviolet radiation-induced DNA damage in primary melanocytes. Exp.Dermatol. 23:509-511.

182. Park J, Halliday GM, Surjana D and Damian DL (2010) Nicotinamide prevents ultraviolet radiation-induced cellular energy loss. Photochem.Photobiol. 86:942-948.

183. Jacobson EL, Shieh WM and Huang AC (1999) Mapping the role of NAD metabolism in prevention and treatment of carcinogenesis. Mol.Cell Biochem. 193:69-74.

184. Thompson BC, Halliday GM and Damian DL (2015) Nicotinamide enhances repair of arsenic and ultraviolet radiation-induced DNA damage in HaCaT keratinocytes and ex vivo human skin. PLoS.One. 10:e0117491.

185. Fang EF, Scheibye-Knudsen M, Brace LE, Kassahun H, SenGupta T, Nilsen H, Mitchell JR, Croteau DL and Bohr VA (2014) Defective mitophagy in XPA via PARP-1 hyperactivation and NAD(+)/SIRT1 reduction. Cell 157:882-896. doi: 10.1016/j.cell.2014.03.026

186. Altenhofer S, Radermacher KA, Kleikers PW, Wingler K and Schmidt HH (2015) Evolution of NADPH Oxidase Inhibitors: Selectivity and Mechanisms for Target Engagement. Antioxid.Redox.Signal. 23:406-427.

187. Hosseini M, Mahfouf W, Serrano-Sanchez M, Raad H, Harfouche G, Bonneu M, Claverol S, Mazurier F, Rossignol R, Taieb A and Rezvani HR (2015) Premature skin aging features rescued by inhibition of NADPH oxidase activity in XPC-deficient mice. J.Invest Dermatol. 135:1108-1118.

188. Raad H, Serrano-Sanchez M, Harfouche G, Mahfouf W, Bortolotto D, Bergeron V, Kasraian Z, Dousset L, Hosseini M, Taieb A and Rezvani HR (2017) NADPH Oxidase-1 Plays a Key Role in Keratinocyte Responses to UV Radiation and UVB-Induced Skin Carcinogenesis. J.Invest Dermatol.

189. Ha SJ, Lee J, Park J, Kim YH, Lee NH, Kim YE, Song KM, Chang PS, Jeong CH and Jung SK (2018) Syringic acid prevents skin carcinogenesis via regulation of NoX and EGFR signaling. Biochem Pharmacol 154:435-445. doi: 10.1016/j.bcp.2018.06.007

190. Guillermo-Lagae R, Deep G, Ting H, Agarwal C and Agarwal R (2015) Silibinin enhances the repair of ultraviolet B-induced DNA damage by activating p53-dependent nucleotide excision repair mechanism in human dermal fibroblasts. Oncotarget. 6:39594-39606.

191. Katiyar SK, Mantena SK and Meeran SM (2011) Silymarin protects epidermal keratinocytes from ultraviolet radiation-induced apoptosis and DNA damage by nucleotide excision repair mechanism. PLoS.One. 6:e21410.

192. Izzotti A, D'Agostini F, Bagnasco M, Scatolini L, Rovida A, Balansky RM, Cesarone CF and De FS (1994) Chemoprevention of carcinogen-DNA adducts and chronic degenerative diseases. Cancer Res. 54:1994s-1998s.

193. Feng D, Huang H, Yang Y, Yan T, Jin Y, Cheng X and Cui L (2015) Ameliorative effects of N-acetylcysteine on fluoride-induced oxidative stress and DNA damage in male rats' testis. Mutat.Res.Genet.Toxicol.Environ.Mutagen. 792:35-45.

194. Duzenli U, Altun Z, Olgun Y, Aktas S, Pamukoglu A, Cetinayak HO, Bayrak AF and Olgun L (2019) Role of N-acetyl cysteine and acetyl-l-carnitine combination treatment on DNA-damage-related genes induced by radiation in HEI-OC1 cells. Int J Radiat Biol 95:298-306. doi: 10.1080/09553002.2019.1547847

195. Choi HR, Shin JW, Na JI, Nam KM, Lee HS and Park KC (2015) Novel Antioxidant Tripeptide "ACQ" Can Prevent UV-Induced Cell Death and Preserve the Number of Epidermal Stem Cells. Oxid.Med.Cell Longev. 2015:359740.

196. Rodriguez JA, Nespereira B, Perez-Ilzarbe M, Eguinoa E and Paramo JA (2005) Vitamins C and E prevent endothelial VEGF and VEGFR-2 overexpression induced by porcine hypercholesterolemic LDL. Cardiovasc.Res. 65:665-673.

197. Farris PK (2005) Topical vitamin C: a useful agent for treating photoaging and other dermatologic conditions. Dermatol.Surg. 31:814-817.

198. Petruk G, Raiola A, Del GR, Barone A, Frusciante L, Rigano MM and Monti DM (2016) An ascorbic acid-enriched tomato genotype to fight UVA-induced oxidative stress in normal human keratinocytes. J.Photochem.Photobiol.B 163:284-289.

199. Stojanovic S, Sprinz H and Brede O (2001) Efficiency and mechanism of the antioxidant action of trans-resveratrol and its analogues in the radical liposome oxidation. Arch.Biochem.Biophys. 391:79-89.

200. Jagdeo J, Adams L, Lev-Tov H, Sieminska J, Michl J and Brody N (2010) Dose-dependent antioxidant function of resveratrol demonstrated via modulation of reactive oxygen species in normal human skin fibroblasts in vitro. J.Drugs Dermatol. 9:1523-1526.

201. Karunasinghe N, Ryan J, Tuckey J, Masters J, Jamieson M, Clarke LC, Marshall JR and Ferguson LR (2004) DNA stability and serum selenium levels in a high-risk group for prostate cancer. Cancer Epidemiol.Biomarkers Prev. 13:391-397.

202. Seo YR, Sweeney C and Smith ML (2002) Selenomethionine induction of DNA repair response in human fibroblasts. Oncogene 21:3663-3669.

203. Bera S, De RV, Rachidi W and Diamond AM (2013) Does a role for selenium in DNA damage repair explain apparent controversies in its use in chemoprevention? Mutagenesis 28:127-134.

204. Katiyar SK, Vaid M, van SH and Meeran SM (2010) Green tea polyphenols prevent UV-induced immunosuppression by rapid repair of DNA damage and enhancement of nucleotide excision repair genes. Cancer Prev.Res.(Phila) 3:179-189.

205. Meeran SM, Akhtar S and Katiyar SK (2009) Inhibition of UVB-induced skin tumor development by drinking green tea polyphenols is mediated through DNA repair and subsequent inhibition of inflammation. J.Invest Dermatol. 129:1258-1270.

206. Vaid M, Sharma SD and Katiyar SK (2010) Proanthocyanidins inhibit photocarcinogenesis through enhancement of DNA repair and xeroderma pigmentosum group A-dependent mechanism. Cancer Prev.Res.(Phila) 3:1621-1629.

207. Thiele JJ (2001) Oxidative targets in the stratum corneum. A new basis for antioxidative strategies. Skin Pharmacol.Appl.Skin Physiol 14 Suppl 1:87-91.

208. Ritter EF, Axelrod M, Minn KW, Eades E, Rudner AM, Serafin D and Klitzman B (1997) Modulation of ultraviolet light-induced epidermal damage: beneficial effects of tocopherol. Plast.Reconstr.Surg. 100:973-980.

209. Krol ES, Kramer-Stickland KA and Liebler DC (2000) Photoprotective actions of topically applied vitamin E. Drug Metab Rev. 32:413-420.

210. Alli E, Solow-Cordero D, Casey SC and Ford JM (2014) Therapeutic targeting of BRCA1-mutated breast cancers with agents that activate DNA repair. Cancer Res. 74:6205-6215.

211. Mazouzi A, Battistini F, Moser SC, Ferreira da SJ, Wiedner M, Owusu M, Lardeau CH, Ringler A, Weil B, Neesen J, Orozco M, Kubicek S and Loizou JI (2017) Repair of UV-Induced DNA Damage Independent of Nucleotide Excision Repair Is Masked by MUTYH. Mol.Cell 68:797-807.

212. Pawlowska E, Wysokinski D and Blasiak J (2016) Nucleotide Excision Repair and Vitamin D--Relevance for Skin Cancer Therapy. Int J Mol Sci 17:372. doi: 10.3390/ijms17040372

213. Le May N, Egly JM and Coin F (2010) True lies: the double life of the nucleotide excision repair factors in transcription and DNA repair. J Nucleic Acids 2010. doi: 10.4061/2010/616342

214. Aune GJ, Furuta T and Pommier Y (2002) Ecteinascidin 743: a novel anticancer drug with a unique mechanism of action. Anticancer Drugs 13:545-55.

215. Barret JM, Cadou M and Hill BT (2002) Inhibition of nucleotide excision repair and sensitisation of cells to DNA cross-linking anticancer drugs by F 11782, a novel fluorinated epipodophylloid. Biochem Pharmacol 63:251-8.

216. Rai KR, Peterson BL, Appelbaum FR, Kolitz J, Elias L, Shepherd L, Hines J, Threatte GA, Larson RA, Cheson BD and Schiffer CA (2000) Fludarabine compared with chlorambucil as primary therapy for chronic lymphocytic leukemia. N Engl J Med 343:1750-7. doi: 10.1056/nejm200012143432402

217. Bulgar AD, Snell M, Donze JR, Kirkland EB, Li L, Yang S, Xu Y, Gerson SL and Liu L (2010) Targeting base excision repair suggests a new therapeutic strategy of fludarabine for the treatment of chronic lymphocytic leukemia. Leukemia 24:1795-9. doi: 10.1038/leu.2010.166

218. Yamauchi T, Kawai Y and Ueda T (2002) Inhibition of nucleotide excision repair by fludarabine in normal lymphocytes in vitro, measured by the alkaline single cell gel electrophoresis (Comet) assay. Jpn J Cancer Res 93:567-73.

219. Wang Q, Fan S, Eastman A, Worland PJ, Sausville EA and O'Connor PM (1996) UCN-01: a potent abrogator of G2 checkpoint function in cancer cells with disrupted p53. J Natl Cancer Inst 88:956-65.

220. Jiang H and Yang LY (1999) Cell cycle checkpoint abrogator UCN-01 inhibits DNA repair: association with attenuation of the interaction of XPA and ERCC1 nucleotide excision repair proteins. Cancer Res 59:4529-34.

221. Tessitore A, Cicciarelli G, Del VF, Gaggiano A, Verzella D, Fischietti M, Vecchiotti D, Capece D, Zazzeroni F and Alesse E (2014) MicroRNAs in the DNA Damage/Repair Network and Cancer. Int.J.Genomics 2014:820248.

222. Crosby ME, Kulshreshtha R, Ivan M and Glazer PM (2009) MicroRNA regulation of DNA repair gene expression in hypoxic stress. Cancer Res. 69:1221-1229.

223. Josson S, Sung SY, Lao K, Chung LW and Johnstone PA (2008) Radiation modulation of microRNA in prostate cancer cell lines. Prostate 68:1599-1606.

224. Friboulet L, Barrios-Gonzales D, Commo F, Olaussen KA, Vagner S, Adam J, Goubar A, Dorvault N, Lazar V, Job B, Besse B, Validire P, Girard P, Lacroix L, Hasmats J, Dufour F, Andre F and Soria JC (2011) Molecular Characteristics of ERCC1-Negative versus ERCC1-Positive Tumors in Resected NSCLC. Clin.Cancer Res. 17:5562-5572.

225. Lehmann AR, McGibbon D and Stefanini M (2011) Xeroderma pigmentosum. Orphanet.J.Rare.Dis. 6:70.

226. Brash DE, Rudolph JA, Simon JA, Lin A, McKenna GJ, Baden HP, Halperin AJ and Ponten J (1991) A role for sunlight in skin cancer: UV-induced p53 mutations in squamous cell carcinoma. Proc.Natl.Acad.Sci.U.S.A 88:10124-10128.

227. Niedernhofer LJ (2008) Nucleotide excision repair deficient mouse models and neurological disease. DNA Repair (Amst) 7:1180-1189.

228. Soufir N, Ged C, Bourillon A, Austerlitz F, Chemin C, Stary A, Armier J, Pham D, Khadir K, Roume J, Hadj-Rabia S, Bouadjar B, Taieb A, de VH, Benchiki H, Grandchamp B and Sarasin A (2010) A prevalent mutation with founder effect in xeroderma pigmentosum group C from north Africa. J.Invest Dermatol. 130:1537-1542.

229. Fu L, Xu X, Ren R, Wu J, Zhang W, Yang J, Ren X, Wang S, Zhao Y, Sun L, Yu Y, Wang Z, Yang Z, Yuan Y, Qiao J, Izpisua Belmonte JC, Qu J and Liu GH (2016) Modeling xeroderma pigmentosum associated neurological pathologies with patients-derived iPSCs. Protein Cell 7:210-221.

230. Venema J, van HA, Karcagi V, Natarajan AT, van Zeeland AA and Mullenders LH (1991) Xeroderma pigmentosum complementation group C cells remove pyrimidine dimers selectively from the transcribed strand of active genes. Mol.Cell Biol. 11:4128-4134.

231. Itoh T, Linn S, Ono T and Yamaizumi M (2000) Reinvestigation of the classification of five cell strains of xeroderma pigmentosum group E with reclassification of three of them. J.Invest Dermatol. 114:1022-1029.

232. Hwang BJ, Toering S, Francke U and Chu G (1998) p48 Activates a UV-damaged-DNA binding factor and is defective in xeroderma pigmentosum group E cells that lack binding activity. Mol.Cell Biol. 18:4391-4399.

233. de Laat WL, Sijbers AM, Odijk H, Jaspers NG and Hoeijmakers JH (1998) Mapping of interaction domains between human repair proteins ERCC1 and XPF. Nucleic Acids Res. 26:4146-4152.

234. States JC, McDuffie ER, Myrand SP, McDowell M and Cleaver JE (1998) Distribution of mutations in the human xeroderma pigmentosum group A gene and their relationships to the functional regions of the DNA damage recognition protein. Hum.Mutat. 12:103-113.

235. Shell SM and Zou Y (2008) Other proteins interacting with XP proteins. Adv.Exp.Med.Biol. 637:103-112.

236. Shah P and He YY (2015) Molecular regulation of UV-induced DNA repair. Photochem.Photobiol. 91:254-264.

237. Robles AI and Harris CC (2001) p53-mediated apoptosis and genomic instability diseases. Acta Oncol. 40:696-701.

238. Itin PH, Sarasin A and Pittelkow MR (2001) Trichothiodystrophy: update on the sulfur-deficient brittle hair syndromes. J.Am.Acad.Dermatol. 44:891-920.

239. Thorel F, Constantinou A, Dunand-Sauthier I, Nouspikel T, Lalle P, Raams A, Jaspers NG, Vermeulen W, Shivji MK, Wood RD and Clarkson SG (2004) Definition of a short region of XPG necessary for TFIIH interaction and stable recruitment to sites of UV damage. Mol.Cell Biol. 24:10670-10680.

240. Bessho T (1999) Nucleotide excision repair 3' endonuclease XPG stimulates the activity of base excision repairenzyme thymine glycol DNA glycosylase. Nucleic Acids Res. 27:979-983.

241. Barreto G, Schafer A, Marhold J, Stach D, Swaminathan SK, Handa V, Doderlein G, Maltry N, Wu W, Lyko F and Niehrs C (2007) Gadd45a promotes epigenetic gene activation by repair-mediated DNA demethylation. Nature 445:671-675.

242. Cooper PK, Nouspikel T, Clarkson SG and Leadon SA (1997) Defective transcription-coupled repair of oxidative base damage in Cockayne syndrome patients from XP group G. Science 275:990-993.

243. Park CH, Bessho T, Matsunaga T and Sancar A (1995) Purification and characterization of the XPF-ERCC1 complex of human DNA repair excision nuclease. J.Biol.Chem. 270:22657-22660.

244. Volker M, Mone MJ, Karmakar P, van HA, Schul W, Vermeulen W, Hoeijmakers JH, van DR, van Zeeland AA and Mullenders LH (2001) Sequential assembly of the nucleotide excision repair factors in vivo. Mol.Cell 8:213-224.

245. Masutani C, Kusumoto R, Yamada A, Dohmae N, Yokoi M, Yuasa M, Araki M, Iwai S, Takio K and Hanaoka F (1999) The XPV (xeroderma pigmentosum variant) gene encodes human DNA polymerase eta. Nature 399:700-704.

246. Cleaver JE (1972) Xeroderma pigmentosum: variants with normal DNA repair and normal sensitivity to ultraviolet light. J.Invest Dermatol. 58:124-128.

247. Krokan HE and Bjoras M (2013) Base excision repair. Cold Spring Harb.Perspect.Biol. 5:a012583.

248. Shimizu Y, Iwai S, Hanaoka F and Sugasawa K (2003) Xeroderma pigmentosum group C protein interacts physically and functionally with thymine DNA glycosylase. EMBO J. 22:164-173.

249. de Melo JT, de Souza Timoteo AR, Lajus TB, Brandao JA, de Souza-Pinto NC, Menck CF, Campalans A, Radicella JP, Vessoni AT, Muotri AR and Agnez-Lima LF (2016) XPC deficiency is related to APE1 and OGG1 expression and function. Mutat.Res. 784-785:25-33.

250. Rezvani HR, Ged C, Bouadjar B, de VH and Taieb A (2008) Catalase overexpression reduces UVB-induced apoptosis in a human xeroderma pigmentosum reconstructed epidermis. Cancer Gene Ther. 15:241-251.

251. Rezvani HR, Kim AL, Rossignol R, Ali N, Daly M, Mahfouf W, Bellance N, Taieb A, de VH, Mazurier F and Bickers DR (2011) XPC silencing in normal human keratinocytes triggers metabolic alterations that drive the formation of squamous cell carcinomas. J.Clin.Invest 121:195-211.

252. Meira LB, Reis AM, Cheo DL, Nahari D, Burns DK and Friedberg EC (2001) Cancer predisposition in mutant mice defective in multiple genetic pathways: uncovering important genetic interactions. Mutat.Res. 477:51-58.

253. Wu YH, Wu TC, Liao JW, Yeh KT, Chen CY and Lee H (2010) p53 dysfunction by xeroderma pigmentosum group C defects enhance lung adenocarcinoma metastasis via increased MMP1 expression. Cancer Res. 70:10422-10432.

254. Colton SL, Xu XS, Wang YA and Wang G (2006) The involvement of ataxia-telangiectasia mutated protein activation in nucleotide excision repair-facilitated cell survival with cisplatin treatment. J.Biol.Chem. 281:27117-27125.

255. Ray A, Mir SN, Wani G, Zhao Q, Battu A, Zhu Q, Wang QE and Wani AA (2009) Human SNF5/INI1, a component of the human SWI/SNF chromatin remodeling complex, promotes nucleotide excision repair by influencing ATM recruitment and downstream H2AX phosphorylation. Mol.Cell Biol. 29:6206-6219.

256. Kim ST, Lim DS, Canman CE and Kastan MB (1999) Substrate specificities and identification of putative substrates of ATM kinase family members. J.Biol.Chem. 274:37538-37543.

257. Le May N, Mota-Fernandes D, Velez-Cruz R, Iltis I, Biard D and Egly JM (2010) NER factors are recruited to active promoters and facilitate chromatin modification for transcription in the absence of exogenous genotoxic attack. Mol Cell 38:54-66. doi: 10.1016/j.molcel.2010.03.004

258. Bidon B, Iltis I, Semer M, Nagy Z, Larnicol A, Cribier A, Benkirane M, Coin F, Egly JM and Le May N (2018) XPC is an RNA polymerase II cofactor recruiting ATAC to promoters by interacting with E2F1. Nat Commun 9:2610. doi: 10.1038/s41467-018-05010-0

259. Muotri AR, Marchetto MC, Zerbini LF, Libermann TA, Ventura AM, Sarasin A and Menck CF (2002) Complementation of the DNA repair deficiency in human xeroderma pigmentosum group a and C cells by recombinant adenovirus-mediated gene transfer. Hum Gene Ther 13:1833-44. doi: 10.1089/104303402760372936

260. Arnaudeau-Bégard C, Brellier F, Chevallier-Lagente O, Hoeijmakers J, Bernerd F, Sarasin A and Magnaldo T (2003) Genetic correction of DNA repair-deficient/cancer-prone xeroderma pigmentosum group C keratinocytes. Hum Gene Ther 14:983-96. doi: 10.1089/104303403766682241

261. Magnaldo T (2004) Xeroderma pigmentosum: from genetics to hopes and realities of cutaneous gene therapy. Expert Opin Biol Ther 4:169-79. doi: 10.1517/14712598.4.2.169

262. Zahid S and Brownell I (2008) Repairing DNA damage in xeroderma pigmentosum: T4N5 lotion and gene therapy. J Drugs Dermatol 7:405-8.

263. Helalat SH, Moradi M, Heidari H, Rezaei F, Yarmohamadi M, Sayadi M, Dadashkhan S and Eydi F (2020) Investigating the efficacy of UVSE protein at repairing CPD and 6-4 pp DNA damages in human cells. J Photochem Photobiol B 205:111843. doi: 10.1016/j.jphotobiol.2020.111843

264. Yang W (2011) Surviving the sun: repair and bypass of DNA UV lesions. Protein Sci 20:1781-9. doi: 10.1002/pro.723

265. Jia P and Zhao Z (2017) Impacts of somatic mutations on gene expression: an association perspective. Brief.Bioinform. 18:413-425.

266. Fitzgerald DM and Rosenberg SM (2019) What is mutation? A chapter in the series: How microbes "jeopardize" the modern synthesis. PLoS Genet 15:e1007995. doi: 10.1371/journal.pgen.1007995

267. Guarente L (1993) Synthetic enhancement in gene interaction: a genetic tool come of age. Trends Genet. 9:362-366.

268. Forsburg SL (2001) The art and design of genetic screens: yeast. Nat.Rev.Genet. 2:659-668.

269. Hodgkin J (2005) Genetic suppression. WormBook.:1-13.

270. van LJ, Pons C, Mellor JC, Yamaguchi TN, Friesen H, Koschwanez J, Usaj MM, Pechlaner M, Takar M, Usaj M, VanderSluis B, Andrusiak K, Bansal P, Baryshnikova A, Boone CE, Cao J, Cote A, Gebbia M, Horecka G, Horecka I, Kuzmin E, Legro N, Liang W, van LN, McNee M, San Luis BJ, Shaeri F, Shuteriqi E, Sun S, Yang L, Youn JY, Yuen M,

Costanzo M, Gingras AC, Aloy P, Oostenbrink C, Murray A, Graham TR, Myers CL, Andrews BJ, Roth FP and Boone C (2016) Exploring genetic suppression interactions on a global scale. Science 354.

271. Sahu AD, J SL, Wang Z, Zhang G, Iglesias-Bartolome R, Tian T, Wei Z, Miao B, Nair NU, Ponomarova O, Friedman AA, Amzallag A, Moll T, Kasumova G, Greninger P, Egan RK, Damon LJ, Frederick DT, Jerby-Arnon L, Wagner A, Cheng K, Park SG, Robinson W, Gardner K, Boland G, Hannenhalli S, Herlyn M, Benes C, Flaherty K, Luo J, Gutkind JS and Ruppin E (2019) Genome-wide prediction of synthetic rescue mediators of resistance to targeted and immunotherapy. Mol Syst Biol 15:e8323. doi: 10.15252/msb.20188323

272. Galarneau G, Palmer CD, Sankaran VG, Orkin SH, Hirschhorn JN and Lettre G (2010) Fine-mapping at three loci known to affect fetal hemoglobin levels explains additional genetic variation. Nat Genet 42:1049-51. doi: 10.1038/ng.707

273. Flannick J, Thorleifsson G, Beer NL, Jacobs SB, Grarup N, Burtt NP, Mahajan A, Fuchsberger C, Atzmon G, Benediktsson R, Blangero J, Bowden DW, Brandslund I, Brosnan J, Burslem F, Chambers J, Cho YS, Christensen C, Douglas DA, Duggirala R, Dymek Z, Farjoun Y, Fennell T, Fontanillas P, Forsen T, Gabriel S, Glaser B, Gudbjartsson DF, Hanis C, Hansen T, Hreidarsson AB, Hveem K, Ingelsson E, Isomaa B, Johansson S, Jorgensen T, Jorgensen ME, Kathiresan S, Kong A, Kooner J, Kravic J, Laakso M, Lee JY, Lind L, Lindgren CM, Linneberg A, Masson G, Meitinger T, Mohlke KL, Molven A, Morris AP, Potluri S, Rauramaa R, Ribel-Madsen R, Richard AM, Rolph T, Salomaa V, Segre AV, Skarstrand H, Steinthorsdottir V, Stringham HM, Sulem P, Tai ES, Teo YY, Teslovich T, Thorsteinsdottir U, Trimmer JK, Tuomi T, Tuomilehto J, Vaziri-Sani F, Voight BF, Wilson JG, Boehnke M, McCarthy MI, Njolstad PR, Pedersen O, Groop L, Cox DR, Stefansson K and Altshuler D (2014) Loss-of-function mutations in SLC30A8 protect against type 2 diabetes. Nat Genet 46:357-63. doi: 10.1038/ng.2915

274. Sharma S and Petsalaki E (2018) Application of CRISPR-Cas9 Based Genome-Wide Screening Approaches to Study Cellular Signalling Mechanisms. Int.J.Mol.Sci. 19.

275. Willingham AT, Deveraux QL, Hampton GM and Aza-Blanc P (2004) RNAi and HTS: exploring cancer by systematic loss-of-function. Oncogene 23:8392-8400.

276. Zambrowicz BP, Abuin A, Ramirez-Solis R, Richter LJ, Piggott J, BeltrandelRio H, Buxton EC, Edwards J, Finch RA, Friddle CJ, Gupta A, Hansen G, Hu Y, Huang W, Jaing C, Key BW, Jr., Kipp P, Kohlhauff B, Ma ZQ, Markesich D, Payne R, Potter DG, Qian N, Shaw J, Schrick J, Shi ZZ, Sparks MJ, Van SI, Vogel P, Walke W, Xu N, Zhu Q, Person C and Sands AT (2003) Wnk1 kinase deficiency lowers blood pressure in mice: a gene-trap screen to identify potential targets for therapeutic intervention. Proc.Natl.Acad.Sci.U.S.A 100:14109-14114.

277. Schulte J, Sepp KJ, Wu C, Hong P and Littleton JT (2011) High-content chemical and RNAi screens for suppressors of neurotoxicity in a Huntington's disease model. PLoS.One. 6:e23841.

278. Manson MD (2000) Allele-specific suppression as a tool to study protein-protein interactions in bacteria. Methods 20:18-34.

279. Prelich G (1999) Suppression mechanisms: themes from variations. Trends Genet. 15:261-266.

280. Novelli J, Ahmed S and Hodgkin J (2004) Gene interactions in Caenorhabditis elegans define DPY-31 as a candidate procollagen C-proteinase and SQT-3/ROL-4 as its predicted major target. Genetics 168:1259-73. doi: 10.1534/genetics.104.027953

281. Lissemore JL, Currie PD, Turk CM and Maine EM (1993) Intragenic dominant suppressors of glp-1, a gene essential for cell-signaling in Caenorhabditis elegans, support a role for cdc10/SWI6/ankyrin motifs in GLP-1 function. Genetics 135:1023-34.

282. Erdeniz N, Dudley S, Gealy R, Jinks-Robertson S and Liskay RM (2005) Novel PMS1 alleles preferentially affect the repair of primer strand loops during DNA replication. Mol.Cell Biol. 25:9221-9231.

283. Rogalski TM, Gilchrist EJ, Mullen GP and Moerman DG (1995) Mutations in the unc-52 gene responsible for body wall muscle defects in adult Caenorhabditis elegans are located in alternatively spliced exons. Genetics 139:159-69.

284. Aoki Y, Nakamura A, Yokota T, Saito T, Okazawa H, Nagata T and Takeda S (2010) In-frame dystrophin following exon 51-skipping improves muscle pathology and function in the exon 52-deficient mdx mouse. Mol Ther 18:1995-2005. doi: 10.1038/mt.2010.186

285. Glass RE, Nene V and Hunter MG (1982) Informational suppression as a tool for the investigation of gene structure and function. Biochem.J. 203:1-13.

286. Beier H and Grimm M (2001) Misreading of termination codons in eukaryotes by natural nonsense suppressor tRNAs. Nucleic Acids Res. 29:4767-4782.

287. Buvoli M, Buvoli A and Leinwand LA (2000) Suppression of nonsense mutations in cell culture and mice by multimerized suppressor tRNA genes. Mol.Cell Biol. 20:3116-3124.

288. O'Neill VA, Eden FC, Pratt K and Hatfield DL (1985) A human opal suppressor tRNA gene and pseudogene. J.Biol.Chem. 260:2501-2508.

289. Raimondeau E, Bufton JC and Schaffitzel C (2018) New insights into the interplay between the translation machinery and nonsense-mediated mRNA decay factors. Biochem.Soc.Trans. 46:503-512.

290. Finkel RS (2010) Read-through strategies for suppression of nonsense mutations in Duchenne/ Becker muscular dystrophy: aminoglycosides and ataluren (PTC124). J.Child Neurol. 25:1158-1164.

291. Hodgkin J, Papp A, Pulak R, Ambros V and Anderson P (1989) A new kind of informational suppression in the nematode Caenorhabditis elegans. Genetics 123:301-313.

292. Spartz AK, Herman RK and Shaw JE (2004) SMU-2 and SMU-1, Caenorhabditis elegans homologs of mammalian spliceosome-associated proteins RED and fSAP57, work together to affect splice site choice. Mol.Cell Biol. 24:6811-6823.

293. Slavov N, Semrau S, Airoldi E, Budnik B and van OA (2015) Differential Stoichiometry among Core Ribosomal Proteins. Cell Rep. 13:865-873.

294. Kabir MA and Sherman F (2008) Overexpressed ribosomal proteins suppress defective chaperonins in Saccharomyces cerevisiae. FEMS Yeast Res. 8:1236-1244.

295. Magtanong L, Ho CH, Barker SL, Jiao W, Baryshnikova A, Bahr S, Smith AM, Heisler LE, Choy JS, Kuzmin E, Andrusiak K, Kobylianski A, Li Z, Costanzo M, Basrai MA, Giaever G, Nislow C, Andrews B and Boone C (2011) Dosage suppression genetic interaction networks enhance functional wiring diagrams of the cell. Nat.Biotechnol. 29:505-511.

296. Baryshnikova A, Costanzo M, Kim Y, Ding H, Koh J, Toufighi K, Youn JY, Ou J, San Luis BJ, Bandyopadhyay S, Hibbs M, Hess D, Gingras AC, Bader GD, Troyanskaya OG, Brown GW, Andrews B, Boone C and Myers CL (2010) Quantitative analysis of fitness and genetic interactions in yeast on a genome scale. Nat.Methods 7:1017-1024.

297. Avery L and Wasserman S (1992) Ordering gene function: the interpretation of epistasis in regulatory hierarchies. Trends Genet. 8:312-316.

298. Park W, Mosteller RD and Broek D (1997) Identification of a dominant-negative mutation in the yeast CDC25 guanine nucleotide exchange factor for Ras. Oncogene 14:831-836.

299. Jones SN, Roe AE, Donehower LA and Bradley A (1995) Rescue of embryonic lethality in Mdm2-deficient mice by absence of p53. Nature 378:206-208.

300. Tye BK and Sawyer S (2000) The hexameric eukaryotic MCM helicase: building symmetry from nonidentical parts. J.Biol.Chem. 275:34833-34836.

301. Shuman HA and Beckwith J (1979) Escherichia coli K-12 mutants that allow transport of maltose via the beta-galactoside transport system. J.Bacteriol. 137:365-373.

302. Maruyama IN, Miller DM and Brenner S (1989) Myosin heavy chain gene amplification as a suppressor mutation in Caenorhabditis elegans. Mol.Gen.Genet. 219:113-118.

303. Liu G, Yong MY, Yurieva M, Srinivasan KG, Liu J, Lim JS, Poidinger M, Wright GD, Zolezzi F, Choi H, Pavelka N and Rancati G (2015) Gene Essentiality Is a Quantitative Property Linked to Cellular Evolvability. Cell 163:1388-1399.

304. Jarvik J and Botstein D (1975) Conditional-lethal mutations that suppress genetic defects in morphogenesis by altering structural proteins. Proc.Natl.Acad.Sci.U.S.A 72:2738-2742.

305. Prelich G (2012) Gene overexpression: uses, mechanisms, and interpretation. Genetics 190:841-854.

306. Szamecz B, Boross G, Kalapis D, Kovacs K, Fekete G, Farkas Z, Lazar V, Hrtyan M, Kemmeren P, Groot Koerkamp MJ, Rutkai E, Holstege FC, Papp B and Pal C (2014) The genomic landscape of compensatory evolution. PLoS.Biol. 12:e1001935.

307. Menne TF, Goyenechea B, Sanchez-Puig N, Wong CC, Tonkin LM, Ancliff PJ, Brost RL, Costanzo M, Boone C and Warren AJ (2007) The Shwachman-Bodian-Diamond syndrome protein mediates translational activation of ribosomes in yeast. Nat.Genet. 39:486-495.

308. Hashimoto K, Nakashima N, Ohara T, Maki S and Sugino A (1998) The second subunit of DNA polymerase III (delta) is encoded by the HYS2 gene in Saccharomyces cerevisiae. Nucleic Acids Res. 26:477-485.

309. Booher R and Beach D (1987) Interaction between cdc13+ and cdc2+ in the control of mitosis in fission yeast; dissociation of the G1 and G2 roles of the cdc2+ protein kinase. EMBO J. 6:3441-3447.

310. Sandrock TM, O'Dell JL and Adams AE (1997) Allele-specific suppression by formation of new protein-protein interactions in yeast. Genetics 147:1635-1642.

311. Motter AE, Gulbahce N, Almaas E and Barabási AL (2008) Predicting synthetic rescues in metabolic networks. Mol Syst Biol 4:168. doi: 10.1038/msb.2008.1

312. Echeverri CJ and Perrimon N (2006) High-throughput RNAi screening in cultured cells: a user's guide. Nat.Rev.Genet. 7:373-384.

313. Zender L, Spector MS, Xue W, Flemming P, Cordon-Cardo C, Silke J, Fan ST, Luk JM, Wigler M, Hannon GJ, Mu D, Lucito R, Powers S and Lowe SW (2006) Identification and validation of oncogenes in liver cancer using an integrative oncogenomic approach. Cell 125:1253-1267.

314. Xue HY, Ji LJ, Gao AM, Liu P, He JD and Lu XJ (2016) CRISPR-Cas9 for medical genetic screens: applications and future perspectives. J.Med.Genet. 53:91-97.

315. Moder M, Velimezi G, Owusu M, Mazouzi A, Wiedner M, Ferreira da SJ, Robinson-Garcia L, Schischlik F, Slavkovsky R, Kralovics R, Schuster M, Bock C, Ideker T, Jackson SP, Menche J and Loizou JI (2017) Parallel genome-wide screens identify synthetic viable interactions between the BLM helicase complex and Fanconi anemia. Nat.Commun. 8:1238.

316. Deans AJ and West SC (2009) FANCM connects the genome instability disorders Bloom's Syndrome and Fanconi Anemia. Mol.Cell 36:943-953.

317. Lam JK, Chow MY, Zhang Y and Leung SW (2015) siRNA Versus miRNA as Therapeutics for Gene Silencing. Mol.Ther.Nucleic Acids 4:e252.

318. Yang D, Buchholz F, Huang Z, Goga A, Chen CY, Brodsky FM and Bishop JM (2002) Short RNA duplexes produced by hydrolysis with Escherichia coli RNase III mediate effective RNA interference in mammalian cells. Proc.Natl.Acad.Sci.U.S.A 99:9942-9947.

319. Graat HC, Witlox MA, Schagen FH, Kaspers GJ, Helder MN, Bras J, Schaap GR, Gerritsen WR, Wuisman PI and van Beusechem VW (2006) Different susceptibility of osteosarcoma cell lines and primary cells to treatment with oncolytic adenovirus and doxorubicin or cisplatin. Br.J.Cancer 94:1837-1844.

320. Moffat J, Grueneberg DA, Yang X, Kim SY, Kloepfer AM, Hinkle G, Piqani B, Eisenhaure TM, Luo B, Grenier JK, Carpenter AE, Foo SY, Stewart SA, Stockwell BR, Hacohen N, Hahn WC, Lander ES, Sabatini DM and Root DE (2006) A lentiviral RNAi library for human and mouse genes applied to an arrayed viral high-content screen. Cell 124:1283-1298.

321. Brummelkamp TR, Fabius AW, Mullenders J, Madiredjo M, Velds A, Kerkhoven RM, Bernards R and Beijersbergen RL (2006) An shRNA barcode screen provides insight into cancer cell vulnerability to MDM2 inhibitors. Nat.Chem.Biol. 2:202-206.

322. Iorns E, Lord CJ, Turner N and Ashworth A (2007) Utilizing RNA interference to enhance cancer drug discovery. Nat.Rev.Drug Discov. 6:556-568.

323. Luo J, Emanuele MJ, Li D, Creighton CJ, Schlabach MR, Westbrook TF, Wong KK and Elledge SJ (2009) A genome-wide RNAi screen identifies multiple synthetic lethal interactions with the Ras oncogene. Cell 137:835-48. doi: 10.1016/j.cell.2009.05.006

324. Springer PS (2000) Gene traps: tools for plant development and genomics. Plant Cell 12:1007-1020.

325. Carette JE, Guimaraes CP, Wuethrich I, Blomen VA, Varadarajan M, Sun C, Bell G, Yuan B, Muellner MK, Nijman SM, Ploegh HL and Brummelkamp TR (2011) Global gene disruption in human cells to assign genes to phenotypes by deep sequencing. Nat.Biotechnol. 29:542-546.

326. Velimezi G, Robinson-Garcia L, Munoz-Martinez F, Wiegant WW, Ferreira da Silva J, Owusu M, Moder M, Wiedner M, Rosenthal SB, Fisch KM, Moffat J, Menche J, van Attikum H, Jackson SP and Loizou JI (2018) Map of synthetic rescue interactions for the Fanconi anemia DNA repair pathway identifies USP48. Nat Commun 9:2280. doi: 10.1038/s41467-018-04649-z

327. Swinney DC and Anthony J (2011) How were new medicines discovered? Nat.Rev.Drug Discov. 10:507-519.

328. Kaelin WG, Jr. (2005) The concept of synthetic lethality in the context of anticancer therapy. Nat.Rev.Cancer 5:689-698.

329. Lee J and Bogyo M (2013) Target deconvolution techniques in modern phenotypic profiling. Curr.Opin.Chem.Biol. 17:118-126.

330. Qu D, Weygant N, Yao J, Chandrakesan P, Berry WL, May R, Pitts K, Husain S, Lightfoot S, Li M, Wang TC, An G, Clendenin C, Stanger BZ and Houchen CW (2019) Overexpression of DCLK1-AL Increases Tumor Cell Invasion, Drug Resistance, and KRAS Activation and Can Be Targeted to Inhibit Tumorigenesis in Pancreatic Cancer. J Oncol 2019:6402925. doi: 10.1155/2019/6402925

331. Hinterndorfer M and Zuber J (2019) Functional-genetic approaches to understanding drug response and resistance. Curr Opin Genet Dev 54:41-47. doi: 10.1016/j.gde.2019.03.003

332. Morgan-Lappe S, Woods KW, Li Q, Anderson MG, Schurdak ME, Luo Y, Giranda VL, Fesik SW and Leverson JD (2006) RNAi-based screening of the human kinome identifies Akt-cooperating kinases: a new approach to designing efficacious multitargeted kinase inhibitors. Oncogene 25:1340-1348.

333. Rathert P, Roth M, Neumann T, Muerdter F, Roe JS, Muhar M, Deswal S, Cerny-Reiterer S, Peter B, Jude J, Hoffmann T, Boryń Ł M, Axelsson E, Schweifer N, Tontsch-Grunt U, Dow LE, Gianni D, Pearson M, Valent P, Stark A, Kraut N, Vakoc CR and Zuber J (2015) Transcriptional plasticity promotes primary and acquired resistance to BET inhibition. Nature 525:543-547. doi: 10.1038/nature14898

334. Pan D, Kobayashi A, Jiang P, Ferrari de Andrade L, Tay RE, Luoma AM, Tsoucas D, Qiu X, Lim K, Rao P, Long HW, Yuan GC, Doench J, Brown M, Liu XS and Wucherpfennig KW (2018) A major chromatin regulator determines resistance of tumor cells to T cell-mediated killing. Science 359:770-775. doi: 10.1126/science.aao1710

335. Bigenzahn JW, Collu GM, Kartnig F, Pieraks M, Vladimer GI, Heinz LX, Sedlyarov V, Schischlik F, Fauster A, Rebsamen M, Parapatics K, Blomen VA, Muller AC, Winter GE, Kralovics R, Brummelkamp TR, Mlodzik M and Superti-Furga G (2018) LZTR1 is a regulator of RAS ubiquitination and signaling. Science 362:1171-1177. doi: 10.1126/science.aap8210

336. Miyamoto DT, Zheng Y, Wittner BS, Lee RJ, Zhu H, Broderick KT, Desai R, Fox DB, Brannigan BW, Trautwein J, Arora KS, Desai N, Dahl DM, Sequist LV, Smith MR, Kapur R, Wu CL, Shioda T, Ramaswamy S, Ting DT, Toner M, Maheswaran S and Haber DA (2015) RNA-Seq of single prostate CTCs implicates noncanonical Wnt signaling in antiandrogen resistance. Science 349:1351-6. doi: 10.1126/science.aab0917

337. Livak KJ and Schmittgen TD (2001) Analysis of relative gene expression data using real-time quantitative PCR and the 2(-Delta Delta C(T)) Method. Methods 25:402-8. doi: 10.1006/meth.2001.1262

338. Fayyad N, Kobaisi F, Beal D, Mahfouf W, Ged C, Morice-Picard F, Fayyad-Kazan M, Fayyad-Kazan H, Badran B, Rezvani HR and Rachidi W (2020) Xeroderma Pigmentosum C (XPC) Mutations in Primary Fibroblasts Impair Base Excision Repair Pathway and Increase Oxidative DNA Damage. Front Genet 11:561687. doi: 10.3389/fgene.2020.561687

339. Matallana-Surget S, Meador JA, Joux F and Douki T (2008) Effect of the GC content of DNA on the distribution of UVB-induced bipyrimidine photoproducts. Photochem Photobiol Sci 7:794-801. doi: 10.1039/b719929e

340. Douki T and Cadet J (2001) Individual determination of the yield of the main UV-induced dimeric pyrimidine photoproducts in DNA suggests a high mutagenicity of CC photolesions. Biochemistry 40:2495-501. doi: 10.1021/bi0022543

341. Kuschal C, DiGiovanna JJ, Khan SG, Gatti RA and Kraemer KH (2013) Repair of UV photolesions in xeroderma pigmentosum group C cells induced by translational readthrough of premature termination codons. Proc Natl Acad Sci U S A 110:19483-8. doi: 10.1073/pnas.1312088110

342. Flowing Software version 2.5.1 bPT, Turku Centre for Biotechnology University of Turku, Finland, In colaboration with Turku Bioimaging. URL http://flowingsoftware.btk.fi/.

343. R Core Team (2018). R: A language and environment for statistical computing. R Foundation for Statistical Computing V, Austria. URL http://www.R-project.org/.

344. Feuerstein TJ, Rossner R and Schumacher M (1997) How to express an effect mean as percentage of a control mean? J Pharmacol Toxicol Methods 37:187-90. doi: 10.1016/s1056-8719(97)00017-8

345. van Oijen MG, Medema RH, Slootweg PJ and Rijksen G (1998) Positivity of the proliferation marker Ki-67 in noncycling cells. Am J Clin Pathol 110:24-31. doi: 10.1093/ajcp/110.1.24

346. Tu Y, Ji C, Yang B, Yang Z, Gu H, Lu CC, Wang R, Su ZL, Chen B, Sun WL, Xia JP, Bi ZG and He L (2013) DNA-dependent protein kinase catalytic subunit (DNA-PKcs)-SIN1 association mediates ultraviolet B (UVB)-induced Akt Ser-473 phosphorylation and skin cell survival. Mol Cancer 12:172. doi: 10.1186/1476-4598-12-172

347. Yogosawa S and Yoshida K (2018) Tumor suppressive role for kinases phosphorylating p53 in DNA damage-induced apoptosis. Cancer Sci 109:3376-3382. doi: 10.1111/cas.13792

348. Boopathy GTK and Hong W (2019) Role of Hippo Pathway-YAP/TAZ Signaling in Angiogenesis. Front Cell Dev Biol 7:49. doi: 10.3389/fcell.2019.00049

349. Yu X, Long YC and Shen HM (2015) Differential regulatory functions of three classes of phosphatidylinositol and phosphoinositide 3-kinases in autophagy. Autophagy 11:1711-28. doi: 10.1080/15548627.2015.1043076

350. Black JO (2016) Xeroderma Pigmentosum. Head Neck Pathol 10:139-44. doi: 10.1007/s12105-016-0707-8

351. Mouret S, Charveron M, Favier A, Cadet J and Douki T (2008) Differential repair of UVB-induced cyclobutane pyrimidine dimers in cultured human skin cells and whole human skin. DNA Repair (Amst) 7:704-12. doi: 10.1016/j.dnarep.2008.01.005

352. Courdavault S, Baudouin C, Charveron M, Canguilhem B, Favier A, Cadet J and Douki T (2005) Repair of the three main types of bipyrimidine DNA photoproducts in human keratinocytes exposed to UVB and UVA radiations. DNA Repair (Amst) 4:836-44. doi: 10.1016/j.dnarep.2005.05.001

353. Pushpakom S, Iorio F, Eyers PA, Escott KJ, Hopper S, Wells A, Doig A, Guilliams T, Latimer J, McNamee C, Norris A, Sanseau P, Cavalla D and Pirmohamed M (2019) Drug repurposing: progress, challenges and recommendations. Nature Reviews Drug Discovery 18:41-58. doi: 10.1038/nrd.2018.168

354. Basu AK (2018) DNA Damage, Mutagenesis and Cancer. Int J Mol Sci 19. doi: 10.3390/ijms19040970

355. Einav S, Gerber D, Bryson PD, Sklan EH, Elazar M, Maerkl SJ, Glenn JS and Quake SR (2008) Discovery of a hepatitis C target and its pharmacological inhibitors by microfluidic affinity analysis. Nat Biotechnol 26:1019-27. doi: 10.1038/nbt.1490

356. Richter JM, Schaefer M and Hill K (2014) Clemizole hydrochloride is a novel and potent inhibitor of transient receptor potential channel TRPC5. Mol Pharmacol 86:514-21. doi: 10.1124/mol.114.093229

357. Kashfi SM, Golmohammadi M, Behboudi F, Nazemalhosseini-Mojarad E and Zali MR (2013) MUTYH the base excision repair gene family member associated with colorectal cancer polyposis. Gastroenterol Hepatol Bed Bench 6:S1-s10.

358. Kobaisi F, Fayyad N, Sulpice E, Badran B, Fayyad-Kazan H, Rachidi W and Gidrol X (2020) High-throughput synthetic rescue for exhaustive characterization of suppressor mutations in human genes. Cellular and Molecular Life Sciences. doi: 10.1007/s00018-020-03519-6

359. Cadet J and Wagner JR (2013) DNA base damage by reactive oxygen species, oxidizing agents, and UV radiation. Cold Spring Harb Perspect Biol 5. doi: 10.1101/cshperspect.a012559

360. Vivanco I and Sawyers CL (2002) The phosphatidylinositol 3-Kinase AKT pathway in human cancer. Nat Rev Cancer 2:489-501. doi: 10.1038/nrc839

361. Sarbassov DD, Guertin DA, Ali SM and Sabatini DM (2005) Phosphorylation and regulation of Akt/PKB by the rictor-mTOR complex. Science 307:1098-101. doi: 10.1126/science.1106148

362. Persad S, Attwell S, Gray V, Delcommenne M, Troussard A, Sanghera J and Dedhar S (2000) Inhibition of integrin-linked kinase (ILK) suppresses activation of protein kinase B/Akt and induces cell cycle arrest and apoptosis of PTEN-mutant prostate cancer cells. Proc Natl Acad Sci U S A 97:3207-12. doi: 10.1073/pnas.060579697

363. Wang QE, Han C, Zhao R, Wani G, Zhu Q, Gong L, Battu A, Racoma I, Sharma N and Wani AA (2013) p38 MAPK- and Akt-mediated p300 phosphorylation regulates its degradation to facilitate nucleotide excision repair. Nucleic Acids Res 41:1722-33. doi: 10.1093/nar/gks1312

364. Perelman B, Dafni N, Naiman T, Eli D, Yaakov M, Feng TL, Sinha S, Weber G, Khodaei S, Sancar A, Dotan I and Canaani D (1997) Molecular cloning of a novel human gene encoding a 63-kDa protein and its sublocalization within the 11q13 locus. Genomics 41:397-405. doi: 10.1006/geno.1997.4623

365. Yang Y, He S, Wang Q, Li F, Kwak MJ, Chen S, O'Connell D, Zhang T, Pirooz SD, Jeon YH, Chimge NO, Frenkel B, Choi Y, Aldrovandi GM, Oh BH, Yuan Z and Liang C (2016) Autophagic UVRAG Promotes UV-Induced Photolesion Repair by Activation of the CRL4(DDB2) E3 Ligase. Mol Cell 62:507-19. doi: 10.1016/j.molcel.2016.04.014

366. Zhao Z, Oh S, Li D, Ni D, Pirooz SD, Lee JH, Yang S, Lee JY, Ghozalli I, Costanzo V, Stark JM and Liang C (2012) A dual role for UVRAG in maintaining chromosomal stability independent of autophagy. Dev Cell 22:1001-16. doi: 10.1016/j.devcel.2011.12.027

ANNEX

SUPPLEMENTARY FIGURE

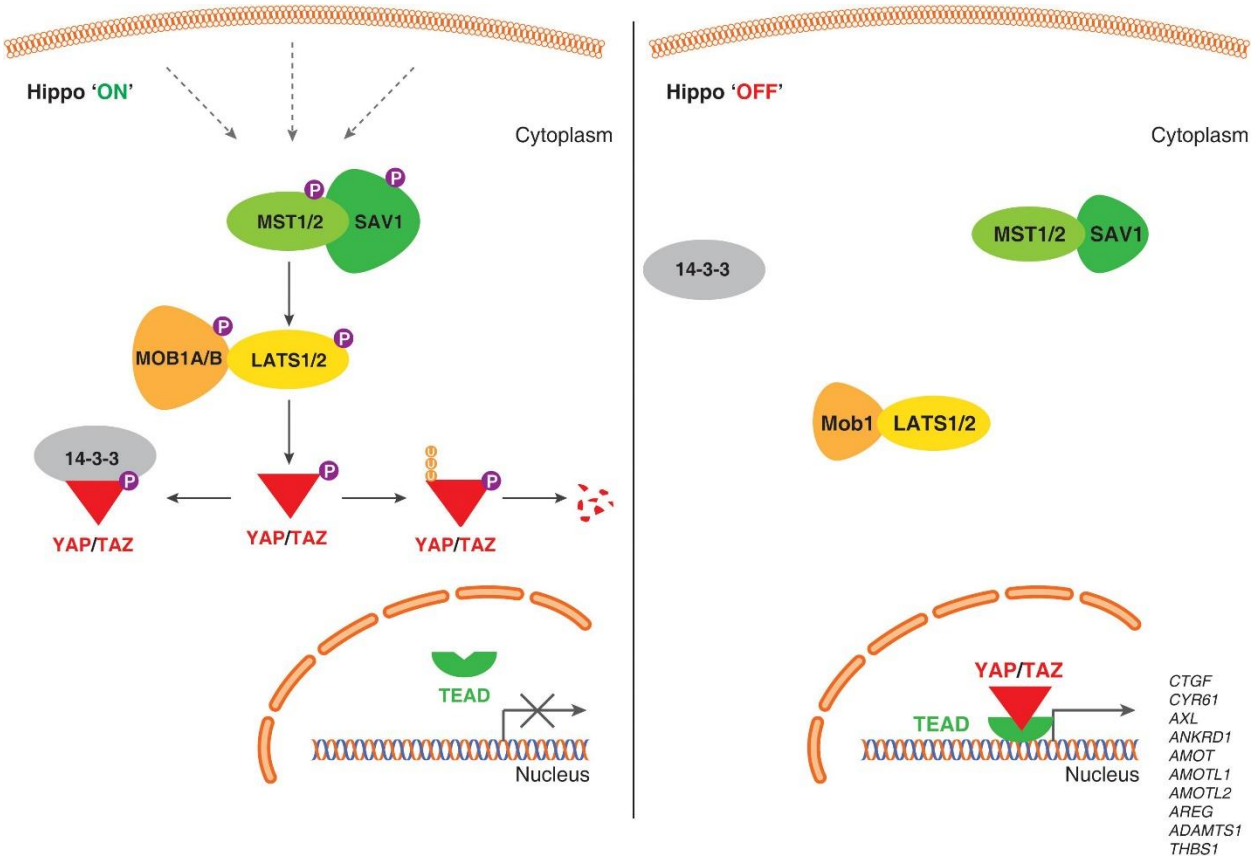

Supplementary Figure 1: Hippo pathway signaling cascade

Upon the activation of the Hippo pathway (left panel) several downstream proteins will become phosphorylated including sequentially the MST1/MST2, LATS1/LATS2 kinases and YAP/TAZ. Phosphorylation of the latter leads to the recruitment of 14-3-3 proteins to the YAP/TAZ complex leading to its cytoplasmic retention or proteolytic degradation. However, during the inactive hippo signaling (right panel) YAP/TAZ can freely localize to the nucleus in the absence of upstream phosphorylating signals. In the nucleus, YAP/TAZ complexes with TEADs transcription factor to regulate the expression of various genes essential for proliferation, survival and migration[348].

PUBLICATIONS

* Isoconazole and Clemizole Hydrochloride Partially Reverse the Xeroderma Pigmentosum C Phenotype

Farah Kobaisi [a, b], Eric Sulpice [a], Caroline Barette [d], Nour Fayyad [c], Marie-Odile Fauvarque[d], bassam Badran [b], Mohammad Fayyad-Kazan [b], Hussein Fayyad-Kazan [b], Xavier Gidrol [a] and Walid Rachidi [a]*

International Journal of Molecular Science, Published

https://www.mdpi.com/1422-0067/22/15/8156

* Xeroderma Pigmentosum C a valuable tool to decipher the signaling pathways in skin cancers

Ali Nasrallah, Nour Fayyad, **Farah Kobaisi**, Bassam Badran, Hussein Fayyad-Kazan, Mohammad Fayyad- Kazan, Michel Seve, Walid Rachidi

Oxidative Medicine and Cellular Longevity, Published

https://www.hindawi.com/journals/omcl/2021/6689403/

* Implication of Ultraviolet Irradiation in Photo-carcinogenesis

Farah Kobaisi [a, b], Eric Sulpice [a], Mohammad Fayyad-Kazan [b], Ali Nasrallah [a], Xavier Gidrol [a], Hussein Fayyad-Kazan [b] and Walid Rachidi [a]

Book Chapter, Published

https://videleaf.com/implication-of-ultraviolet-irradiation-in-photo-carcinogenesis/

*Link between Base Excision Repair (BER), Reactive Oxygen Species (ROS), and Cancer

Nour Fayyad[1], **Farah Kobaisi** [2,3], Mohammad Fayyad-Kazan[3] , Ali Nasrallah[2],

Hussein Fayyad-Kazan[3] and Walid Rachidi[2]

Book Chapter, Published

https://videleaf.com/link-between-base-excision-repair-ber-reactive-oxygen-species-ros-and-cancer/

* Xeroderma Pigmentosum C (XPC) mutations in primary fibroblasts impair base excision repair pathway and increase oxidative DNA damage.

Fayyad N.[*], **Kobaisi F**.[*], Beal D., Mahfouf W., GED C., Morice-picard F., Fayyad-kazan M., Fayyad-kazan H., Badran B., Reza-Rezvani H., Rachidi W.

Frontiers in Genetics, November 2020, https://pubmed.ncbi.nlm.nih.gov/33329698/

* High-throughput synthetic rescue for exhaustive characterization of suppressor mutations in human genes.

Farah Kobaisi et al. Journal of Cellular and Molecular Life Science, 2020 April 8, **Volume Cover**, https://pubmed.ncbi.nlm.nih.gov/32270227/

* RNA interference and Chemical-Based High Content Screening for the Normalization of XPC Phenotype: **Abstract Submission**
Kobaisi, F. et al., Journal of Investigative Dermatology, Volume 139, Issue 9, S306, https://doi.org/10.1016/j.jid.2019.07.450

* Signaling Pathways, Chemical and Biological Modulators of Nucleotide Excision Repair: The Faithful Shield against UV Genotoxicity.
Kobaisi F, Fayyad N, Rezvani HR, Fayyad-Kazan M, Sulpice E, Badran B, Fayyad-Kazan H, Gidrol X, Rachidi W.
Oxid Med Cell Longev. 2019 Aug 7; 2019:4654206. doi:10.1155/2019/4654206. eCollection 2019. Review.
https://www.ncbi.nlm.nih.gov/pubmed/31485292

To be completed article entitled:
* Kinome-RNAi based High content screening to identify targets for reversal of Xeroderma Pigmentosum C phenotype.

ORAL PRESENTATIONS AND POSTERS

*Invited Speaker for D2ONCO, CLARA, March 30, 2021

*CLARA March-April 2021-Lyon- e-Poster (Online Conf.)

* ESDR 18-21 September 2019- Bordeaux-Poster

* EDISCE scientific day-28 May 2019-UGA-Poster

* Biobeirut 8 25-26 October 2018- Lebanese University-Poster

* FRON 15 September 2018-USJ-Invited Speaker

PUBLISHED ARTICLE

International Journal of
Molecular Sciences

MDPI

Article

Isoconazole and Clemizole Hydrochloride Partially Reverse the Xeroderma Pigmentosum C Phenotype

Farah Kobaisi [1,2], Eric Sulpice [1], Caroline Barette [3], Nour Fayyad [4], Marie-Odile Fauvarque [3], Bassam Badran [2], Mohammad Fayyad-Kazan [2], Hussein Fayyad-Kazan [2], Xavier Gidrol [1] and Walid Rachidi [1,*]

1 Biomics, IRIG-BGE U1038, INSERM, Univ. Grenoble Alpes, 38000 Grenoble, France; farahkobaisi@gmail.com (F.K.); eric.sulpice@cea.fr (E.S.); xavier.gidrol@cea.fr (X.G.)
2 Laboratory of Cancer Biology and Molecular Immunology, Faculty of Sciences I, Lebanese University, Hadath, Lebanon; bassam.badran@ul.edu.lb (B.B.); mfayyadk@gmail.com (M.F.-K.); hfayyadk@gmail.com (H.F.-K.)
3 CEA/IRIG/Gen & Chem, Univ. Grenoble Alpes, 38000 Grenoble, France; caroline.barette@cea.fr (C.B.); marie-odile.fauvarque@cea.fr (M.-O.F.)
4 SYMMES/CIBEST UMR 5819 UGA-CNRS-CEA, IRIG/CEA-Grenoble, Univ. Grenoble Alpes, 38000 Grenoble, France; nour.fayyad.94@hotmail.com
* Correspondence: walid.rachidi@univ-grenoble-alpes.fr; Tel.: +33-438-785-011

Citation: Kobaisi, F.; Sulpice, E.; Barette, C.; Fayyad, N.; Fauvarque, M.-O.; Badran, B.; Fayyad-Kazan, M.; Fayyad-Kazan, H.; Gidrol, X.; Rachidi, W. Isoconazole and Clemizole Hydrochloride Partially Reverse the Xeroderma Pigmentosum C Phenotype. *Int. J. Mol. Sci.* **2021**, *22*, 8156. https://doi.org/10.3390/ijms22158156

Academic Editors: Giovanni Minervini, Castrense Savojardo and Emanuela Leonardi

Received: 22 June 2021
Accepted: 27 July 2021
Published: 29 July 2021

Abstract: Xeroderma Pigmentosum protein C (XPC) is involved in recognition and repair of bulky DNA damage such as lesions induced by Ultra Violet (UV) radiation. *XPC*-mutated cells are, therefore, photosensitive and accumulate UVB-induced pyrimidine dimers leading to increased cancer incidence. Here, we performed a high-throughput screen to identify chemicals capable of normalizing the XP-C phenotype (hyper-photosensitivity and accumulation of photoproducts). Fibroblasts from XP-C patients were treated with a library of approved chemical drugs. Out of 1280 tested chemicals, 16 showed ≥25% photo-resistance with RZscore above 2.6 and two drugs were able to favor repair of 6-4 pyrimidine pyrimidone photoproducts (6-4PP). Among these two compounds, Isoconazole could partially inhibit apoptosis of the irradiated cells especially when cells were post-treated directly after UV irradiation while Clemizole Hydrochloride-mediated increase in viability was dependent on both pre and post treatment. No synergistic effect was recorded following combined drug treatment and the compounds exerted no effect on the proliferative capacity of the cells post UV exposure. Amelioration of XP-C phenotype is a pave way towards understanding the accelerated skin cancer initiation in XP-C patients. Further examination is required to decipher the molecular mechanisms targeted by these two chemicals.

Keywords: XPC; DNA repair; UV; skin cancer; chemical screen; DNA damage

1. Introduction

The skin is a barrier that shields our body against pathogens, mechanical, chemical and physical stress and water loss [1]. However, direct contact with the environment makes it highly susceptible to different stimulants such as xenobiotics and UV radiation that can disrupt skin cells' metabolism [2]. Solar UV radiation is sub-classified into UVA (320–400 nm), UVB (280–320 nm) and UVC (200–280 nm). UVB irradiation, comprising 5% of solar UV radiation, generates direct damages to the DNA in the form of dimeric pyrimidine photoproducts: Cyclobutane pyrimidine dimers (CPD), 6-4 pyrimidine-pyrimidone photoproducts (6-4PP), and Dewar isomers [3]. UVB also contributes to the generation of double-strand breaks [4] via collapsing the replication forks at dimer sites [5] and triggering the formation of reactive oxygen species (ROS) [6]. The majority of UVB-induced mutations are C → T or CC → TT transitions [7]. In wild-type situation/healthy individuals, these lesions can be removed by a process termed nucleotide excision repair (NER). The latter is divided into global genome repair (GGR) occurring throughout the genome and

transcription-coupled repair (TCR) in actively transcribed genes [8]. GGR and TCR differ in their recognition step. On the one hand, XPC-Rad23B-Centrin2 and XPE -DDB1 are required for damage recognition in GGR. 6-4PP can be readily recognized by XPC while CPDs require also the cooperation of XPE-DDB1 [9]. On the other hand, CSA and CSB proteins are required for the recognition step of TCR. The following steps converge between the two sub-pathways where helicase XPD and XPB, as part of the TFIIH, are recruited to allow unwinding of the region around the damaged bases. XPA is then employed for damage verification while the nucleases XPF and XPG mediate the incision 5′ and 3′ to the damage allowing its removal, thus creating a gap. This gap is then filled by synthesizing damage-free DNA via polymerases and is eventually ligated, thus sealing the nick [10]. Failure of this repair mechanism leads to the accumulation of DNA damage, generation of mutations and cell transformation. Hereditary mutations in one of the NER proteins can hinder the repair process and lead to the generation of a wide range of diseases. Mutations in TCR sub-pathway underlie the origin of Cockayne Syndrome (CS) and UV-Sensitive Syndrome (UVSS), while patients with *Xeroderma Pigmentosum* (XP), trichothiodystrophy (TTD), XP-CS, XP-TTD and Cerebro-oculo-facio-skeletal Syndrome (COFS) are lacking proficiency in either GGR or both sub-pathways. Some of these diseases are characterized by an early onset of skin tumors. Several studies indicated that the origin of skin tumorigenesis could be mutations in different genes: *TP53* for squamous cell carcinoma [11], hedgehog signaling genes for basal cell carcinoma [12] and BRAF and RAS genes for melanoma [13]. It is thus an expected outcome for NER deficiency to be associated with skin carcinogenesis due to the mutagenic profile of the accumulated DNA damage and the UVB characteristic mutational profile seen in genes involved in carcinogenesis.

Xeroderma Pigmentosium C (XP-C) is a rare autosomal recessive genodermatosis. XP-C patients carry a mutation in the NER DNA damage recognition protein recognizing helix distortions opposite to pyrimidine dimers, notably 6-4PP distorting the helix at a higher angle compared to CPDs [14]. This mutation generates a diseased phenotype characterized by extreme photosensitivity and the accumulation of UV–DNA lesions. The onset of skin cancer is early in XP-C patients, often in childhood, who present a 2000 and 10,000 fold increase compared to healthy individuals in the risk of melanoma and non-melanoma skin cancers, respectively. Currently, there is no treatment for XP-C syndrome but only preventive measures including UV shielding and protection. In addition to its role in NER, XPC is also involved in several other DNA repair pathways or cellular mechanisms. For instance, XPC also participates in the initial phase of Base Excision Repair (BER), especially in the removal of oxidative DNA damage as in the case of XP-C deficient cells showing great sensitivity to the latter [15,16]. XPC has also a role in the regulation of cellular homeostasis. Silencing of XPC leads to a decrease in catalase activity leading to an increase in the levels of reactive oxygen species [17]. In addition, another study demonstrated that the accumulation of damage due to XPC deficiency increases the activation of DNA-dependent protein kinases ultimately leading to the activation of AKT1 [18]. The latter leads to the activation of NADPH oxidase1 (NOX1) which produces ROS [19]. XPC was also reported to be involved in transcription regulation. Bidon et al. demonstrated that XPC, even in the absence of DNA damage, interacts with E2F1 favoring the recruitment of ATAC (histone acetyl transferase) complex to gene promoters, thus conveying to XPC the title of RNA polymerase II cofactor [20]. These additional functions of XPC can explain the fact that XP-C patients also exhibit tumors in non-photo-exposed areas where the tumorigenesis is not linked directly to UVB induced DNA damage pointing out towards other tumorigenic pathways mediated via XPC [21].

In this study, we screened a library of approved FDA and EMA chemical drugs on XP-C patient-derived fibroblasts with the aim to identify compounds that could help in normalizing or at least ameliorating the XP-C-associated cell phenotype following UV exposure. We identified two drugs, isoconazole and clemizole hydrochloride, that can partially reverse this phenotype. This attempt of drug repurposing aims at the identification of new roles for existing drugs whose pharmacodynamics, pharmacokinetics and toxicology

characteristics are already well established, thus speeding up the benefits of the use of these drugs for a new therapeutic purpose for XP-C patients who do not have any treatment option presently.

2. Results

2.1. Characterization of XP-C and Wild-Type (WT) Fibroblasts Used in This Study

2.1.1. XPC Protein Expression Is Lost in XP-C Cells Compared to WT Cells

The expression of XPC protein was examined in both WT and XP-C cells immortalized from patient primary fibroblasts. Immuno-staining of both cells using an antibody against the XPC protein was carried out. In contrast to WT cells, XP-C cells showed a total absence of XPC protein (Figure 1a).

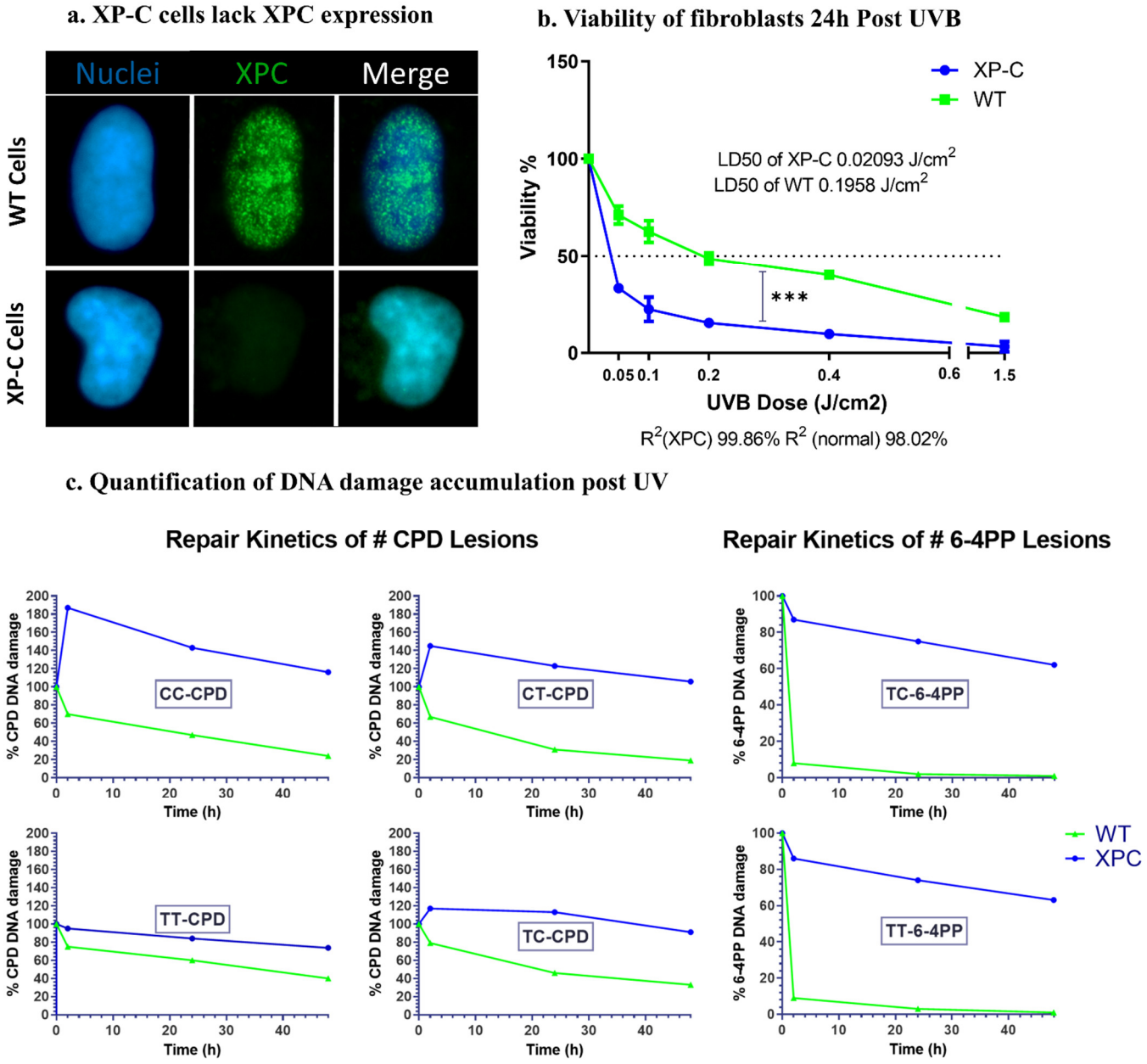

Figure 1. Characterization of XP-C and WT cells. (**a**) XP-C cells lack the expression of XPC protein. XP-C and WT cells were fixed and stained with anti-XPC antibody to analyze its differential expression in both cell lines. XP-C cells, unlike WT cells, do not manifest XPC protein expression in their nuclei. (**b**) Viability of fibroblasts 24 h post UVB. XP-C cells manifest significantly increased photosensitivity compared to WT cells. Both XP-C and WT cells were seeded in 96-well plates to be

irradiated at 80% confluency with increasing UVB doses, then their viability was quantified 24 h later by the incubation with PrestoBlue. XP-C cells show a sharper significant decrease in viability as a function of increased UVB dose compared to WT cells. Viability was calculated by means of percent of control with 100% control being non-irradiated cells. *** $p < 0.001$, unpaired *t*-test. Results presented are the mean of three technical replicates ± SEM. (**c**) Quantification of DNA damage accumulation post UV. WT cells manifest faster repair kinetics of both CPD and 6-4PP lesions post UV compared to impaired repair in XP-C cells. Both cell lines were subjected to UVB then incubated for different time points post UV. At each time points, cells were collected, their DNA extracted and digested to be then analyzed by LC-MS/MS. Four different CPD lesion types were quantified with TT-CPD being the most frequent. Normal cells show a decrease in the % of CPD lesions as a function of time signifying repair with different kinetics per lesion time. XP-C cells, however, manifest an increase in CPD lesion at 2 h post UV and continue to have a large amount of lesion % as time elapses, a sign of impaired repair. Two lesion types were quantified for 6-4PP with TC-6-4PP being more abundant. Similar to CPD, impaired repair is visualized in XP-C cells manifested by a slow decrease in lesion % as a function of time compared to the normal cells, which in contrast to CPD lesions show even faster repair for 6-4PP. CPD: cyclobutane pyrimidine dimer, 6-4PP: 6-4 photoproducts, WT: wild type, XP-C: Xeroderma Pigmentosum C, LD50: lethal dose 50, R^2: coefficient of determination.

2.1.2. Increased Photosensitivity of XP-C Cells in Response to UVB Irradiation Compared to WT Cells

To examine the photosensitivity of XP-C cells relative to WT, both kinds of cell lines were seeded until 80% confluency then subjected to increasing doses of UVB. Twenty-four hours after UV treatment, cell viability was recorded as a measurement of the cells' reducing capacity (Presto blue, Thermofisher Scientific, Waltham, MA, USA). Viability was normalized based on the calculation of the percentage of viability compared to the viability of control non-irradiated cells set as 100% viability. Both cell lines showed a decrease in viability as a function of increased UVB doses. XP-C cells were more photosensitive compared to the WT ones showing a sharper significant decrease in viability at each UVB dose ($p < 0.001$). The UVB dose leading to 50% of mortality was determined for both XP-C and wild-type cells (LD50). XP-C cells showed a much lower LD50 (about 0.02 J/cm^2) compared to WT cells (about 0.19 J/cm^2) (Figure 1b). These results confirm the strong sensitivity to UVB of XP-C cells used in this study as described in the other model [22].

2.1.3. Absence of XPC Impairs DNA Repair of UVB-Induced Lesions

XPC protein is essential for the lesion recognition step of GGR [23]. For that, we aimed to determine the effect of *XPC* mutation on the repair of lesions. The two major photoproducts generated after UVB exposure are CPDs and 6-4PPs that are formed between pyrimidine dimers, either TT, TC, CT or CC. The cells were seeded until 80% confluency then irradiated at 0.02 J/cm^2, corresponding to the previously determined XP-C LD50, then collected post UVB treatment at different time points. In order to monitor DNA lesions, DNA was extracted and digested to be analyzed by LC-MS/MS. For CPDs, the four different lesion types were quantified. WT cells showed a decrease in different CPDs lesions' amounts as a function of time to reach a minimum after 48 h indicating efficient repair of DNA damage, while in contrast, XP-C cells showed constant elevated amounts of lesions as a function of time (Figure 1c). It should be noted that not all lesions were present in the DNA in the same quantities: the majority of CPD lesions were of TT-CPD nature followed by TC-CPD, CT-CPD, while the least abundant lesion was CC-CPD in both kinds of cells. In addition, the repair kinetics in wild-type cells differed between lesion types with the fastest repair observed for the CT-CPD. Only the TT and TC lesions could be detected for the 6-4PPs, as the two remaining lesions were less frequent. 6-4PPs were repaired faster than CPD with total repair 24 h post UV in WT cells compared to the higher amount of lesions in XP-C cells. There were no discrepancies in the repair kinetics between the TT and TC 6-4PP lesions in normal cells (Figure 1c). Taken together, our results show that wild-type but not XP-C cells efficiently repair photoproducts resulting from UVB irradiation.

2.2. Primary Screen Identified 16 Candidate Compounds That Increase XP-C Cells Viability Post UVB Irradiation

To identify compounds that would correct the photosensitive phenotype of XP-C cells, we did set up a robotic assay in 96-well microplate to monitor cell viability after UVB irradiation (see methods and Supplementary Figure S1, see Supplementary Materials). The robustness of the assay was calculated as a Z′ factor [24] at various UVB doses on a Z′ plate including 48 bioactive controls mimicking the desired effect (here, non-irradiated protected XPC cells in DMSO) and 48 bioinactive controls (here, irradiated cells in DMSO). A library of 1280 FDA and EMA approved drugs (Prestwick Library) was then screened on XP-C cells at 10 μM for 24 h in duplicates using this assay. Briefly, following drug treatment, the cells were UVB irradiated at 0.05 J/cm^2 based on Z′ Factor calculation (Supplementary Figure S1), then post-treated with the same drugs and incubated at 37 °C for an additional 24 h period before the measurement of cell viability. In this setup, the effect of drug treatment on cell viability can be either preventive or curative to the UVB-induced damage. The bioactivity of each tested compound, signifying the drugs' beneficial effects on photo-resistance, was calculated by determining the fluorescence of each well with respect to the fluorescence of non-irradiated DMSO treated wells set as 100% (bioactive control) and irradiated DMSO treated wells set as 0% (bioinactive control). The robust Z score was also calculated per plate as an additional normalization technique [24]. The hit selection was based on two criteria: compounds that possess a bioactivity ≥25% and a robust Z score ≥2.5. Sixteen molecules were identified as primary hits on this basis and selected for further characterization of their bioactivity on XP cells (Figure 2).

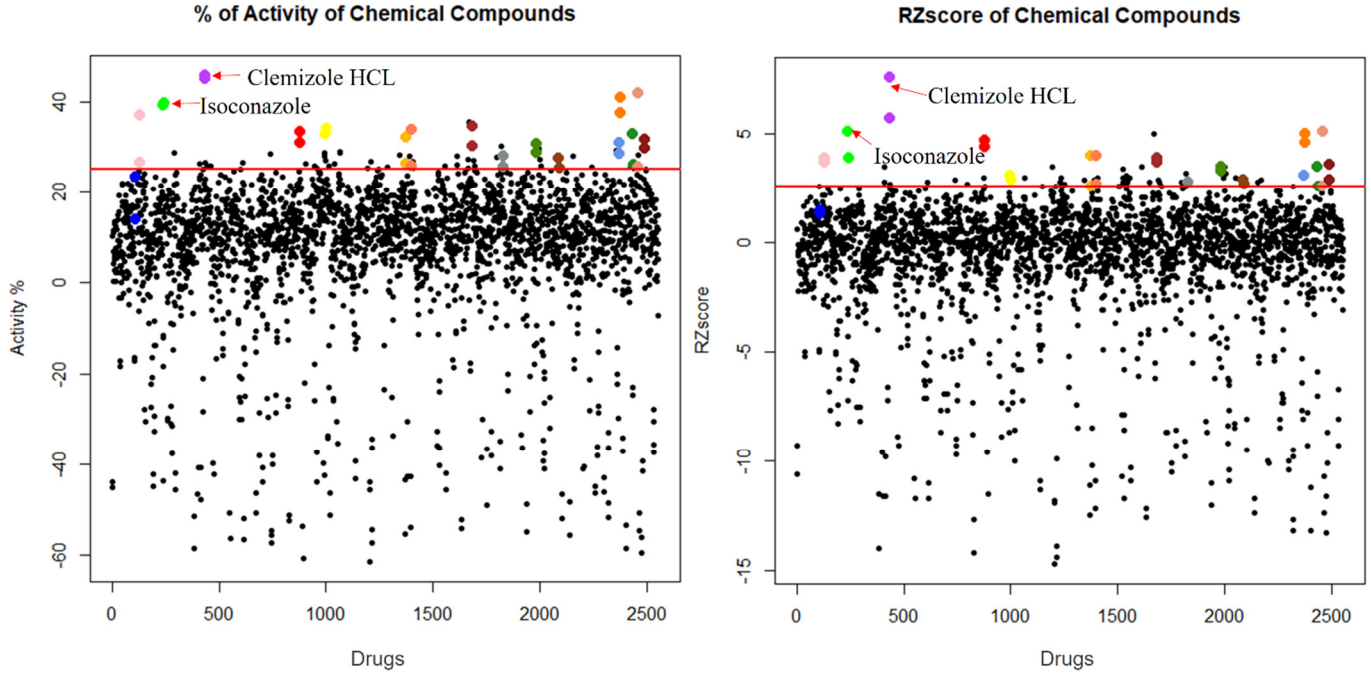

Figure 2. Identification of 16 compounds reversing XP-C photo-sensitivity upon UVB irradiation. Prestwick library of chemical drugs was screened on XP-C cells. The cells were treated with the library for 24 h, then further on, irradiated. Post Irradiation, the cells were then incubated with the library for an additional 24 h prior to having their viability assessed 24 h post UV via the addition of Presto Blue reagent and the recording of the fluorescent values. Based on two different normalization criteria, control based % of activity and non-control based RZscore, 16 compounds were selected manifesting >25% increase or >2.5 value for both % of activity and RZscore respectively. % Activity was calculated by normalizing the obtained values between the interval of 100% donated to non-irradiated DMSO treated cells and 0% that donated irradiated DMSO treated cells. RZscore was measured by normalizing the fluorescence values to the median and median absolute deviation. RZscore: Robust Z score.

2.3. Selection of Three Bioactive Drugs Increasing XP-C Cells Viability after UVB Irradiation

In order to select the most efficient compounds showing robust activity on XPC viability among the 16 primary hits, a secondary screen was carried out using the same assay as the initial primary screen. Additional conditions were included together with the initial screen's conditions. The drugs were indeed screened at three different concentrations (1, 5 and 10 µM). Moreover, the cells were irradiated at two doses of either 0.02 J/cm^2 or 0.05 J/cm^2. Finally, each drug was screened in triplicate in each of the different irradiation conditions and drug concentrations. The same viability readout was measured as for the primary screen. The acetohexamide drug was also added as a positive control as it was reported to increase XP-A cells' viability in response to UV irradiation [25] where XPA is a protein involved in the damage verification process downstream damage recognition post irradiation [26]. For each drug, a dose-response curve of bioactivity as a function of drug concentration (in µM) was plotted for the different doses tested. The drugs that showed the highest bioactivity were isoconazole, clemizole hydrochloride and bifonazole, inducing a significant 20 to 40% increase in XP-C cell viability with p-value < 0.001 depending on the UVB exposition and drug concentration. In contrast, the acetohexamide only mediated a 20% increase in viability of XPC cells and displayed no increased bioactivity when applying increasing concentrations to the cells (Figure 3). This secondary screen defines three promising drugs protecting XPC cells from UVB toxicity.

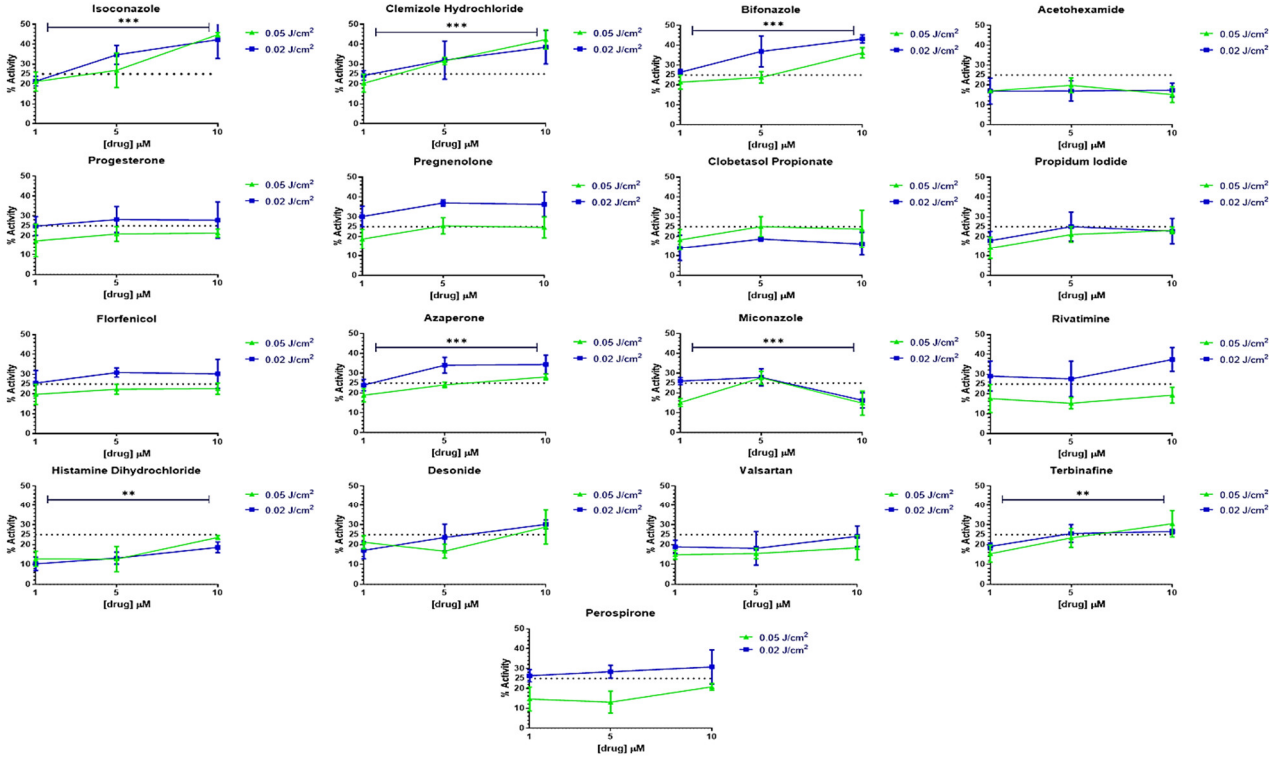

Figure 3. Confirmation of primary screen hits and the identification of the 3 most effective compounds. XP-C cells were treated with the different primary screen candidate compounds at three different concentrations (1, 5 & 10 µM), then subjected to two UVB doses (0.02 & 0.05 J/cm^2) after which their viability was measured 24 h later by the addition of PrestoBlue. It should be noted that pre- and post-irradiation treatment with the drugs was carried out. The three compounds showing the increased drug bioactivity as a function of increased concentrations are isoconazole, clemizole hydrochloride and bifonazole, showing the highest protection against UV irradiation. % Activity was calculated by determining the relative % of fluorescence with respect to non-irradiated DMSO treated cells set as 100% and irradiated DMSO treated cells set as 0%. The dotted line represents a threshold of 25% Activity. The statistical significance of the effect of two UVB doses and the three drug concentration on the % activity was conducted by using 2-way ANOVA ** $p < 0.01$, *** $p < 0.001$. The figures represent triplicates ±SD.

2.4. Identification of Drugs That Promote the Repair of DNA Damage

In order to determine the mechanisms of action of the 16 primary hits and acetohexamide, we tested whether they could promote DNA repair activity in XP-C cells. For that, DNA damage analysis was carried out after cells were treated with the 17 drugs and irradiated at a dose of 0.05 J/cm^2 using the same protocol as for the primary screen. After the measurement of bioactivity, the plates were fixed and immuno-stained with an anti-6-4PP antibody for the quantification of the amount of DNA damage following UVB irradiation in the presence of drug or not (Supplementary Figure S2). It should be noted that the amount of DNA damage induced at time zero after UVB irradiation was the same for either treated or non-treated cells. The positive control showing maximal DNA damage was the DMSO treated irradiated cells while the negative control with minimal damage is the non-irradiated DMSO treated cells. XP-C cells treated with either isoconazole or clemizole hydrochloride showed a significant decrease in the amount of 6-4PP at the single-cell level compared to untreated controls, suggesting enhanced repair activity due to drug treatment. This decrease in DNA damage was significant at a 5 μM concentration for both drugs ($p < 0.001$) while not at 1μM, which may be a too weak concentration, or at 10 μM, where the difference was not found to be significant (Figure 4). These results thus identified isoconazole and clemizole hydrochloride as two drugs promoting DNA repair in response to UVB irradiation in XP-C cells.

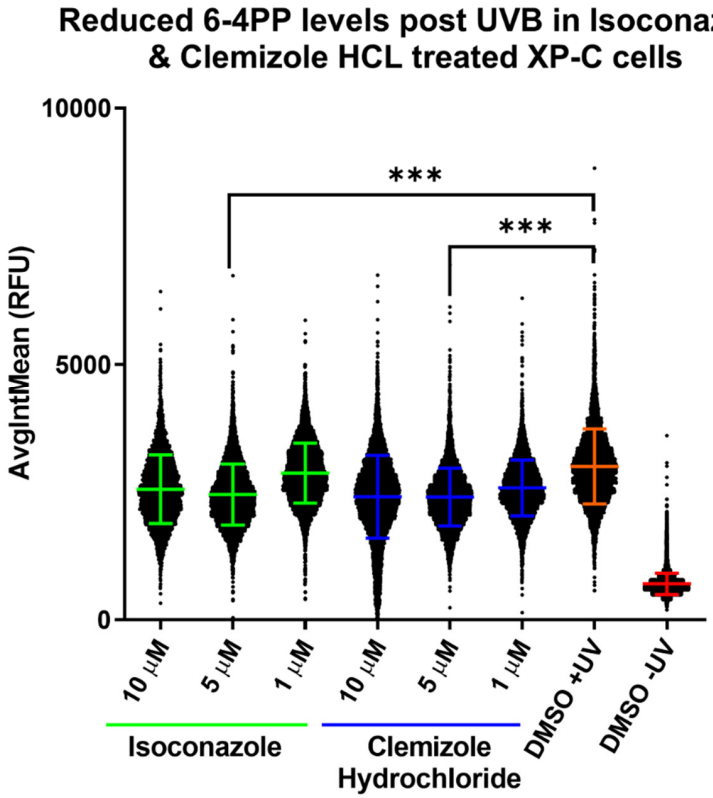

Figure 4. Identification of compounds enabling repair of 6-4PP in XP-C cells. XP-C cells were treated with the 16 primary screen candidate hits at three different concentrations (1, 5 & 10 μM) with pre- and post-irradiation treatments. Irradiation was carried out at a dose of 0.05 J/cm^2. 24 h post UV the cells were fixed and stained with 6-4PP antibodies for the quantification of DNA damage. Fluorescence intensities of individual cells for each condition were quantified and more than 1000 cells per condition were analyzed. Among the 16 hits, only isoconazole and Clemizole hydrochloride enabled a decrease in the amount of DNA damage post UV shown here. Almost 20% repair of 6-4PP DNA damage was recorded for both drugs at a concentration of 5μM which was found to be significant. DNA damage quantification in DMSO treated irradiated cells was used as positive control showing the maximum amount of DNA damage while quantification of 6-4PP in DMSO treated

non-irradiated cells was taken as a negative control with the minimum amount of detected damage. *** $p < 0.001$, freedman non-parametric test with Dunn's post hoc analysis. Up to 10,000 cells were analyzed per condition with ±SD.

2.5. Dose-Response Analysis of Drug Bioactivity as a Function of UVB Doses in XP-C and WT Cells

To further characterize the effect of isoconazole and clemizole hydrochloride drugs on XP-C cells versus wild-type cell viability enhancement, UV dose-response experiments were carried out. In contrast to the previous experiments, the dose-response analysis here was performed on both the XP-C and WT cell lines and viability was normalized to that of non-irradiated cells (fixed at 100%). This task aims to decipher whether the effect of the two drugs on cell viability is specific to XP-C cells or also valid in WT cells. The two cell lines were treated with either isoconazole, clemizole hydrochloride or DMSO, then subjected to increasing UVB doses. Both drugs enabled enhanced photo-resistance to the increasing UVB doses in both XP-C and WT compared to DMSO treated cells (Figure 5a,b). Such photo-resistance was significant for both drugs in XP-C cells with a p-value < 0.05. However, in WT cells, the treatment with isoconazole showed significant photo-resistance against increased UV doses irradiation (p-value < 0.05), unlike clemizole hydrochloride whose increase in viability was not significant. In conclusion, this protective effect may not be specific to XP-C cells as a similar protective effect was also shown for the WT cells. This is consistent with their observed ability to increase DNA repair efficiency.

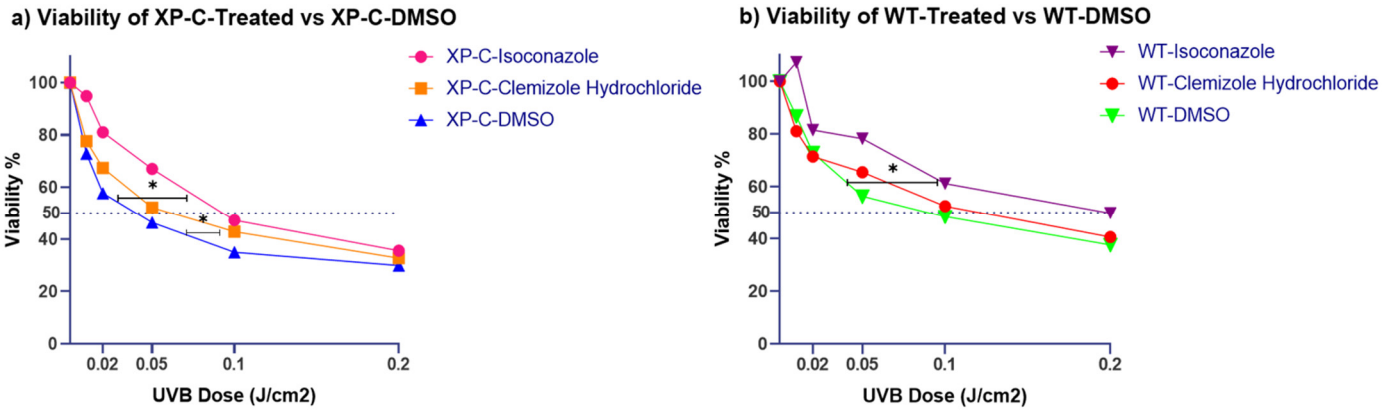

Figure 5. Isoconazole and Clemizole Hydrochloride viability analysis post UVB in both XP-C and WT cell lines. XP-C and WT cells were treated with either drugs or DMSO (pre- and post-irradiation treatment), then subjected to increased UVB doses. Their viability was further on assessed 24 h post UV by the incubation with PrestoBlue. (**a**) Viability of XP-C treated cells vs. DMSO. Both drugs enabled significant (p value < 0.05) protection of XP-C cells from UVB induced death with isoconazole having a more protective effect. (**b**) Viability of WT treated cells vs. DMSO. Drug mediated protection against UVB irradiation was also evident in treated WT cells and not unique to XP-C cells. Only isoconazole mediated protection was significant with p value < 0.05. Viability was calculated by determining the percent of control with respect to non-irradiated DMSO treated cells taken as 100% viable. * p-value < 0.05, Repeated Measure one way ANOVA with Dunnett's multiple comparison test. The experiments were carried out in triplicates.

2.6. Investigation of Pre- Versus Post-Drug Treatment Efficacy

As mentioned above, the chemical treatment consisted of two phases, a pre-irradiation treatment to test the preventative effect of the drug and a post-irradiation treatment to examine its curative effect. In order to determine which treatment phase had a more essential role in the XP-C cells phenotypic normalization, the two phases of treatment were analyzed separately via the determination of drug bioactivity. It should be noted that bioactivity is defined by the ability of the drugs to impose an effect on living matter, which

in this case, is its ability to increase photo-resistance of the cells between non-irradiated cells set at 100% and irradiated non-treated cells set at 0%. The effect of each of the pre- or post-treatment was compared to that of the combined pre- plus post-treatment regimen. For isoconazole, the post-irradiation treatment was sufficient to induce similar protection as the combined treatment at both 5 and 10 µM (with no significant differences) while the pre-treatment had no effect on XP-C cells viability at any of the tested concentrations (Figure 6a). At 10 µM, the difference in bioactivity was significant between pre and post-treatment as well as between the pre-and combined treatment with a p-value < 0.01, signifying that both pre-treatment and combined regimens share significant protection compared to pretreatment. In the case of clemizole hydrochloride, the pre-irradiation treatment showed slight bioactivity reaching 20% increased cell viability at the highest concentration of drug of 10 µM. The post-treatment, however, was again more effective than the pre-treatment on XP-C viability reaching an average of 50% increase of cell viability at 10 µM. The combination of both pre-and post-irradiation treatments showed the highest bioactivity with a significant difference compared to the pretreatment at both 5 and 10 µM p-value < 0.05, and no significant difference with the post-treatment only. Thus, despite a slight protective potential of clemizole hydrochloride, both drugs (isoconazole and clemizole hydrochloride) may essentially serve as curative remedy post-UVB irradiation.

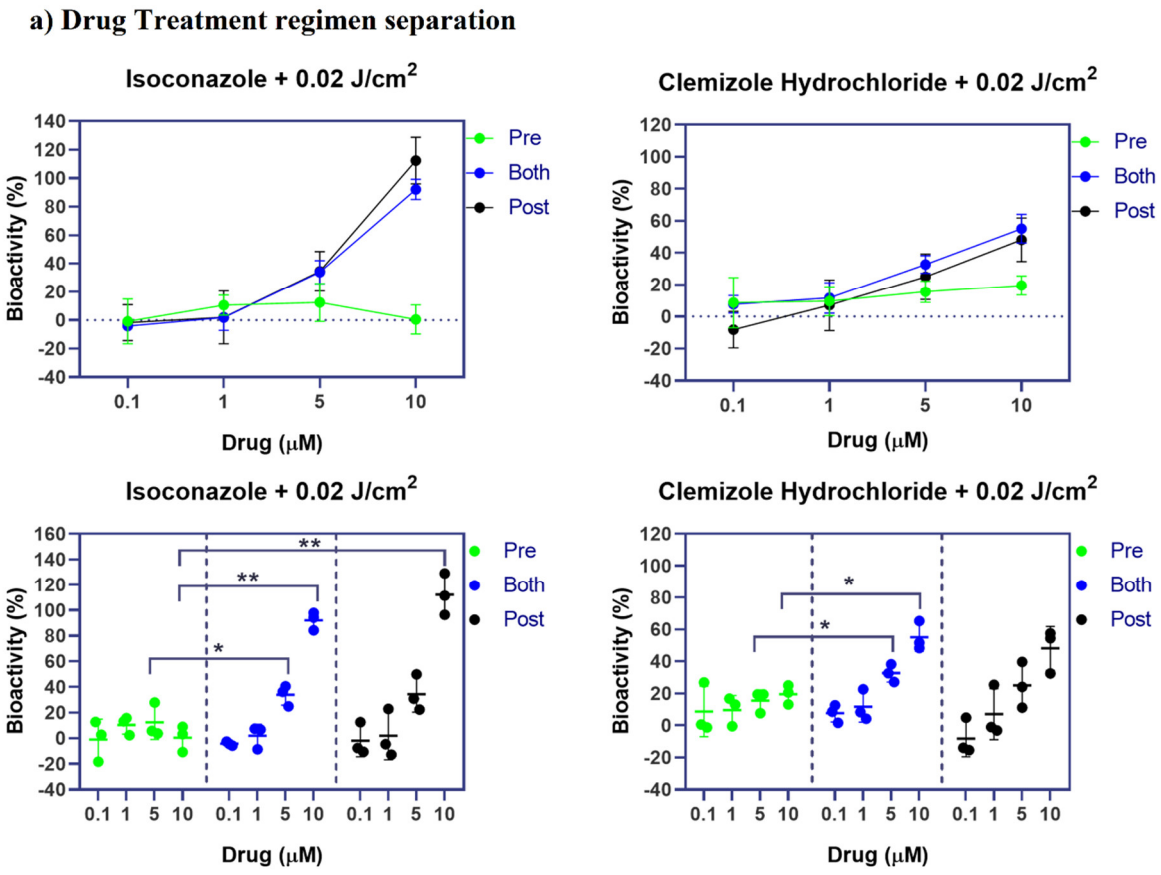

Figure 6. *Cont.*

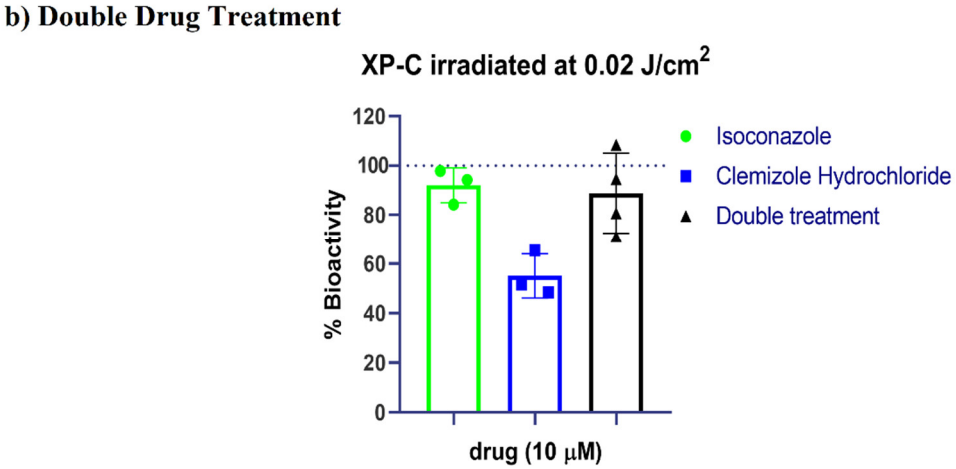

Figure 6. Drug treatment regimen separation and double drug treatment. To determine which treatment regimen was more effective, XP-C cells were treated with the drugs either pre-irradiation, post-irradiation or both pre and post-irradiation. Drug Bioactivity % was then calculated 24 h post UV. Such calculation is based on determining the relative percentage considering non-irradiated DMSO treated samples as 100% and irradiated ones as 0%. Thus, the obtained fluorescence values normalized to these two controls. (**a**) Drug treatment regimen separation. Isoconazole post-irradiation or both treatments showed a significant p value < 0.01 increase in bioactivity at 10 μM, while only both treatments showed significant enhancement of bioactivity at 5 μM compared to pre-treatment procedure. Clemizole hydrochloride, however, seems to have better bioactivity when both pre and post-irradiation regimes were used where the increase of bioactivity was significant, p value < 0.05 for both 5 μM and 10 μM treatment compared to pre-treatment at each concentration, respectively. Moreover, double drug treatment was also carried out to test whether both drugs possess synergistic or additive effect. (**b**) Double drug treatment. XP-C cells were treated with either Isoconazole, clemizole hydrochloride or double treated at 10 μM, then irradiated at 0.02 J/cm^2. % of drug bioactivity was measured 24 h later. Double treatment showed the same protective profile as isoconazole with no added protection against UVB irradiation. * p value < 0.05, ** p value < 0.01, 2-way ANOVA with Tukey's multiple comparison test. The experiments were performed in triplicate with ±SD.

2.7. Double Drug Treatment Has no Synergistic nor Additive Effect

Both compounds, isoconazole and clemizole hydrochloride, have an azole ring in their structure (and may thus target the same molecular biological target or similar mechanisms). We, therefore, examined whether the combined treatment with both drugs at 10 μM could improve further or not the acquired photo-resistance compared to single-drug treatment. Accordingly, XP-C cells were treated with either drug alone or with both and then subjected to irradiation at a dose of 0.02 J/cm^2. The double treatment had the same bioactivity as the single treatment with isoconazole with no benefit (Figure 6b). Hence, no synergetic effect was obtained upon double drug treatment.

2.8. Isoconazole and Clemizole Hydrochloride Do Not Affect Cell Proliferation

In a first step, and in order to analyze the proliferative state of the irradiated cells and whether the different treatments can modify this profile, cells were stained with Ki67 antibodies and analysis was carried out at the single-cell level. Ki67 antigen was expressed during all phases of the cell cycle (G1, S, G2 and M) but not in quiescent cells. Both XP-C and WT cell lines were positive to Ki67, signifying that the cells are not in quiescent state post UV. Cells treated with either DMSO, isoconazole, clemizole hydrochloride or both drugs showed no difference in the Ki67 expression profile (Supplementary Figure S3).

Ki67 antibodies stain cells in various stages of the cell cycle, and it was previously reported that some non-proliferating cells tend to test positive for Ki67 due to antigen retention [27]. Moreover, bulky adducts generated by UV tend to block the progression of replication forks, decreasing DNA replication. Therefore, in a second step, EdU incorporation assay was performed to clarify whether this positive staining was due to antigen retention or whether rather the cells were capable of recovering from the DNA replication

blockade following different treatments. It should be noted that EdU insertion into DNA allows the identification of cells with active DNA synthesis that generally occurs during S phase. XP-C cells were treated with either DMSO, isoconazole or clemizole hydrochloride in a pre-and post-treatment regime and then irradiated with UV to be finally cultured in the presence of EdU at different time points (2 h or 4 h post UV). Cells were then collected and stained to be analyzed by flow cytometry. When comparing the course of EdU incorporation in DMSO treated cells over the different time points post UV, it was clear that the intensity of EdU decreases as a function of time till becoming null at 24 h post UV. This signifies that the cells were no longer able to undergo DNA replication at 24 h post UV. No increase in the EdU MFI (mean fluorescence intensity) for the drugs compared to DMSO treatment was recorded (Figure 7c). Isoconazole had a slight effect on increasing EdU positive population at 2 h post UV with $p < 0.01$ (Figure 7b) which might either be attributes to a slight increase in cell proliferation or an increase in translesion synthesis allowing more DNA synthesis upon drug treatment. Both drugs, however, failed to increase DNA replication beyond that, showing similar effects to DMSO (Figure 7b). These results indicate that cell proliferation does not seem to be the major mechanism underlying the protective effect induced by these drugs.

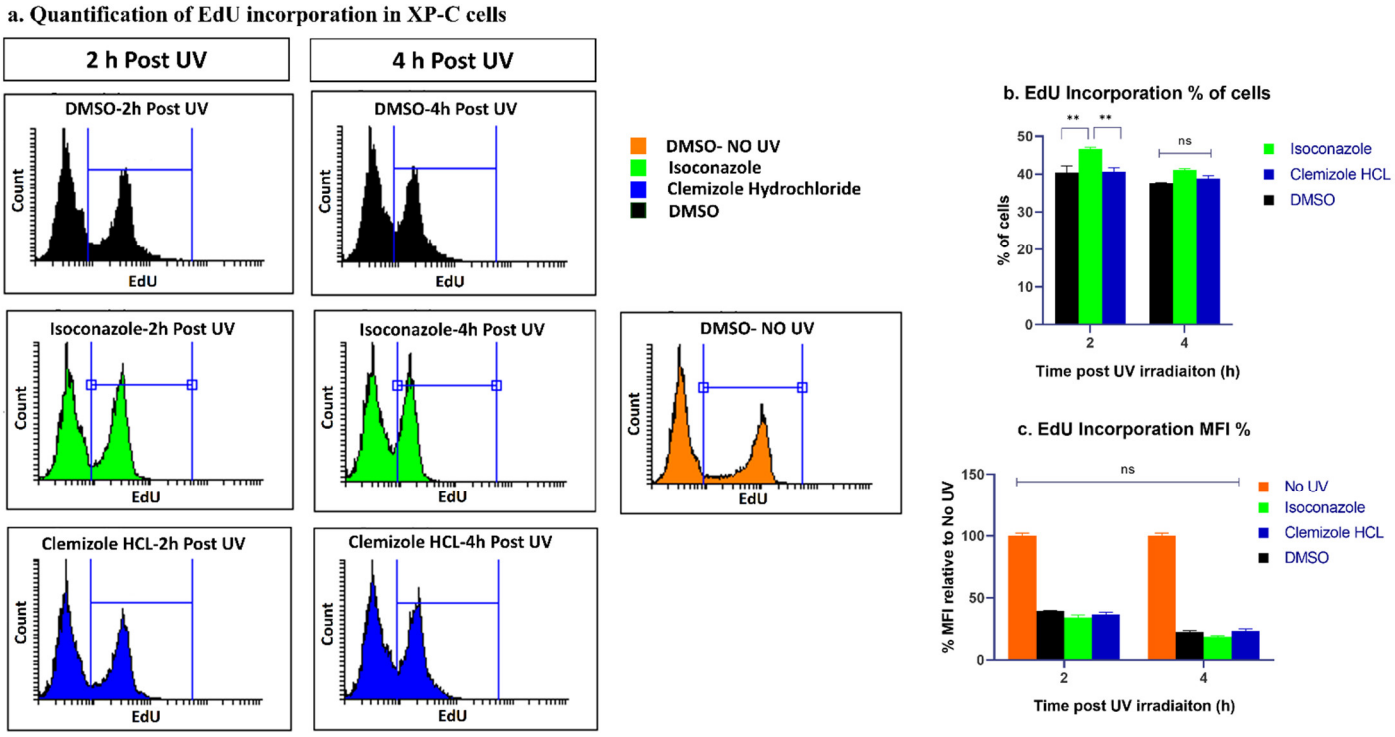

Figure 7. Same EdU incorporation profile is evident between drugs or DMSO treated XP-C cells. XP-C cells were treated with the different drugs or DMSO, then irradiated at 0.02 J/cm^2. Prior to the end of the post UVB incubation, the cells were incubated in the presence of EdU. Cells were further on collected, stained and analyzed by flow cytometry. No difference is seen between the mean fluorescence intensity of the EdU positive populations between the different treatment condition at either 2 or 4 h post UV. It should be noted that as incubation time post UV increases, the mean fluorescence intensity of EdU positive population decreases. Quantification of both the mean fluorescence intensity (MFI) and EdU positive population percentage were carried out. Two-way ANOVA was used to compare between the two independent variables (time post UV and nature of the drug treatment) and the dependent variable of either EdU population percentage or MFI, ** $p < 0.01$, ns: not significant. The experiments were carried out in triplicates with ±SD. (**a**) Quantification of EdU incorporation in XP-C cells, (**b**) EdU Incorporation %of cells, (**c**) EdU Incorporation MFI %.

2.9. Isoconazole and Not Clemizole Hydrochloride Increases Live Cell Population in the Course of Apoptosis and Necrosis Analysis

In an attempt to decipher the cellular mechanisms of photo-resistance of the drug treatment, different cell phenotypes were analyzed. Apoptosis was therefore quantified using Cell Event which allows the indirect measurement of caspase 3/7 activity, key downstream players in the apoptosis activation cascade. XP-C cells were therefore treated with either drug or DMSO followed by UVB irradiation then staining with Cell Event and PI 24 h post UV. The samples were analyzed by flow cytometry. Out of the two drugs, Isoconazole showed a decrease in Cell Event % cells reaching 23.35% as well as lower PI-positive population percentage (9.57%) compared to DMSO treated cells, showing higher population percentages of 41.23% and 11.57% (Figure 8a-right panel), respectively, but was not found significant. However, the increase in the levels of the live cell population originating from this decrease in both apoptotic and necrotic populations was significantly regulated compared to that of DMSO (p-value < 0.05) or to that of clemizole hydrochloride (p-value < 0.01). On the other hand, clemizole hydrochloride did not show any decrease in both quantified parameters. These results suggest that, unlike isoconazole, it is probably not via the reduction of apoptosis that the clemizole hydrochloride mediates its protective role (Figure 8b). Similar outputs were also detected in WT cells (Supplementary Figure S4).

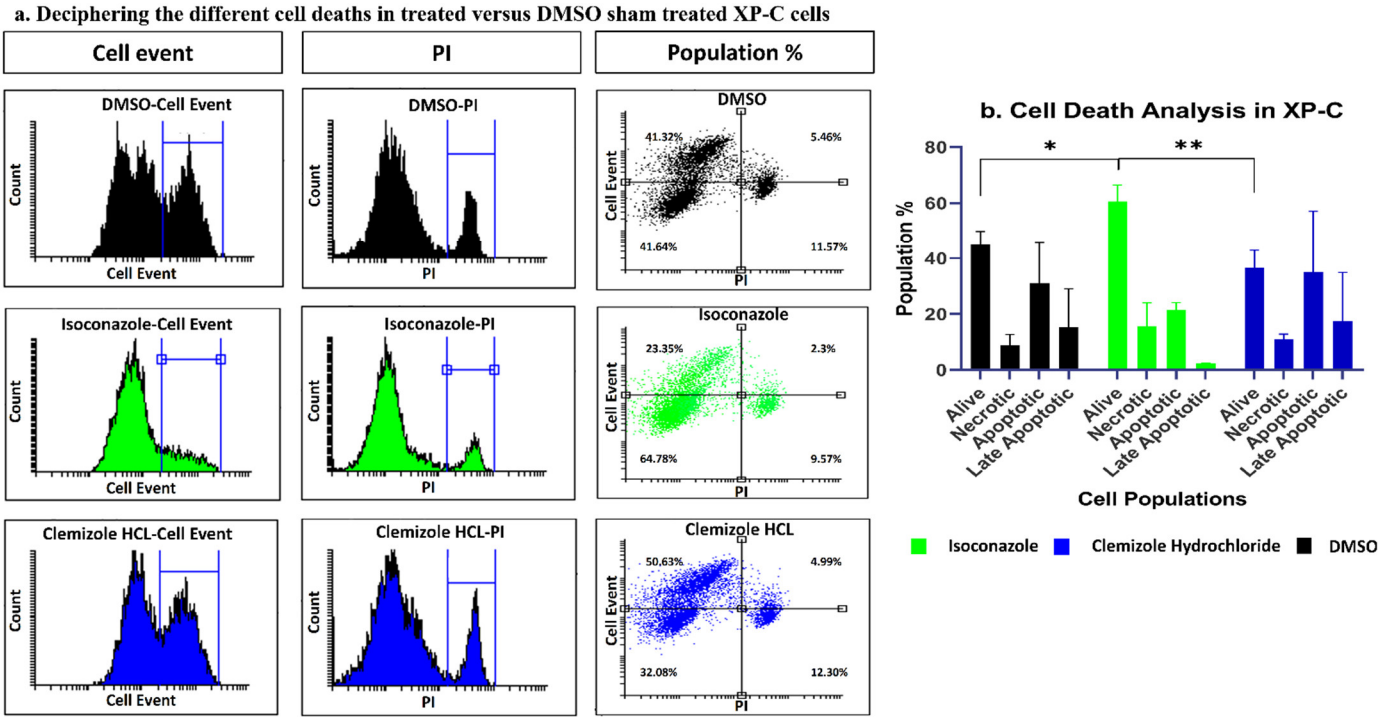

Figure 8. Isoconazole but not clemizole hydrochloride increases live cell population of XP-C cells post UV. XP-C cells were treated with the different drugs or DMSO then irradiated. CellEvent caspase 3/7 marker was added post UV then cells were collected. PI was added just before analysis on a flow cytometer. Isoconazole treatment decreased the percentage of apoptotic cells post UV compared to DMSO treated cells. Clemizole hydrochloride, however, had no effect so it is perhaps via another mechanism that this drug mediates its mode of action. Student t-test. ** $p < 0.01$, * $p < 0.05$. The experiments were carried out in triplicates with ±SD. (**a**) Deciphering the different cell deaths in treated versus DMSO sham treated XP-C cells, (**b**) Cell Death Analysis in XP-C.

3. Discussion

The presented work identified two drugs, isoconazole and clemizole hydrochloride, that could partially reverse the XP-C characteristic phenotype: increased photosensitivity

and absence of DNA damage repair of photoproducts. In addition, both drugs also enabled photo-protection in WT cells exposed to high doses of UVB irradiation.

XP-C patient cells carry a mutation in the *XPC* gene required for the recognition of DNA damage. This mutation renders the cells photosensitive [28] and unable to repair UVB induced DNA damage. Here we confirmed the photosensitive profile of XP-C as they show a significantly (p-value < 0.001) reduced viability compared to WT cells as a function of increased UV doses. Such cells lack the XPC proteins, as confirmed by immunostaining, signifying that such a mutation leads to the complete loss of the XPC protein. Moreover, upon the quantification of the different UVB induced DNA lesions by LC-MS/MS, it was evident that XP-C cells manifest slower repair kinetics compared to WT cells. UVB induced lesions include either CPD or 6-4PP that are formed between two adjacent pyrimidines giving four possible lesions T-T, C-C, C-T and T-C [29]. The most abundantly formed lesions are the T-T and T-C lesions for both the CPD and the 6-4PP. In WT cells, both lesion types of 6-4PP are readily repaired by the cells a few hours post irradiation, while CPDs require more time, with lesion dependent repair kinetics being the slowest repair for T-T, T-C, C-C then C-T, CPD showing the fastest repair, confirmed by us and others [30]. XP-C cells show no or reduced repair for both CPD and 6-4PP different lesion types as a function of time.

Drug repurposing is the process of testing previously approved drugs, used for a particular therapeutic purpose, for their potential use in the treatment of other common or rare diseases. This cuts down drug discovery costs and the long process of toxicity and pharmacokinetics testing [31]. For that, our aim was to test a library of 1280 approved drugs for their potential use in normalizing the XP-C phenotype. XP-C cells were treated with the compounds at 10 μM for 24 h then irradiated with UVB and then treated again with the same compounds at the same concentration for an additional period of 24 h. The overall viability of the treated cells, proportional to the amount of metabolically active cells, was then measured via incubation with PrestoBlue. The fluorescent values obtained were normalized via either the calculation of drug activity %, control based with 100% for non-irradiated DMSO treated cells and 0% for irradiated ones or via the calculation of the non-control based RZscore. Drugs that showed an activity ≥25% with an RZscore above 2.6 were selected as primary hits to be confirmed via a secondary screening which were 16 drugs. Acitohexamide was added to the secondary screen drug list due to its previously described photo-protective effect on XPA cells via the enabling of damage repair [25]. Isoconazole, clemizole hydrochloride and bifonazole manifested the highest bioactivity after secondary screening enabling photo-protection in XP-C cells compared to DMSO treated controls with a range of 20 to 40% increase of cell viability depending on the conditions. However, the enabling of photo-resistance is not sufficient by itself for a satisfying curative outcome. The persistence of cells with accumulated DNA damage can lead to the conversion of such lesions into mutations which, depending on their localizations, can lead to carcinogenesis [32]. The main lesion in XP cells mediating the UV signature mutation is the C-C lesion where the slow repair of such lesion in XP cells compared to its fast repair in WT cells favors the deamination and induction of mutations [29]. Therefore, photo-resistance should be associated with increased DNA damage repair in the perspective of therapeutic treatment. Indeed, we tested the capacity of the 16 primary hits and acetohexamide in mediating the decrease of DNA damage post UVB irradiation. Out of this collection, two compounds, isoconazole and clemizole hydrochloride, decreased the amount of DNA damage post UV in XP-C cells by about 20% (p-value < 0.001 at 5 μM).

Isoconazole is an azole antifungal drug with no reported data on its effect in sun-shielding upon its use on the skin, while clemizole hydrochloride is a Histamine H1 antagonist. Other documented functions for clemizole hydrochloride include its role in the treatment of HCV infection [33] and its blocking effect on TRPC5 ion channels [34]. These functions fail to explain these drugs' effect on XP-C cells, suggesting possible alternative mode(s) of action than the ones documented that need(s) to be further on explored.

One similar approach to ours was conducted on XP-A cells, where the anti-diabetic drug acetohexamide was found to be effective in reducing the cells' photosensitivity and enabling damage repair [25], mediating the identification of an additional mode of action for this drug not related to its documented effect. Acetohexamide had minimal effect in the reversal of XP-C phenotype when tested in our screen, yet we managed to identify other drugs that can aid in this phenotypic partial reversal. Acetohexamide enabled the degradation of MUTYH, a protein involved in the removal of adenine residues mispaired with 8-oxo-guanine residues after oxidative stress [35]. The authors hypothesized that the degradation of such protein might be enabling spatial access of the lesions to other repair machinery independent of nucleotide excision repair [25] which was not yet further explored to date. It is therefore possible that the hit drugs identified in this study might similarly impose spatial access effect or that they interfere with one or several mediators of DNA repair, a hypothesis which needs to be further on examined.

Collectively, our data show that isoconazole and clemizole hydrochloride mediated an increase in cell viability post UV irradiation and enabled to a lower extent the repair of accumulated DNA damage in the form of UVB-induced 6-4PP. Isoconazole, on the one hand, mediated a curative effect post UV irradiation by enabling the decrease of apoptotic cells' population as measured by flow cytometry with Cell Event caspase 3/7 activity staining. Clemizole hydrochloride's effect, on the other hand, was both preventative pre UV and curative post UV irradiation showing a p-value < 0.05, while the difference between the post-irradiation alone and the pre-irradiation treatment was not significant. Such an effect is mediated via a yet unknown mechanism. The simultaneous double treatment with both drugs revealed no synergistic or additive effect. This suggests that both drugs interfere with a similar biological process or target which is consistent with the fact that they share a similar chemical scaffold (azole ring). Moreover, both drugs were shown not to affect the cells' proliferation rate. The photoprotective effect of the drugs was also evident in WT cells post UV irradiation signifying the involvement of a protective pathway indirectly related to the mutated *XPC* gene. This work will mark the first attempt in discovering compounds for the amelioration of the XP-C phenotype, yet the exact regulated target needs to be further on explored to allow the identification of the effectors aiding in this phenotypic reversal and thus paving a way for a potential therapy for this yet untreatable genodermatosis.

4. Materials and Methods

4.1. Cell Line

Wild type (AG10076) and XP-C (GM15983) immortalized patient derived-fibroblasts were purchased from Coriell Biorepository. XP-C fibroblasts possess a two-base pair shift mutation at codon 431 of the *XPC* gene. The cells were cultured in DMEM high glucose, GlutaMAX media (Gibco, Waltham, MA, USA) supplemented with 10% FBS and 1% penicillin/streptomycin at 37 °C in a 5% CO_2 incubator.

4.2. Chemical Drug Screening

The Prestwick chemical library was utilized. It consists of 1280 drugs of high chemical and pharmacological diversity. The drugs are all approved (FDA, EMA or other agencies). The drugs cover all main ATC groups and are dedicated to either CNS, cardiovascular, metabolism or infectiology diseases with either enzymatic or GPCRs targets. The library was screened at a final concentration of 10 μM. For the screening procedure, the cells were incubated with the drugs for 24 h then media was recuperated and the cells washed with PBS. Irradiation was carried out in the presence of PBS. Following that same drug, containing media were returned back to the cells for the course of post treatment to be incubated for further 24 h before the assessment of the readouts.

4.3. UV Dose-Response

To examine the photosensitivity of XP-C cells relative to WT in response to UVB irradiation, both cells were seeded in 96 well plates until 80% confluency, washed with

PBS, then subjected to increasing doses of UVB. Twenty-four hours post UV, the viability of the cells was recorded as a measurement of the cells' reducing capacity by PrestoBlue (Thermofisher Scientific, Waltham, MA, USA) according to the manufacturer's suggestion. The LD50 for each cell line was calculated.

4.4. XPC Immuno-Staining and Associated Microscopy

For the characterization of XPC expression, both cell lines were fixed with 4% paraformaldehyde followed by permeabilization using 0.2% Triton X-100 and saturation with 3% FBS in PBS. Primary antibody targeting XPC (mouse monoclonal, Thermofisher Scientific, Waltham, MA, USA) was utilized followed by incubation with Alexa Fluor 488-coupled secondary antibody (goat anti-mouse, Invitrogen, Waltham, MA, USA). Nuclear DNA was counter-stained with Hoechst (Sigma-Aldrich, Burlington, MA, USA). Cell images were acquired by the Zen Axio-observer at 40X.

4.5. LC-MS/MS DNA Damage Quantification

The quantification of pyrimidine dimers (CPD & 6-4PP) was carried out by LC-MS/MS according to previous protocol [36]. Briefly, both cell lines were seeded in 100 mm dishes until sub-confluency where they were subjected to a UVB dose of 0.01 J/cm^2. At different time points post UV (0, 2, 24 and 48 h), the cells were collected and their DNA extracted with Qiagen DNEasy Kit (Hilden, Germany). Sample preparation was carried out in two steps; the first includes incubation of DNA for 2 h at 37 °C and pH 6 in the presence of nuclease P1, DNase II and phosphodiesterase II. The pH was then raised to 8 by the addition of Tris. A second incubation period in the presence of phosphodiesterase I and alkaline phosphatase at 37 °C for 2 h yielded digested DNA with normal bases as nucleosides and photoproducts as dinucleoside monophosphates. Samples were then injected on an HPLC system (Agilent, Massy, France) connected to a reverse-phase HPLC column (150_2mm ID, 5 mm particle size, ODB, France). The detection was provided first by a UV detector aimed at quantifying normal nucleosides. Photoproducts were detected by a tandem mass spectrometer (API 3000, SCIEX, Thorn hill, ON, Canada) used in the reaction-monitoring mode as previously described [37]. The four CPDs and the four 6-4PPs (TT, TC, CT and CC derivatives) were quantified individually in the same HPLC run. Results were expressed in the number of lesions per million normal bases.

4.6. 6-4PP DNA Damage Staining and Quantification

For the quantification of DNA damage, cells were seeded until confluency, then subjected to UVB irradiation at a dose of 0.02 J/cm^2. Twenty-four hours post UV, the cells were stained according to a previous protocol [38], consisting first of cell fixation with 4% paraformaldehyde, and permeabilized with 0.2% Triton X-100. Cells were further on treated with 2M HCL to denaturate the DNA and thus allow access to the DNA damage-targeting antibody. After saturation, the cells were incubated with 6-4PP antibody (64M-2 cosmo bio, Japan) followed by AF488 secondary antibody (Invitrogen, Waltham, MA, USA) and the DNA was counterstained with Hoechst (Sigma Aldrich, Burlington, MA, USA). Image acquisition and quantification were carried out by a Cell-insight NXT high content screening platform at 10X magnification. Single-cell fluorescence was quantified for all the cells under each particular treatment condition.

4.7. Ki67 Staining and Single-Cell Quantification

The cells were seeded until sub-confluency, then subjected to UVB irradiation at a dose of 0.02 J/cm^2. Twenty-four hours post-irradiation, the cells were fixed with 4% paraformaldehyde and permeabilized with 0.2% Triton X-100. After saturation, the cells were incubated with ki67 antibody (clone MIB-1, Clinisciences, France) followed by AF488 secondary antibody (Invitrogen, Waltham, MA, USA), and the DNA was counterstained with Hoechst (Sigma Aldrich, Burlington, MA, USA). Image acquisition and quantification

were carried out by Cell-insight NXT high content screening platform at 10X magnification. Single-cell fluorescence was quantified for all the cells under each particular treatment condition.

4.8. EdU Cell Proliferation Assay

Cell health and genotoxicity can be assessed by measuring the cell's ability to proliferate via the incorporation of the nucleoside analog EdU. The latter can be further on quantified by a click-it covalent reaction between an azide and alkyne catalyzed by copper. For that, both cell lines were seeded in 100 mm dishes subjected to different forms of treatment followed by irradiation. Sham irradiated and sham-treated controls were also utilized. Two hours before the end of post UV incubation, EdU was diluted in the cell media at different time points. The cells were then collected and stained according to the manufacturer's protocol. The samples were analyzed by flow cytometry (FACScan, BD LSRII flow cytometer, BD Biosciences, Franklin Lakes, NJ, USA). The post analysis was carried out using flowing software [39] (Turku Bioimaging, Finland).

4.9. Cell Event-PI Cell Death Quantification

To follow the effect of treatment on the induction of apoptosis post UV irradiation, CellEvent (Thermofisher Scientific) was utilized, which allows the measurement of caspase 3/7 activity. For that, cells were seeded in 100 mm dishes, treated with the molecules, irradiated, then Cell Event was added post UV and incubated for 24 h. The cells were then collected and PI was added before their analysis by flow cytometer (FACScan, BD LSRII flow cytometer, BD Biosciences). The post analysis was carried using flowing software [39] (Turku Bioimaging, Finland).

4.10. Statistical Analysis

Drug screening hit selection and single-cell analysis was carried out using R software [40]. Statistical analysis was conducted using GraphPad Prism v.8 after data normalization and quantification of normality to allow the choice of the respective statistical test (parametric or non-parametric) for each particular set of experiments.

Supplementary Materials: The following are available online at https://www.mdpi.com/article/10.3390/ijms22158156/s1, Figure S1: Primary Screen UV dose optimization and reproducibility assessment. Figure S2: Single-cell analysis of nuclear DNA damage quantification. Figure S3: Drug treatment has no effect on ki67 proliferation marker expression. Figure S4: Isoconazole and not clemizole hydrochloride decreases the population % of apoptotic WT cells post UV.

Author Contributions: F.K. performed all the experiments and wrote the manuscript. E.S. aided in flow cytometry, data normalization and manuscript revision. C.B. designed and performed the chemical primary screening. M.-O.F. supervised the screening campaign. N.F. assisted in the LC-MS/MS experiment. X.G., H.F.-K. and W.R. supervised the project. M.F.-K. and B.B. revised the manuscript. All authors have read and agreed to the published version of the manuscript.

Funding: F.K. is supported by a fund from the Lebanese University (UL) and Alternative Energies and Atomic Energy Commission (CEA). W.R.'s contribution was funded by ANR grant PG2HEAL (ANR-18-CE17-0017) and supported by the French National Research Agency in the framework of the "Investissements d'avenir" program (ANR-15-IDEX-02). Automated molecular screening has been performed through the ChemBioFrance infrastructure at the Grenoble Alpes Probes and Drug Discovery platform (GAP2D). Support of the Labex GRAL, ANR-10-LABX-49-01 financed within the University of Grenoble Alpes graduate school CBH-EUR-GS (ANR-17-EURE-0003) is acknowledged.

Institutional Review Board Statement: Not applicable.

Informed Consent Statement: Not applicable.

Data Availability Statement: Not applicable.

Acknowledgments: This article was previously published as a pre-print on research square accessed on 16th February 2021 (https://www.researchsquare.com/article/rs-197694/v1).

Conflicts of Interest: The authors declare that the research was conducted in the absence of any commercial or financial relationships that could be construed as a potential conflict of interest.

References

1. Tan, N.S.; Wahli, W. The emerging role of Nrf2 in dermatotoxicology. *EMBO Mol. Med.* **2014**, *6*, 431–433. [CrossRef]
2. Gegotek, A.; Skrzydlewska, E. The role of transcription factor Nrf2 in skin cells metabolism. *Arch. Dermatol. Res.* **2015**, *307*, 385–396. [CrossRef] [PubMed]
3. Ravanat, J.L.; Douki, T.; Cadet, J. Direct and indirect effects of UV radiation on DNA and its components. *J. Photochem. Photobiol. B* **2001**, *63*, 88–102. [CrossRef]
4. Slieman, T.A.; Nicholson, W.L. Artificial and solar UV radiation induces strand breaks and cyclobutane pyrimidine dimers in Bacillus subtilis spore DNA. *Appl. Environ. Microbiol.* **2000**, *66*, 199–205. [CrossRef]
5. Baumstark-Khan, C.; Hentschel, U.; Nikandrova, Y.; Krug, J.; Horneck, G. Fluorometric analysis of DNA unwinding (FADU) as a method for detecting repair-induced DNA strand breaks in UV-irradiated mammalian cells. *Photochem. Photobiol.* **2000**, *72*, 477–484. [CrossRef]
6. Rastogi, R.P.; Singh, S.P.; Hader, D.P.; Sinha, R.P. Detection of reactive oxygen species (ROS) by the oxidant-sensing probe 2′,7′-dichlorodihydrofluorescein diacetate in the cyanobacterium Anabaena variabilis PCC 7937. *Biochem. Biophys. Res. Commun.* **2010**, *397*, 603–607. [CrossRef] [PubMed]
7. Armstrong JD and Kunz BA (1990) Site and strand specificity of UVB mutagenesis in the SUP4-o gene of yeast. *Proc. Natl. Acad. Sci. USA* **1990**, *87*, 9005–9009. [CrossRef]
8. Kobaisi, F.; Fayyad, N.; Rezvani, H.R.; Fayyad-Kazan, M.; Sulpice, E.; Badran, B.; Fayyad-Kazan, H.; Gidrol, X.; Rachidi, W. Signaling Pathways, Chemical and Biological Modulators of Nucleotide Excision Repair: The Faithful Shield against UV Genotoxicity. *Oxidative Med. Cell. Longev.* **2019**, *2019*, 4654206. [CrossRef] [PubMed]
9. Spivak, G. Nucleotide excision repair in humans. *DNA Repair* **2015**, *36*, 3–18. [CrossRef] [PubMed]
10. Iyama, T.; Wilson, D.M., III. DNA repair mechanisms in dividing and non-dividing cells. *DNA Repair* **2013**, *12*, 620–636. [CrossRef] [PubMed]
11. Giglia-Mari, G.; Sarasin, A. TP53 mutations in human skin cancers. *Hum. Mutat.* **2003**, *21*, 217–228. [CrossRef] [PubMed]
12. Tampa, M.; Georgescu, S.R.; Mitran, C.I.; Mitran, M.I.; Matei, C.; Scheau, C.; Constantin, C.; Neagu, M. Recent Advances in Signaling Pathways Comprehension as Carcinogenesis Triggers in Basal Cell Carcinoma. *J. Clin. Med.* **2020**, *9*, 3010. [CrossRef] [PubMed]
13. Curtin, J.A.; Fridlyand, J.; Kageshita, T.; Patel, H.N.; Busam, K.J.; Kutzner, H.; Cho, K.H.; Aiba, S.; Bröcker, E.B.; LeBoit, P.E.; et al. Distinct sets of genetic alterations in melanoma. *N. Engl. J. Med.* **2005**, *353*, 2135–2147. [CrossRef]
14. Melis, J.P.; Luijten, M.; Mullenders, L.H.; van Steeg, H. The role of XPC: Implications in cancer and oxidative DNA damage. *Mutat. Res.* **2001**, *728*, 107–117. [CrossRef] [PubMed]
15. D'Errico, M.; Parlanti, E.; Teson, M.; de Jesus, B.M.; Degan, P.; Calcagnile, A.; Jaruga, P.; Bjoras, M.; Crescenzi, M.; Pedrini, A.M.; et al. New functions of XPC in the protection of human skin cells from oxidative damage. *EMBO J.* **2006**, *25*, 4305–4315. [CrossRef] [PubMed]
16. Fayyad, N.; Kobaisi, F.; Beal, D.; Mahfouf, W.; Ged, C.; Morice-Picard, F.; Fayyad-Kazan, M.; Fayyad-Kazan, H.; Badran, B.; Rezvani, H.R.; et al. Xeroderma Pigmentosum C (XPC) Mutations in Primary Fibroblasts Impair Base Excision Repair Pathway and Increase Oxidative DNA Damage. *Front. Genet.* **2020**, *11*, 561687. [CrossRef]
17. Rezvani, H.R.; Ged, C.; Bouadjar, B.; de Verneuil, H.; Taieb, A. Catalase overexpression reduces UVB-induced apoptosis in a human xeroderma pigmentosum reconstructed epidermis. *Cancer Gene Ther.* **2008**, *15*, 241–251. [CrossRef]
18. Rezvani, H.R.; Kim, A.L.; Rossignol, R.; Ali, N.; Daly, M.; Mahfouf, W.; Bellance, N.; Taieb, A.; de Verneuil, H.; Mazurier, F.; et al. XPC silencing in normal human keratinocytes triggers metabolic alterations that drive the formation of squamous cell carcinomas. *J. Clin. Investig.* **2011**, *121*, 195–211. [CrossRef]
19. Raad, H.; Serrano-Sanchez, M.; Harfouche, G.; Mahfouf, W.; Bortolotto, D.; Bergeron, V.; Kasraian, Z.; Dousset, L.; Hosseini, M.; Taieb, A.; et al. NADPH Oxidase-1 Plays a Key Role in Keratinocyte Responses to UV Radiation and UVB-Induced Skin Carcinogenesis. *J. Investig. Dermatol.* **2017**, *137*, 1311–1321. [CrossRef]
20. Bidon, B.; Iltis, I.; Semer, M.; Nagy, Z.; Larnicol, A.; Cribier, A.; Benkirane, M.; Coin, F.; Egly, J.M.; Le May, N. XPC is an RNA polymerase II cofactor recruiting ATAC to promoters by interacting with E2F1. *Nat. Commun.* **2018**, *9*, 2610. [CrossRef]
21. Chen, Z.; Yang, J.; Wang, G.; Song, B.; Li, J.; Xu, Z. Attenuated expression of xeroderma pigmentosum group C is associated with critical events in human bladder cancer carcinogenesis and progression. *Cancer Res.* **2007**, *67*, 4578–4585. [CrossRef]
22. de Feraudy, S.; Ridd, K.; Richards, L.M.; Kwok, P.Y.; Revet, I.; Oh, D.; Feeney, L.; Cleaver, J.E. The DNA damage-binding protein XPC is a frequent target for inactivation in squamous cell carcinomas. *Am. J. Pathol.* **2010**, *177*, 555–562. [CrossRef]
23. Pascucci, B.; D'Errico, M.; Parlanti, E.; Giovannini, S.; Dogliotti, E. Role of nucleotide excision repair proteins in oxidative DNA damage repair: An updating. *Biochemistry* **2011**, *76*, 4–15. [CrossRef]
24. Birmingham, A.; Selfors, L.M.; Forster, T.; Wrobel, D.; Kennedy, C.J.; Shanks, E.; Santoyo-Lopez, J.; Dunican, D.J.; Long, A.; Kelleher, D.; et al. Statistical methods for analysis of high-throughput RNA interference screens. *Nat. Methods* **2009**, *6*, 569–575. [CrossRef]

25. Mazouzi, A.; Battistini, F.; Moser, S.C.; da Ferreira, S.J.; Wiedner, M.; Owusu, M.; Lardeau, C.H.; Ringler, A.; Weil, B.; Neesen, J.; et al. Repair of UV-Induced DNA Damage Independent of Nucleotide Excision Repair Is Masked by MUTYH. *Mol. Cell* **2017**, *68*, 797–807. [CrossRef]
26. Borszéková Pulzová, L.; Ward, T.A.; Chovanec, M. XPA: DNA Repair Protein of Significant Clinical Importance. *Int. J. Mol. Sci.* **2020**, *6*, 2182. [CrossRef] [PubMed]
27. van Oijen, M.G.; Medema, R.H.; Slootweg, P.J.; Rijksen, G. Positivity of the proliferation marker Ki-67 in noncycling cells. *Am. J. Clin. Pathol.* **1998**, *110*, 24–31. [CrossRef] [PubMed]
28. Black, J.O. Xeroderma Pigmentosum. *Head Neck Pathol.* **2016**, *10*, 139–144. [CrossRef]
29. Mouret, S.; Charveron, M.; Favier, A.; Cadet, J.; Douki, T. Differential repair of UVB-induced cyclobutane pyrimidine dimers in cultured human skin cells and whole human skin. *DNA Repair* **2008**, *7*, 704–712. [CrossRef] [PubMed]
30. Courdavault, S.; Baudouin, C.; Charveron, M.; Canguilhem, B.; Favier, A.; Cadet, J.; Douki, T. Repair of the three main types of bipyrimidine DNA photoproducts in human keratinocytes exposed to UVB and UVA radiations. *DNA Repair* **2005**, *4*, 836–844. [CrossRef]
31. Pushpakom, S.; Iorio, F.; Eyers, P.A.; Escott, K.J.; Hopper, S.; Wells, A.; Doig, A.; Guilliams, T.; Latimer, J.; McNamee, C.; et al. Drug repurposing: Progress, challenges and recommendations. *Nat. Rev. Drug Discov.* **2019**, *18*, 41–58. [CrossRef]
32. Basu, A.K. DNA Damage, Mutagenesis and Cancer. *Int. J. Mol. Sci.* **2018**, *19*, 970. [CrossRef] [PubMed]
33. Einav, S.; Gerber, D.; Bryson, P.D.; Sklan, E.H.; Elazar, M.; Maerkl, S.J.; Glenn, J.S.; Quake, S.R. Discovery of a hepatitis C target and its pharmacological inhibitors by microfluidic affinity analysis. *Nat. Biotechnol.* **2008**, *26*, 1019–1027. [CrossRef] [PubMed]
34. Richter, J.M.; Schaefer, M.; Hill, K. Clemizole hydrochloride is a novel and potent inhibitor of transient receptor potential channel TRPC5. *Mol. Pharmacol.* **2014**, *86*, 514–521. [CrossRef] [PubMed]
35. Kashfi, S.M.; Golmohammadi, M.; Behboudi, F.; Nazemalhosseini-Mojarad, E.; Zali, M.R. MUTYH the base excision repair gene family member associated with colorectal cancer polyposis. *Gastroenterol. Hepatol. Bed Bench* **2013**, *6*, S1–S10. [PubMed]
36. Matallana-Surget, S.; Meador, J.A.; Joux, F.; Douki, T. Effect of the GC content of DNA on the distribution of UVB-induced bipyrimidine photoproducts. *Photochem. Photobiol. Sci.* **2008**, *7*, 794–801. [CrossRef]
37. Douki, T.; Cadet, J. Individual determination of the yield of the main UV-induced dimeric pyrimidine photoproducts in DNA suggests a high mutagenicity of CC photolesions. *Biochemistry* **2001**, *40*, 2495–2501. [CrossRef]
38. Kuschal, C.; DiGiovanna, J.J.; Khan, S.G.; Gatti, R.A.; Kraemer, K.H. Repair of UV photolesions in xeroderma pigmentosum group C cells induced by translational readthrough of premature termination codons. *Proc. Natl. Acad. Sci. USA* **2013**, *110*, 19483–19488. [CrossRef]
39. Flowing Software Version 2.5.1 bPT, Turku Centre for Biotechnology University of Turku, Finland, In Colaboration with Turku Bioimaging. Available online: http://flowingsoftware.btk.fi/ (accessed on 16 February 2021).
40. R Core Team. R: A Language and Environment for Statistical Computing. R Foundation for Statistical Computing V, Austria. 2018. Available online: http://www.R-project.org/ (accessed on 16 February 2021).

SIGILLUM UNIVERSITATIS GRATIANOPOLITANÆ
1339